Nodal and paranodal auto-antibodies in immune-mediated peripheral neuropathies:

clinical-serological characterisation and pathogenic mechanisms



Janev Fehmi
St Johns College
University of Oxford

Supervisors:
Associate Professor Simon Rinaldi
Professor David Bennett

2024

Acknowledgements

Undertaking this research project was made possible by the generous funding from both Guarantors of Brain and the GBS|CIDP Foundation International. I am incredibly grateful for their prolonged support and flexibility. Ultimately though, the support, expertise, and friendship of my supervisors, family, and those working around me in the laboratory have been key to the enjoyment and completion of this project.

Simon has not merely supervised me, but rather guided me through five (and counting) years of navigating a new world consisting of running endlessly failing experiments and more publication rejections than I ever thought possible in my short research career thus far. He has managed to provide me with enough support and encouragement to steer me away from too many diversions and keep my optimism afloat, but allowed me sufficient space to find my own way on what has been a rather steep learning curve. He has been a friend, and he has always made me feel as if he were walking a path alongside, rather than in front of me.

Dave has been an inspiring, overarching presence throughout my time in Oxford. I am so grateful for his wise words, not just in a formal capacity with regards to the DPhil and its overall direction, but also those provided over a pint after a soggy summer punting excursion. It remains a mystery to me how he manages to achieve everything he does, whilst being accessible to even the most junior (me) members of the lab, and always making time for a pint and a chat. There must be more hours in his day than mine.

Tom Vale, one of the first people I met in the laboratory in Oxford, with our shared love of coffee breaks and his passion for fine wines, it was quite clear we would become lab besties. Outside of the laboratory, he has actually provided me with a place to live for a third of my DPhil, been an infinite source of wine recommendations (and indeed wine itself), but most importantly a great friend.

Alex Davies, there are no words. You might possess some of the finest qualities in a human I have ever come across. Patience, tolerance, generosity, and a meticulous work ethic. You have been a troubleshooting sounding board, and always made time to listen and provide help when I have (so often) needed it. You also seem to live in this world where there are more hours in a day than the rest of us.

Last, but by no means least, my husband Ali has had to put up with continuously moving goal posts of a three (to 6) year DPhil, interrupted by the birth of our two wild gems, Florence and Joni (apparently writing papers on maternity leave was not a reliable ambition). Ali has been the best rock one could ever hope for, living mainly on the M4 between Bristol and Oxford for the best part of two years, and making all the right supportive gestures for me to keep going (a little faster for the write up if possible). He and the girls are the main reason I will look back on so many of my memories from Oxford so fondly.

Table of Contents

1 INTRODUCTION 1

1.1 Abstract 1

1.2 Overview of Inflammatory and immune-mediated peripheral neuropathies 3

1.2.1 Spectrum of diseases 3

1.2.2 Clinical presentation of GBS and CIDP 4

1.2.3 Diagnostic challenges 6

1.2.4 Current immunotherapies 7

1.2.5 Pathogenic mechanisms 8

1.3 Specialised regions of the peripheral nerve 15

1.3.1 The Node of Ranvier 16

1.3.2 The paranodal junction 17

1.3.3 The Juxtaparanode and compact myelin 18

1.4 The Autoimmune Nodopathies 19

1.4.1 Emerging antibodies targeting antigens at the node and paranode 19

1.4.2 Overview of phenotypic characteristics 20

1.4.3 Clinical and serological characteristics of individual nodal and paranodal antibody cohorts 25

1.4.4 Pathogenicity of (para)nodal antibodies 32

1.5 Aims of this thesis 39

2 METHODOLOGY 40

2.1 Abstract 40

2.2 Cell based assays (CBA) 41

2.2.1 DNA plasmid amplification 41

2.2.2 DNA plasmid purification 41

2.2.3 Human Embryonic Kidney (HEK) cell transfection 42

2.2.4 Immunoassay and interpretation 43
2.2.5 Complement binding assays 44
2.3 Enzyme-linked immunosorbent assay (ELISA) 45
2.4 Myelinated co-cultures (human-induced pluripotent stem cell-derived) 46
2.4.1 Human-induced pluripotent stem cell (hiPSC) differentiation, and plating of sensory neurons 46
2.4.2 Sensory neuron precursor freezing (for development of a higher throughput method of sera screening on 96 well plates) 47
2.4.3 Schwann cell harvesting and myelination of sensory neurons with rat Schwann cells 48
2.4.4 Immunoassay for topographical human IgG binding 48
2.4.5 Initial and subsequent validation of screening human sera for IgG binding 49
2.4.6 Complement binding assays 50
2.4.7 Complement-dependent cytotoxicity (CDC) assay using CytotoxGlo 51
2.4.8 Detection of fluid biomarkers (NfL and CNTN1 protein) 52
2.5 Human sera sampling, serological and clinical profiling, data analysis 53
2.5.1 Analysis of clinical and serological associations in anti-pan-neurofascin antibody cohort 54
2.5.2 Analysis of clinical and serological associations in anti-CNTN1 antibody and nephrotic syndrome cohort 55
2.6 Western blot 55
2.6.1 Cell line lysate preparation 55
2.6.2 Rat tissue lysate preparation (brain, kidney, sciatic nerve) 55
2.6.3 Human tissue lysate preparation (podocyte, whole kidney) 56
2.6.4 Immune complex detection (CNTN1) 57
2.6.5 Polyacrylamide gel (PAGE) electrophoresis and immunoblotting 57
2.7 Data analysis 58
2.7.1 Analysis of clinical and serological associations in anti-pan-neurofascin antibody cohort 58
2.7.2 Analysis of clinical and serological associations in anti-CNTN1 antibody and nephrotic syndrome cohort 59
2.8 CNTN1 identification in mouse and human tissue–- Immunohistochemistry 59
2.8.1 Mouse sciatic nerve teased fibres 59

2.8.2 Human kidney and brain 60

3 RESULTS 62

3.1 Diagnostic assays and screening tools used to detect nodal and paranodal antibodies 62

3.1.1 Abstract 62

3.1.2 ELISA 63

3.1.3 Live CBA using HEK cells 63

3.1.4 A comparison of sensitivity and specificity of ELISA and CBA 70

3.1.5 Myelinated co-cultures as a screening tool for the presence of established and novel peripheral nerve-reactive antibodies 76

3.1.6 Discussion 86

3.2 Clinical-serological phenotype of patients seropositive for (para)nodal auto-antibodies 89

3.2.1 Abstract 89

3.2.2 Overall cohort screened (BioSPIN and diagnostic service cohorts) 90

3.2.3 PanNF-antibody cohort 110

3.2.4 CNTN1-antibody AN cohort with neuropathy and nephropathy 122

3.2.5 Discussion 139

3.3 Mechanistic studies of nodal and paranodal auto-antibody-mediated pathogenicity 146

3.3.1 Abstract 146

3.3.2 Topographical patterns of antibody binding in myelinated co-cultures and investigation of in-vitro evidence of pathogenicity 147

3.3.3 Evidence of complement activation 158

3.3.4 Assessment of complement dependent neuronal injury 172

3.3.5 Discussion 178

4 CONCLUSION AND FUTURE WORK 184

5 BIBLIOGRAPHY 188

6 APPPENDIX 220

List of Figures

Figure 1: Clinical phenotypes in inflammatory neuropathies 4

Figure 2: Conduction abnormalities classically seen in nodo-paranodopathies 14

Figure 3: Organisation and structure of myelinated axon domains 16

Figure 4: Immunoreactivity of IgG from a CNTN1-positive patient on CBA before and after pre-adsorption confirm their specificity for Contactin-1 65

Figure 5: Pattern of IgG reactivity with CNTN1 antibody positive sera with transfected HEK cells 66

Figure 6: Commercial anti-Caspr1 and -CNTN1 antibody staining in HEK cells 67

Figure 7: Pattern of IgG reactivity with Caspr1 antibody-positive sera with transfected HEK cells 67

Figure 8: Reactivity of sera against Caspr1 in ELISA 68

Figure 9: Comparison between neurofascin-155 monospecific and pan-neurofascin antibody reactivity on cell-based assays 69

Figure 10: Subclass specificity and comparison between CBA and ELISA for sera from 8 PanNF AIN patients 73

Figure 11: A comparison between CBA and ELISA of end-point titre and subclass specificity of CNTN1 antibodies 74

Figure 12: End-point titre comparison between CBA and ELISA for all (para)nodal seropositive patients 75

Figure 13: Optimisation of hiPSC-derived sensory neuron differentiation and patient cohort screened for IgG binding in myelinated co-cultures 78

Figure 14: Generation of stocks of sensory neuron precursors and development of a high throughput culture system of human stem cell-derived sensory neurons myelinated with rat Schwann cells 79

Figure 15: Patterns of positive immunostaining: IgG reactivity detected in myelinated co-cultures 81

Figure 16: Inter-assay, inter-experimenter and inter-observer agreement of positive immunoreactivity of serum samples on myelinating co-cultures 82
Figure 17: Discrepancies in topographical IgG binding patterns 83
Figure 18: Patterns of positive IgG immunostaining observed in patients seronegative for (para)nodal antibodies (validation study) 84
Figure 19: Topographical IgG binding patterns from patient and control sera samples in myelinated co-cultures 85
Figure 20: Total proportion of autoimmune nodopathy patients detected through screening. 92
Figure 21: Patient cohort positive for nodal and paranodal antibodies (total 120) 92
Figure 22: Clinical characteristics of the seropositive (AIN) vs seronegative patient cohort 94
Figure 23: modified Rankin score (mRS) for (para)nodal antibody seropositive (86) and seronegative (182) cohorts. 95
Figure 24: Clinical characteristics in each (para)nodal antibody group (table, heat map and bar chart) 97
Figure 25: Patient IgG subclass testing: CBA appearances, heat map and tables representing proportion and dominance of IgG subclasses detected within each antibody group 100
Figure 26: Heat map showing IgG subclass positive reactivity scores per patient sample within antibody groups 102
Figure 27: Correlation of (para)nodal antibody titres and mRS. 102
Figure 28: Proportion of seropositive (PNAb+) and seronegative (PNAb-) patients requiring number of treatment modalities 103
Figure 29: Pie charts showing percentage overall treatment responses in the autoimmune nodopathy cohort 104
Figure 30: Alternative immunomodulatory therapy use in autoimmune nodopathy patients 104
Figure 31: Rituximab treatment led to improved clinical outcome than standard therapy (steroids, IVIg, PLEX) alone. 106

Figure 32: Physician reported treatment outcomes of autoimmune nodopathy (PNAb+) patients compared with seronegative suspected immune neuropathy patients (PNAb-) 107
Figure 33: Comparison of treatment responses in 72 autoimmune nodopathy patients with and without IgG4 antibodies 108
Figure 34: Serological, radiological and histological findings. 116
Figure 35: Teased nerve fibre. 117
Figure 36: Modified Rankin scores and CSF protein levels. 118
Figure 37: Treatment timelines of anti-panNF AIN patients 120
Figure 38: Flowchart summarising detection of patients with CIDP, nephrotic syndrome and CNTN1 antibodies through prospective (para)nodal autoantibody screening 125
Figure 39: CNTN1 antibody titres correlate with disease activity. 138
Figure 40: Axonal pattern of IgG binding from CNTN1-positive patients in myelinated neuronal co-cultures is specific to the CNTN1 antigen. 150
Figure 41: Pan-neurofascin serum is specific to NF155 and NF186 in live myelinating co- cultures. 151
Figure 42: Contactin-1 immunoreactivity in kidney immune deposits and peripheral nerve tissue 152
Figure 43: Contactin-1 immunoreactivity in kidney immune deposits for patents 1, 2 and 13 153
Figure 44: LC-MS/MS of CNTN1 peptides. 154
Figure 45: CNTN1 is expressed in healthy human kidney 155
Figure 46: Fall in serum CNTN1 protein is associated with immune complex formation in active disease. . 156
Figure 47: CNTN1-containing immune complexes are present in serum at disease nadir. 157
Figure 48: Heat inactivation eliminates endogenous complement but not antibody binding 159
Figure 49: Assessment of (para)nodal antibody and complement fixation in HEK cells 161
Figure 50: High background staining and complement dose dependent HEK cell cytotoxicity 164
Figure 51: Normal human sera (NHS) binding in myelinated co-cultures. 167
Figure 52: Antibody-containing sera and NHS (top row sera SR1192, bottom row sera BQ008) 168

Figure 53: Factors affecting strength of antibody binding. 169

Figure 54: Complement binding in the presence of antibody-containing sera alone. 170

Figure 55: Complement binding precedes axonal injury in the presence of a source of complement. 171

Figure 56: IgG labelling and complement-dependent cytotoxicity in human sensory neurons. 174

Figure 57: Graphs illustrating figures from table 12 176

Figure 58: Examples of culture appearances seen using confocal microscopy with and without the addition of NHS 20%. 177

Figure 59: CNTN1 protein levels in healthy and nerve injury conditions, from experiment 2. 177

List of Tables

Table 1: Table summarising proportion of (para)nodal antibody seropositive and seronegative samples tested for IgG binding in co-culture during preliminary screening 80

Table 2: Total patients screened for (para)nodal antibodies 91

Table 3: Clinical characteristics of the (para)nodal antibody seropositive (AIN) vs seronegative patient cohort 94

Table 4: Treatment responses and IgG subclass dominance in 72 AIN patients. 109

Table 5: Subclass distribution of pan-neurofascin versus neurofascin-155, contactin-1 and contactin1/caspr1 complex reactive antibodies. 114

Table 6: A comparison of clinical features of panNF AN patients to other antibody cohorts 115

Table 7: Clinical features of panNF antibody positive patients 119

Table 8: Detailed neurophysiological findings. 121

Table 9: Physician reported treatment response by serological group 121

Table 10: Summary of patients with neuropathy, nephrotic syndrome and CNTN1 antibodies 126

Table 11: Key characteristics of 15 patients with immune-mediated neuropathy and nephrotic syndrome with positive anti-CNTN1 antibodies (patients 1-7 and 8-15) 137

Table 12: NfL measurements compared from supernatant extracted from experiment 1 and 2. Assessment of imaging for experiment 2 is ongoing 176

List of Abbreviations

ADAM23 – ADAM metallopeptidase domain 23

AIDP – Acute inflammatory demyelinating polyneuropathy

AMAN – Acute motor axonal neuropathy

AMSAN – Acute motor sensory axonal neuropathy

AIN – Autoimmune nodopathy

AP – Action potential

AQP4 – Aquaporin 4

BioSPIN – Biomarker Investigation and Study of Pathology in Neuropathy

BSA – Bovine serum albumin

CAMs – Cell adhesion molecules

CANOMAD – Chronic ataxic neuropathy, opthalmoplegia, immunoglobulin M, cold agglutinins, and disialosyl antibodies

Caspr1 – Contactin-associated protein 1

CB – Conduction block

CBA – Cell based assay

CCPD – Combined central and peripheral demyelination

CDC – Complement dependent cytotoxicity

CIDP – Chronic immune demyelinating polyneuropathy

CISP – Chronic immune sensory polyradiculoneuropthy

CMAPs – Compound muscle action potentials

CNS – Central nervous system

CNTN1 – Contactin-1

CSF – Cerebrospinal fluid

CV – Conduction velocity

DAB – 3,3′-Diaminobenzidine

DADS – Distal acquired demyelinating symmetric

DMEM – Dulbecco's Modified Eagle Medium

DML – Distal motor latency

DRG – Dorsal root ganglia

EAN – Experimental autoimmune neuritis

ELISA – Enzyme-linked immunosorbent assay

FAE – Fab arm exchange

FBS – Fetal bovine serum

FnIII – Fibronectin type III

GBS – Guillain-Barré syndrome

HEK – Human embryonic kidney

hiPSC – human induced pluripotent stem cells

HRP – Horseradish peroxidase

IgG – Immunoglobulin G

IgM – Immunoglobulin M

IHC – Immunohistochemistry

IVIg – Intravenous Immunoglobulin

JXP – Juxtaparanode

Kv – Potassium ion channel

LB – Lysogeny broth

LGI4 – Leucine rich repeat LGI family member 4

MAC – Membrane attack complex

MADSAM – Multifocal acquired demyelinating sensory and motor neuropathy

MAG – Myelin-associated glycoprotein

MMN – Multifocal motor neuropathy

MRI – Magnetic resonance imaging

Nav – Sodium ion channel

NCS – Nerve conduction studies

NDS – Normal donkey serum

NF155 – Neurofascin-155

NF186 – Neurofascin-186

NfL – Neurofilament light

NHS – Normal human serum

NoR – Node of Ranvier

NrCAM – Neuronal cell adhesion molecule

OD – Optical density

OPD – O-phenylenediamine dihydrochloride

PanNF – Pan-neurofascin

PBS – Phosphate buffered saline

PEG – Polyethylene glycol

PFA – Paraformaldehyde

PLEX – Plasma exchange

PNJ – Paranodal junction

PNS – Peripheral nervous system

RCF – Reversible conduction failure

RNA – Ribonucleic acid

RT – Room temperature

RTX – Rituximab

SCs – Schwann cells

TD – Temporal dispersion

1 INTRODUCTION

1.1 Abstract

The term inflammatory peripheral neuropathy, sometimes used interchangeably with immune-mediated peripheral neuropathy, encompasses a wide range of syndromes, broadly categorised into acute and chronic forms, most commonly Guillain Barré Syndrome (GBS) and Chronic Inflammatory Demyelinating Polyradiculoneuropathy (CIDP), respectively. Their clinical heterogeneity, likely reflecting diverse pathogenic mechanisms, can lead to a delay in diagnosis, in particular for the numerous atypical forms, unnecessary investigations, and trials of ineffective and potentially harmful treatments.

This project focusses on a group of disorders within this category, which have recently been recognised to be pathologically and clinically distinct, and so recently renamed 'Autoimmune Nodopathies' (AIN). Crucially, these have been identified through the discovery of antibodies targeting the antigens Contactin-1 (CNTN1), Caspr1, Neurofascin-155 (NF155) and Neurofascin-186 (NF186) at the node of Ranvier, and adjacent paranodes ((para)nodal antibodies). These are one of a handful of existing serum biomarkers which are currently used in clinical practice with diagnostic and therapeutic impact for patients with immune-mediated peripheral neuropathies (Bellanti et al., 2024).

The node of Ranvier is required for fast and efficient saltatory conduction along myelinated peripheral nerve fibres. This and adjacent perinodal regions are composed of a vast array of highly specialised molecules, involved in complex axoglial interactions, in order to facilitate the tightly regulated structural assembly and maintenance of these regions.

Ganglioside antibody-mediated attack targeting the node and flanking regions has previously been reported in acute axonal neuropathies, though their identification is of limited clinical use in the majority of inflammatory and immune-mediated neuropathies. The (para)nodal antibodies discussed here have been

shown to bind to the nodal regions, leading to structural dismantling and functional disruption. However, their individual mechanisms of pathogenicity are only beginning to be resolved.

The overall aims of my doctoral research are to:

1. Clinically and serologically characterise patients with Autoimmune nodopathies (AIN)
2. Assess the utility of diagnostic assays used to detect (para)nodal antibodies
3. Investigate the mechanisms by which (para)nodal antibodies exert their pathogenic effects

1.2 Overview of Inflammatory and immune-mediated peripheral neuropathies

1.2.1 Spectrum of diseases

Immune-mediated peripheral neuropathies encompass a diverse range of disabling disorders caused by dysregulation of the immune system resulting in damage to the peripheral nervous system (PNS). Peripheral neuropathies are highly prevalent globally (Shahrizaila, 2021), one in ten potentially caused by an autoimmune process (Visser et al., 2015).

Neuropathies have historically been classified in a number of ways, on the basis of clinical characteristics i.e. symmetry, time to nadir, progressive or fluctuating clinical course, and with the advent of neurophysiology by involvement of specific nerve components i.e. axonal or demyelinating, and further by histological appearances resulting from a pathological process. Inflammatory neuropathies are an example of the latter, referring to peripheral neuropathies for which histological evidence of inflammation has been observed. Comprising this group are acute and chronic neuropathy categories, dominated by Guillain-Barré syndrome (GBS) and chronic inflammatory demyelinating polyradiculoneuropathy (CIDP), respectively. Broadly, their underlying pathology is considered to be immune-mediated. Other chronic inflammatory neuropathy syndromes include those arising from aberrant production of a monoclonal protein (paraprotein) or specific pathogenic antibodies i.e. anti-myelin-associated glycoprotein (MAG) neuropathy, multifocal motor neuropathy (MMN), chronic ataxic neuropathy with ophthalmoplegia, M- protein, cold agglutinins and disialosyl ganglioside antibodies (CANOMAD) (**Figure 1**).

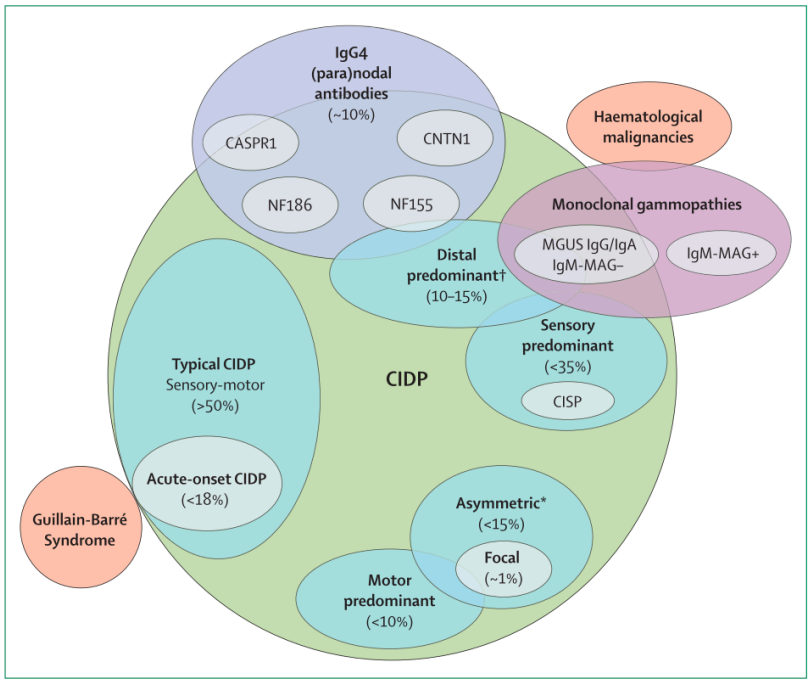


Figure 1: Clinical phenotypes in inflammatory neuropathies

[Taken from (Bunschoten et al., 2019)]

In the following paragraphs I will specifically focus on the clinical and pathological features of GBS and CIDP.

1.2.2 Clinical presentation of GBS and CIDP

GBS is classically characterised by a rapidly progressive ascending and symmetrical sensorimotor neuropathy, reaching peak deficit within 4 weeks, and is the most common cause of acute flaccid paralysis worldwide. It is almost always a monophasic illness. Associated but variably present clinical signs include cranial nerve palsies, ataxia, autonomic disturbance and respiratory failure, with up to a third of patients requiring mechanical ventilation (Henderson et al., 2003; Winer et al., 1988). Additionally, the initial pattern of clinical symptoms can help categorise it into one of the 7 regional variants (Leonhard et al., 2019), though often these overlap with the 'classical' form. Further classification can be made on a neurophysiological basis, into its most common demyelinating form, acute inflammatory demyelinating polyneuropathy (AIDP) or axonal subtypes, acute motor (and sensory) axonal neuropathy (AMAN and AMSAN). A further

supportive, but not specific, diagnostic feature is elevated CSF protein without an increased cell count (Guillain et al., 1999).

CIDP in its 'typical' form is defined clinically by a chronic (reaching nadir beyond 8 weeks of onset) peripheral neuropathy characterised by symmetrical, proximal and distal muscle weakness, with sensory involvement and diminished tendon reflexes, occurring over a relapsing or progressive clinical course. It's now termed 'variant' forms introduce heterogeneity into this umbrella term and include distal (distal acquired demyelinating symmetric; DADS), multifocal (multifocal acquired demyelinating sensory and motor; MADSAM), focal (one limb only), motor, or sensory-predominant (Doneddu et al., 2021). This recent terminology was introduced to bring clarity over previous categorisation of 'atypical' forms of CIDP (Van den Bergh et al., 2021), and aims to represent a variety of clinical presentations which share common histological features and treatment responses. Previous disorders included within the umbrella term of CIDP have now importantly been recognised as their own distinct disease entities, permitting an alternative management approach. These include anti-MAG neuropathies, chronic immune sensory polyradiculopathy (CISP), and autoimmune nodopathies (AIN). The latter are the focus of this thesis and represent a relatively minor proportion of patients fulfilling criteria for CIDP, but specifically found to have antibodies targeting the node of Ranvier (NoR) and adjacent paranodes, as well as additional features including cranial neuropathies, ataxia, and autonomic and respiratory dysfunction, not usually associated with CIDP.

Specific neurophysiological features, including electrodiagnostic criteria supporting demyelination in motor and sensory nerves, are mandatory to confirm a diagnosis of CIDP, though supportive criteria provided by other modalities (response to treatment, imaging or nerve biopsy) can be used to strengthen the diagnosis if neurophysiology is only weakly supportive, or yield a 'possible CIDP' conclusion if no electrodiagnostic criteria are met (Van den Bergh et al., 2021).

1.2.3 Diagnostic challenges

Ultimately, the diagnoses of GBS and CIDP are made on clinical grounds. They are often considered part of a continuous spectrum, one acute and self-limiting, the other chronic and progressive or relapsing, but primarily distinguished by time from onset to nadir. Indeed, typical CIDP can rarely present acutely (A-CIDP), rapidly worsening within 4 weeks, thus mimicking GBS initially. Within the acute phase there are currently no clinical, serological or neurophysiological markers that can reliably distinguish GBS from CIDP. Electrodiagnostic criteria can support a clinical diagnosis in the subacute and chronic phases of both disorders, though they cannot be relied on solely in the face of clinical uncertainty. Thus, reliance on clinical patterns (at least early on in presentation), lack of confirmatory tests, and ambiguity of electrophysiological studies leaves patients frequently exposed to a high risk of misdiagnosis (Allen, 2020; Allen et al., 2018), in particular for CIDP variants.

There are no serological biomarkers available in the clinical setting for CIDP, though neurophysiological criteria predominantly support clinical suspicions (Van den Bergh et al., 2021).

Anti-ganglioside antibodies are available for testing in specific immune-mediated neuropathies, and some are strongly associated with defined subtypes (Emilien & Hugh, 2015). The most clinically relevant IgG antibodies in GBS are anti-GQ1b in the Miller-Fisher syndrome variant (MFS) (Willison et al., 1993), and anti-GM1 in AMAN (Kuwabara et al., 1998). Unfortunately, these are not immediately available to aid in diagnosis, are not always positive, and ultimately do not change therapeutic approach. Some can, however, be helpful in predicting outcome (Thomma et al., 2023).

There are many potential diagnostic and disease activity serological biomarkers that are being developed and validated in a research setting, in particular serum neurofilament light (NfL) as a surrogate for axonal injury (Khalil et al., 2018; Lieverloo et al., 2019; Martín-Aguilar et al., 2021), but accurate, reliable, and cost-effective biomarkers are still lacking. Prospective studies of neuronal damage, and longitudinal data of

relative levels within individual patients, and compared to age and sex-matched controls is needed before these sorts of biomarkers can be utilised in a clinical setting.

The mortality rate in GBS patients is reported to range between 5-10% (Berg et al., 2013; Witsch et al., 2013) and residual disability in both GBS and CIDP affect a significant proportion of patients (Forsberg et al., 2012; Garssen et al., 2006; Querol et al., 2021). These disorders are treatable however, and our understanding of the pathological processes underpinning each, with responsive reclassification in clinical guidelines is paramount to develop and target specific treatments to individual patients.

1.2.4 Current immunotherapies

Prompt treatment of immune-mediated neuropathies is important if axonal Wallerian degeneration, and irreversible damage, is to be avoided. Early diagnosis can be challenging, potentially delaying effective therapies. But even when diagnosis is correctly established, without objective and accurate disease monitoring biomarkers, patients can be overtreated, resulting in unnecessary adverse events.

Currently standard first line treatments for GBS and CIDP are non-specific, and often incompletely effective. They include steroids, for CIDP only, and intravenous immunoglobulin (IVIg) and plasma exchange (PLEX) for both CIDP and GBS (Hughes et al., 2014; Raphaël et al., 2012; Van den Bergh et al., 2021).

Some 80-90% of CIDP patients respond well to one or more of these therapies (Cocito et al., 2010; Oaklander et al., 2017), though they can be less effective in a proportion of patients with CIDP variants (Menon et al., 2021), likely reflecting differing pathophysiology. If patients improve and stabilise on first-line therapies, longer term immunosuppressive agents can be introduced in place of steroids and possibly IVIg, and if a confident diagnosis of CIDP can be given but patients prove refractory to first line treatments, escalation to more potent immunosuppression, namely Rituximab (RTX) or Cyclophosphamide (CYC) is

warranted (Godil et al., 2020). Response to these agents was found to be especially effective in patients found to have a paraprotein or (para)nodal antibody (Querol et al., 2015; Roux et al., 2018). As a last resort, haematopoietic stem cell transplantation can be considered, and is effective but associated with significant mortality and morbidity (Burt et al., 2020).

Treatment in the context of GBS is thought to accelerate recovery (Hughes et al., 2014; Raphaël et al., 2012), but even if administered early, do not necessarily stop disease progression, indicating an untargeted therapeutic approach. The development of novel therapies in GBS hold promise, for example, to specifically reduce the serum IgG levels (Wang et al., 2017; G. Zhang et al., 2017), or targeting the complement pathway (Davidson et al., 2017; McGonigal et al., 2016; Misawa et al., 2018). For these to be most effective however, patients will still need to be appropriately selected on the basis of likely pathological mechanism.

Thus, identifying biomarkers to allow early recognition of GBS and CIDP variants is of particular importance, as these are likely to require alternative therapeutic approaches.

1.2.5 Pathogenic mechanisms

1.2.5.1 Overview

The intact PNS is largely protected from passive diffusion of systemic circulating immune cells into the nerve parenchyma by the blood-nerve barrier. If this is compromised, invasion by activated T-cells can mount an inflammatory response and permit macrophages and proteins (including antibodies) to pass through (Kanda, 2013) potentially leading to nerve injury. What specifically causes this permeability, however, has not been elucidated in immune-mediated neuropathies.

Both humoral and cellular immune mechanisms have been implicated in the pathophysiology of GBS and CIDP, with dominant disease mechanisms emerging for specific subtypes (Ikeda et al., 2019; Yuki et al., 1990). In GBS, differentiating the underlying pathogenesis of axonal variants vs demyelinating forms is

important, as prognosis can differ. Presently, however, there is insufficient data to support treating these variants differently.

Morphological features identified within this broad range of disorders can be heterogeneous and do not clearly define distinct pathogenic mechanisms, probably reflecting different timepoints of sampling in disease course, but also likely the different disease mechanisms at play within patient cohorts.

It is also important to bear in mind that there are a number of common findings, such as nodal/paranodal abnormalities, which can be seen in a variety of peripheral neuropathies, and are not necessarily specific for a single disease or underlying pathogenic mechanism. For example, nodal disorganisation (nodal gap elongation and paranodal dispersion) could be seen in immunofluorescence studies of skin biopsies taken from patients with a range of neuropathies, including CIDP, diabetic, vasculitic and genetic neuropathies (Doppler et al., 2013). Nodal abnormalities could also be characterised using biopsy material from patients with chronic demyelinating or axonal neuropathies (Cifuentes-Diaz et al., 2011). In a super-resolution ultrastructural study, paranodal architecture can be altered in acute axonal, and acute and chronic demyelinating neuropathies within varying diagnostic categories (Appeltshauser et al., 2023).

1.2.5.2 Cellular immunity

Much of our current understanding of primary demyelinating forms of GBS and CIDP stems from nerve biopsies in patients, autopsy series and the use of established animal models. The pathology observed in the ‘experimental autoimmune neuritis’ (EAN) model (WAKSMAN & ADAMS, 1955), induced through immunization with PNS myelin proteins, resembles that seen in humans, even though the mechanism of disease induction is clearly different.

Ultrastructural studies in AIDP and CIDP, reveal a pattern of inflammatory demyelination that can be indistinguishable (Koike et al., 2018, 2020). Immune effector mechanisms considered central to their

immunopathogenesis are activation and invasion of T-cells, allowing macrophages to infiltrate the endoneurium at internodal and sometimes nodal areas, and phagocytose myelin, resulting in inflammatory patchy internodal demyelination. This has remained largely unchanged from Asbury's initial description of "idiopathic polyneuritis" some five decades ago (Asbury et al., 1969). Early pathological studies have demonstrated myelin swelling preceding cellular infiltration (Haymaker & Kernohan, 1949), implying the latter may be a response to an initial insult. Indeed, autoantibody reactivity to peripheral myelin proteins (P0, P2, PMP-22) (Csurhes et al., 2005; Gabriel et al., 2000), and complement myelin deposition (C. E. Hafer-Macko et al., 1996) have been reported in conjunction, suggesting perhaps an overlap of humoral and cellular mechanisms–- an initial autoantibody driven process leading to macrophage-led demyelination (J. M. Vallat et al., 2019). In CIDP, demyelinated axons can also develop a characteristic "onion-bulb" appearance on histology, formed by inefficient proliferating layers of Schwann cell (SC) processes, representative of recurrent demyelination-remyelination (Koike et al., 2018).

The role of Schwann cells (SCs) has more recently been shown to play a part in facilitating macrophage-mediated nerve injury. It has been shown that following macrophage attack, SCs can de-differentiate into demyelinating SCs (Park et al., 2019, 2020), inducing self-myelin clearance, and potentially enabling macrophages to access the SCs within multiple nerve domains, including the node. Indeed demyelinating SCs have been reported in GBS and CIDP patients (Kim et al., 2019).

1.2.5.3 Humoral immunity

The aberrant production of pathogenic autoantibodies by B-cells, is a widely recognised mechanism in the pathogenesis of immune-mediated neuropathies. Multiple antibodies with specificities to proteins and glycolipid antigens, often shown to target the NoR, have been reported in patients with GBS and CIDP, those with the most convincing pathological relevance being redefined as their own disease entity, as in AINs. The different mechanisms proposed for how antibodies exert might their pathogenic effect include i) promoting cell death through FcγR-mediated responses, either by antibody-dependent cellular cytotoxicity

(ADCC) or antibody-dependent cellular phagocytosis (ADCP), via NK cells or macrophages, respectively ii) cross-linking target antigens which are then internalised, iii) activation of the complement pathway or iv) directly blocking the function of the antigenic target, in the absence of inflammation or complement (Kieseier et al., 2006).

In GBS, antecedent infection is thought to trigger an autoantibody-mediated process in a proportion of patients, though a primary target antigen has not been identified to account for the majority of patients. It has, however, been established that some microbial epitopes structurally mimic endogenous peripheral nerve antigens leading to cross-reactive autoimmune injury. A strong link has been made between the most commonly detected preceding infective agent, *Campylobacter jejuni,* and the development of anti-ganglioside antibodies to GM1 at the node in axonal GBS (Yuki et al., 1990) and GQ1b antibodies in Miller-Fisher syndrome (MFS). Anti-GQ1b in the regional GBS variant MFS is the other most clinically relevant antibody in GBS (Willison et al., 1993), though a wider repertoire of antibodies targeting individual or complexes of gangliosides can be found in half of GBS patients (Rinaldi et al., 2013; Van Den Berg et al., 2014; Willison, 2018). This may in fact be an underestimate, given that there is some evidence circulating pathogenic anti-ganglioside antibody levels may be depleted to below detectable levels in a process of neuronal endocytosis (Cunningham et al., 2016). Further, these can determine, at least in part, the phenotypic variant of GBS (Yuki, 2007).

The pathogenicity of anti-ganglioside antibodies has been substantiated through numerous histological observations in patients and animal models. Patients injected with an experimental ganglioside treatment for pain developed GBS with primary axonal degeneration and IgG anti-ganglioside antibodies (Illa et al., 1995). Immunizing rabbits against GM1 and GD1b gangliosides has also reproduced the motor and sensory ataxic axonal phenotypes of GBS, respectively (Kusunoki et al., 1996; Yuki et al., 2001).

Seminal studies using the AMAN rabbit model proposed a pathogenic mechanism now considered common to most anti-ganglioside-mediated neuropathies (Susuki, Rasband, et al., 2007). Here, anti-GM1 IgG antibodies are deposited at the NoR, and complement activation induces MAC pore formation, axonal calcium influx and protease (i.e calpain)-induced axonal injury. The destruction of sodium (Nav) channels and paranodal architecture ensues, manifesting electrophysiologically as potentially reversible conduction block without typical features of inflammatory demyelination ('reversible conduction failure'; RCF), or left unchecked leading to permanent axonal degeneration with poor prognosis (**Figure 2**). This notion of the NoR being the key site of antibody attack is backed up by pathological studies showing macrophages seen in nerve specimens from AMAN patients (C. Hafer-Macko et al., 1996), though these are within the periaxonal space, not on the SC surface, as in AIDP, and there is no evidence of T-cell deposition, inflammation or internodal demyelination. Similarly, in a patient with MFS and anti-GQ1b antibodies, morphological abnormalities could be seen at the node and paranode, with macrophages evident along the axon, but without other histological features of segmental demyelination (Miller et al., 2014).

This concept led to the suggestion that anti-ganglioside antibody-driven neuropathy should be more accurately reclassified as a 'nodo-paranodopathy' (Uncini et al., 2013). This terminology did not gain much ground, however, until the discovery of more recent antibodies targeting nodal cell adhesion molecules (CAMs) (CNTN1, Caspr1, NF155 and 186) (Delmont et al., 2017; Doppler et al., 2016; Ng et al., 2012; Querol et al., 2013), in which patients shared this electrophysiological hallmark (Uncini & Vallat, 2018).

Anti-ganglioside antibodies of the IgM isotype are additionally associated with the chronic immune-mediated motor (MMN) and sensory ataxic (CANOMAD) neuropathies, again implicating complement-mediated lysis and nodal targeting and/or disruption (Uncini et al., 1993; Yuki & Uncini, 2014). Further, in-vitro studies using stem cell-derived human sensory neurons, show IgM antibodies in CANOMAD may require complement to induce axonal degeneration, though demyelination can occur in its absence (Clark et al., 2017).

In the last decade, evidence for antibody involvement in CIDP seems to be catching up with that for GBS, even discounting the discovery of IgG4 (para)nodal antibodies. In one study, IgG from CIDP patients suspected to have autoantibody-mediated disease (determined by response to PLEX), was used to demonstrate IgG anti-myelin reactivity with complement deposition, and induce demyelination and conduction block in immunized rats (W. X. Yan et al., 2000). Antibodies to either LM1 (abundant myelin glycolipid) or more frequently LM1-containing ganglioside complexes (8%) were also identified in 75 CIDP patients (Kuwahara et al., 2013). Another showed serum IgG and IgM reactivity to myelin in 22% and 3%, respectively, of 94 CIDP patients (J. M. Vallat et al., 2019). For those with available biopsies, simultaneous macrophage-mediated demyelination, but no nodal or paranodal pathology, was seen, suggesting concurrent humoral and cell-mediated mechanisms of nerve injury.

In both GBS and CIDP, response to IVIg and PLEX indicate a likely overlap in cellular and humoral processes. IVIg may induce complement inhibitory effects, enhance IgG elimination, and supress inflammatory mediators (Dalakas, 2002). Clearly this could potentially counter either humoral or cellular pathogenic mechanisms, though may provide variable benefit depending on the stage or severity of disease. PLEX separates out and replaces the plasma, thereby in theory removing pathogenic antibodies and inflammatory cytokines, perhaps preferentially benefitting those with antibody-driven disease. In CIDP, many patients also respond very well to steroids, presumably working on the inflammatory demyelination that occurs in the classic form. It is not clear why these have not been found to be effective in the seemingly acute equivalent, AIDP, or in MMN.

Despite robust animal models, and large body of histological data, the current understanding of the immunopathogenesis of GBS and CIDP has not significantly influenced therapeutic approaches in over three decades. Further studies using human-derived live nerve cell cultures, and clinically accessible tissue

activity surrogate biomarkers in patients are needed to uncover the key, modifiable drivers of immune-mediated attack.

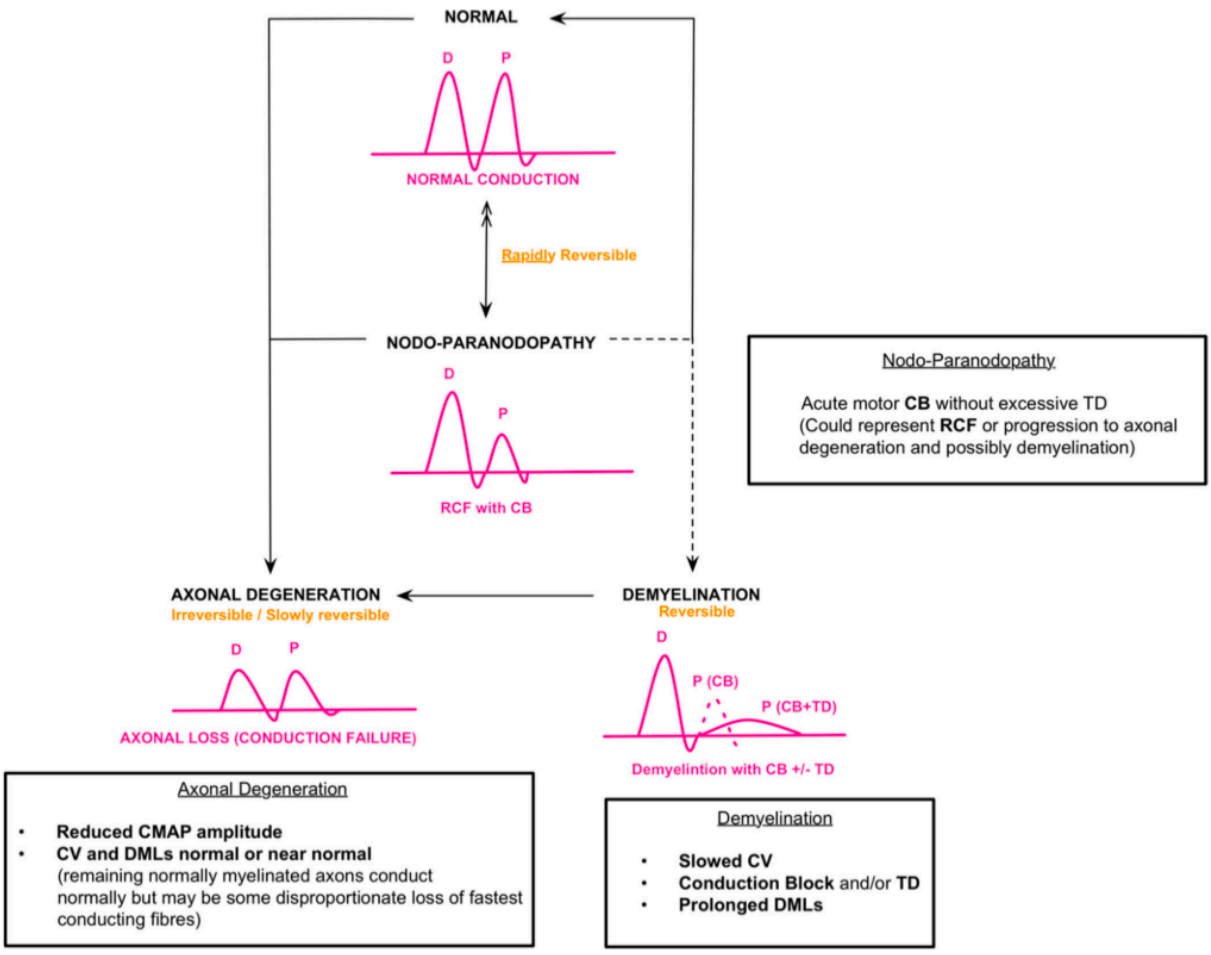


Figure 2: Conduction abnormalities classically seen in nodo-paranodopathies

Suspected evolution of conduction deficits in nodo-paranodopathies (electrophysiological characteristics and appearances in accompanying boxes). CB is defined as a reduction in CMAP amplitude on proximal (P) versus distal (D) nerve stimulation. This has been shown to rapidly revert to normal conduction ('RCF') in some patients, manifesting as rapid clinical improvement and return of the proximal CMAP amplitude to normal. Alternatively, this state could progress to axonal degeneration, revealed by an additional reduction in distal CMAP amplitudes. whether paranodal demyelination or other nodal injury can act as a precursor to classical/segmental demyelination remains to be determined. when such demyelination does occur, reversion to normal conduction can be achieved through remyelination, although over a longer time frame than seen with RCF, and typically in the presence of temporal dispersion (representing differing degrees of myelination and thus conduction velocities between individual nerve fibres). Alternatively, chronically demyelinated axons may subsequently degenerate. The idealised electrophysiological traces represent the waveforms that would be obtained with stimulation both proximally and distally to a site of injury along the intermediate nerve trunk. with pathology at the distal nerve terminal and/or root, this will not be possible, and the electrophysiological findings will be different (see main text for further explanation). CB, conduction block; CMAP, compound muscle action potential; CV, conduction velocity; DML, distal motor latencies; RCF, reversible conduction failure; TD, temporal dispersion.

[Taken from (Fehmi et al., 2018)]

1.3 Specialised regions of the peripheral nerve

The myelination of peripheral nerve neurons by SCs in vertebrates prompts its division into specialised membrane domains, each comprised of a tightly regulated molecular arrangement to ensure efficient saltatory conduction. The NoR are formed at regular intervals, flanked on either side by the paranodal junction (PNJ) and adjacent juxtaparanodal (JXP) regions transitioning to internodal segments consisting of compact myelin (**Figure 3**). Each region is decorated with uniquely organised CAMs which mediate axo-glial interactions. In synergy with cytoskeletal scaffolding proteins, these instruct the localisation of ion channels at the node and JXP, and maintain structural integrity, in turn ensuring the efficient propagation of each action potential (AP). The evolution of super-resolution imaging is strengthening our appreciation of the precision with which molecular alignment in these regions occurs (Appeltshauser et al., 2023; D'Este et al., 2017). Our understanding of dysfunction affecting these regions as a cause or result of disease is deepening, and no doubt will lead to more targeted therapeutic intervention.

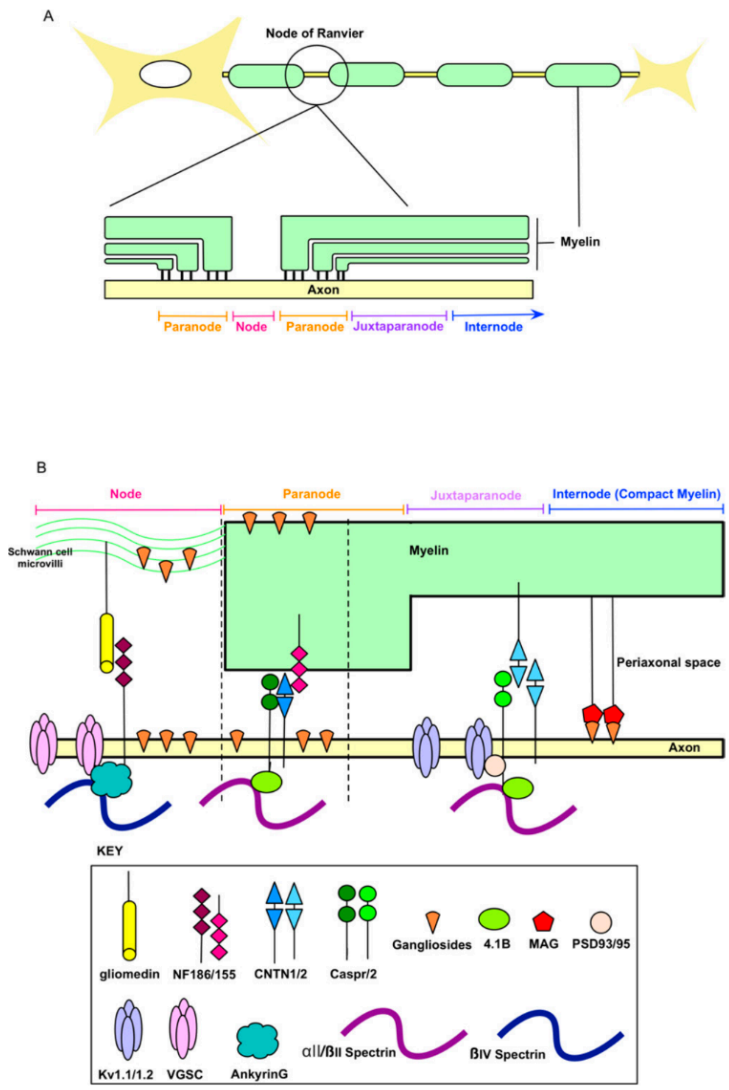


Figure 3: Organisation and structure of myelinated axon domains

(A) *Overview of specialised nodal regions in a myelinated nerve fibre.* ***(B)*** *Molecular components of peripheral nervous system nodes, paranodes and juxtaparanodes. The axonal spectrin cytoskeleton protein mediates binding of ankyrin G to NF186 and vGSCs at the node, 4.1B to the Caspr/ CNTN complex at the paranode, and PSD93/95 with 4.1B to potassium channels at the juxtaparanode (Kv1.1/1.2). Caspr, contactin-associated protein; CNTN, contactin; MAG, myelin-associated glycoprotein (found in non-compact myelin interacting with axonal molecules); NF, neurofascin; , Kv1.1 and 1.2, voltage-gated potassium channels ; vGSC, voltage-gated sodium [Taken from* (Fehmi et al., 2018)]

1.3.1 The Node of Ranvier

The nodes of Ranvier are exposed regions of axolemma, periodically interrupting the compact myelin sheath covering internodal axonal segments. The primary function of the node is to permit rapid depolarisation and propagation of the AP along the axon. This relies on the localisation and clustering of major molecular

components comprising the nodal complex, which include the CAMs NF186 (neuronal form of neurofascin), NrCAM and Gliomedin, voltage-gated Nav channels (in particular Nav1.6), high voltage-activated potassium (Kv) ion channels (Kv3 and Kv7), and cytoskeletal proteins ankyrin G and βIV-spectrin. These act to restrict the nodal intrusion of the PNJ (Thaxton et al., 2011).

During development, NF186 plays a pivotal role in initiating nodal assembly at heminodes (Lambert et al., 1997; Lustig et al., 2001) which form at the end of myelin segments, established through SCs wrapping around axons in multiple layers, and later join to form mature nodes (Vabnick et al., 1996).

NF186 is initially trapped at the nodes from its pre-existing presence in axons (Y. Zhang et al., 2012) through binding to nodal microvilli-secreted components NrCAM and Gliomedin (Eshed et al., 2005; Feinberg et al., 2010). Through the essential recruitment of ankyrin G, ion channels can accumulate and the nodal complex is anchored to βIV-spectrin and the actin cytoskeleton (Dzhashiashvili et al., 2007; Jenkins & Bennett, 2002; Komada & Soriano, 2002; Yang et al., 2004).

1.3.2 The paranodal junction

The PNJs flank the node on either side, marking the ends of each myelin segment, and are the point at which the glia are most closely apposed to the axon. The development of the PNJs provide additional support in nodal assembly and Nav channel clustering, which, even in the absence of NF186, may be sufficient to rescue nodal architecture in the mature node (Amor et al., 2017; Feinberg et al., 2010). The PNJ functions as a diffusion barrier, separating ion channels at the node to those in the JXP, and restricting the lateral movement of axolemmal molecules between domains (Bhat, 2003; C. Zhang et al., 2013). The PNJ is characterised by cytoplasmic loops extending from myelinating SCs, closely spiralling around the axon, known as septate-like junctions. These are tightly adhered to the axolemma by specialised CAMs – a cis-complex of CNTN1 and Caspr1 (Einheber et al., 1997; Peles et al., 1997), interacting in trans to glial-

anchored protein NF155. Caspr1 is bound to 4.1B in the axonal cytoplasm, which in turn anchors the complex to cytoskeletal protein αII/βII spectrin complex (Ogawa et al., 2006).

The integrity of the septate like junctions depend on the presence and interaction of NF155, CNTN1 and Caspr1, their absence in mouse models causing the invasion of Kv channels into the paranode and resulting in conduction defects (Bhat et al., 2001; Boyle et al., 2001; Garcia-Fresco et al., 2006; Pillai et al., 2009).

There is also a strong body of evidence suggesting the complementary role of sulfatides and gangliosides in maintaining the stability of the nodal domains, with deficiencies leading to structural, electrophysiological and clinical abnormalities (Dustin et al., 2023; Ishibashi et al., 2002; McGonigal et al., 2019; Susuki, Baba, et al., 2007). In particular, the extracellular portion of NF155, but not NF186, preferentially binds in *cis* with sulfatides, an interaction essential to its association with lipid rafts and stability within the membrane (McKie et al., 2022).

1.3.3 The Juxtaparanode and compact myelin

The JXP region adjoins the PNJ to the internodal segment, located beneath compact myelin. Low voltage-activated shaker type potassium channels (Kv1.1/Kv1.2) are restricted from the PNJ to JXP regions, regulating refractory repolarisation and maintaining the resting potential of the axonal membrane. These are stabilised in complexes with CAMs contactin-associated protein 2 (Caspr2) on the axonal membrane, and contactin-2 (also known as transient axonal glycoprotein 1; TAG1) in both axonal and glial membranes (Poliak et al., 2003), and further anchored to the axonal spectrin cytoskeleton through scaffolding proteins (PSD93/95 and 4.1B). The ADAM23 protein however, is thought to be the key driving force in the formation and maintenance of Kv1 channel complexes (Kozar-Gillan et al., 2023).

1.4 The Autoimmune Nodopathies

1.4.1 Emerging antibodies targeting antigens at the node and paranode

A new clinical diagnostic category, termed autoimmune nodopathies (AIN), has recently been established, and defines a group of phenotypically distinct antibody-mediated neuropathies by the primary site of autoimmune attack. This avoids the dichotomous, and potentially premature classification of neuropathy subtypes into demyelinating or axonal. This group specifically refers to a peripheral neuropathy associated with antibodies targeting nodal or paranodal CAMs (CNTN1, NF155, NF186, Caspr1), previously encompassed under the umbrella term CIDP.

The new terminology is not inclusive of those with anti-ganglioside antibodies, which originally prompted the use of the term ‘nodo-paranodopathies’, however. This is likely to provide clarity that the detection of nodal and paranodal ((para)nodal) antibodies is diagnostic for an AIN, in contrast to the detection of anti-ganglioside antibodies in GBS, and crucially informs the use of alternative therapies.

This reclassification has importantly shifted the approach to managing patients with acute or subacute disabling neuropathies who are less responsive to standard therapies, such that the national and international guidelines now support the early use of Rituximab (RTX), a B-cell depleting therapy, for these patients (Van den Bergh et al., 2021). It has also provided a renewed interest in pathogenic mechanisms targeting the NoR in immune-mediated neuropathies, and reignited the search for other novel, potentially pathogenic antibodies that are likely to account for a proportion of GBS and CIDP patients who could further benefit from alternative treatments.

Just over a decade ago Devaux *et al* detected autoantibodies targeting the node and paranode of rodent nerves in up to 30% of patients with GBS (both AIDP and AMAN) and CIDP (Devaux et al., 2012). Further, their sera specifically contained antibodies that bound selectively to the CAMs NF186, CNTN1, or

gliomedin. Although the node had already been implicated in axonal GBS, it was only after this study, and subsequent identification of antibodies targeting (para)nodal CAMs that the term ‘nodo-paranodopathy’ started to gain popularity. Since this time, antibodies to NF155, CNTN1, Caspr1 and NF186 (usually with cross-reactivity to NF155, termed ‘PanNF’) have been reported in an increased number of patients initially diagnosed with GBS or CIDP. The presence of anti-gliomedin antibodies could not be reproduced in subsequent studies (Delmont et al., 2017).

1.4.2 Overview of phenotypic characteristics

1.4.2.1 Clinical and serological

As a group, patients with AIN are reported to present with an acute or subacute-onset motor predominant or sensory ataxic symmetrical, non-length dependent polyneuropathy. They are often initially diagnosed with GBS given the aggressive onset, or CIDP once they show a more chronic course, as evidenced by these antibodies consistently being reported in patients diagnosed with such conditions. What distinguishes them from these two disorders, however, are the additional features infrequently associated with GBS, and rarely, if at all, with CIDP. These most commonly include ataxia (sensory or cerebellar), tremor, cranial nerve palsies, respiratory and/or autonomic failure. Crucially, they are poorly responsive to standard immune-suppressive and -modulatory therapies (steroids, IVIg and PLEX). They are phenotypically distinct as a group, though specific clinical features to each antibody group are beginning to emerge in the literature.

The demographic profile of reported cohorts are most often in keeping with adult patients in the 4th-6th decade in life and there is a male preponderance. However, there have been paediatric cases (Burnor et al., 2018; De Simoni et al., 2020; Delmont et al., 2017; R. E. Harris et al., 2023), and with increasing awareness their detection will no doubt increase in frequency. Most international studies report a variable prevalence, but (para)nodal antibodies are probably found in up to 10% of patients with a suspected immune-mediated neuropathy, (Delmont et al., 2020; Doneddu et al., 2018; Martín-Aguilar, Lleixà, & Pascual-Goñi, 2022; Shelly et al., 2021), though have been reported in as high as 18% (Ogata et al., 2015).

Antibodies to (para)nodal antigens were initially, and are still most commonly, reported to be predominantly of the IgG4 subclass, some with lesser reactivity to other subclasses (Miura et al., 2015). However, more recent studies have identified some AIN patients with antibodies that are IgG3 predominant (Appeltshauser et al., 2020; Doppler et al., 2015, 2019; Stengel et al., 2019), with the potential to switch to IgG4 in the more chronic disease phase (Appeltshauser et al., 2020).

The utility of cerebrospinal fluid (CSF) analysis in AIN has not yet been determined. When CNS demyelination has been found in patients with NF155 seropositive AIN, antibodies can be detected in serum and CSF (Kawamura, 2015), and in one of three patients with serum panNF antibodies, CSF antibodies were eventually detected after 6 months (Stengel et al., 2019). CSF protein levels are typically markedly elevated in AIN patients, less so in panNF seropositive patients (Appeltshauser et al., 2022; Stengel et al., 2019). Patchy testing and reporting on CSF analysis, as well as variable timings of lumbar punctures, however, limits the conclusions that can be drawn about the significance of this.

Imaging of the nerve roots using MRI or ultrasound, as in other immune-mediated neuropathies, show thickening and enhancement with contrast of the nerve roots, in particular in anti-NF155 antibody seropositive AIN patients (B. Liu, Zhou, et al., 2023; Ogata et al., 2015).

The most notable shared characteristic amongst this group is the incomplete or only partial/transient response to traditionally used 1st line therapies for inflammatory neuropathies, IVIg in particular. Aggressive and repeated therapy with standard immunosuppressive agents is usually required to achieve at least transient responses, but near complete and sustained recovery requires escalation of immunomodulatory treatment, in most instances RTX has been used (Querol et al., 2015).

Steroids are often used in AIN patients, with reports of moderate but usually transient responses. PLEX has shown good but usually only transient response (A. Davies et al., 2020). Both steroids and PLEX can be

used alongside, or before RTX treatment, respectively, which has consistently been shown to be the most successful agent in treating patients with AIN (Delmont et al., 2020; Dubey et al., 2020; Jiao et al., 2020; B. Liu, Hu, et al., 2023; Martín-Aguilar, Lleixà, Pascual-Goñi, et al., 2022; Pascual-Goñi et al., 2021; Querol et al., 2015; Shelly et al., 2021). The factors determining it's efficacy, however, are not well understood. Further, RTX pre-treatment with PLEX has not so far been proven to be of additional benefit (Martín-Aguilar, Lleixà, Pascual-Goñi, et al., 2022).

As the study of (para)nodal antibody-mediated disease is in its infancy, rates of relapse and longer-term outcomes of AIN patients are only beginning to be reported. Shelly *et al* reported on the outcome of a large cohort of anti-NF155 antibody seropositive patients after at least 5 years follow-up (Shelly et al., 2021). In this group, almost half of patients showed a relapsing course, and relapses were more likely in those with a longer time from onset to treatment and more disability at onset. This was also linked to higher morbidity than those who had not relapsed. At 1 year half of the patients required assistance to mobilise. There was a mortality rate of 12%, although it did not seem the deaths were directly caused by the neuropathy. In another cohort of 40 anti-NF155 antibody seropositive patients, followed up at a median of 3.8 years, mortality rate was 7.5%, and, similar to Shelly *et al*, 75% of those who received RTX (after prior failed therapies) achieved a good outcome (Martín-Aguilar, Lleixà, Pascual-Goñi, et al., 2022).

In contrast, in another study of 11 panNF patients, although morbidity and mortality (18%) was high, even without receiving RTX, three quarters of patients achieved remission or stability (Appeltshauser et al., 2022). The five who had B-cell depleting therapy had a good outcome (max 2 years), and this reversibility from severe disability to functional independence occurred despite many months between onset and RTX treatment.

To more accurately ascertain and compare treatment responses and long-term outcome, prospective studies, ideally in a controlled trial setting, and clearer, shared definitions of what constitutes ‘good’ outcome are clearly needed.

1.4.2.2 Electrophysiology

In general, neurophysiological studies can aid in the classification of GBS as ‘demyelinating’ or ‘axonal’ (Hadden et al., 1998), and are now mandatory in the diagnosis of CIDP, whereby specific criteria must be met in addition to clinical suspicion for a formal diagnosis (Van den Bergh et al., 2021). Slowed conduction velocity (CV), prolonged distal motor latencies (DML), delayed or absent f-wave latencies, and conduction block (CB) are typically associated with inflammatory segmental demyelination. Temporal dispersion (TD) of compound muscle action potentials (CMAPs) is thought to be the electrical correlate of the reparative process of demyelination/remyelination. Reduced CMAPs, with no or very little slowing of CV and DMLs, traditionally signifies axonal degeneration.

The idea of reversible conduction failure (RCF) in motor nerves, whereby CB can be seen without TD of CMAPs (termed ‘axonal’ CB) and rapidly reversed, avoiding subsequent axonal degeneration, was introduced as the mechanism by which patients with ‘axonal’ GBS could demonstrate rapid clinical recovery (Uncini & Kuwabara, 2012). This became known as the pathological correlate of antibodies binding and disrupting the nodal axolemma, aptly named ‘nodo-paranodopathy’ (**Figure 2**). Thus, early CB could be functional in nature and actually reversed, or alternatively progress to axonal degeneration, felt to indicate a poor prognosis. Thereafter, the relevance of serial nerve conduction studies to more accurately phenotypically classify cases of GBS became apparent (Rajabally et al., 2015).

Although there are no unequivocal electrodiagnostic features which confirm a diagnosis of AIN, conduction abnormalities in this group can mimic classic demyelinating neuropathies, almost always meeting the electrodiagnostic criteria for demyelinating GBS or CIDP. Importantly, even in these cases, corresponding

histological analysis of their nerve biopsies do not show classical segmental demyelination, but more subtle nodal and paranodal structural abnormalities (Koike et al., 2017; Manso et al., 2016). Serial neurophysiological studies can of course go on to show progressively reduced CMAPs, indicative of the eventual axonal loss that can ensue if CB is not reversed. Early denervation can also be seen, particularly in anti-CNTN1 or anti-Caspr1 antibody seropositive patients (Pascual-Goñi et al., 2021; Querol et al., 2013). Even in cases of axonal degeneration, complete clinical recovery is still possible (B. Liu, Hu, et al., 2023). Interestingly, in an Caspr1 antibody seropositive case who did have evidence of TD, their nerve biopsy showed axonal degeneration, not demyelination (Doppler et al., 2016). Taken together, these limited data exemplify the pitfalls in relying on a single diagnostic modality, or indeed a single electrophysiological study, to confine patients to phenotypic classifications too early.

Further, the neurophysiological identification of a ‘nodo-paranodopathy’, although important prognostically, may be made more challenging by the difficulty in picking up CB in a proportion of patients who have nodal pathology concentrated at distal nerve terminals, or proximally at the roots. This is because these sites are particularly vulnerable to injury from circulating antibodies and complement (McGonigal et al., 2010), and the detection of CB requires electrical stimulation proximally and distally to the site of injury, which may not be possible in these cases.

Despite parameters that suggest RCF, there are no reliable associations to serological status, or electrophysiological features that distinguish between specific antibodies. However, recent electrophysiological data comparing 40 seronegative CIDP to 22 AIN patients suggested conduction abnormalities were more pronounced in the latter, and cut-offs for specific parameters were predictive of seropositivity to antibodies targeting the NoR (Kouton et al., 2020).

1.4.3 Clinical and serological characteristics of individual nodal and paranodal antibody cohorts

1.4.3.1 Neurofascin-155

Patients with anti-NF155 antibody seropositive AIN constitute the largest cohort of AIN patients reported in the literature, with a particularly high frequency of up to 20% in Asia (Ogata et al., 2015; X. Zhang et al., 2019). These patients are typically younger males, in their 2nd to 5th decade, with a subacute onset, distal and motor predominant polyradiculoneuropathy, associated with sensory ataxia, tremor, rarely combined central and peripheral demyelination (CCPD), with a poor response to IVIg in particular, and significantly improved outcomes with RTX (Burnor et al., 2018; Devaux et al., 2016; Gupta et al., 2023; B. Liu, Zhou, et al., 2023; Martín-Aguilar, Lleixà, Pascual-Goñi, et al., 2022; Ogata et al., 2016; Querol et al., 2014, 2015; Vural et al., 2018; X. Zhang et al., 2019).

In an early study testing 394 serum samples from patients with inflammatory neuropathies for neurofascin antibodies (Ng et al., 2012) two patients were found to have antibodies with strong reactivity to NF155 using enzyme-linked immunosorbent assay (ELISA) and cell based assays (CBA), and were predominantly of the IgG4 subclass. Interestingly they describe another 2 patients, from whom sera initially tested positive only for NF155 on ELISA and were of IgG3 or IgG1 subclasses, but one of which went on to test positive for both NF186 and 155 isoforms (panNF) after immunoprecipitation was performed to purify the antibodies. This illustrates, during earlier reports, that NF155 monospecific antibody-positive patients may have in fact had reactivity to both isoforms, but due to lack of or limited testing modalities used did not detect the antibodies reactive to NF186.

Following this, a further two patients were identified through screening a small Spanish CIDP cohort, with severe, predominantly distal weakness, and refractory to IVIg treatment (Querol et al., 2014). Prompted by this they were able to identify a further two NF155 antibody seropositive patients from another cohort of CIDP patients, specifically selected for being IVIg non-responders. All were predominantly IgG4, with low

concentrations of IgG2. Notably, these patients had disabling tremor, with some cerebellar features. Their antibodies not only stained paranodes, as in the earlier study conducted by Ng *et al*, but additionally rat cerebellum. Subsequent studies confirmed this CNS and PNS reactivity (Kawamura, 2015; Ogata et al., 2016), which to date has not been shown in the other antibody groups.

The largest report to date characterising NF155 positive AIN patients describes a Japanese cohort of 48 seropositive patients, of the IgG4 subclass in 38, IgG3 in 1, and the remainder of an indeterminate IgG subclass (Devaux et al., 2016). These confirm the clinical phenotype already described, notably being younger males, with sensory ataxia and cerebellar features, though fewer had demonstrable CNS demyelinating lesions, though the majority did not respond to IVIg.

Another substantial cohort of NF155 positive AIN patients is characterised by Martín-Aguilar and Lleixà *et al*, who describe 40 patients with IgG4 NF155 antibodies and a severe, progressive symmetrical sensorimotor neuropathy fulfilling criteria for CIDP (Martín-Aguilar, Lleixà, Pascual-Goñi, et al., 2022). Approximately three quarters had additional tremor and/or ataxia, and a third cranial nerve deficits. Almost all patients were treated with IVIg and/or steroids, half with PLEX and over half with RTX, with good response rates considered to be 13%, 28%, 39% and 77% in these respective groups.

Although there have been reports of favourable response to steroids and PLEX in some NF155 patients (Kadoya et al., 2016; Ng et al., 2012) these are often transient, and RTX has led to a much more sustained good response (Demichelis et al., 2018; Jiao et al., 2020; B. Liu, Hu, et al., 2023; Martín-Aguilar, Lleixà, Pascual-Goñi, et al., 2022; Querol et al., 2015; Shelly et al., 2021).

In addition to minor contributions from IgG1-3 subclasses usually reported, IgM NF155 antibodies have specifically been found in patients with idiopathic, genetic and inflammatory neuropathies

(Burnor et al., 2018; Doppler et al., 2018; Shelly et al., 2021). They can share some similar features to NF155 IgG4 patients, though do not adhere to the distinct phenotype described above i.e they respond more favourably to IVIg. More investigation into their prevalence within larger cohorts of neuropathy patients, and those with IgG antibodies, will be important in determining their clinical and pathological relevance.

1.4.3.2 Pan-neurofascin and Neurofascin-186/140

The glial/paranodal (NF155) and neuronal/nodal (NF186 and NF140) isoforms of neurofascin in the PNS are composed of almost identical extracellular domains. There are six shared immunoglobulin domains, and between 3-4 fibronectin III (FnIII) domains. NF155 has a FnIII domain (Fn3-Fn4), not present in either NF186 or NF140, and appears to be the target epitope in patients with monospecific anti-NF155 antibodies (Delmont et al., 2017; Ng et al., 2012; Stengel et al., 2019). NF186 shares the configuration of 3 FnIII domains with NF140 but has an additional FnIII and mucin domain (Mucin-Fn5), which is likely the target for NF186 antibodies (Ng et al., 2012).

Following the identification of anti-NF186 IgG antibodies in a rat model of GBS (Lonigro & Devaux, 2009), the earliest report of IgM or IgG antibodies targeting NF186 at the node in humans was over a decade ago, in eight patients mainly with the AMAN variant of GBS (Devaux et al., 2012).

Delmont *et al* went on to characterise the clinical phenotypes of 5 patients in whom antibodies mainly targeting NF186 and NF140 were detected, with lesser reactivity to NF155 (Delmont et al., 2017). Interestingly, by ELISA, the serum IgG from 4 patients had reactivity to all three isoforms, and 1 patient showed reactivity to only NF186, suggesting different target epitopes, and probably a variety within this cohort of 'PanNF' reactive and NF186 monospecific sera. Nevertheless, the IgG from all 5 patients bound nodes in teased nerve fibres, compared to the IgG from patients with anti-NF155 monospecific antibodies in the same study, which bound the paranodes. Due to these nodal-predominant binding patterns, the 5 patients were referred to as NF186/140 antibody positive. In comparison to previously reported cohorts of NF155

and seronegative CIDP patients, the five anti-NF186/140 antibody patients had a more severe neuropathy, in two patients requiring mechanical ventilation in intensive care. There was a higher incidence of cranial nerve deficits, and despite most also having sensory ataxia, as in NF155 patients, none had tremor. This was also the first time associated conditions had been reported in the AIN group, notably nephrotic syndrome, and IgG4-mediated retroperitoneal fibrosis. Their neurophysiological profile was representative of AIN patients in general i.e. demyelinating with CB, or axonal. Uncharacteristic for this group, 3 were reported to respond well to IVIg (although one also had steroids and RTX), and two others to steroids. One of the most severely affected patients, with antibodies targeting all three isoforms, had predominantly IgG3, rather than IgG4, antibodies. A subsequent study described another similarly affected patient, again requiring mechanical ventilation, also with IgG3 panNF antibodies with strong reactivity to nodes (J. M. Vallat et al., 2018). In both cases IVIg was felt not to be of benefit, and went on to receive PLEX and steroids with good effect.

In another study, 3 PanNF AIN patients were described, again with IgG3 antibodies, targeting NF186 and NF155 (Stengel et al., 2019). Patients notably had a fulminant disease course characterised by an acute-onset quadriplegia with associated features (except one with low antibody titre) including cranial neuropathies, autonomic dysfunction and respiratory insufficiency requiring mechanical ventilation. One patient died, and the others partially and completely recovered with steroids and PLEX, respectively. Antibodies from patient sera bound both nodes and paranodes in murine teased fibres, in contrast to Delmont *et al* who found only nodal staining in their NF186/140-predominantly reactive cohort (Delmont et al., 2017). Interestingly, upon pre-incubation of the panNF sera with NF155-transfected cells, all (para)nodal staining was abrogated, but pre-incubation with NF186-transfected cells left weak residual paranodal staining, indicating the presence of antibodies with varying epitopes rather than one shared target. In keeping with this, using binding assays of truncated neurofascin mutants, all 3 patients' antibodies targeted the shared Ig domains, with one patient having additional reactivity to the Fn3 domain specific to NF155.

The largest data set of panNF AIN patients has been described by Appeltshauser *et al*, in whom predominantly IgG3 and IgG4 antibodies to all three neurofascin isoforms were detected in 11 patients, in comparison to patients with anti-NF155 antibodies, with mostly IgG4 and IgG2 (Appeltshauser et al., 2022). Patients presented with an aggressive-onset, symmetrical, proximal and distal, predominantly motor neuropathy with a monophasic disease course, with less frequently reported sensory ataxia and tremor than the NF155 antibody-positive patients in the same cohort, but significantly more frequent cranial neuropathies and autonomic/respiratory dysfunction and greater disability scores. Both antibody groups responded similarly to treatments, with poor or unsustained responses to IVIg and steroids, a slightly more favourable initial, but again unsustained, response to PLEX in the NF155 group, and induction of clinical and serological remission using repeated doses of RTX. Of note, 3 panNF patients went into remission without B-cell depleting therapy.

Most recently, another group of AIN patients with neurofascin antibodies have been reported at a high frequency (17%) in China, with the highest number of patients (13) harbouring antibodies monospecific to NF186 to date, as well as 20 with a NF155 positive AIN, and no panNF positive patients (B. Liu, Zhou, et al., 2023). The NF186 monospecific group differed from those with anti-NF155 antibodies, with a more acute onset and minimal sensory ataxia and tremor. However, they did not replicate the severe phenotype of panNF patients, and lacked the additional features i.e. cranial neuropathies, autonomic/respiratory. Both NF186 and NF155 patients responded well to RTX, reasonably to PLEX, and neither to IVIg. But the NF186 group responded more favourably to steroids. Serologically IgM, in addition to IgG, could be detected in one patient, and IgG subclass could only be characterised in under a third, mainly IgG1-3.

1.4.3.3 Contactin-1

Anti-CNTN1 antibodies were initially identified in a handful of GBS and CIDP patients (Devaux et al., 2012), and clinical characteristics of anti-CNTN1 seropositive patients originally reported by Querol *et al* as having an acute onset, severe, distal-predominant motor neuropathy with sensory ataxia and poor response

to IVIg in older (6th-7th decade) male patients (Querol et al., 2013). Subsequent descriptions of anti-CNTN1 patients have largely echoed this phenotype, though several other cohorts have brought to light some additional features, such as nephrotic syndrome caused by membranous glomerulonephritis (MGN) (Delmont et al., 2020; Miura et al., 2015; Taieb et al., 2019), and paraproteinaemic or oncological associations (Dubey et al., 2020).

Compared to anti-NF155 antibody AIN, cranial nerve involvement (Delmont et al., 2020) has been reported more frequently, and tremor (Cortese et al., 2020; Delmont et al., 2020) less frequently but more than in seronegative CIDP cases. A few patients have even presented similarly to a purely sensory ataxic variant of CIDP (CISP) (Dubey et al., 2020). As with the other antibody groups, IVIg has consistently been ineffective in patients with IgG4 anti-CNTN1 antibodies, though more favourable in isolated cases where IgG3 is the predominant subclass in the acute phase (Doppler et al., 2015, 2017). Steroids and PLEX can be effective but rarely lead to sustained recovery, and as in other AIN patients, RTX or second-line immunomodulation (cyclophosphamide and azathioprine) has been shown to induce remission (Delmont et al., 2020; Dubey et al., 2020).

1.4.3.4 Caspr1 and Contactin-1/ Caspr1 complex

Antibodies to Caspr1 are the less frequently observed, and even fewer patients have antibodies reactive to the CNTN1/Caspr1 complex but neither antigen individually (Pascual-Goñi et al., 2021; Querol et al., 2013). Clinical features appear to be similar between these groups and those with anti-CNTN1 antibodies, with a GBS-like presentation, severe predominantly motor deficit, with a higher rate of sensory ataxia and neuropathic pain. Unlike the other (para)nodal antibody subgroups, Caspr1 or CNTN1/caspr1 antibody-positive patients have been found to harbour IgG2 or 3 subclass antibodies, particularly at disease onset, which may have a favourable response to IVIg (Appeltshauser et al., 2020).

The earliest reports of sera containing antibodies monospecific to Caspr1 was in 2 patients presenting with an acute and subacute sensorimotor polyradiculoneuropathy, being notable for the severe neuropathic pain as a distinguishing feature from other antibody groups (Doppler et al., 2016). Both achieved remission, one patient responding to treatment with PLEX, the other more resistant to first line therapy and requiring RTX. These patients had IgG3 anti-Caspr1 antibodies. Similarly, in a further study, 4 patients were found to have IgG2 or IgG3 antibodies to either Caspr1 alone or the CNTN1/Caspr1 complex, and developed a moderate to severe quadriparesis with dominant sensory symptoms in a few, and all notably with neuropathic pain (Appeltshauser et al., 2020). Interestingly 2 out of 4 patients responded well to IVIg, and the other two improved with PLEX.

1.4.3.5 LGI4 and juxtaparanode (JXP) associated neuropathies

Antibodies targeting Caspr2 at the juxtaparanode have been described in large cohorts of patients with more varied neurological phenotypes, typically presenting with peripheral nerve hyperexcitability (e.g fasciculations/cramps), alone or in a syndrome with other features of 'neurological irritability' i.e. neuromyotonia, seiuzures, limbic encephalitis, insomnia and dysautonomia (Lancaster et al., 2011). Caspr2 autoimmunity in patients manifesting with these predominantly CNS phenotypes are well recognised now and are shown to have antibodies against caspr2 alone or as part of a Kv channel complex with LGI1 (Leucine-rich, glioma inactivated 1 protein) (Binks et al., 2018; Irani et al., 2010; Klein et al., 2012, 2013; Lancaster et al., 2011; van Sonderen et al., 2016).

Confirmed sensorimotor polyneuropathy has been reported in 17% of an anti-Caspr2 antibody positive patient cohort (Klein et al., 2013). Individual reports associate Caspr2 antibodies with GBS-like presentations with variable response to standard treatments (Rosch et al., 2014; Tüzün et al., 2013). However, anti-caspr2 autoantibodies have not yet been linked to a distinct neuropathy phenotype.

There has been even less light shed on contactin-2 as a potential antigenic target, though interestingly IVIg responsiveness in CIDP patients have been linked to single nucleotide polymorphisms within the gene encoding contactin-2, potentially implicating it as a significant contributory molecule (Iijima et al., 2009).

In the last year, IgG4 autoantibodies targeting the juxtaparanodal protein LGI4 (Leucine-rich, glioma inactivated 4 protein) have been found by one group in four CIDP patients, with a subacute sensorimotor polyneuropathy (X. Zhang et al., 2023).

1.4.4 Pathogenicity of (para)nodal antibodies

Despite many shared clinical features between the AINs, there is evidence that the pathomechanisms for each antibody subgroup differs. To date, CNTN1 and NF155 antibodies have the strongest level of evidence to confirm pathogenicity (Doppler et al., 2019; Manso et al., 2016, 2019). Ultrastructural analysis from human biopsy specimens, and in vitro studies provide additional data, though passive transfer animal models are lacking for Caspr1 and NF186/PanNF antibodies.

1.4.4.1 Evidence of pathogenicity (overview)

Clinical and serological observations gathered from AIN patient cohorts so far adheres to a distinct clinical phenotype, with a high specificity of (para)nodal antibodies (Rinaldi et al., 2022), as well as antibody titres paralleling disease activity, falling to undetectable levels in line with clinical remission (Appeltshauser et al., 2020, 2022; Delmont et al., 2017; Querol et al., 2015). It therefore seems reasonable to assume these antibodies are pathogenic.

In line with this, there is existing data to suggest that if these specific antigenic targets underwent genetic ablation, or were absent during development, nodal and paranodal architecture is disrupted, interrupting saltatory conduction and causing severe clinical neurological deficit (Bhat et al., 2001; Boyle et al., 2001; Garcia-Fresco et al., 2006; Pillai et al., 2009; Taylor et al., 2017; Thaxton et al., 2011).

Further supporting pathogenicity of these (para)nodal antibodies are ultrastructural studies of sural nerve biopsies from patients with AINs, which reveal the pathological process (and IgG4 deposition) to be limited to the node and paranode, with the most characteristic features being axo-glial dismantling and paranodal loop detachment, and the absence of overt macrophage mediated inflammatory demyelination (Koike et al., 2017). Loss of myelinated fibres in more chronic cases, endoneurial oedema and axonal degeneration are also frequently seen (Koike et al., 2017; Ogata et al., 2015). Morphological alterations can also be seen at the node (elongation) and paranode (loss of NF155 and caspr1 staining) of myelinated fibres in skin biopsies of patients with AINs (Cortese et al., 2020). It should be noted, however, that similar morphological changes can be seen in skin biopsies from patients with demyelinating neuropathies (Doppler et al., 2013).

1.4.4.2 Neurofascin 155

Ng *et al* provided the first supportive data of NF155 antibodies from patient sera binding to paranodes and co-localising with Caspr1 in rat spinal cord tissue (Ng et al., 2012). They and another group also mapped the epitopes recognised by NF155 seropositive patients, concluding that the majority bind to the FNIII domains (Devaux et al., 2016). Devaux *et al* further demonstrated peripheral paranodal binding of IgG4 from the sera of 38 anti-NF155 antibody-positive patients on teased fibres, and also antibody staining of murine brain tissue (3 of these patients had clinical evidence of additional central demyelination). In line with several other studies, compared with seronegative CIDP control patients, sural nerve biopsies from AIN patients revealed no evidence of inflammatory cell infiltrates or macrophages, and only occasional demyelination in the presence of extensive axonal degeneration (Koike et al., 2017; Ogata et al., 2015; J.-M. Vallat et al., 2017). In particular, widening of the NoR, the absence of septate-like junctions located at the paranodes, and terminal myelin loop detachment from the axon were reported, and suggested NF155 antibodies significantly disrupted the paranodal barrier (Koike et al., 2017; J.-M. Vallat et al., 2017, 2019).

In a passive transfer animal model, anti-NF155 IgG4 antibodies isolated from patients were shown to exert a direct pathogenic effect on NF155 formation in vivo (Manso et al., 2019). Firstly, in vitro and in vivo exposure of rat sciatic nerve to IgG4 NF155 antibodies showed IgG binding to surface antigens on the glial surface at Schmidt-Lanterman incisures (previously known) and what was likely the Schwann cell microvilli overlying the node (new data). Further, IgG did not penetrate or alter the paranodal domain, even after prolonged exposure. Secondly, by injecting the antibodies in neonatal and adult animals, before and after node/paranode formation, respectively, they showed that depletion of NF155 occurred in both instances, but formation of septate like junctions of the paranodal myelin loops was significantly reduced only in neonatal rats. However, after repeated injection in mature rats, the stability of the paranodal junction was eventually compromised. Finally, the animals injected with patient antibodies developed clinical deficits and conduction abnormalities replicating some of those seen in patients. Despite suspicions that the IgG4 antibodies may exert their effect by blocking the axo-glial complex (Manso et al., 2016), this study confirmed, by the in vivo assays, and an in vitro cell aggregation assay, that the interaction between NF155 and CNTN1/Caspr1 was not affected, but rather the NF155 was clustered and depleted.

These findings were further supported by a very recent study, which found NF155 IgG bound to the node more than the paranode of rat sciatic nerve after incubation in vitro, or intrathecal injection in vivo, though only if repeated (Hecker et al., 2023). This paralleled a clinical phenotype resembling patients with AIN.

Shedding light on a potentially significant determinant of pathogenicity, a recent study investigated whether the unique characteristic of IgG4 antibodies being able to exchange it Fab arms (Fab-arm exchange; FAE) is contributing to the pathogenicity of (para)nodal antibodies (Jentzer et al., 2022), as is the case in some cases of myasthenia gravis with IgG4 antibodies to muscle-specific kinase (MuSK) (Huijbers et al., 2019). IgG4 are initially monospecific and bivalent for a target antigen but can undergo a process of random exchange of their fragment antigen-binding (Fab) arms. Initially, Jentzer *et al* established that NF155 AIN patients have variable levels of monospecific IgG4 antibodies, and these correlated with titres of anti-NF155 IgG4

antibodies in patient sera. They generated in vitro either bivalent (and monospecific) or monovalent (and bispecific) IgG4 antibodies from 2 NF155 AIN patients, and alongside native anti-NF155 IgG4 antibodies from the same patients, injected these into rats. After 2 days they observed that the native and the bivalent antibodies markedly impaired paranode formation upon teased nerve fibre immunostaining, but the monovalent antibodies did not, similar to controls (Jentzer et al., 2022).

1.4.4.3 Pan-neurofascin and neurofascin 186

Animal neurofascin 186 IgG and IgM have already been demonstrated to worsen neuritis in animal models of EAN (Ng et al., 2012; W. Yan et al., 2014), as well as cause axonal injury in CNS disease models (Lindner et al., 2013; Mathey et al., 2007). This supports the potential of panNF or NF186 antibodies to be pathogenic in humans, though passive transfer animal models are lacking.

Using human NF186 or panNF-reactive IgG, pathogenicity has so far only been implicated through the analysis of patient nerve biopsy or in vitro studies. Although in the original report of patients with panNF antibodies there was no study of pathogenicity, the authors speculated that these antibodies, which bound predominantly to the node (in comparison to NF155 antibodies which bound to paranodes), would exert any pathogenic effect to the nodal complex (Delmont et al., 2017). Avid nodal binding in teased nerve was corroborated in a subsequent study using the serum of a NF140/186 IgG3 antibody-positive patient, additionally associated with nodal complement deposition (J. M. Vallat et al., 2018). Ultrastructural analysis of their sural nerve further supported nodal, but not paranodal, alterations notable for the absence of Schwann cell microvilli, replaced with cytoplasmic extensions from adjacent SC processes occluding the nodal gap, which has been consistently demonstrated in two subsequent studies (Appeltshauser et al., 2022; B. Liu, Zhou, et al., 2023).

In contrast, more recent in vitro analysis of the pathogenicity of panNF antibodies has shown more extensive pathogenic effects on the nodal, as well as paranodal domains (Appeltshauser et al., 2022). Serum and

purified IgG incubation assays to live myelinated neurons from 4 seropositive patients were performed during and after myelination. In both conditions, the number of intact nodes was significantly reduced, and those remaining were elongated with dispersion of nodal proteins; caspr1 and NF155 proteins lost leading to dismantling and shortening of the paranodes in the panNF group, compared to anti-NF155 positive patient sera and healthy controls. Again complement was potentially implicated in the pathomechanism of panNF antibodies as C1q fixation in ELISA and CBA, inducing toxicity, was evident, in comparison to anti-NF155 antibodies.

1.4.4.4 Contactin-1

Pathogenicity of anti-CNTN1 antibodies isolated from AIN patient sera has been proven in vitro, using myelinated DRG cultures (Labasque et al., 2014) and dermal myelinated fibres (Doppler et al., 2015), and in vivo (Doppler et al., 2019; Manso et al., 2016).

An initial study by Labasque *et al* was the first to find anti-CNTN1 IgG4 from patient sera may act pathologically by blocking the interaction of paranodal axo-glial CAMs (NF155, caspr/CNTN1) (Labasque et al., 2014). This was demonstrated using cell aggregation assays, as well as in myelinated DRG rat cultures, in which significantly reduced caspr1 staining at paranodes was observed in the presence of anti-CNTN1 IgG4 antibodies from patient sera. This suspicion was later confirmed when intraneural injection of anti-CNTN1 IgG4, but not IgG1, antibodies into EAN rat models were able to access paranodes over 3 days, induced marked motor conduction failure and ataxia, and lead to the selective loss of the paranodal complex caspr/CNTN1/NF155 (Manso et al., 2016). In a subsequent passive transfer experiment, Lewis rats were again injected with anti-CNTN1 antibodies isolated from patients in the acute (predominantly IgG3 subclass), and chronic (predominantly IgG4) phase of their disease (Doppler et al., 2019), though binding of patient IgG was only just detectable at the edge of the paranode at 2 days, and only in up to a third of animals injected with purified IgG3 antibodies. The rats injected with ‘acute’ IgG3 antibodies appeared to

have a more severe clinical phenotype (predominantly weakness) and conduction block (which was reversible) than those injected with IgG4, and only very mild nodal structural alterations were observed. Of note complement deposition was detected at some paranodes of the animals injected with anti-CNTN1 IgG3, but not IgG4 from the chronic patient. Again, there were no findings to suggest an inflammatory process was responsible for the pathological findings.

Although scarce, some in vitro models have further corroborated the (para)nodal destruction and absence of inflammatory cells seen in animal studies, for example in sural nerve patient biopsies (Koike et al., 2017), and in anti-CNTN1 antibody-positive patient dermal myelinated fibres, which revealed nodal gap lengthening, and loss of paranodal caspr1 and neurofascin immunoreactivity (Doppler et al., 2015).

Recently, the effect of anti-CNTN1 IgG3 and IgG4 antibodies on the surface expression of CNTN1 in other cell types has also been investigated (Grüner et al., 2021). By incubating patient IgG with mouse DRG or cerebellar neurons they were able to reduced levels of CNTN1 expression. Further, although sodium channels were not reduced in density, recordings from anti-CNTN1 antibody-treated DRG showed sodium currents to be markedly decreased, most pronounced with IgG3 vs IgG4 antibody-containing sera, compared with healthy control sera. This supports findings from previous data, showing anti-CNTN1 IgG3 inducing a more severe clinical and electrophysiological deficit in the absence of marked structural abnormality.

Lastly, using a similar approach to anti-NF155 antibodies, but yielding contrary results, monovalent (and bispecific) anti-CNTN1 antibodies made up a large proportion of anti-CNTN1 IgG4 antibodies in patient sera from a recent study (Taieb et al., 2023), i.e. the majority had undergone FAE. These also correlated with titres of anti-CNTN1 antibodies, though not clinical severity. However, like the native IgG4 antibodies, the monovalent anti-CNTN1 antibodies invaded the paranodes fully in vivo, suggesting the potential to alter the paranodal complex, though specific studies were not performed to demonstrate this.

1.4.4.5 Caspr1

Nerve biopsy analysis from Caspr1 patients, similar to other AIN patients, have shown axonal degeneration, gross (para)nodal distortion, and some loss of myelinated fibres, but no segmental demyelination (Doppler et al., 2016; Pascual-Goñi et al., 2021). Myelinated fibres from the skin biopsy of one Caspr1 IgG4 antibody positive patient showed elongation of nodes and again paranodal disruption, evidenced by the loss of caspr1 and NF155 staining (Cortese et al., 2020). In the same study, the authors propose caspr1 antibodies may act in a similar way to CNTN1 antibodies, by acting to functionally block axo-glial interacting cells. By purifying different caspr1 antibody isotypes IgG1 and IgG4 from the same patient, they showed that the addition of IgG4, but not IgG1, to a cell aggregation assay inhibited cells expressing the CNTN1/caspr1 complex from binding to cells expressing NF155. Using an in vitro (incubating mouse sciatic nerve with caspr IgG) and in vivo assay (intraneural injection into animals) they again confirmed that IgG4, but not IgG1, partially penetrated and bound to paranodes.

1.4.4.6 Caspr2 and LGI4

Although pathogenicity studies for Caspr2 antibodies in peripheral neuropathies are lacking, Caspr2 has a dominant role clustering Kv channels at the juxtaparanode. It is therefore credible that the impairment or loss of Kv channels would lead to disturbed maintenance of the membrane resting potential, and uninhibited depolarization of the NoR (Chiu & Ritchie, 1984).

Although in the single study identifying anti-LGI4 antibodies in CIDP patients, incubation of rat Schwann cell cultures with patient IgG did not affect LGI4 protein expression (X. Zhang et al., 2023), the crucial role of the LGI family, and specifically LGI4 in peripheral nerve myelination is recognised (Bermingham et al., 2006; Kegel et al., 2013) Thus, although the pathogenicity of LGI4 antibodies remains to be verified, the hypothesis that they can induce a peripheral neuropathy is tenable.

1.5 Aims of this thesis

The overall aims of my doctoral research are to:

1. Clinically and serologically characterise patients with Autoimmune Nodopathies
2. Assess the utility of diagnostic assays used to detect (para)nodal antibodies
3. Investigate the mechanisms by which (para)nodal antibodies exert their pathogenic effects

2 METHODOLOGY

2.1 Abstract

Sera for patients suspected to have an immune-mediated neuropathy was collected via the observational study 'BioSPIN' and through a national diagnostic service. Cell based assays (CBA) using transfected HEK cells to test patient sera for IgG reactivity to nodal and paranodal targets were used as the gold standard for antibody detection, and enzyme-linked immunosorbent assays (ELISA) used to as an ancillary, usually confirmatory test in addition. IgG reactivity to specific (para)nodal antigens could also be confirmed using immunoadsorption assays, to demonstrate absence of IgG binding after depletion with free protein antigen. To identify topographical IgG binding from autoimmune nodopathy patient sera in vitro, an experimental model of human-induced pluripotent stem cell-derived live myelinated co-cultures was used. This model was also the core technique used to assess antibody-induced and complement dependent neuronal injury and cytotoxicity. In a CNTN1 antibody-positive cohort with suspected concurrent antibody-mediated renal disease, CNTN1 antibody-antigen immune complexes were isolated using immunoprecipitation, and detected in sera and tissue lysate using western blot, and in neural/renal tissue using immunohistochemistry.

2.2 Cell based assays (CBA)

2.2.1 DNA plasmid amplification

LB agar plates and LB broth were prepared for bacterial colonisation by mixing 32g LB agar powder (Invitrogen, 22700025) and 20g LB powder (Sigma, L3022), respectively, per 1L distilled water, and autoclaving for 15 minutes at 121°C. By an open flame, Kanamycin (10 mg/ml stock, diluted to 50 µg/ml) or Ampicillin (100 mg/ml stock, diluted to 100 µg/ml) were added, depending on DNA plasmid for amplification (NF155; Kanamycin).Using a sterile pipette, 25ml of agar was transferred to each 10cm petri dish, lid replaced and once set turned upside down, sealed with parafilm and stored at 4°C for future use. Using a sterile pipette tip, bacterial stocks were pricked/scraped by an open flame, spread onto the agar plate, and incubated at 37°C overnight. Bacterial colonies for each desired plasmid were then picked with sterile pipette tips and dropped into separate 15ml falcons filled with 5ml of LB broth (with corresponding antibiotic), left on a shaker for 4 hours at 37°C to establish 'starter cultures'. Starter cultures could be frozen down, diluted 3:1 in glycerol, for future use. Or for further growth, 1.5ml of each starter culture was added to 500ml LB broth in 3L conical flasks (2 flasks per plasmid) and left on a shaker (250rpm) at 32°C for 3 days.

2.2.2 DNA plasmid purification

Approximately 300ml LB broth/bacteria mixtures were transferred to plastic bottles and centrifuged (4600g, 15 mins), supernatant discarded, and DNA purified using the Invitrogen PureLink HiPure Plasmid Megaprep Kit (catalog No: K210008XP). Specifically, to lyse and precipitate DNA, resuspension buffer (maximum 50ml per DNA) and RNAse was added and vortexed to resuspend each pellet. The same volume of lysis buffer was added, and the solution inverted for 5 minutes. The same volume of precipitation buffer (N3) was added and bottle inverted again. To clarify the cell lysate, the cell filtration cartridge was attached to a sterile 1L stericup receiver flask, and the lysate poured into it, let to stand for at least 2 minutes, and then connected to a vacuum source. Wash buffer was added, and upon vacuum clarified lysate containing DNA plasmid was

collected. To bind the DNA, a binding cartridge was attached to a new stericup and washed with 100ml of equilibrium buffer (supernatant discarded) prior to the cell lysate being loaded and filtered. Wash buffer was filtered through twice, and the flow-through discarded. To elute the DNA, elution buffer was added and the vacuum pulsed. The filter was stored for further pulsing if required. The eluate was transferred to 30ml sterile tubes (max 17.5ml/tube) and DNA was precipitated with 0.7 volume isopropanol/volume eluate, and centrifuged (4°C, 30 mins, >12000g). The supernatant was discarded, and pellet gently washed and resuspend with 70% ethanol (20ml per tube), prior to vortexing gently. This was centrifuged again this time for 10 min, supernatant gently aspirated from the pellet, and allowed to air dry for 10 minutes. TE buffer (500µl) was added and vortexed, and a nanodrop was used to measure the concentration of DNA (230nm). The purified DNA was stored at 4°C, or -20°C for longer term use.

2.2.3 Human Embryonic Kidney (HEK) cell transfection

Human embryonic kidney 293T ("HEK") cells were expanded in T75 flasks in Dulbecc''s Modified Eagle Medium (DMEM)/10% fetal bovine serum (FBS) (both Gibco, Life Technologies)/antibiotic-antimycotic (anti-anti) media until confluent, washed in PBS, incubated with TrypLE (Gibco, Life Technologies) for 5 minutes before being centrifuged (500g, 5 minutes). 13mm round glass coverslips were pre-stored in 100% ethanol, air dried, and pre-coated in Poly-L-Lysine (Sigma-Aldrich, P4707) (stock at 1mg/ml – dilute to 20µg/ml for coating in PBS) for 1 hour, aspirated and dried for a further 2 hours. HEK cell pellets were resuspended in DMEM/FBS/anti-anti, counted, and plated onto coverslips in 24 well plates at a density of 75,000 cells/well. These were incubated (37°C, 1 hour), wells topped up to 300µl/ well, and incubated (37°C) overnight. Once cells were 60-80% confluent, usually by the following day, cells were co-transfected with contactin-1 (*CNTN1*, EXA1153-MO29 Genecopoeia, Maryland, US) and contactin-associated protein ('1') (*CASPR1*, EXMO417-MO2 Genecopoeia, Maryland, US), or mono-transfected with either neurofascin-155 (NF155, *NFASC*) (RC228652, Origene), neurofascin-186 (NF186, courtesy of Jerome Devaux, University of Marseille), or one of the above CNTN1 and Caspr1 constructs (if sera was positive for IgG reactivity to co-transfected cells). Prior to transfection, media from wells was aspirated and replaced

with 250µl DMEM/FBS per well, without anti-anti. DNA plasmids were diluted in DMEM (1µg for single-transfection, 0.5µg each for co-transfection), and Jet-PEI transfection reagent (101-10; Polyplus) in DMEM (2µg PEI for single-transfection, 3µg co-transfection). The PEI mixture was dripped into the DNA mixture at 1:1 ratio and rested for 30 minutes, prior to dripping 100µl of the relevant solution into each coverslip, and incubating at (37°C) overnight. On day 3 media in each well was replaced and incubated for a following 24 hours prior to sera incubation.

2.2.4 Immunoassay and interpretation

Patient sera were initially screened for IgG reactivity to mono-transfected (NF155, NF186) or co-transfected (CNTN1/Caspr1), at 1:100 or 1:40, respectively. Sera was diluted in DMEM/1% bovine serum albumin (BSA), and co-incubation (1hr RT) with commercial primary antibody chicken anti-neurofascin, (1:1000) (AF3235, R&D systems, Bio-Techne), was used to confirm successful transfection and assess for co-localisation with any bound human IgG. Sera was incubated with live HEK cells for 1 hour at room temperature (RT). If positive IgG reactivity was detected at first screen, they were subsequently titrated out to 1:6400, and incubation with CNTN1 and Caspr1 mono-transfected cells was performed if IgG reacted with co-transfected cells. Cells were washed with DMEM/20 mM HEPES, fixed with 4% paraformaldehyde (PFA), and washed again with PBS. Permeabilization with ice-cold methanol (25 minutes) was performed only in wells with co-transfected cells, and subsequent incubation (1hr RT) with commercial primary antibodies mouse anti-Caspr1, (1:1000) (P97846, Neuromab), or goat anti-contactin-1 (1:1000) (AF904, R&D systems) was performed to assess for successful transfection and IgG co-localisation. Secondary antibody incubation (45 mins in the dark, RT) was with goat anti-human IgG-Fc specific-Alexa Fluor 488 (1:750) (Cat no. H10120; Life Tech), goat anti-mouse Alexa Fluor 546 (1:1000) (A11003; Life Tech), and goat anti-Chicken Alexa Fluor 546 1:1000 (Cat no. A11040; Life Tech) diluted in DMEM/HEPES/1% BSA. Unconjugated mouse anti-human IgG subclass 1-4 antibodies (1:100) (I2513, I25635, I7260 I7385; Sigma Life Sciences) were used with a fluorescently tagged tertiary antibody goat anti-mouse Alexa Fluor 488 (1:750) (A11029, Life Tech) to determine antibody subclass, if required on subsequent testing. Cells were

washed with DMEM/HEPES, then PBS, and incubated with DAPI (’',6-Diamidino-2-Phenylindole, Dihydrochloride, Invitrogen) (5 minutes, RT) before washing in PBS and imaged for positive IgG staining using light microscopy, or mounted onto glass slides and stored at -20°C for imaging using fluorescence confocal microscopy (LSM 700, Zeiss). Each sera was scored qualitatively by an observer using a numerical scale of 1-4 in increasing fluorescence intensity from human IgG membrane staining (1= minimum threshold of positivity). To further confirm antibody reactivity to specific antigen targets, sera were pre-adsorbed by incubating with 1µg of either CNTN1 protein (10383-H08H, Sino Biological Inc), human recombinant neurofascin-155 (8208-NF, R&D systems) or neurfascin-186 (TP329070, OriGene Technologies) overnight at 4°C, prior to re-application to HEK cells. Abrogation of IgG binding to the corresponding transfected HEK cells confirmed specificity.

2.2.5 Complement binding assays

For complement binding assays, after 1 hour sera incubation, cells were washed with DMEM/HEPES and incubated with normal (healthy) human sera (NHS) diluted to 20% in DMEM/HEPES for 1 hour at RT. Following fixation with PFA, cells were incubated with primary antibody rabbit anti-C3c (Dako A0062) at a 1:200 dilution in DMEM/HEPES/1% BSA for 1 hour at RT. Instead of using goat anti-Chicken Alexa Fluor 546, neurofascin transfection was confirmed using biotinylated anti-chicken IgY (1:1000) (BA9010, Vector Laboratories), + Pacific Blue (1:500, S11222, Life Technologies), and C3c was labelled with secondary antibody goat anti-rabbit IgG AF546 (1:400, A11010, ThermoFisher Scientific). Aquaporin-4 antibody-(AQP4) positive patient sera was used as a positive control (1:250) of complement binding in AQP4 transfected HEK cells (AQP4-EGFP plasmid, provided by Professor Sarosh Irani).

2.3 Enzyme-linked immunosorbent assay (ELISA)

The following ELISA methodology is taken from a prior publication detailing the identification of IgG1 antibodies in patients with pan-neurofascin antibodies, for which I am first author (Fehmi, Davies, et al., 2021).

Wells of Nunc Maxisorp ELISA plates (Fisher Scientific) were originally coated with human recombinant neurofascin-155 (NF155) (8208-NF, R&D systems), NF186 (TP329070, OriGene Technologies) or CNTN1 (10383-H08H, Sino Biological Inc) diluted to 1mg/ml in PBS (100ul/well), and left overnight at 4°C. Caspr protein (2418-CR R&D Systems) became commercially available for testing at a later date. Blank wells were incubated with PBS only. The coating solution was flicked off and wells blocked with 5% milk/PBS (1hr, RT). Patient sera (1:100) was screened by incubation in 5% milk (1hr, RT), flicked off and washed five times by PBS. Wells were incubated with secondary antibody anti-human IgG (Fc-specific) peroxidase-conjugated anti-human IgG (A0170, Sigma) (1:3000 in 5% milk, 1hr RT) and washed as before. Detection reaction was activated using o-Phenylenediamine dihydrochloride (OPD, Sigma) (20 mins in the dark), and ceased with 4M H_2SO_4. Optical densities (OD) were measured at 492nm, and those measured at greater than 0.1 (above uncoated blank wells) were considered positive. Serial doubling dilutions (1:100 to 1:6400) were used to determine end-point titres, and IgG subclass specificity tested for using subclass specific, HRP-conjugated secondary antibodies (1:1000) (MH1715, MH1722, MH1732, MH1742; Thermo Fisher Scientific).

To assess the specificity of the subclass specific secondary antibodies used in the CBA, recombinant human IgG subclass proteins (HCA049, HCA50, HCA178, HCA193, HCA194, HCA195, Bio-Rad) were coated as above, and then exposed to the unconjugated mouse anti-human IgG subclass 1-4 antibodies for 1h at room temperature (IgG1 1:1000, IgG2 1:250, IgG3 1:100, IgG4 1:250). Following a wash step, a HRP anti-mouse- IgG antibody (A4416, Sigma) was applied at 1:1000 for 1h, washed off, and binding detected as

before. A standard curve was created for each subclass antibody using duplicate wells coated with the recombinant subclass proteins on the same plate as patient sera, and the limit of the blank (highest detectable analyte in duplicate blank wells) and limit of detection (lowest analyte concentration distinguishable from the blank) for each subclass were calculated (Armbruster & Pry, 2008). Optical densities 5 standard deviations of a low concentration analyte above the limit of the blank were considered positive.

2.4 Myelinated co-cultures (human-induced pluripotent stem cell-derived)

2.4.1 Human-induced pluripotent stem cell (hiPSC) differentiation, and plating of sensory neurons

The following co-culture methodology is taken from a recent publication identifying the link between autoimmune neuropathy and membranous glomerulonephritis, for which I am first author (Fehmi et al., 2023).

Human fibroblasts reprogrammed to pluripotent stem cells (iPSC) from two healthy control lines (AD2 and AD3) were obtained from the StemBANCC consortium at the University of Oxford. iPSC were differentiated to sensory neurons using a combination of small-molecule mediated dual-SMAD inhibition and WNT activation according to a previous protocol (Chambers et al., 2012) in 6 well culture plates coated with hESC-qualified matrigel (Corning, 354277). On day 11 of differentiation, sensory neuron precursors were washed with 1ml per well of PBS containing dNase I (100U/ml), lifted using TyrpLE dissociation reagent, and centrifuged (5 mins, 500g) to a pellet. These were seeded onto 13 mm diameter glass coverslips (approximately 20,000 cells per coverslip) in 24-well plates, or 96-well flat glass-bottom imaging plates (Greiner Bio-One 96 well Sensoplate™ 655892) (approximately 5,000 – 10,000 cells per well), previously coated with poly-D-lysine (PDL) (10 µg/mL) overnight and reduced growth-factor matrigel (Corning) for 1 hour (RT). Neurons were maintaines with neurobasal media supplemented with N2 (Cat. 17502-048), B27 (Cat 12587-010), Glutamax (Cat. 35050-038) and antibiotic-antimycotic (Cat. 15240-062) (all Gibco, Life

Technologies) ('complete' neurobasal) plus recombinant human β-NGF (rhNGF) (Cat. 450-01, Peprotech), NT3 (Cat. 450-03, Peprotech), GDNF (Cat. 450-10, Peprotech), and BDNF (Cat. PHC7074, Life Technologies) (all growth factors 25 ng/ml), supplemented with Rho-associated, coiled-coil containing protein kinase (ROCK) inhibitor (10 μM) (Tocris, Bio-Techne) on days 11–12, CHIR99021 (3 μM) (Sigma) on days 11–14 and cytosine arabinoside (Ara-C) (1 μM) (Sigma) on days 12–14 to remove proliferating, non-neuronal cells. Neurons were matured by incubation at 37°C in 5% CO_2 for 4 weeks with twice-weekly medium changes.

2.4.2 Sensory neuron precursor freezing (for development of a higher throughput method of sera screening on 96 well plates)

On day 11 of differentiation, sensory neuron precursors are either cryopreserved for later use or seeded directly onto 96-well plates for maturation and myelination. For cryopreservation, cells are dissociated by washing with PBS containing dNase I (100 U/ml), then TrypLE dissociation reagent prior to incubation for 5 min at 37°C. The cell suspension is centrifuged (500g, 5 min) and resultant pellet resuspended in 'complete' neurobasal media as specified in the 'iPSC differentiation' protocol, plus recombinant human β-NGF, NT3, GDNF, BDNF (all growth factors 25 ng/ml), CHIR99021 (3 μM) (Sigma) and ROCK inhibitor (1:1000 of 10 μM stock) (Tocris, Bio-Techne), 'plating media'. The cell suspension is diluted 1:1 with chilled 2X freeze media (20% DMSO, 80% charcoal-stripped FBS) and immediately transferred to cryovials (1 ml per vial at $2x10^6$ cells per ml) for storage at -80C overnight, and to a gaseous nitrogen tank thereafter. When required, cells can be thawed in a water bath, collected in PBS for centrifugation (400g, 5 min), and resuspended in the below medium. Cells can be thawed in a water bath and collected in PBS for centrifugation (5 min, 400g), resuspended in 'plating media', and plated on 96 well glass-bottom plates (pre-coated with PDL and matrigel as before).

2.4.3 Schwann cell harvesting and myelination of sensory neurons with rat Schwann cells

Primary Schwann cells were isolated from the sciatic nerves of rat pups (P2-3). Mother and pups were killed by rising concentration of CO2 in accordance with Schedule 1 of the UK Home Office Animals (Scientific Procedures) Act 1986. Sciatic nerves were rapidly dissected and digested in a mixture of collagenase (3mg/ml) (Worthington, Lorne Labs) and dispase II (3.5mg/mL) (Roche) for 1 h at 37°C with frequent gentle agitation. Nerves were washed in DMEM + FBS (10%) and gently triturated using a fire-polished glass Pasteur pipette. Dissociated cells were seeded into matrigel -coated tissue culture flasks overnight and expanded in Schwann cell expansion medium containing charcoal-stripped FBS (10%) (Sigma), Forskolin (4 µM), recombinant human NRG1-β1 EGF domain (80 ng/mL) (Cat. 396-HB, R&D Systems) and recombinant murine NGF (10 ng/ml) (Cat. 450-34, Peprotech) in DMEM/F12 (Gibco). Cells were treated overnight with 5–10 µM Ara-C to eliminate fibroblasts. Expanded Schwann cells were added to the neuronal cultures (5,000 – 10,000 cells per 96-well) and allowed to proliferate and align with the axons for 1 week in basal media containing: (CS-FBS) (10%), insulin (5 mg/ml) (Sigma) with holo-transferrin (100 mg/mL) (Sigma), rhNGF (25 ng/mL) (Peprotech) (Sigma), Selenium (25 ng/mL) (Sigma), 25 ng/ml thyroxine (Sigma), progesterone (30 ng/ml) (Sigma), triiodothyronine (25 ng/mL) (Sigma) and putrescine 8 mg/mL (Sigma) [collectively known as ‘Sato mix’ – use at 1:100 from stock] in DMEM/F12 media (Gibco, Life Technologies). From this point on, cultures were maintained in ‘myelination medium’ containing: 5% CS-FBS, ascorbic acid (25 µg/mL), phenol-free matrigel (1:300) (Corning, 356231) or Geltrex (Thermo, A1413302) and hrNGF (25 ng/mL) in ‘complete’ neurobasal medium. Myelinating cultures were matured for at least 4 weeks before use in subsequent experiments.

2.4.4 Immunoassay for topographical human IgG binding

The following co-culture methodology is taken from a recent publication identifying the link between autoimmune neuropathy and membranous glomerulonephritis, for which I am first author (Fehmi et al., 2023).

Sera were assessed for topographical binding using mature myelinated co-cultures. These were incubated with patient sera diluted at 1:100 in N2 'complete' neurobasal media with 1% BSA and human nerve growth factor (NGF) (25 ng/ml) for 1 h at 37°C. For pre-adsorption assays patient sera was first incubated with 1ug of CNTN1 protein (10383-H08H, Sino Biological Inc), human recombinant neurofascin-155 (8208-NF, R&D systems) or neurfascin-186 (TP329070, OriGene Technologies) overnight, at 4°C, prior to application of cultures. Cultures were washed with PBS and fixed with 2% PFA for 30 min at room temperature. After washing sequentially with PBS and DMEM (including 20 mM HEPES) cultures were incubated with goat anti-human IgG AF488 (1:750) (A11013, ThermoFisher Scientific) in DMEM/HEPES/1% BSA for 1h at room temperature. Cultures were washed sequentially with DMEM/HEPES and PBS and then permeabilised with ice cold methanol (30-45 minutes on ice). Cultures were blocked with 5% normal goat serum (NGS) in PBS before incubation with primary antibodies chicken anti-Neurofilament 200 (1:10,000) (4680; Abcam) and rat anti-myelin basic protein (1:500) (Ab7349, Abcam) over night at 4°C. Secondary antibody incubation was with biotinylated goat anti-chicken IgY (1:500) (BA9010, Vector Laboratories), goat anti-rat IgG Alexa Fluor 546 (1:1000, 1hr, RT) (A11081, Life Tech) followed by streptavidin pacific blue (1:500,45 mins, RT) (S11222, Life Technologies), or goat anti-rabbit IgG Alexa Fluor 546 (1:400) (Cat no. A11010: ThermoFisher Scientific) and biotinylated goat anti-rat IgG (1:1000) (Cat no. BA9400; Vector lab), followed by Streptavidin pacific blue. Coverslips were mounted onto glass slides with Vectorshield (H1000, Vector), if using 24 well plates, and fluorescence images of IgG nodal labelling in myelinating cultures were acquired on a laser scanning confocal microscope (LSM 700, Zeiss) using the x63 or x20 objectives. 10-15 z-sections at 0.5 µm interval were exported as maximum projection images. Brightness and contrast were adjusted for presentation.

2.4.5 Initial and subsequent validation of screening human sera for IgG binding

Sera samples from patients suspected to have inflammatory neuropathies, other neurological diseases, or healthy control sera were initially tested in a preliminary stage for IgG binding in myelinated co-cultures (as described above) on an ad-hoc basis. Results from 3 different experimenters over this time were collated.

These had all been previously tested in a CBA for the presence of nodal and paranodal antibodies (NF155 and 186, CNTN1 and caspr1). If one or more experimenters deemed a sample positive for IgG reactivity to any neuronal components the overall result for that sample was recorded as positive. Otherwise these were scored as negative. A smaller cohort of these seropositive and seronegative patients or healthy controls from those tested in the preliminary phase (total 47 samples) were selected to validate IgG reactivity in neuron co-cultures and investigate whether variability in cell line, experimenter or observer would significantly influence this outcome. Assays were performed by two of the experimenters, using two different cell lines on two separate occasions. All samples were further analysed by both experimenters. Experimenters were blinded to serological antibody status during the immunostaining and observation of IgG binding by confocal microscopy.

Using 96 well plates to identify IgG binding in preliminary screening and validation studies of seronegative and seropositive human samples, a maximum of 68 sera samples per plate were tested for topographical IgG binding (as described above in 'immunoassay for topographical human IgG binding'). The experimenter was blinded to sample antibody serotype for each experiment. After washing secondary antibodies off with PBS the plate was sealed and stored in the dark at 4°C until further analysis. Criteria necessary for inclusion upon imaging were clearly visible axons and myelination with at least 3 nodes of Ranvier visible for analysis. Confocal acquisition settings were adjusted as required per observer and samples scored as positive or negative in the first instance, and IgG reactivity to neuronal components further categorised as binding to axons, nodes, myelinating or non-myelinating SCs. Images for samples scored as positive were saved for subsequent comparison.

2.4.6 Complement binding assays

Mature myelinated co-cultures were incubated with patient sera alone or with the addition of a source of complement (NHS 5%, 10% or 20%). Media or NHS alone were used as controls. Heat inactivated NHS (warmed at 37ºC for 30 minutes) was also incubated in place of NHS to assess the effects of healthy sera

without (or significantly reduced) activated complement. Sera were used at 1:100 dilution and incubated with live cultures for 1 hour on cover slips as previously described, washed with PBS and fixed with 2% PFA for 30 minutes. After a further wash with PBS then DMEM/HEPES cultures were incubated with primary antibody rabbit anti-C3c (1:100, A0062; Dako), or if testing for concurrent human IgG binding secondary antibody goat anti-human IgG (H+L) 568 (Life Tech, A21090, 1:750), diluted in DMEM/20mM HEPES/1% BSA for 1 hour on an orbital shaker at room temperature. After washing with DMEM/HEPES and PBS cultures were permeabilised with MeOH for 30 mins on ice, washed with PBS and blocked with 5% NGS in PBS for 1 hour. Incubation with primary antibodies chicken anti-Neurofilament 200 (1:10,000) (4680; Abcam), and if assessing for myelin rat anti-myelin basic protein (1:500) (Ab7349, Abcam), diluted in 1% NGS/PBS, was performed for 4 hours at 4°C. After washing with PBS, cultures were incubated for 1 hour at room temp with goat anti-rabbit IgG (H+L) Alexa Fluor 488 (1:1000, A11008, Life Tech) to label complement, biotinylated goat anti-chicken IgY (1:500) (BA9010, Vector Laboratories) for axons, and goat anti-rat IgG Alexa Fluor 546 (1:1000, A11081, Life Tech) if assessing for myelin. After washing with PBS incubation was with tertiary antibody streptavidin pacific blue (1:500,45 mins, RT) (S11222, Life Technologies) to label axons. After a further wash and mounting step images were visualised using fluorescence confocal microscopy at x20.

2.4.7 Complement-dependent cytotoxicity (CDC) assay using CytotoxGlo™

Ninety-six well luminescence plates (Corning 96-well Flat Clear Bottom White Polystyrene TC-treated Microplates, 3610) were prepared with PDL and Matrigel coating as previously described, and seeded with differentiated sensory neuron precursors (20,000 cells/well). After 4 weeks neurons were mature enough to use for CDC assays. Patient sera or control antibody (positive control of complement mediated cytotoxicity was EG4) was diluted to the desired concentration (1.25-40 µg/ml EG4, 1:50,000-1:5 patient sera) in supplemented neurobasal media including 1% BSA. All plates had duplicate or triplicate wells for each sample. NHS was added to a final concentration of between 12.5-50%. Negative control wells included media only, and NHS without antibody or patient sera at each concentration. These control conditions were

also used as ‘maximum lysis’ wells, whereby a luminescence value could be obtained for total lysis of all cells in a well. Media was removed by flicking the plate, and 50 µl media containing serum or antibody replaced in each well, mixed on orbital shaker and incubated for 1h at 37ºC. For wells with additional NHS, 50µl (neat if final concentration of NHS 50%, otherwise diluted to reach relevant final concentration) of freshly thawed NHS was added (not to ‘maximum lysis’ controls – serum components prevent lysis by digitonin) for 2hr at 37ºC. Assay buffer from the Promega Cytotoxicity kit (G9291) was added to each well (except maximum lysis controls), and lysis buffer (containing digitonin) to maximum lysis control wells. Wells were mixed again on the orbital shaker, and the relevant NHS mixture finally added to the maximum lysis controls immediately prior to adding CytotoxGlo reagent to all wells, incubating for 15 minutes in the dark and reading on a luminescence plate reader (gain 2000). In between each step of adding reagents the plates were mixed on the orbital shaker (600 rpm, 1 min at RT). Final volumes were equal between all wells with the same proportion of lysis buffer. The percentage of cytotoxicity was calculated using the following calculation: % cytotoxicity = [(luminescence reading – average ‘media only’ 0 µg/ml well reading)/(average max lysis well reading – average ‘media only’ 0 µg/ml well reading)] x100

2.4.8 Detection of fluid biomarkers (NfL and CNTN1 protein)

Supernatant was collected from myelinated co-cultures incubated with media (controls), or antibody-containing sera samples known to cause injury to axons (GQ1b antibody causing ‘axonal injury’ sera) or myelin (unknown antibody, ‘demyelination’ sera) in the presence of a source of complement. Specifically, 100µl of heat inactivated sera at 1:50 was incubated with co-cultures (as previously described, except 1% BSA was not used to avoid interference with measurement of NfL or CNTN1 protein) for 1 hour. 50µl was removed and replaced with 50µl NHS diluted to a final concentration of 20% and supplemented with patient sera (1:50) to avoid diluting the original concentration of antibody. For wells without additional NHS the same procedure was followed but without the addition of NHS. This was left in the incubator for a further hour (‘1 hour’ condition) or 24 hours (’24 hour’ condition) prior to collecting the supernatant (stored at -80ºC for further analysis), and performing the immunoassay (as previously described). Both NfL and

CNTN1 protein were measured by an external collaborating laboratory in Amsterdam. Serum CNTN1 protein levels were measured on the Luminex® platform according to the manufacturer's instructions (Human Magnetic Luminex Assay, R&D systems) as previously described (Wieske et al., 2021). Samples were coded randomly and analysed in duplicate. Measurements with a coefficient of variation >15% and outliers were repeated. Serum NfLwas measured using a Simoa assay as described previously (Lieverloo et al., 2019).

Two experiments were performed at different timepoints. 'Experiment 1' was performed using 24 well plates, with neurons plated onto 13mm round coverslips (single well per condition). 'Experiment 2' was performed at a later date on a 96 well plate platform (triplicate wells per condition), and additionally NfL and CNTN1 protein levels were measured at baseline (in media containing sera prior to exposure to cultures). Further, sera samples were only heat inactivated in experiment 2.

2.5 Human sera sampling, serological and clinical profiling, data analysis

Serum samples of patients suspected to have an immune mediated neuropathy were sent to the Oxford neuroimmunology laboratory for diagnostic testing of (para)nodal antibodies from national and international centres. They were all tested for CNTN1 and Caspr1 (co-transfected at initial screen), NF155 and NF186 antibodies, and if found positive were typed for IgG subclass, and end-point titre determined. A voluntary clinical proforma was sent to referring clinicians requesting patient details, initial clinical presentation and any treatments (and responses) administered prior to sample testing. Multiple efforts were made to contact referring clinicians of those who tested positive, but those without returned clinical data could only be included in subsequent analysis for the purpose of antibody reactivity and subclass. Initially patients with suspected inflammatory/immune-mediated neuropathies seen in Oxford were recruited to an observational study 'Bio-SPIN'. This study was approved by the NHS National Research Ethics Service Committee (South Central – Oxford A, 14/SC/0280). The use of de-identified clinical data from other patients to audit

the relative value of available and novel methods to determine autoantibodies, based on the gold standard of immune-mediated clinical phenotypes, was approved by the Oxford University Hospitals NHS Trust clinical audit leads (ID 5106). Follow-up data (clinical course and outcome, response to treatment) could only be obtained for patients recruited to Bio-SPIN, thus seropositive patients from the diagnostic cohort were contacted at a later date to recruit to Bio-SPIN for the purposes of obtaining follow up data. Study data for all autoimmune nodopathy patients recruited to BioSPIN were collected using REDCap electronic data capture tools hosted at the University of Oxford (P. A. Harris et al., 2009, 2019). Further analysis to compare (para)nodal antibody-positive vs seronegative patients, or patients in different antibody groups was also performed using Microsoft excel (version 16.77.1) and GraphPad Prism 10 (version 10.0.3).

2.5.1 Analysis of clinical and serological associations in anti-pan-neurofascin antibody cohort

The following analysis methodology is taken from a prior publication detailing the identification of IgG1 antibodies in patients with pan-neurofascin antibodies, for which I am first author (Fehmi, Davies, et al., 2021).

Contingency data for the presence or absence of 10 core clinical features (diagnostic category, onset/progression, ataxia, tremor, neuropathic pain, cranial nerve palsy, autonomic dysfunction, respiratory involvement, nephrotic syndrome, and MRI abnormalities) were analysed by Chi-square tests without family- wise correction for error rate. For subsequent comparisons between panNF positive patients, NF155 antibody positive patients, and seronegative patients, Fisher's exact test was used. Point estimates of the odds ratio are reported, with 95% confidence intervals calculated by the Baptista-Pike method. The widths of the intervals have not been adjusted for multiplicity and as such the inferences drawn may not be reproducible. The nadir modified Rankin score and CSF protein level at diagnosis were compared by the Kruskal-Wallis test with Dunn's correction for multiple comparisons.

2.5.2 Analysis of clinical and serological associations in anti-CNTN1 antibody and nephrotic syndrome cohort

Statistical analysis was performed using GraphPad Prism 8 (version 8.0.2). Statistical significance for contingency data was assessed by Fishers exact test. Differences between CNTN1 antibody titres in remission versus in active disease, and in serum CNTN1 levels in the presence or absence of nephrotic syndrome, were assessed by the Mann-Whitney test. A p-value of<0.05 was considered significant.

2.6 Western blot

2.6.1 Cell line lysate preparation

The following methodology in sections 2.6.1 to 2.6.5 detailing cell and tissue lysate preparation as well as western blotting are taken from a recent publication linking CNTN1-associated neuropathy with nephrotic syndrome, for which I am the first author (Fehmi et al., 2023).

CNTN1-transfected HEK cells and iPSC-derived neurons were cultured as described, washed once in PBS, lifted into suspension with TrypLE Express (12604-021, Gibco) and centrifuged at 500g for 5 minutes. The pellets were resuspended in RIPA buffer (R0278, Sigma) and Halt protease inhibitor cocktail (1:100) (1862209, ThermoFisher Scientific), rested on ice for 15 minutes before re-pipetting to homogenise. After a further 30 minutes with gentle inversion at 4°C and re-pipetting to homogenise they are centrifuged at 4°C for 5 minutes at 10g. Protein quantification of the supernatant (for cell line and all tissue lysates) was determined using the Pierce™ BCA protein assay kit (23225, ThermoFisher scientific) prior to storage at -80°C until required for use in western blot.

2.6.2 Rat tissue lysate preparation (brain, kidney, sciatic nerve)

Rat tissue was harvested from a six-week old male Wistar rat immediately following Schedule 1 killing by rising concentration of CO_2. Dissected tissues were immediately frozen on dry ice stored at -80°C. For lysis,

tissues were weighed, cut into ~1mm sections, then incubated with RIPA buffer and protease inhibitor cocktail (1:100) (300µl lysis buffer per 0·1g tissue) at 4°C for 20 minutes with gentle inversion. Tissues were homogenised on ice with a handheld homogeniser and lysates were centrifuged at 10,000g for 5 minutes at 4°C prior to transfer of supernatant.

2.6.3 Human tissue lysate preparation (podocyte, whole kidney)

Cortical tissue from fresh frozen healthy human kidney was dissected into two 200 mg pieces, each transferred to 2ml microcentrifuge tubes (QIAGEN) on ice and incubated with 1ml of RIPA buffer, Pepstatin A and 1:100 Halt™ PIC. A 5mm steel bead (QIAGEN) was added to each tube and samples were homogenised on ice at 30Hz using a tissue homogeniser for a total of 10 minutes, with 2 minute cycles at 1 minute intervals. The homogenates were placed on a rotator at 4°C for 2 h before being centrifuged at 5100g at 4°C for 30 minutes. The supernatant was transferred to a clean tube and centrifuged again at 15800g 4°C for 15 minutes. This final supernatant was stored at -20°C until further use in western blotting.

Human podocytes from an immortalised cell line (kindly provided by Professor Moin Saleem, University of Bristol) were grown in Roswell Park Memorial Institute (RPMI) 1640 medium (Cat no. 31870-025, Gibco), 1% Insulin-Transferrin-Selenium (ITS) (Cat no. 41400-045, Gibco), 10% FBS, 1% Penicillin Streptomycin and 5mM L-glutamine at 33°C , the medium only supplemented with the latter when the cells were passaged (twice weekly) or medium was changed (three times weekly). They were subsequently incubated at 37°C for two weeks to allow for differentiation into podocytes. These were washed in PBS, lifted with Trypsin-EDTA (0·05%) and centrifuged at 200 x g for 5 minutes. The pellet was resuspended thoroughly in RIPA buffer and Halt PIC and kept on ice for 15 minutes before further homogenisation and centrifugation at 4°C at maximum speed for 15 minutes. The supernatant was collected and transferred to a clean sample tube for storage at -80°C.

2.6.4 Immune complex detection (CNTN1)

An adaptation of a previously described methods was used (Harkiss & Brown, 1979; Lux et al., 2013) . Poly(ethylene)glycol (PEG MW~6000, 81260) (Cat no. 81260, Sigma) was dissolved in borate buffer (0.1 M boric acid, 25 mM disodium tetraborate, 75 mM NaCl, pH 8.4) to make a 12.5% stock solution and a 2.5% wash solution. To precipitate immune complexes (iCs) from sera, 50 µl of borate buffer and 50 µl of 0.2 M EDTA were added to 300µl of test serum in an Eppendorf tube. After mixing briefly, 100 µl of 12.5% PEG was added (final PEG concentration 2.5%, which should preferentially precipitate immune complexes while free antigens and antibodies remain soluble). After mixing briefly again, the tube was incubated at 4°C overnight. After centrifugation (2000g, 30 min, 4°C) the supernatants were removed and pellets resuspended with 1 ml of 2.5% PEG. The tube was vortexed to re-suspend the pellets, and centrifuged again. After aspirating the supernatants, the PEG precipitates containing iCs (PEG-IC) were re-suspended in 30 µl of pre-warmed PBS at 37 °C (1hr rotating). A sample (5ul) of the supernatant from this last step (depleted of iCs), in parallel to the same volume of PEG-IC was run on the western blot (see below).

2.6.5 Polyacrylamide gel (PAGE) electrophoresis and immunoblotting

For the analysis of CNTN1 in anti-CNTN1 antibody-positive patients with nephrotic syndrome, cell lysates, tissue homogenates, immune complex precipitation samples, and human recombinant CNTN1 protein (10383-H08H, Sino Biological) were reduced and denatured by mixing with sample reducing agent, (B0009, Thermofisher) and LDS sample buffer (B0008, Thermofisher) before heating at 70°C for 15 mins. They were loaded (5-60µg rat tissue, 40µg podocyte fraction or 30µg whole kidney including glomeruli for human kidney lysates) onto an 8% polyacrylamide gel (Bolt Bis-tris plus; ThermoFisher Scientific) for electrophoresis and run at 150V 400mA on a mini gel tank (A25977, Thermofisher) . Separated proteins were transferred onto a nitrocellulose membrane (LC2000, ThermoFisher) and blocked with 5% non-fat milk in Tris-buffered saline plus 0·1% Tween 20 (TBS-T) before incubation with either goat anti-CNTN1 (1:12,000) (AF904, R&D Systems) (Note: This antibody is cross-reactive to human, mouse and rat CNTN1) or CNTN1 antibody-positive patient sera from patients 1-4, 13 and 16 at 1:500, and P14 at 1:100, in milk,

overnight at 4°C. P16 was additionally pre-incubated with recombinant CNTN1 protein prior to gel electrophoresis to demonstrate abrogation of CNTN1 reactivity and antibody specificity. Secondary antibody incubation was with either peroxidase conjugated anti-goat IgG (705-036; Jackson ImmunoResearch; 1:2000) or anti-human IgG4 (MH1742, Thermofisher), respectively. Protein detection was performed using ECL Prime detection reagent (RPN2232, GE Healthcare).

For any samples that were initially pre-adsorbed, patient sera was first incubated with 1ug of CNTN1 protein (10383-H08H, Sino Biological Inc) prior to loading.

2.7 Data analysis

2.7.1 Analysis of clinical and serological associations in anti-pan-neurofascin antibody cohort

The following methodology for obtaining clinical analysis comparative data has been taken from a prior publication outlining patients with pan-neurofascin antibodies (Fehmi, Davies, et al., 2021) and CNTN1 antibody-associated neuropathy and nephropathy (Fehmi et al., 2023).

Contingency data for the presence or absence of 10 core clinical features (diagnostic category, onset/progression, ataxia, tremor, neuropathic pain, cranial nerve palsy, autonomic dysfunction, respiratory involvement, nephrotic syndrome, and MRI abnormalities) were analysed by Chi-square tests without family- wise correction for error rate. For subsequent comparisons between panNF positive patients, NF155 antibody positive patients, and seronegative patients, Fisher's exact test was used. Point estimates of the odds ratio are reported, with 95% confidence intervals calculated by the Baptista-Pike method. The widths of the intervals have not been adjusted for multiplicity and as such the inferences drawn may not be reproducible. The nadir modified Rankin score and CSF protein level at diagnosis were compared by the Kruskal-Wallis test with Dunn's correction for multiple comparisons.

2.7.2 Analysis of clinical and serological associations in anti-CNTN1 antibody and nephrotic syndrome cohort

Statistical analysis was performed using GraphPad Prism 8 (version 8.0.2). Statistical significance for contingency data was assessed by Fishers exact test. Differences between CNTN1 antibody titres in remission versus in active disease, and in serum CNTN1 levels in the presence or absence of nephrotic syndrome, were assessed by the Mann-Whitney test. A p-value of<0.05 was considered significant.

2.8 CNTN1 identification in mouse and human tissue–- Immunohistochemistry

2.8.1 Mouse sciatic nerve teased fibres

The following methodology detailing immunolabelling of mouse teased nerve fibres and human kidney and brain (section 2.8.2) have been taken from a recent publication identifying CNTN1 antibodies as a link between neuropathy and nephropathy, for which I am first author (Fehmi et al., 2023).

Sciatic nerves were harvested from a six-week old male C57BL/6 mouse immediately following Schedule 1 killing by rising concentration of CO_2 and were post-fixed overnight in 4% PFA in 0.1M PBS. For teased fibres the sciatic nerve sheath was removed and smaller nerve bundles transferred to a drop of distilled water on a Superfrost slide. Individual fibres were teased from the bundle and air-dried. Nerve fibres were permeabilised in 100% acetone, 10 min at -20°C, washed 3x in PBS and blocked in 5% fish gelatin in PBS + 0.1% triton-X for 1 hr at room temperature. Patient sera were diluted 1:200 in 0.5% fish gelatin and 0.01% triton-X., including guinea pig anti-Caspr (1:1000) (Bhat et al., 2001) (a gift from Dr Manzoor Bhat, UT Health Science Center San Antonio) and incubated overnight at 4°C in a humidified chamber. The next day slides were washed with PBS and counterstained with goat anti-human IgG Alexa 488 (1:750) (A11013) and goat anti-guinea pig IgG Alexa 568 (1:1000) (A11075, ThermoFisher) in 0.5% fish gelatin and 0.01% triton-

X for 1h at room temperature. After washing in PBS, slides were mounted with Vectorshield (H1000, Vector) and imaged with confocal microscopy (Zeiss LSM 700).

2.8.2 Human kidney and brain

Fresh frozen human kidney cortex normal tissue (Request no. 19/A157) and paraffin-embedded kidney biopsy tissues (Request no. 19/A071) were obtained from the Oxford Centre for Histopathology Research (OCHRe) under REC approval number 14/SC/0280. For tissue sections, kidney biopsy samples obtained under local anaesthesia were collected in either phosphate buffer or Michel's medium, before being placed into formalin (4%) and then processed and embedded according to standards clinical lab protocols. Thereafter, samples were stored at room temperature until needed for cutting. Fresh human kidney tissue was resected from two patients undergoing nephrectomy for renal cell carcinoma. Approximately 0.5 cm^3 of kidney tissue or cortex were flash frozen in liquid nitrogen and transferred to cryotubes for storage in liquid nitrogen at -80 °C. Sample 1: Whole kidney (Male, aged 63). Sample 2: Whole kidney and cortex (Male aged 65). Additional kidney biopsies were provided by the MRC/Kidney Research UK National DNA Bank for Glomerulonephritis.

Fresh frozen human frontal cortex tissues of normal aged brain from a healthy donor were obtained from the Oxford Brain Bank (Request no. OBB553) under REC approval number 15/SC/0639 (59 year old male; post-mortem delay 1 day; frontal cortex from right hemisphere snap frozen in liquid nitrogen; storage in -80 freezer since May 2013; pathological diagnosis – normal aged brain). Additional formalin-fixed and paraffin embedded healthy human cerebral cortex (HP-210) and kidney tissue sections (HP-901) were purchased from Zyagen (San Diego, CA, USA). Peripheral blood mononuclear cells (PBMC) were isolated from the whole blood of a healthy donor (40 year old male; venepuncture collected in sodium heparin tubes; Lymphocyte density gradient centrifugation; cryopreservation in 10% DMSO, 40% foetal bovine serum, 50% RPMI; storage in gaseous nitrogen since February 2019).

2.8.2.1 Human kidney diaminobenzidine (DAB) immunohistochemistry for CNTN1.

Sections of kidney biopsy tissue from patients 1, 2, 13 and 14 (Supplementary Table 1), as well as PLA_2R+ patients and healthy human donors, were immunostained in parallel for CNTN1 by DAB immunohistochemistry. Formalin-fixed, paraffin embedded human tissue sections (3-5 μm) sections were rehydrated through two 5 min changes each of xylene, 3 min of 100% ethanol, 1 min of 95% ethanol, and 5 min of 80% ethanol to distilled water. Tissue slides were incubated in near-boiling citrate-EDTA buffer (citric acid 10 mM, EDTA 2·5 mM, tween-20 0·05%, pH 6·2 with NaOH) for 20 min, and after cooling washed with PBS. Blocking and permeabilization was performed by incubating sections with 10% normal donkey serum (NDS) and 0·3% triton-X in PBS for 1h at room temperature. Primary antibody incubation was with goat anti-CNTN1 (1:800; 2·5 μg/ml) (AF904, R&D systems; lot EPC021808A) overnight at 4°C in 1% NDS and 0·03% triton-X in PBS. The following day after washing in PBS, incubated with horse anti-goat biotin (1:200) (BA9500, Vector labs) in 1% NDS and 0·03% triton-X in PBS for 90 minutes at room temperature. After washing in PBS, endogenous peroxidase activity was quenched by 3% H_2O_2 in PBS for 30 min. Sections were washed in azide-free PBS and incubated with ABC reagent (Vectorstain Elite ABC HRP kit, Vector, PK-6100) 30 min at room temperature, followed by wash with distilled water. Sections were developed by incubating with DAB reagent (SK-4100, DAB peroxidase substrate Kit, Vector) 1-5 min and stopped stain by rinsing in water. Sections were counterstained with haematoxylin (Mayer's) solution (51275, Sigma), dehydrated back through alcohol series with two changes each: 95% ethanol (30 s), 100% ethanol (30 s), xylene (30 s) and mounted with DPX and coverslip. Sections were imaged on an upright bright-field microscope fitted with digital camera. CNTN1 antibody concentration was established empirically prior to experiments by titration on positive control tissue (healthy human brain cortex) (HP-210, Zyagen) and compared with staining where the primary antibody was omitted.

3 RESULTS

3.1 Diagnostic assays and screening tools used to detect nodal and paranodal antibodies

3.1.1 Abstract

Since the detection of one or more of the (para)nodal antibodies is required to diagnose a patient with a peripheral neuropathy as having an 'autoimmune nodopathy' (AIN), their accurate detection is essential. International testing centres use multiple assays to detect nodal and paranodal antibodies, including ELISA, live or fixed CBA, and IHC of animal teased nerve fibres. Each with different performance characteristics, it is challenging to establish a reliable platform on which to define meaningful characteristics and cut-off values for clinical application.

Inter-laboratory studies comparing different diagnostic assays used shows a high rate of overall concordance in returning positive or negative antibody results between centres (Rinaldi et al., 2022). CBA was found to be the most accurate for testing (para)nodal antibodies, and should be used as the primary method for detection. Live CBA and ELISA within the Oxford neuroimmunology laboratory are highly specific (100%) and very sensitive (92.1% and 79.4%, respectively) in detecting these antibodies (Rinaldi et al., 2022). Separately performed, intra-laboratory comparative studies between ELISA and live CBA concluded that ELISA was as, if not more, reliable than CBA at detecting NF155, CNTN1 and Capsr1 antibodies in patient sera, but less reliable for NF186 mono-specific antibodies.

Myelinated co-cultures of pluripotent human stem cell-induced sensory neurons and rat SCs can be used more experimentally to screen for IgG binding to neuronal structures from patient sera, and although show characteristic binding patterns in each antibody group, are not always positive despite CBA-confirmed antibody positivity, and cannot distinguish between specific antibody.

3.1.2 ELISA

ELISA was used as a method to confirm equivocal test results yielded through CBA, and samples positive for CNTN1, Caspr1 and NF155. ELISA had a lower pick-up rate for the detection of anti-NF186 and anti-NF155 antibodies in panNF antibody-positive sera compared to CBA (**Figure 10C**), thus was not used for this purpose. Overall (not including samples tested for the inter-laboratory study – see section 3.1.4), samples from 66 individual suspected (para)nodal antibody-positive patients have been tested for each antigen target (except Caspr1 as a commercially available protein was not available at the time of testing) using ELISA, of which 88% (58/66) were deemed positive.

3.1.3 Live CBA using HEK cells

3.1.3.1 IgG reactivity to Contactin-1, Caspr1, and the CNTN1/Caspr1 complex

Live CBAs using transfected HEK cells were used routinely, and as the gold standard, to assess for the presence of (para)nodal antibodies in patient sera. Different patterns of IgG binding could be seen when patient sera was applied to CNTN1/Caspr1 co-transfected cells, though identifying the exact antigenic target has not always been clear.

Sera demonstrating IgG binding to CNTN1/Caspr1 co-transfected cells and CNTN1 mono-transfected cells were considered anti-CNTN1 positive. Even in untransfected cells faint membrane reactivity can be seen when anti-CNTN1 antibody-containing sera is applied, thought to be due to a low level of endogenous expression of CNTN1 in HEK cells (**Figure 4**). Despite this, IgG binding from anti-CNTN1 antibody containing sera to CNTN1/Caspr1 co-transfected and CNTN1 mono-transfected cells was clearly discernible over background staining of untransfected cells, and co-localised well with commercial CNTN1 antibodies applied to the same cells, though did not bind to Caspr1 mono-transfected cells (**Figure 5**). Further, staining was abrogated when CNTN1 antibody-positive sera was pre-adsorbed with CNTN1 protein (**Figure 4**).

At first, if IgG from patient sera was found to bind to CNTN1/Caspr1 co-transfected HEK cells but not to CNTN1 mono-transfected cells, they were considered, by default, anti-Caspr1 antibody positive. Subsequent testing of these sera specifically against Caspr1 mono-transfected cells showed positive IgG staining in some sera, but not all. This raised the question of what the exact antigenic target was, if not CNTN1 or Caspr1 individually i.e. CNTN1/Caspr1 complex, but also given the endogenous expression of CNTN1, if positive IgG binding is seen in Caspr1 mono-transfected cells we cannot reliably say these antibodies are targeting Caspr1 alone. This pattern of staining was also observed in another, international, diagnostic laboratory (Dr Luis Querol, Barcelona) carrying out similar experiments. Collaborative work between our laboratory and that of Dr Querol went on to show that within both Oxford and Barcelona patient cohorts, some sera, aside from CNTN1 monospecific antibodies, contained antibodies targeting Caspr1 only, or the CNTN1/Caspr1 complex but neither individually (Pascual-Goñi et al., 2021). In this study, we contributed patients' sera to a cohort of 15 CIDP patients, all of whom had antibodies reactive against the CNTN1/Caspr1 co-transfected HEK cells, but not to mono-transfected CNTN1 cells, in order to further explore their likely specific antigenic target. In co-transfected cells, as we had seen previously, all sera showed IgG better co-localised with commercial CNTN1, vs Caspr1, antibodies, despite none binding to CNTN1 mono-transfected cells. Five also did not show any individual binding to Caspr1 mono-transfected cells.

In our own experiments, we could show that without the addition of patient sera, commercial antibodies individually targeting Caspr1 or CNTN1 antigen targets bind to HEK cells co-transfected with CNTN1/Caspr1, and both individually bind to cells mono-transfected with their respective antigen targets (**Figure 6**). However, in co-transfected cells, the commercial antibodies do not seem to co-localise well, either binding preferentially to different cells, or to the inner and outer membrane within the same cell. Anti-Caspr1 positive sera showed better IgG co-localisation with commercial anti-CNTN1 rather than anti-Caspr1 antibodies (**Figure 7**), also demonstrated by Pascual-Goñi *et al* (Pascual-Goñi et al., 2021).

Anti-CNTN1 and anti-Caspr1 antibody-positive sera showed positive reactivity in ELISA to CNTN1 or Caspr1 protein coated plates, respectively. In our laboratory CNTN1 and Caspr1 were not co-plated, but further collaboration with Pascual-Goñi *et al* did demonstrate reactivity to the complex in ELISA, and sera containing only Caspr1 reactive antibodies were positive in Caspr1 mono-coated ELISA plates, with enhanced signal seen when CNTN1 protein was additionally coated (Pascual-Goñi et al., 2021). Notably, higher Caspr1 ELISA titres were seen in sera that were positive in Caspr1 mono-transfected CBA, compared with sera that were negative in Caspr1 mono-transfected CBA, further suggesting that the sensitivity of CBA to Caspr1 reactivity can be increased with the addition of CNTN1 (**Figure 8**).

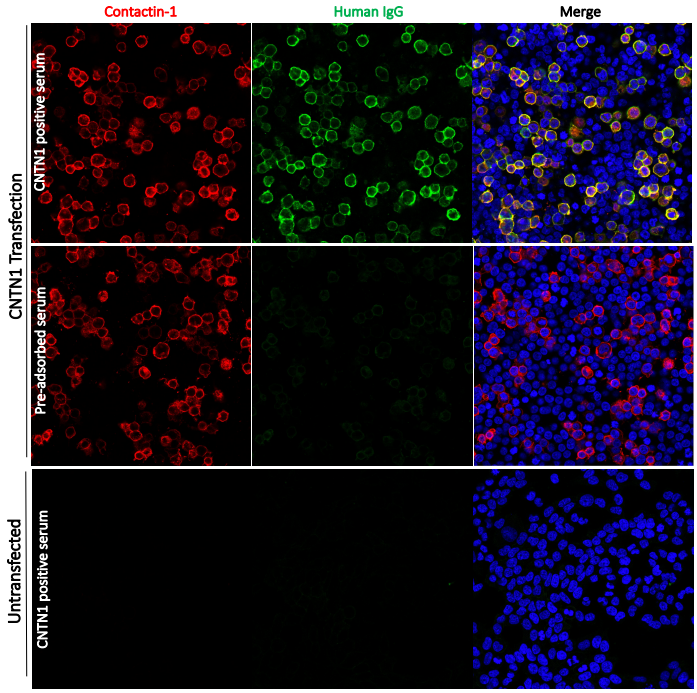


***Figure 4**: Immunoreactivity of IgG from a CNTN1-positive patient on CBA before and after pre-adsorption confirm their specificity for Contactin-1*

IgG from CNTN1-positive sera react with only CNTN1-transfected HEK cells (top panel; commercial CNTN1 stain in red, patient IgG green, cell nuclei in blue). Further, reactivity is abrogated or significantly diminished when pre-adsorbed with CNTN1 protein (middle panel), comparable to no reactivity seen following incubation with untransfected cells (bottom panel). [Supplementary figure 37 from (Fehmi et al., 2023)*]*

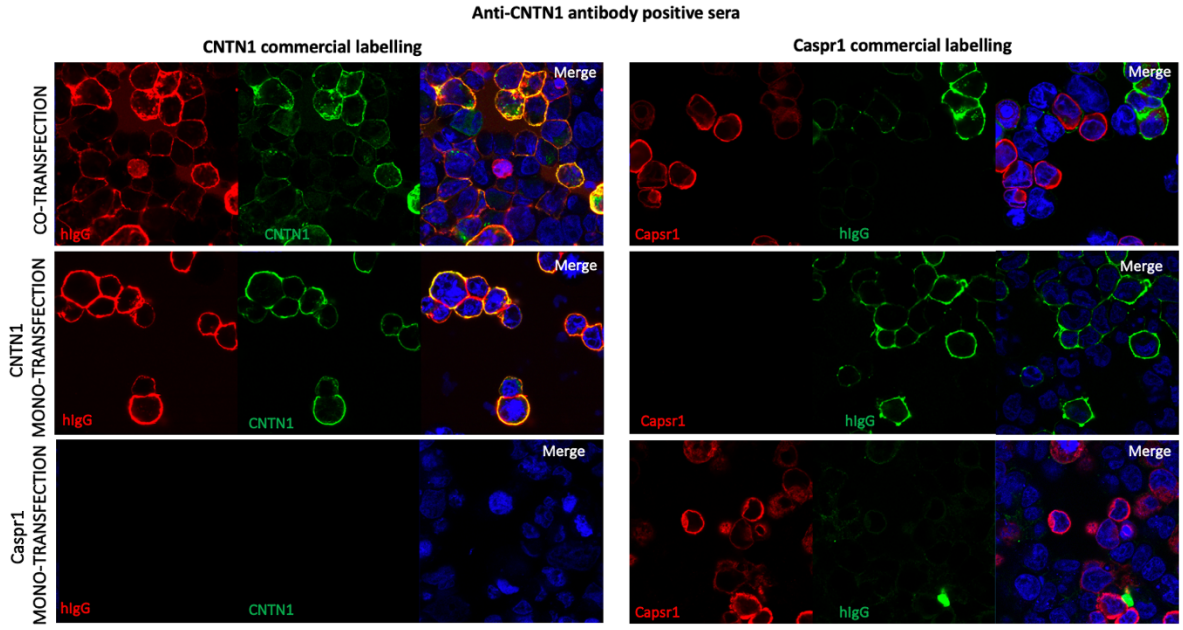


Figure 5: Pattern of IgG reactivity with CNTN1 antibody positive sera with transfected HEK cells

Top panel: Sera positive for antibodies targeting CNTN1 only will show IgG cell membrane reactivity (hIgG in red or green if CNTN1 or Caspr1 commercial antibodies used, respectively) in HEK cells co-transfected with CNTN1 and Caspr1, which co-localises with commercial CNTN1 antibody but not Caspr1 commercial antibody. Middle and bottom panels: anti-CNTN1 positive sera only shows IgG staining in CNTN1 mono-transfected cells (no hIgG staining in Caspr1 mono-transfection panel)

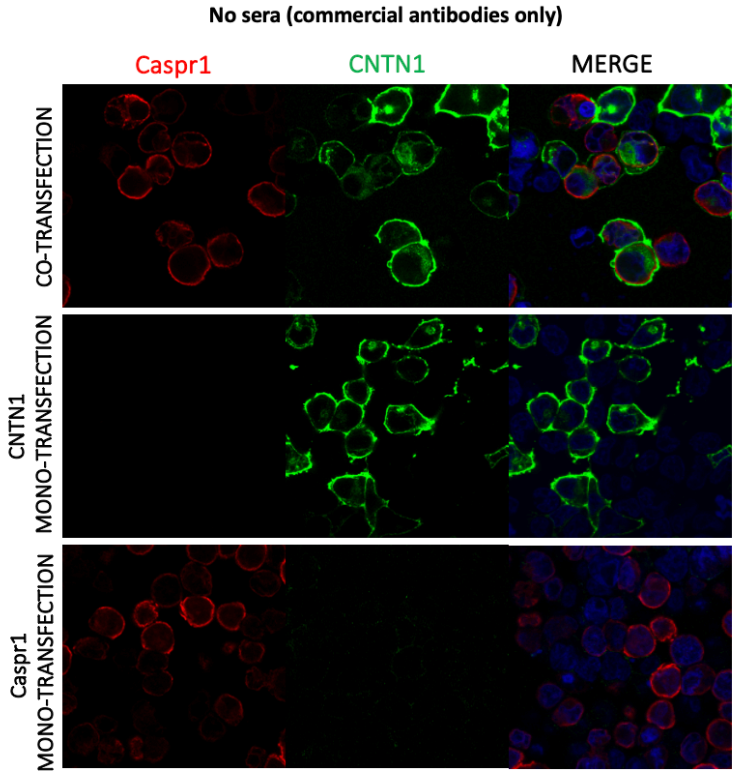


Figure 6: Commercial anti-Caspr1 and -CNTN1 antibody staining in HEK cells

Commercial antibodies targeting Caspr1 or CNTN1 show membrane staining if untreated HEK cells are co-transfected with CNTN1 and Caspr1 (top panel, red and green respectively), though do not co-localise well. Both antibodies are specific to their target (middle panel – anti-Caspr1 antibodies do not stain CNTN1 mono-transfected cells) (bottom panel–- anti-CNTN1 antibodies do not stain Caspr1 mono-transfected cells)

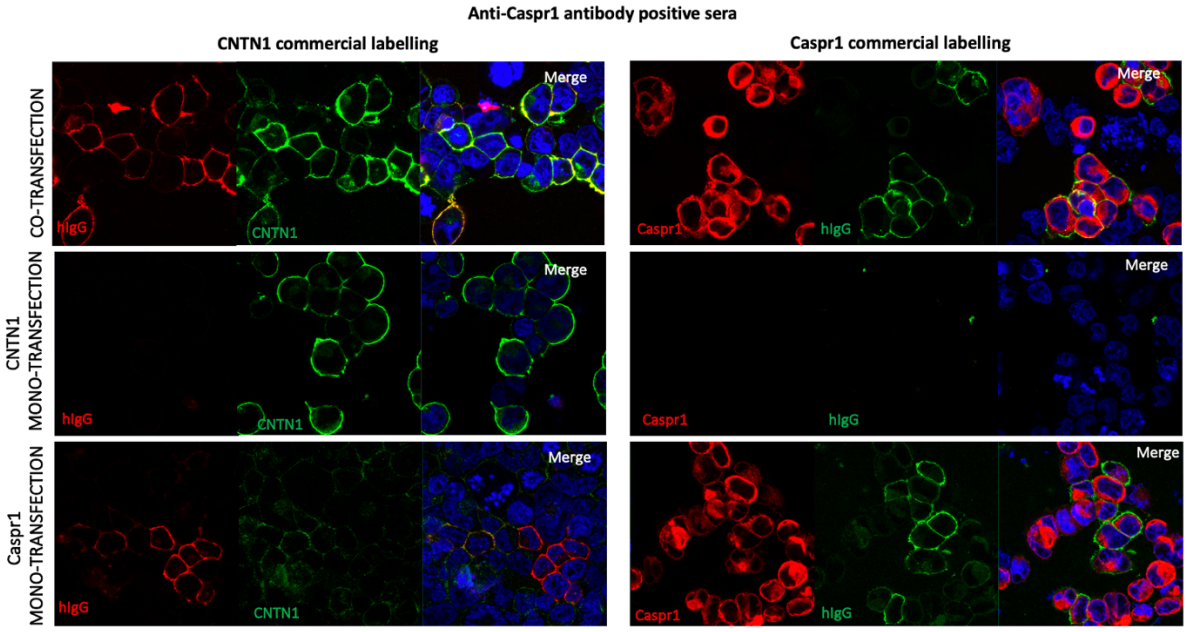


Figure 7: Pattern of IgG reactivity with Caspr1 antibody-positive sera with transfected HEK cells

Top panel: Sera positive for antibodies targeting Caspr1 only will show IgG cell membrane reactivity (hIgG in red or green if CNTN1 or Caspr1 commercial antibodies used, respectively) in HEK cells co-transfected with CNTN1 and Caspr1, which co-localises better with commercial anti-CNTN1 than anti-Caspr1 antibody. Middle and bottom panels: anti-Caspr1 positive sera only shows IgG staining in Caspr1 mono-transfected cells (no hIgG staining in CNTN1 mono-transfection panel)

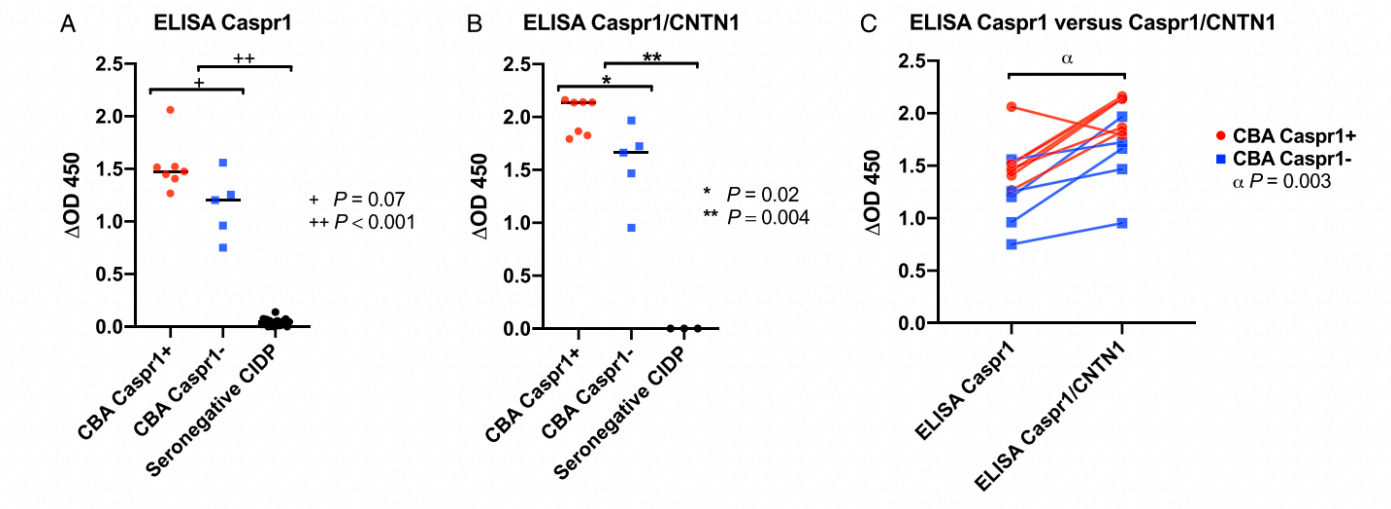


Figure 8: Reactivity of sera against Caspr1 in ELISA

Sera from patients with antibodies reactive to CNTN1/Caspr1 co-transfected HEK cells, and negative against CNTN1 monotransfected cells, were positive in **(A)** Caspr1 and **(B)** Caspr1/CNTN1 ELISA. Generally optical densities (ODs) were higher if CNTN1 and Caspr1 were co-plated (C) (p=0.003). ODs were higher (in both types of ELISA–- A and B) in sera which were positive, vs negative, in the Caspr1 mono-transfected CBA. [Adapted from (Pascual-Goñi et al., 2020)]

3.1.3.2 IgG reactivity to NF155 and NF186

Patient sera reactive to a neurofascin isoform could be classified as either NF155, NF186, or panNF (NF155/NF186/NF140 reactivity) positive on CBA (**Figure 9**). Specificity to each isoform was confirmed by pre-adsorbing sera with the individual target protein, which abrogated binding to that target, but not other isoforms **Figure 9C**). PanNF sera demonstrated IgG binding to both NF186 and NF155 transfected cells; IgG labelling to NF186-transfected cells could be abrogated through pre-adsorption with NF186 (**Figure 9D**), and NF155-transfected cells through pre-adsorption with NF155 (data not shown).

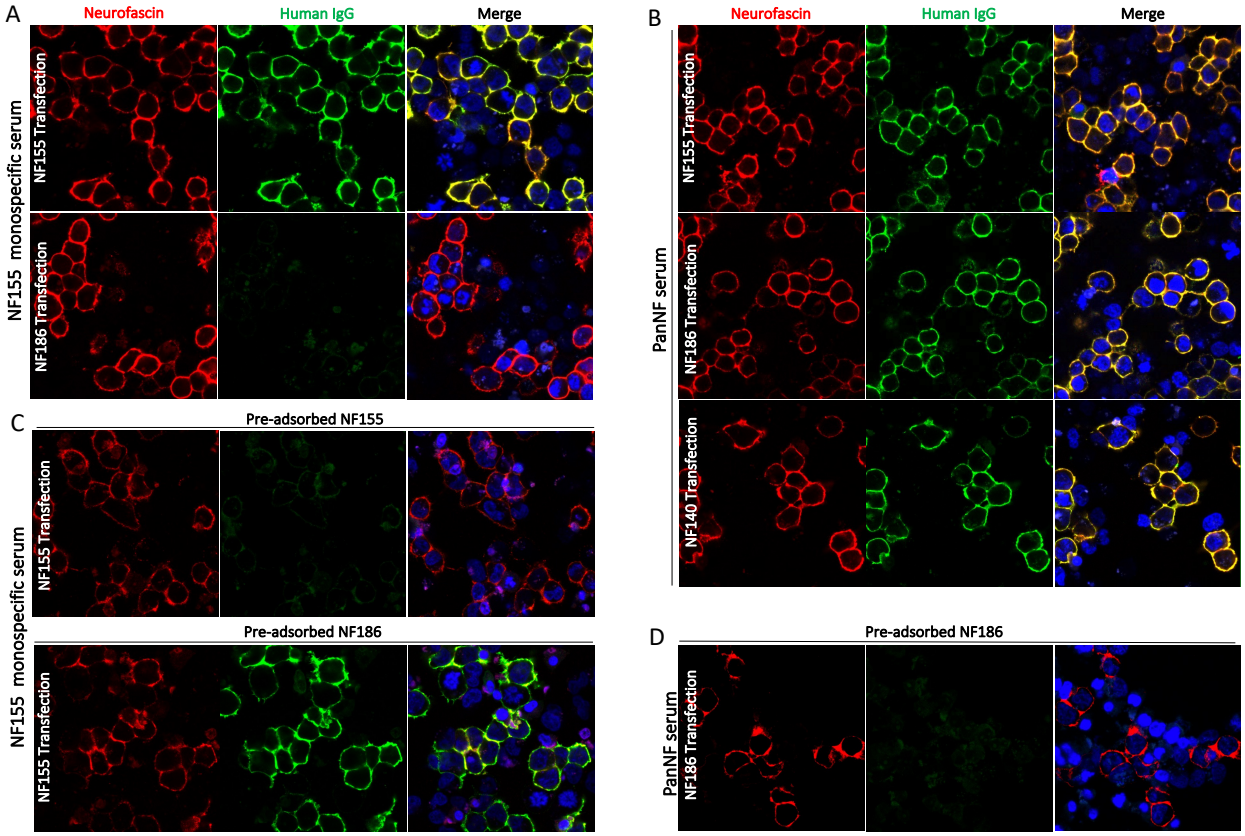


Figure 9: Comparison between neurofascin-155 monospecific and pan-neurofascin antibody reactivity on cell-based assays

(A) *Neurofascin (NF)-155 monospecific serum contains IgG (green) which reacts exclusively with the membrane of NF155 and not NF186 transfected cells (commercial neurofascin antibody, red). IgG4, IgG2 and IgG1 subclass antibodies are present in this example.* ***(B)*** *PanNF sera (patient 6) contains IgG reactive against NF155, NF186, and NF140 transfected cells. Reactivity to all three neurofascin isoforms was found in all patients. Only IgG1 subclass antibodies with this reactivity are detected.* ***(C)*** *Pre-adsorption of NF155 monospecific serum with NF155 protein, but not NF186 protein, abrogates IgG binding to NF155 transfected cells, in contrast to panNF sera, for which no IgG labelling to NF186 transfected cells can be seen after pre-adsorption with NF186 protein* ***(D).*** *Same results are obtained using NF155 transfected cells and pre-adsorption with NF155 protein.[Supplementary figure 1 from* (Fehmi, Davies, et al., 2021)]

3.1.4 A comparison of sensitivity and specificity of ELISA and CBA

In collaboration with four international (para)nodal antibody testing centres, we were able to perform an inter-laboratory validation study to assess the sensitivity and specificity of methods across laboratories used to detect (para)nodal antibodies in a diagnostic setting, including live and fixed CBA, ELISA, and IHC (Rinaldi et al., 2022). Each centre submitted up to 44 sera samples, pre-defined in each centre as 1) (para)nodal-antibody positive sera (from patients who were immunotherapy treatment-responsive), 2) seronegative inflammatory neuropathy or 3) other disease/healthy control sera. An independent centre received the samples and redistributed 170 identical samples to each centre for blinded testing (60 paranodal antibody positive including 10 pre-diluted samples, 108 seronegative: 51 inflammatory neuropathies, 57 healthy or other diseases, and 2 further samples not included in final analysis), performing final analysis of the results. Our test centre (Oxford) was found to return results yielded from CBA and ELISA overall as 96% sensitive (48/50 samples tested positive with either CBA or ELISA) and 100% specific (108/108 all negative for paranodal antibodies). Within specific antibody groups all of the CNTN1 antibody-positive samples (15) were identified by both CBA (co-transfected and monotransfected) and ELISA (100% sensitivity). Caspr1 positive sera (8) were only tested by ELISA if positive binding on co-transfected CBA was identified in our lab, though in one another laboratory Caspr1 mono-transfected CBA were only positive for 4/8 of these samples (50% sensitive). Of the NF155 (15), panNF (10), and NF186 (2) positive sera samples, all tested positive on CBA (100% sensitivity), though 1 NF155, 3 panNF, and 2 NF186 of those samples were negative on ELISA (93%, 70% and 0% sensitivity, respectively). Of the 15 duplicate samples, 14/15 (93%) were reproduced within out laboratory, indicating good intra-lab reproducibility. Further, retesting the samples Oxford originally submitted, results were 100% consistent for positivity/negativity (95.8% for dominant IgG subclass identification). IgG subclass analysis was more frequently detected using CBA than ELISA, and IgG1 and 4 testing were more reproducible than IgG2 and 3.

In keeping with this, using fewer samples in an intra-laboratory (only within Oxford) comparison of CBA vs ELISA, end point titres suggested that these methods were comparable for the detection of anti-CNTN1

(**Figure 10C**, **Figure 11A, Figure 12**), anti-Caspr1 and anti-NF155 monospecific antibodies (**Figure 12**). However, end-point titres for pan-NF antibody-positive sera reactive against NF155 or NF186 proteins were consistently lower or negative on ELISA compared with CBA (shown for 8 patients in **Figure 10C** and 16 patients in **Figure 12**). Further, detection of subclass specificity was comparable in ELISA and CBA for all except anti-pan-NF antibodies, for which IgG1 subclass reactivity was strong on CBA but infrequently detectable using ELISA (shown for published anti-panNF patient cohort in **Figure 10B** and anti-CNTN1 cohort in **Figure 11B and C**).

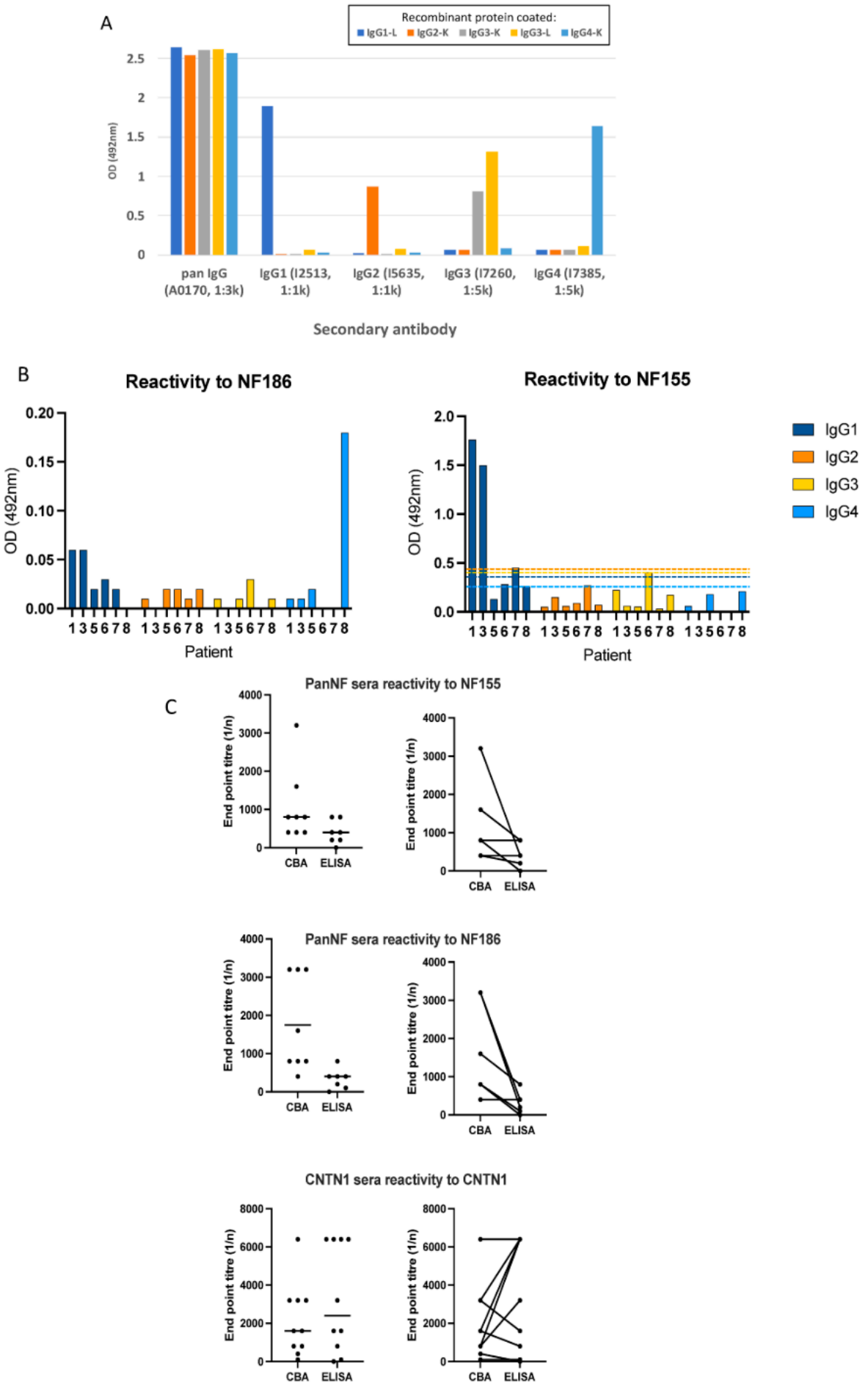

A
Recombinant protein coated:
IgG1-L
IgG2-K
IgG3-K
IgG3-L
IgG4-K
OD (492nm)
pan IgG (A0170, 1:3k)
IgG1 (I2513, 1:1k)
IgG2 (I5635, 1:1k)
IgG3 (I7260, 1:5k)
IgG4 (I7385, 1:5k)
Secondary antibody
B
Reactivity to NF186
Reactivity to NF155
OD (492nm)
Patient
IgG1
IgG2
IgG3
IgG4
C
PanNF sera reactivity to NF155
PanNF sera reactivity to NF186
CNTN1 sera reactivity to CNTN1
End point titre (1/n)
CBA
ELISA

Figure 10: Subclass specificity and comparison between CBA and ELISA for sera from 8 PanNF AIN patients

(A) *A pan-IgG secondary antibody detects all 5 human IgG recombinant proteins similarly. The subclass antibodies produce a signal only in wells coated with recombinants of their specified subclass.* **(B)** *Sera from patients in this cohort are tested for antibody subclass reactivity to either NF186 or NF155. Cut-off optical density values for each subclass are indicated by the dotted lines (IgG1 0.35, IgG2 0.42, IgG3 0.40, IgG4 0.26), thus P1, 3 and 7 are positive for IgG1 antibodies only by ELISA. All other sera and subclass combinations result in OD results below the limits of detection.* **(C)** *End point titres on the cell-based assay (CBA) are consistently higher than by ELISA for both NF155 and NF186 antibodies but ELISA is at least equally as sensitive to the CBA for CNTN1 positive sera. The panels on the left-hand side show the individual data points and mean titre, the panels to the right show the same data with lines linking individual patients' results across the 2 assays. [Supplementary figure 3 extracted from* (Fehmi, Davies, et al., 2021)*]*

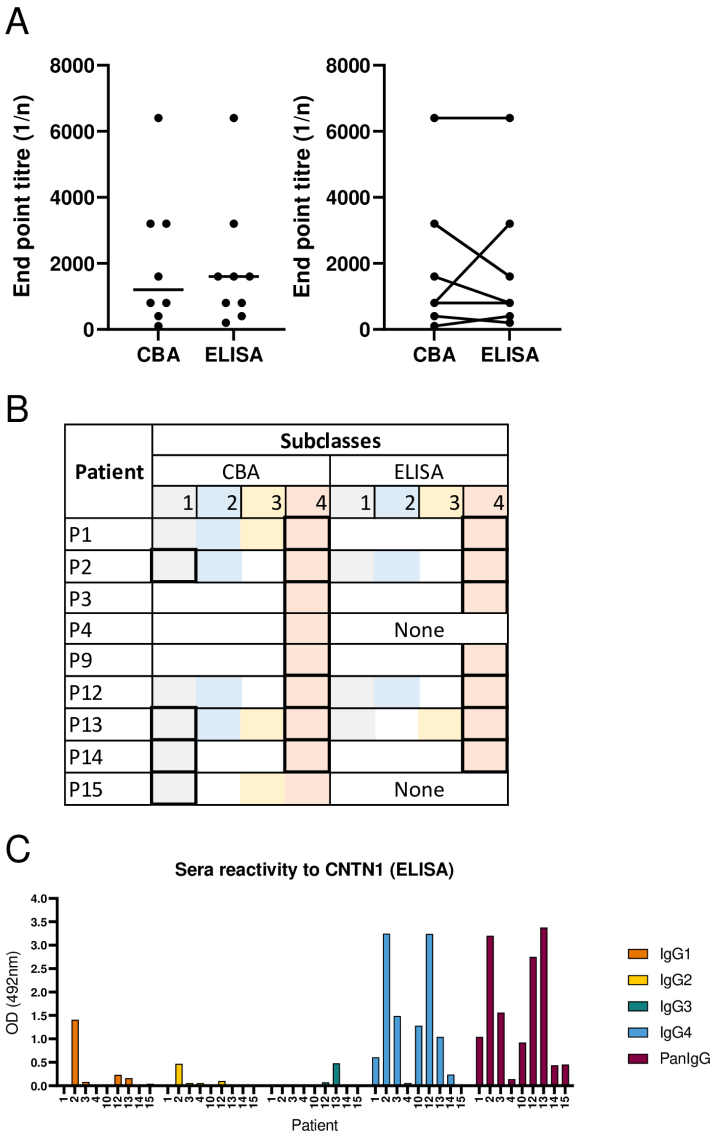


Figure 11: A comparison between CBA and ELISA of end-point titre and subclass specificity of CNTN1 antibodies

(A) *The average end-point titre for CNTN1 antibody detection was slightly higher using ELISA compared with CBA, though antibodies were detected in all the 9 patient sera samples available locally for testing using both assays (titre for P09 was only tested on ELISA so no data point is shown for CBA). The mean titre is indicated by the lines on left-hand graph, and lines linking individual patients' results across 2 assays can be seen on the right-hand graph. There were 2 patients with titres of 3200 on CBA (both 1600 on ELISA) and 2 with titres of 800 on CBA, thus these data points are merged.* **(B)** *For the same 9 patients, antibody subclass testing revealed specificity mainly to IgG4 in both assays, but often with the presence of other subclasses. The predominant subclass, assessed by visual scoring of the fluorescence intensity of IgG binding to transfected cells in CBA, is indicated by a boldly outlined box. IgG1 was deemed to be the predominant subclass in P15, and equally dominant in P2, P13 and P14. No subclass was detected on ELISA for P4 and P15.* **(C)** *Optical density (OD) is shown as a quantitative measure for each IgG subclass and pan-IgG in the ELISA for the same patients. [Supplementary figure S2 from* (Fehmi et al., 2023)*]*

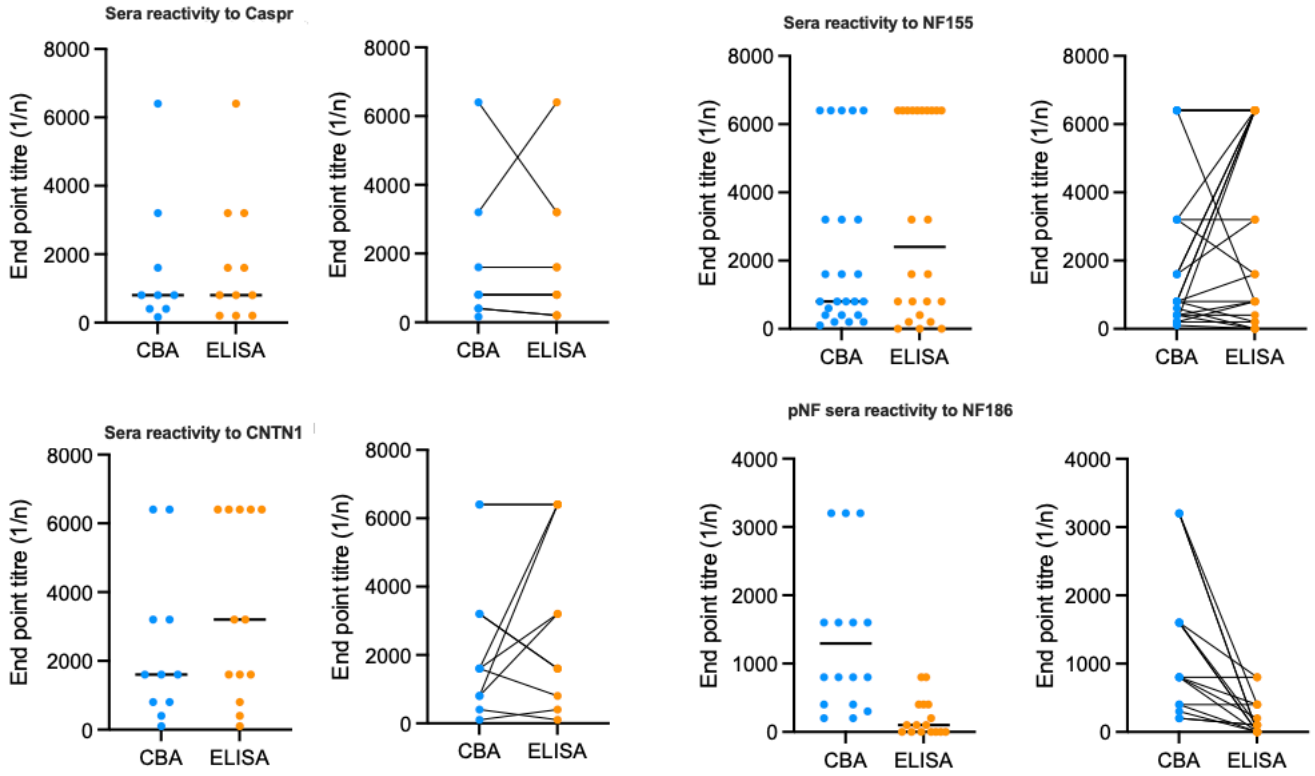


Figure 12: End-point titre comparison between CBA and ELISA for all (para)nodal seropositive patients

End point titres on the cell-based assay (CBA) are consistently higher than by ELISA for NF155 and NF186 antibodies in panNF (pNF) positive sera (panNF reactivity only shown against NF186). ELISA is at least equally as sensitive to the CBA for NF155 mono-specific, caspr1 and CNTN1 positive sera. The panels on the left-hand side show the individual data points and mean titre, the panels to the right show the same data with lines linking individual patients' results across the 2 assays.

3.1.5 Myelinated co-cultures as a screening tool for the presence of established and novel peripheral nerve-reactive antibodies

Myelinated sensory neuronal co-cultures can be used to identify topographical IgG binding from patient sera to axonal and/or glial structures in a live in vitro model. Through the development of using a 96 well platform to establish these cultures, and the introduction of a cryopreservation step at the point at which precursor cells can be matured into sensory neurons (work by Dr Alex Davies, University of Oxford) (**Figure 13** and **Figure 14**), we screened 253 patient sera samples for IgG labelling (**Table 1**). Sixty were known to be (para)nodal antibody-positive by CBA, 162 seronegative, and 31 healthy control sera.

We found cultures to be positive for IgG labelling in both antibody-seronegative (8%; 14/162), and CBA-confirmed (para)nodal antibody positive patient sera (58%; 35/60), though only detectable in half to three-quarters of patients in the latter group (**Figure 15**). Sera containing CNTN1 or Caspr1-reactive antibodies stained axons and were the groups most likely to have positive IgG staining in culture (82% CNTN1, 80% CNTN1/Caspr1 positive). NF155 reactive antibodies stained the nodal and/or glial structures, whereas panNF reactive antibodies typically stained nodes with occasional axonal reactivity. There was no significant correlation between higher CBA antibody titres and detectable IgG binding in culture ($p=0.52$ for CNTN1/Caspr1, $p=0.24$ for panNF, 0.47 for NF155 positive samples, using unpaired t-test to compare means) (**Figure 15**).

The 14 CBA-seronegative samples positive for IgG staining in co-culture were rated by two independent observers. Seven of these labelled axons or nodes, and 7 glial structures. One of the healthy control samples was initially scored as showing an axonal pattern of staining, though was deemed negative on repeat testing.

Through a subsequent validation study, 56 of these samples, including 33 seropositive, 11 seronegative and 12 healthy control sera, were retested at two further timepoints, by two different experimenters (blinded to

sample ID), using neurons differentiated from two different stem cell lines. Manual analysis for the presence or absence of IgG binding and topographical labelling under confocal fluorescence microscopy was performed for each plate by each experimenter, and scores documented prior to unblinding. There was good inter-assay, inter-experimenter, and inter-observer correlation of IgG reactivity scored as positive or negative (**Figure 16**) (Fleiss' Kappa score 0.709, z=30.9 using 'Bangdiwala' agreement chart). Repeat imaging of a subset of plates using an automated imaging system reduced the rate of overall agreement of positive IgG binding (kappa score 0.635, z=34.2).

Agreement of IgG binding to specific neuronal and glial structures once rated at positive was less concordant, even where agreement on overall positivity was **Figure 19**). Some examples of discrepencies in binding patterns are provided in **Figure 17** and predominantly occurred when there was felt to be binding to the nodal region in addition and separately to another structure i.e. axon or myelin by one observer but not another. IgG binding seen in (para)nodal antibody negative patient sera included both neuronal and glial structures, and was seen in patients with a range of suspected immune-mediated neuropathies (**Figure 18**).

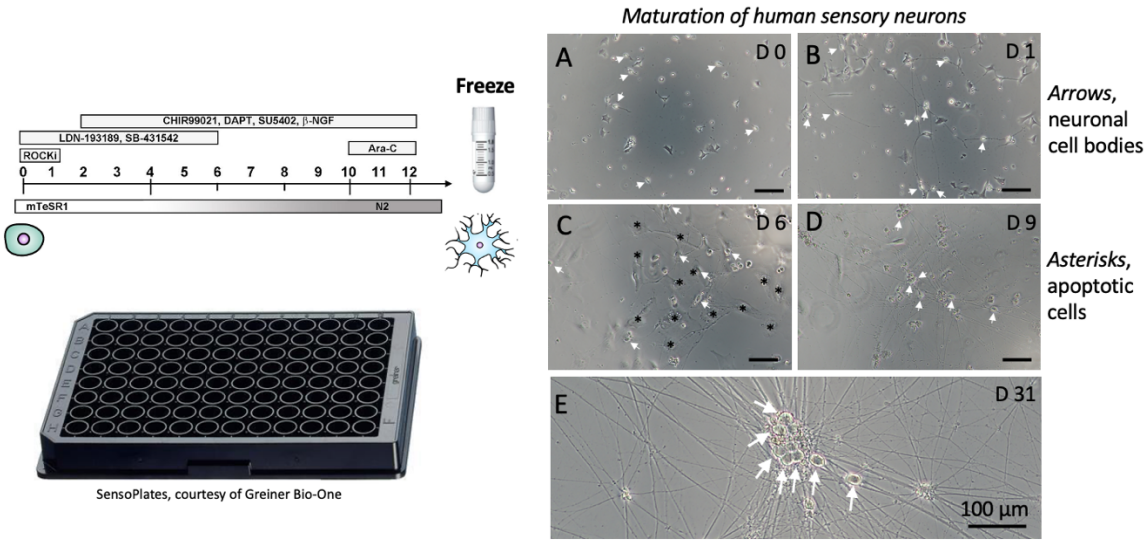


Figure 13: Optimisation of hiPSC-derived sensory neuron differentiation and patient cohort screened for IgG binding in myelinated co-cultures

(*A)* *Differentiation of sensory neurons from hiPSCs (cryopreserved in bulk on day 11), seeded in 96 well microplates and matured for up to four weeks. Maturation and incubation with rat Schwann cells lead to mature myelinated co-cultures by 8 weeks after neurons are initially seeded. Myelin basic protein (MBP) reveals the compact myelin internodes of neurofilament positive neurons (NF200). DAPI (4', 6-diamidino-2-phenylindole) stains Schwann cell and neuronal nuclei.* ***B)*** *Sera samples screened for specific IgG reactivity are taken from seropositive, seronegative and healthy control patients. [adapted from* (Clark et al., 2017)]

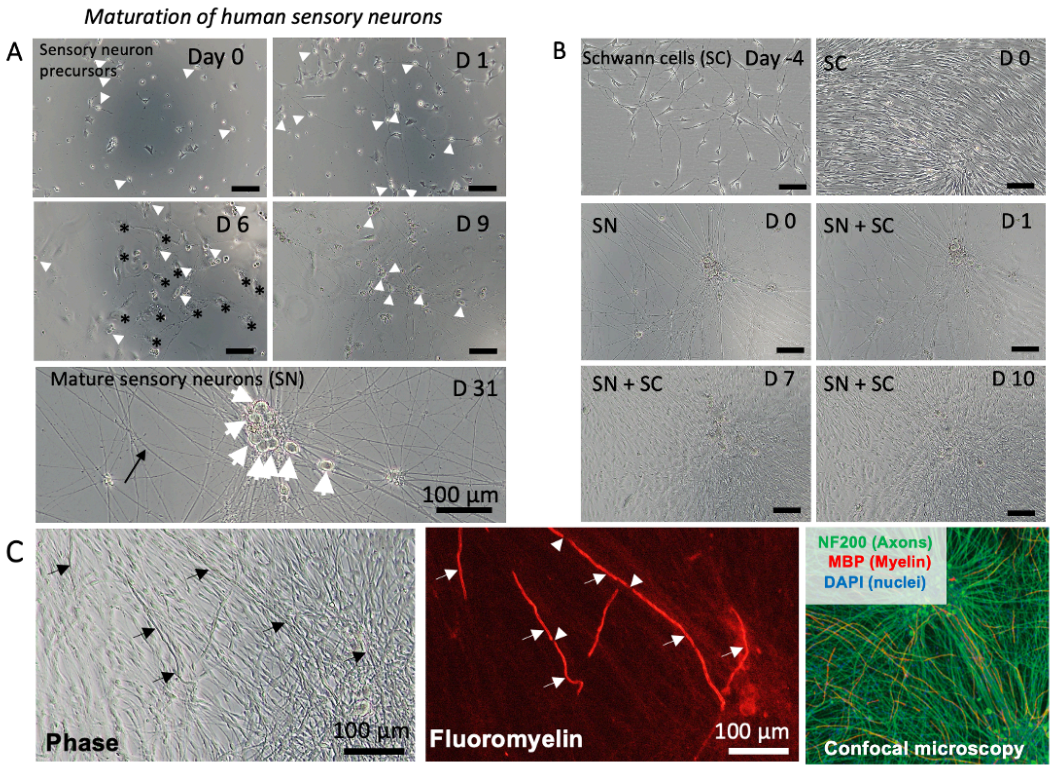


Figure 14: Generation of stocks of sensory neuron precursors and development of a high throughput culture system of human stem cell-derived sensory neurons myelinated with rat Schwann cells

[Adapted from (Clark et al., 2017) by Dr Alex Davies]

(A) *Light microscopy showing maturation of human sensory neurons (white arrows: neuronal cell bodies, black asterisks: apoptotic cells, black arrow: axon).* ***(B)*** *Expansion (4 days) and seeding of rat Schwann cells onto neuronal cultures.* ***(C)*** *mature myelinated neurons can be visualised under light microscopy (internodes indicated by arrows), using fluoromyelin to stain live cultures for internodal myelin, and confocal fluorescence microscopy (x20 magnification) with axons (neurofilament 200 – NF200 stain in green), myelin (Myelin Basic Protein – MBP in red) and nuclei (4',6-diamidino-2-phenylindole – DAPI blue).*

Cohort		Number of patients	Age (mean)	Gender M:F
Seropositive (by CBA)	**NF155**	22	59.4	7.5:1
	Pan-NF	17	50.2	1.8:1
	CNTN1	11	58.7	4.5:1
	CNTN1/Caspr1	10	57.46	2.3:1
Seronegative (by CBA)		162	57.9	1.4:1
Healthy Controls (seronegative by CBA)		31	TBC	TBC
TOTAL		**253**		

Table 1: Table summarising proportion of (para)nodal antibody seropositive and seronegative samples tested for IgG binding in co-culture during preliminary screening

Sera from all 60 patients seropositive for (para)nodal antibodies (confirmed on cell based assay), 160 seronegative (patients with suspected immune-mediated neuropathies), and 31 healthy controls, were applied to the cultures and assessed by a blinded observer and scored as either positive or negative for IgG immunolabelling. During the preliminary stage of testing these were tested ad-hoc, by one or more investigators and observers blinded to serological status of each sample, using one of three different stem cell lines, at different times. Mean age was comparable between cohorts, and in the seropositive group patients were predominantly male. Abbreviations: CNTN1 – Contactin-1; Caspr1 – Contactin-associated protein-1; NF155 – Neurofasin155; PanNF - Pan-neurofascin

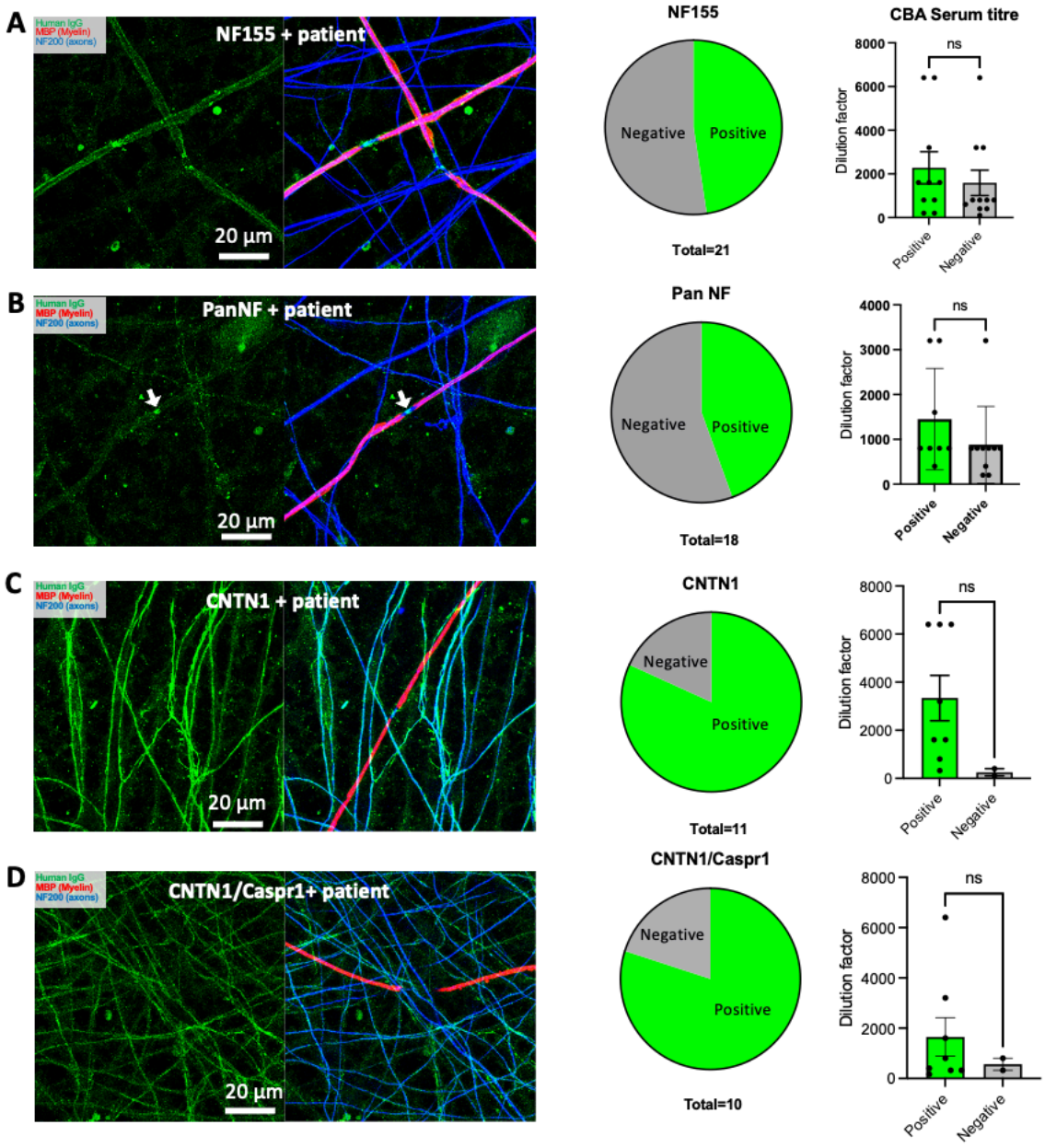


Figure 15: Patterns of positive immunostaining: IgG reactivity detected in myelinated co-cultures

Confocal fluorescence microscopy images show typical human IgG (green) staining patterns for ***(A)*** *NF155 (nodal and/or myelin staining in 48%),* ***(B)*** *panNF (nodal, with occasional axonal staining in 44%),* ***(C,D)*** *CNTN1 or CNTN1/caspr1 (axonal staining in 82% and 80%, respectively) seropositive patients tested. Pie charts represent the proportion of sera showing positive and negative IgG reactivity in co-culture that were previously found to be positive for that antibody on a CBA. Bar charts with error bars show the end-point titre of each sera sample on CBA. Although there was no significant correlation between higher titres and positive IgG reactivity in co-culture there was a trend with CNTN1 and CNTN1/caspr1 antibody seropositive samples.*

Abbreviations: CIDP – Chronic inflammatory demyelinating polyradiculoneuropathy; CISP - Chronic immune sensory polyradiculopathy; GBS - Guillain-Barré syndrome

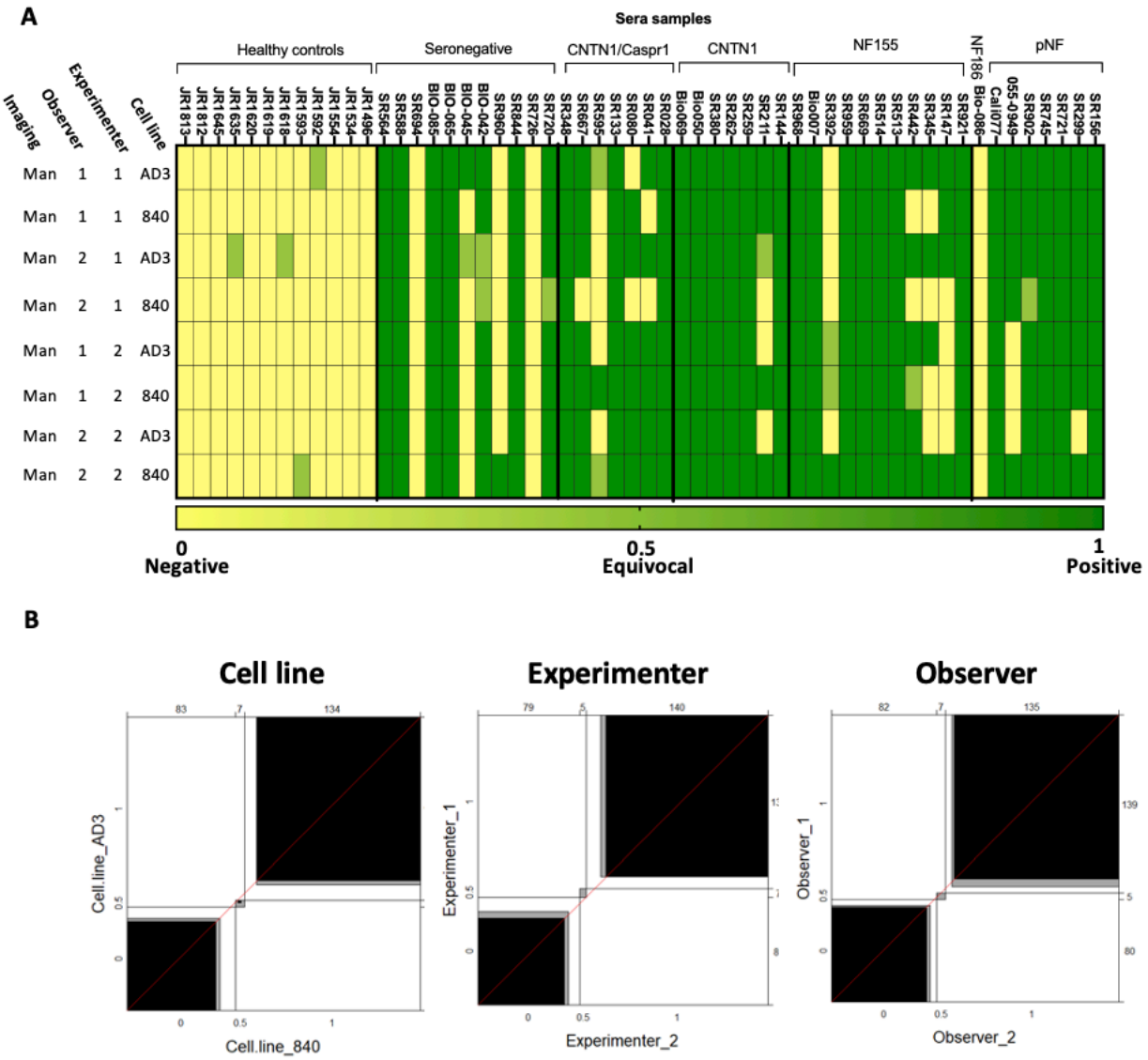


Figure 16: Inter-assay, inter-experimenter and inter-observer agreement of positive immunoreactivity of serum samples on myelinating co-cultures

(A) Heat map showing rating of IgG positivity in a live co-culture assay after exposure to patient serum samples (n=56) from different serological cohorts. For overall agreement of sample reactivity assessed under different conditions a Fleiss' Kappa statistic for m Raters was performed: Subjects = 56, Raters = 8. Kappa = 0.709 (z = 30.9). ***(B-D)*** *Agreement ('Bangdiwala') charts for pairs of variables(Bangdiwala & Shankar, 2013): Cell line (B), Experimenter (C) and Observer (D). Agreement is not substantially influenced by any one variable. Abbreviations: Man – manual*

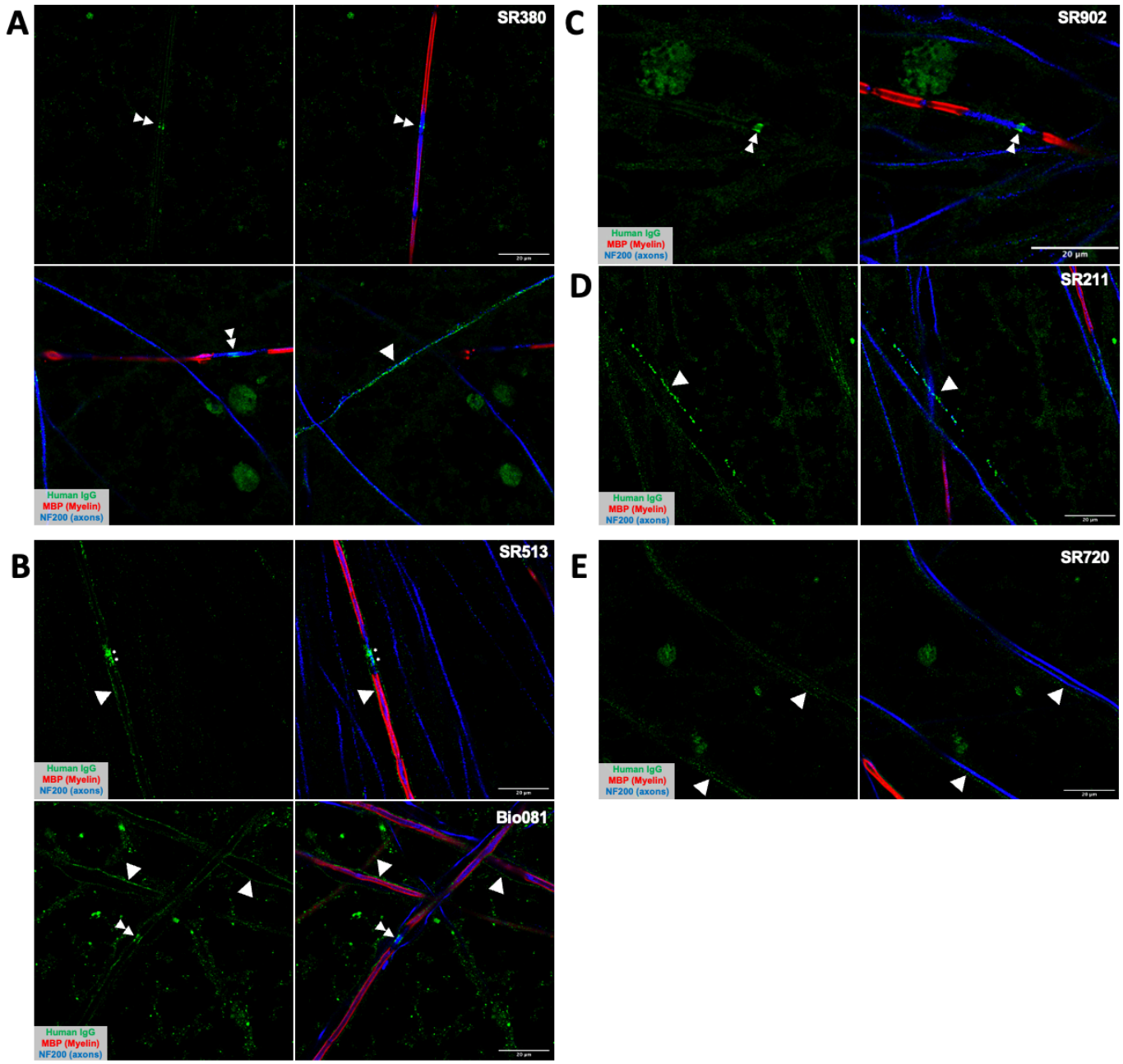


Figure 17: Discrepancies in topographical IgG binding patterns

Discrepancies in IgG binding observations were most often when multiple neuronal structures were labelled, for example ***(A)*** *nodal binding (double arrow head) in the context of axonal IgG labelling (large arrow head bottom right), where one observed may consider this to be independent binding of node and axon, and another may interpret this as axonal IgG binding with concurrent binding at the exposed axolemma in the nodal region. Similarly, in the context of IgG binding to the myelinating Schwann cell (large arrow heads)* ***(B)*** *paranodal (asterix) and nodal (double arrowhead) labelling can be seen, which may be documented as either independent binding of the paranode, or just Schwann cell IgG binding with increased intensity of signal where the two cells meet in the nodal region. Subtle patterns of* ***(C)*** *nodal* ***(D)*** *axonal, and* ***(E)*** *non-myelinating Schwann cell (all indicated by yellow arrows) can also cause discrepancies in agreement of IgG staining.*

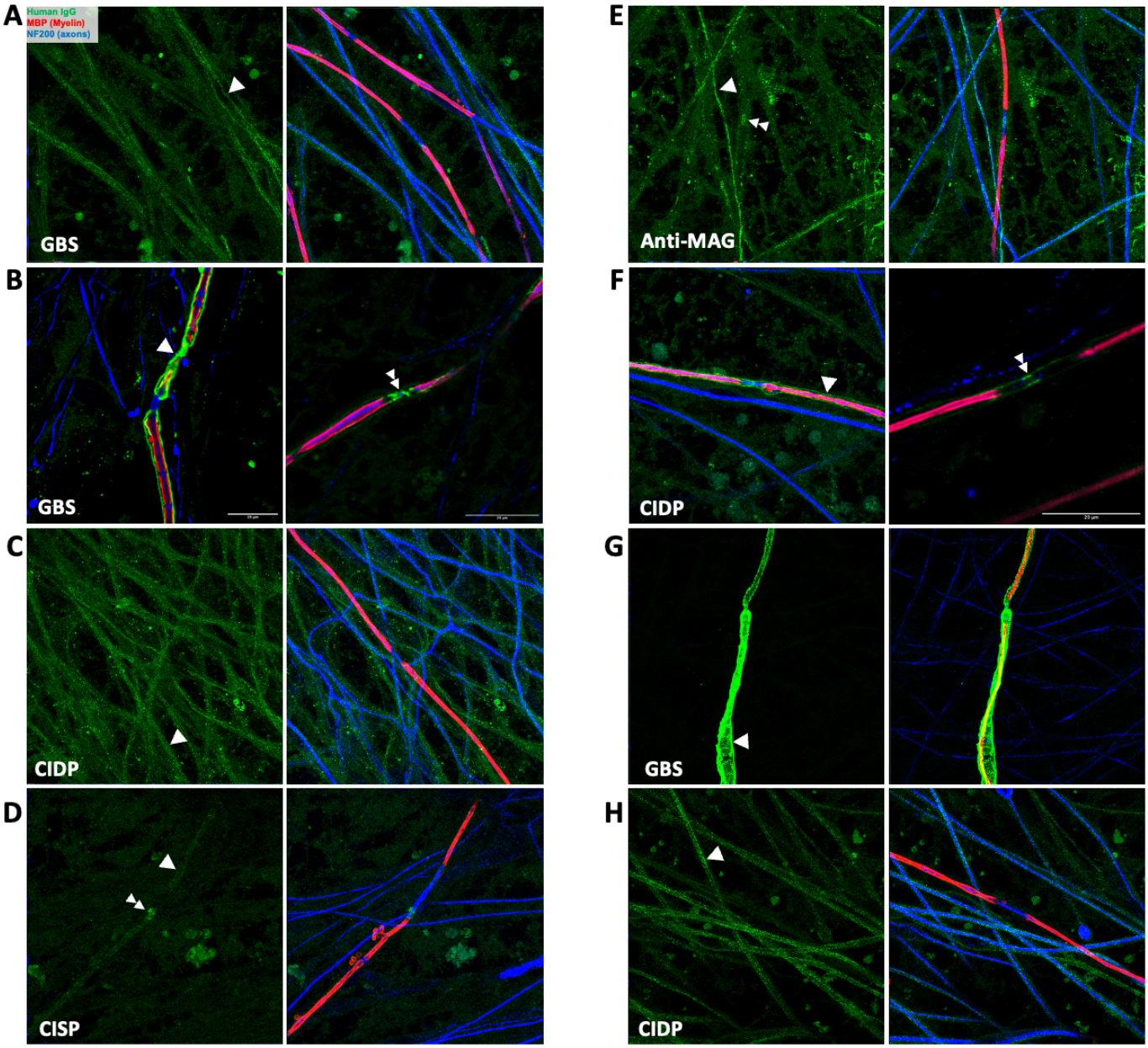


Figure 18: Patterns of positive IgG immunostaining observed in patients seronegative for (para)nodal antibodies (validation study)

Sera from patients found to be negative for (para)nodal antibodies on CBA showed IgG binding (arrow heads) in myelinated co-cultures on the validation screen to the non-myelinating Schwann cells ***(A, C, H),*** *myelinating Schwann cells alone* ***(G)*** *or with nodal binding (double arrow heads -* ***B, D, F****), and axonal with nodal binding* ***(E)****. The diagnosis for each patient is stated on the images.*

Abbreviations: GBS – Guillain Barré syndrome; CISP – Chronic Immune Sensory Polyradiculopathy; Anti-MAG – Anti-Myelin associated protein; CIDP – Chronic Inflammatory Demyelinating Polyradiculoneuropathy

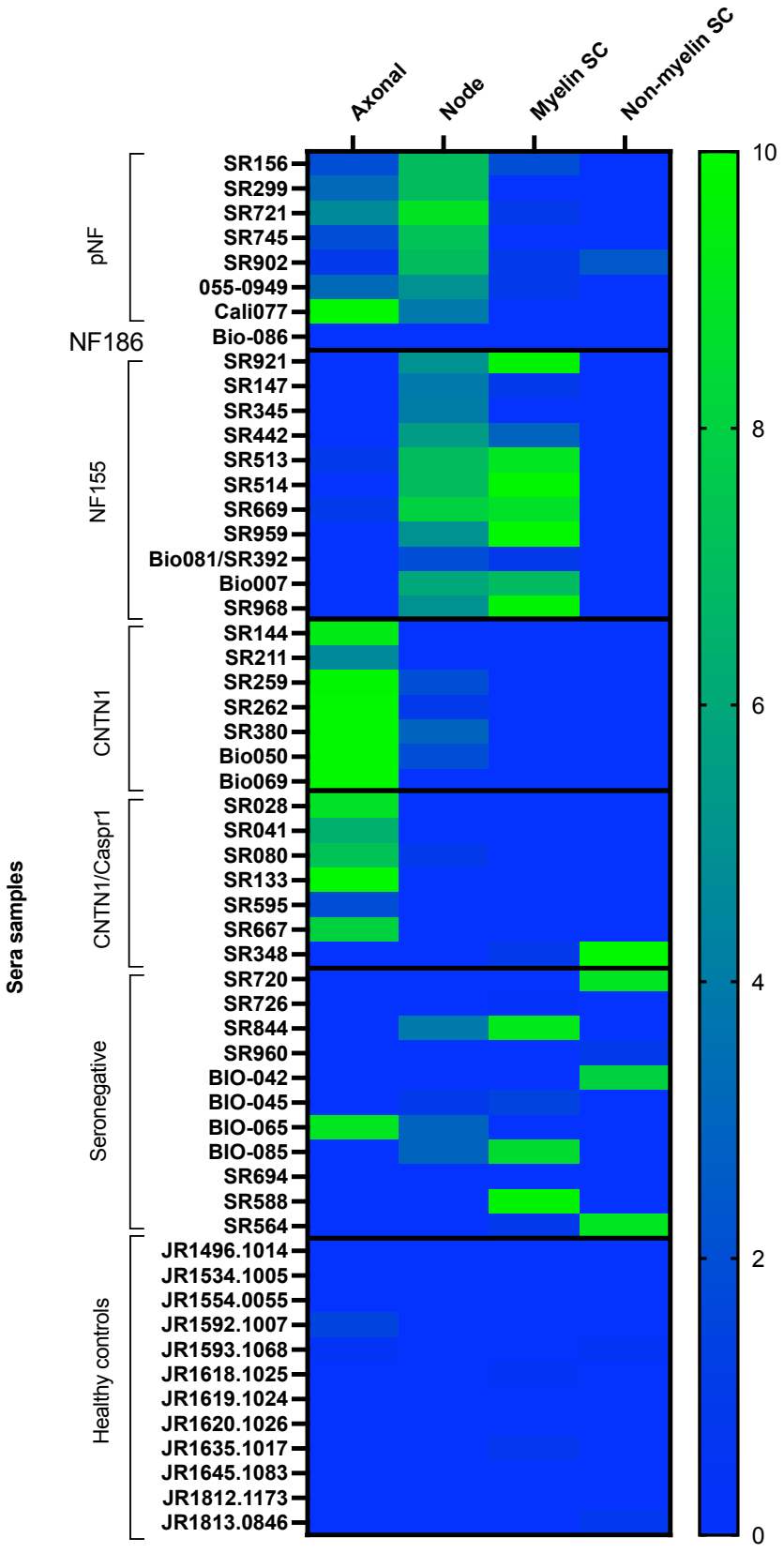


Figure 19: Topographical IgG binding patterns from patient and control sera samples in myelinated co-cultures

Heat map showing topographical binding pattern of IgG in samples tested in the validation cohort. Positivity scores (green) were rated from 4 rating scores (2 replicates from 2 different observers).

3.1.6 Discussion

The live CBA was concluded to be the most sensitive and specific assay to detect nodal and paranodal antibodies in patient sera, both within our laboratory (vs ELISA) and between international testing centres (vs fixed CBA, ELISA and IHC) (Rinaldi et al., 2022). Further, there was good intra- and inter-laboratory reproducibility of results. In particular, we found ELISA could be as or more sensitive upon testing for antibody mono-reactivity to CNTN1, Caspr1 and NF155, making it useful as a confirmatory test in addition to CBA, particularly when equivocal staining patterns were seen on CBA. However, it was less likely to pick up panNF antibodies using either NF155 or NF186 protein coating. Given strong reactivity could be seen in CBA using panNF antibody containing sera, this was likely due to the conformational differences in protein epitope used for ELISA versus in their native membrane conformation in CBA.

Other testing laboratories that have previously reported on sera positive for (para)nodal antibodies exposed patient sera to CNTN1, Caspr1 or NF155 mono-transfected cells. Through performing testing to NF186 transfected cells we were able to additionally identify anti-NF186 mono-specific antibodies, and also anti-panNF antibodies, whereas this latter group may have been previously reported as anti-NF155 antibody-positive sera. This suggests there was most likely an under-reporting of panNF/NF186 positive AIN patients, which is clinically relevant given from our panNF cohort (as described in section 3.2.3 ‘PanNF-antibody cohort’) (Fehmi, Davies, et al., 2021), and a prior report of a small panNF cohort (Stengel et al., 2019), it is clear that their presentation is more rapid, severe, and refractory to standard treatments. This emphasises the importance of testing both neuronal and glial isoforms of neurofascin.

In collaboration with Dr Luis Querol’s laboratory in Barcelona, Spain, we have also identified a small cohort of patients who have sera reactive to the CNTN1/Caspr1 complex but not to either antigen individually (Pascual-Goñi et al., 2021). This highlights the importance of testing sera against CNTN1 and Caspr1 mono-

transfected HEK cells if they are found to be reactive to CNTN1/Caspr1 co-transfected. Pascual-Goñi et al importantly revealed that antibodies binding the CNTN1/Caspr1 complex should be considered a single subgroup within the autoimmune nodopathies. A high proportion of these sera demonstrated weaker reactivity to Caspr1 if transfected alone in a CBA, and although also positive for caspr1 in ELISA, the signal was enhanced with the addition of CNTN1 protein i.e. although these antibodies mainly target Caspr1, optimal reactivity is achieved by Caspr1 forming a complex with CNTN1. Only half of this cohort reported neuropathic pain, though notable features included early axonal motor involvement on neurophysiological studies and a high proportion with sensory ataxia. Response to IVIg was incomplete and there was a clear benefit with RTX (90% responded).

The main limitations of using live CBA to detect these antibodies are that membrane IgG staining can be subtle and/or difficult to distinguish between high background signal. Accurate and consistent detection and rating of positivity (1-4) relies on negative, weak and strong positive controls being used for each assay run, in order to control for differences in cell batches and transfection efficiency. Manual interpretation of positive reactivity using an arbitrary scale additionally relies on consistency of the observer. Developing a stably transfected HEK cell line, and using the same, experienced operator to run and interpret the assays may ensure more efficiency and accuracy of results, though potentially decreasing protein expression levels over time could introduce variability.

The use of myelinated co-cultures to screen the sera of patients suspected to have an immune-mediated neuropathy has not been reported before, and is a novel approach for antibody discovery in these patients. We have shown that using sera with a known (para)nodal antibody (detected by CBA), typical IgG binding patterns of axonal and glial structures can be seen in vitro for more than three-quarters of CNTN1 and Caspr1 patients (axonal), and almost half of neurofascin patients (nodal +/- glial or axonal). This does not appear to be titre dependent, though sample sizes were small. This perhaps indicates that, particularly with neurofascin reactivity, regardless of end point titre in CBA, binding and reactivity is dependent on

accessibility, density and conformation of the epitope in their more native environment, versus overexpression in a CBA. Binding of NF155 and panNF antibodies to the node but not the paranode suggests different conditions and as yet unknown external factors may be required to allow permeability of the tight paranodal myelin loops to antibodies. It is unclear why panNF antibodies also show subtle binding to sensory axons in culture, and NF155 antibodies to glial structures (rat derived). This may suggest cross reactivity to molecules only present in this model of peripheral nerves.

This in vitro model of a myelinated sensory peripheral nerve currently provides the closest resemblance to the native assortment of nodal and paranodal molecules in humans, though despite reproducible binding patterns seen for each individual antibody group, it cannot reliably be used to identify the culprit antibody in patients with a suspected nodopathy.

The optimisation of this assay to provide more efficient and reproducible results is underway. We have already shown that there is good reproducibility of the detection of positive IgG reactivity in culture, and that cell line, and different experimenters and observers do not significantly affect this. By using a 96 well platform to screen larger batches of patient sera, and automated imaging to detect positive IgG reactivity, we will be able to further optimise the reliability of this assay, and have a more robust model in which to identify potential candidates for antibody discovery. By correlating positive IgG binding in culture to the clinical details of patients we can additionally learn more about the clinical relevance of these findings, and potentially support clinical evidence that a neuropathy is likely to be immune-mediated, despite the absence of a defined pathogenic antibody being identified through targeted protein assays.

3.2 Clinical-serological phenotype of patients seropositive for (para)nodal auto-antibodies

3.2.1 Abstract

Between 2015 and 2023, through screening a cohort of patients with a suspected immune-mediated or inflammatory peripheral neuropathy, 121 (6.2%) patients were positive for a (para)nodal antibody (autoimmune nodopathy -AIN), and 1819 were negative. AIN patients demonstrated a distinct clinical phenotype compared to seronegative counterparts, in keeping with that already described in the literature. This is typified by a severe motor and sensory, proximal and distal, symmetrical neuropathy which has an acute or subacute onset, is associated with atypical features (not commonly seen in other inflammatory neuropathies), and responds poorly to standard therapies used in inflammatory neuropathies. An aggressive onset and severe course of disease was significantly more frequent in panNF patients, whilst nephrotic syndrome was significantly associated with patients harbouring anti-CNTN and anti-panNF antibodies.

Although there are no electrophysiological or histological features that are unequivocally diagnostic of AINs, and they often meet electrodiagnostic criteria for CIDP, they show characteristic hallmarks of antibody-mediated attack at the node. Strongly reactive IgG4 and IgG1 (para)nodal antibodies were found in all antibody groups, contrary to prior literature implicating only IgG4 in the majority of patients. In keeping with other cohorts reported, a potent complement-activating IgG subclass was identified almost exclusively in panNF antibody patients (IgG1 in our cohort, IgG3 in others). AIN patients were more likely to respond (clinically and serologically) favourably to CD20 B-cell depleting therapy (RTX) and were less likely to relapse on this treatment. So far, antibody titres seem to correlate with clinical course and show promise as not just diagnostic, but also prognostic serum biomarkers.

3.2.2 Overall cohort screened (BioSPIN and diagnostic service cohorts)

The following work characterising the clinical and serological features of panNF and CNTN1 antibody-positive AIN patients has previously been published (Fehmi, Davies, et al., 2021; Fehmi et al., 2023).

From January 2015 to date (August 2023 at the time of writing), sera samples from 146 patients with a confirmed or suspected inflammatory peripheral neuropathy from NHS trusts within the UK have been collected, with written consent, as part of an observational study (BioSPIN) and tested for antibodies targeting CNTN1, caspr1, NF155 and NF186. Sera from 90 patients with neurological diseases (70 other antibody-mediated CNS neurological disorders, 20 with multiple sclerosis), as well as 120 patients with non-neurological diseases, and 120 healthy subjects have also been tested as controls. Since August 2017, and with collection ongoing, serum samples from patients with suspected inflammatory neuropathies have been received from other clinical centres for diagnostic testing of (para)nodal antibodies (not recruited to a study).

In total, to date (07/08/2023) through both cohorts (BioSPIN and diagnostic) there have been 121 patients identified with AINs, positive for either CNTN1, caspr1, CNTN1/caspr1 complex, NF155, NF186 or PanNF antibodies. This accounts for 6.2% of the total patients with suspected immune-mediated neuropathies screened (121/1940), or 5.3% if control samples from patients with neurological and other diseases and healthy subjects are included (121/2270) (**Table 2** and **Figure 21**).

Of the AIN patients, they were most frequently positive for NF155 (46), panNF (26), CNTN1 (23), Caspr1 (16), NF186 (5), and CNTN1/Caspr1 (4) antibodies (**Figure 21**), accounting for 2.4%, 1.3%, 1.2%, 0.8%, 0.26% and 0.2%, respectively.

BioSPIN cohort	Seronegative	**99**
	Seropositive	47
Diagnostic cohort	Seronegative	1720
	Seropositive	73
Controls	Neurological disease	90
	Non-neurological disease	120
	Healthy	120
	TOTAL	2270

Table 2: Total patients screened for (para)nodal antibodies

From both BioSPIN and diagnostic cohorts a total of 120 patients are seropositive i.e. said to have an autoimmune nodopathy. A total of 330 patient samples acted as controls (neurological or other disease, and healthy).

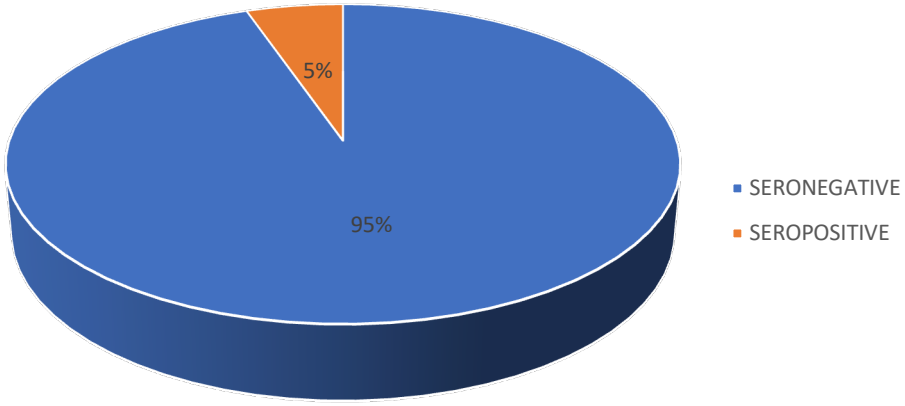


Figure 20: Total proportion of autoimmune nodopathy patients detected through screening.

*120 patients were seropositive amongst a total of 2270 patients (**Table 2**)*

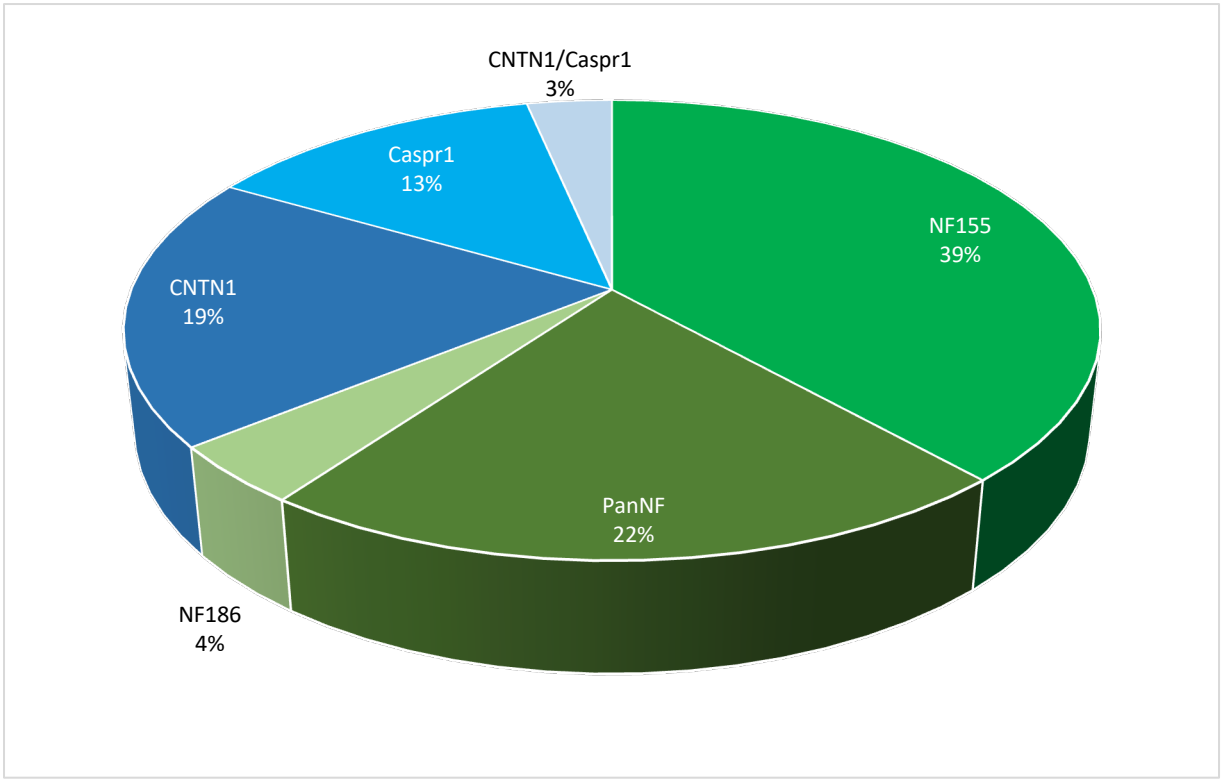


Figure 21: Patient cohort positive for nodal and paranodal antibodies (total 120).

In order of frequency: NF155 (47), panNF (26), CNTN1 (23), Caspr1 (16), NF186 (5), CNTN1/Caspr1 (4)

Serological data (antibody reactivity and subclass if reactive) is available for all those screened. Variable clinical data is currently available for 196 seronegative patients (suspected or confirmed immune-mediated peripheral neuropathy) and 88 (para)nodal seropositive patients.

3.2.2.1 Demographic and clinical characteristics

In comparison to the (para)nodal seronegative cohort (PNAb-) (with available clinical data), (para)nodal positive (PNAb+) or AIN patients were significantly more frequently initially diagnosed with GBS (43% vs 21%, p=0.0002) with an acute or subacute onset of disease (53% vs 30%, p=0.0005), and had more severe disease (79% mRs >=4 vs 40%, p= 0.0001) with a median mRS of 3 (able to walk) in the seronegative and 4 (unable to walk) in the seropositive group. They also more frequently had associated clinical features, though only the association of nephrotic syndrome reached statistical significance (61% vs 3%, p=0.0001). CSF protein levels were higher, and nerve root or plexus abnormalities (thickening and/or contrast enhancement) were more frequently observed in the AIN group. Gender and age were similar between the groups overall (**Table 2** and **Figure 22**).

	PNAb positive (n=88)			PNAb negative (n=194)			p-value
Age (median, range)	56.5 (2-81)			61 (3-90)			
	Y	**N**	**%**	**Y**	**N**	**%**	
Male sex	58	30	66	124	70	64	0.7892
Initial clinical diagnosis of GBS	37	50	43	38	147	21	0.0002
Acute/subacute onset	46	41	53	56	128	30	0.0005
Ataxia	41	46	47	62	96	39	0.2794
Tremor	27	60	31	39	115	25	0.3686
Neuropathic pain	38	45	46	49	85	37	0.2008
Cranial nerve palsy	28	59	32	41	115	26	0.3739
Autonomic dysfunction	16	62	21	9	62	13	0.2727
Respiratory involvement	17	70	20	25	160	14	0.2113
Nephrotic syndrome	54	34	61	5	142	3	0.0001
MRI plexus/root abnromalities	26	30	46	15	38	28	0.0745
nadir mRs >=4	68	18	79	75	112	40	0.0001
nadir mRs (median, range)	4 (1-6)			3 (1-6)			
CSF protein (g/L) (median, range)	1.8 (0-10)			0.87 (0.18-6)			
CSF WCC (cells/uL) (median, range)	1 (0-90)			NA			
Rasied CSF WCC (>5/uL)	13	63	17	NA			

Table 3: Clinical characteristics of the (para)nodal antibody seropositive (AIN) vs seronegative patient cohort

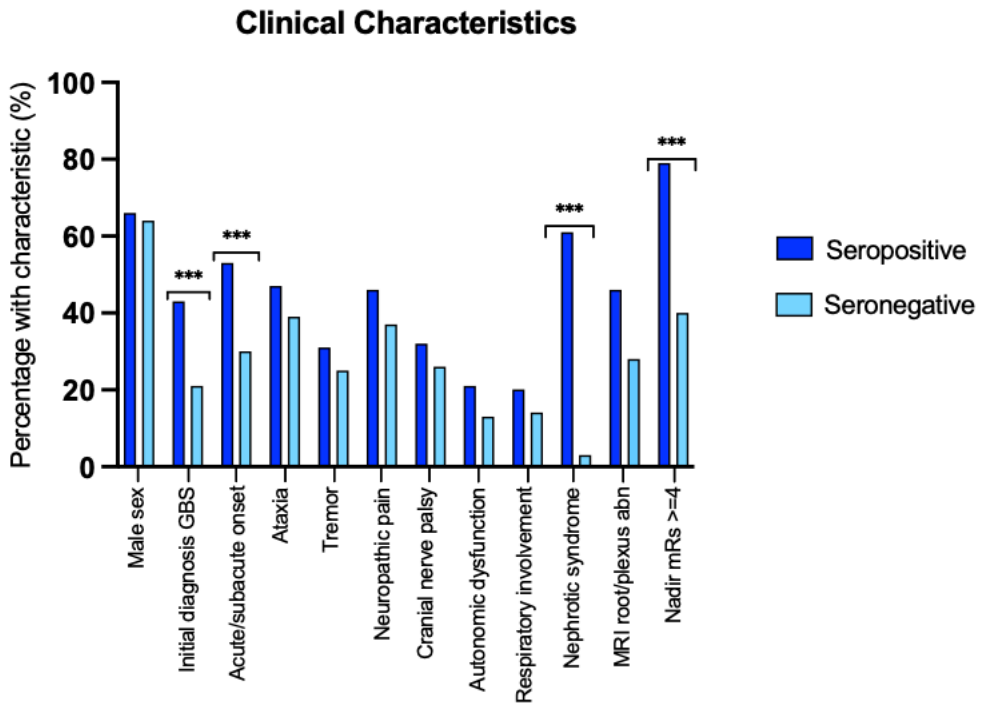


Figure 22: Clinical characteristics of the seropositive (AIN) vs seronegative patient cohort

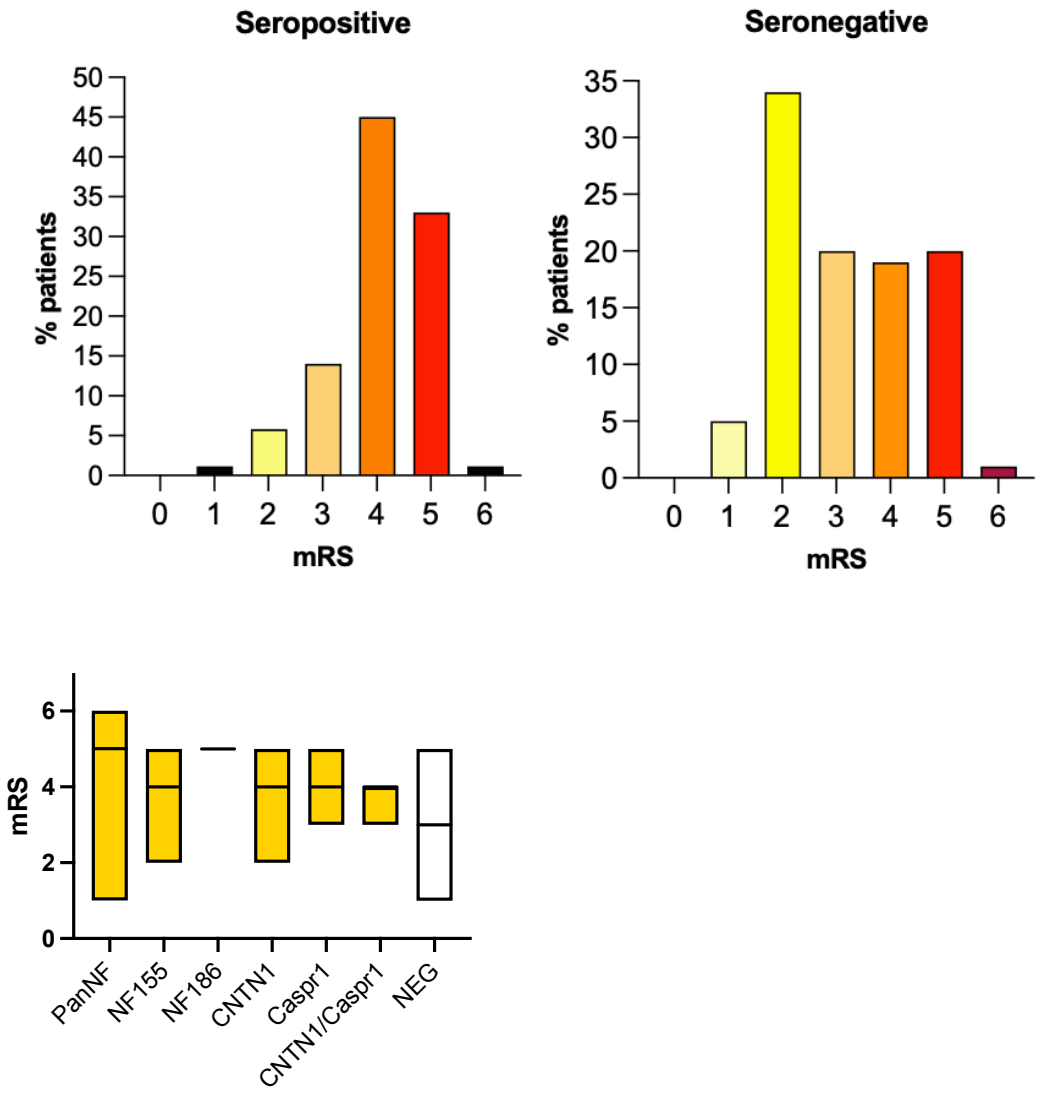


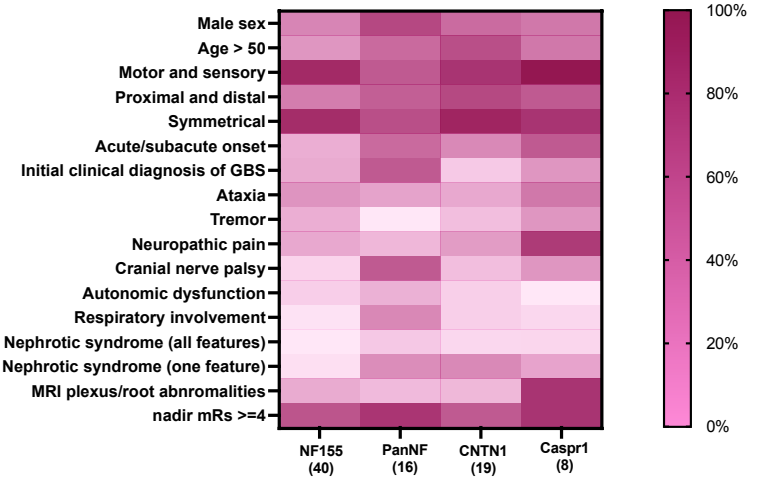
Figure 23: modified Rankin score (mRS) for (para)nodal antibody seropositive (86) and seronegative (182) cohorts.

The two top graphs compare the proportion of patients with each mRS scored at nadir, with a breakdown of each antibody subgroup and median mRS in the below chart. Overall, the median mRS in the seropositive group was 4, and the seronegative group 3. In the seropositive group the mRS in the panNF (16 patients) and NF186 (2 patients) antibody groups were higher than the NF155 (40 pts), CNTN1 (16 pts) Caspr1 (9 pts) and CNTN1/Caspr1 (3 pts) groups.

Within the AIN cohort, at the time of writing (19/9/2023) data was available for 40 patients with anti-NF155 antibodies, 19 CNTN1, 16 panNF, 8 Caspr1, 2 NF186, and 3 CNTN1/Caspr1 complex antibodies.

A comparison of clinical characteristics between each antibody subgroup (not including NF186 monoreactivity or CNTN1/Caspr1 complex due to such low numbers) shows all antibody groups are predominantly male and over the age of 50, and present with a motor and sensory, symmetrical, proximal and distal peripheral neuropathy (**Figure 24**). PanNF and Caspr1 positive patients present most frequently with an acute or subacute onset, with panNF patients in particular, as a result initially suspected to have GBS. Ataxia was common in all groups (41-63%), and to a lesser extent tremor (29-50%), though the latter was not reported at all in the panNF group. Neuropathic pain was notable in the Caspr1 cohort, whereas cranial nerve palsy, autonomic dysfunction and respiratory insufficiency were more frequently associated with panNF antibody positive patients. Nephrotic syndrome (defined by peripheral oedema, hypoalbuminaemia and proteinuria) was reported in almost a quarter of panNF patients, but also in Caspr1 and CNTN1 groups (14%), but at least half of patients in these groups were noted to have just one feature of nephrotic syndrome. Nerve root hypertrophy or signal enhancement on MRI was evident in about a third of patients from all groups, but was notably high in Caspr1. Disability was severe (mRS >=4) in at least three quarters of each antibody group, in particular panNF and Caspr1.

Antibody subgroup	NF155	PanNF	CNTN1	Caspr1
Number of patients	(40)	(16)	(19)	(8)
	% patients			
Male sex	58	81	68	63
Age > 50	50	69	79	63
Motor and sensory	92	75	88	100
Proximal and distal	61	73	81	75
Symmetrical	91	79	94	88
Acute/subacute onset	38	69	56	75
Initial clinical diagnosis of GBS	40	75	22	50
Ataxia	51	44	41	63
Tremor	38	0	29	50
Neuropathic pain	41	33	47	86
Cranial nerve palsy	15	75	29	50
Autonomic dysfunction	19	36	18	0
Respiratory involvement	5	56	18	13
Nephrotic syndrome (all features)	0	23	13	14
Nephrotic syndrome (one feature)	7	54	56	43
MRI plexus/root abnromalities	40	31	33	88
nadir mRs >=4	77	88	75	88



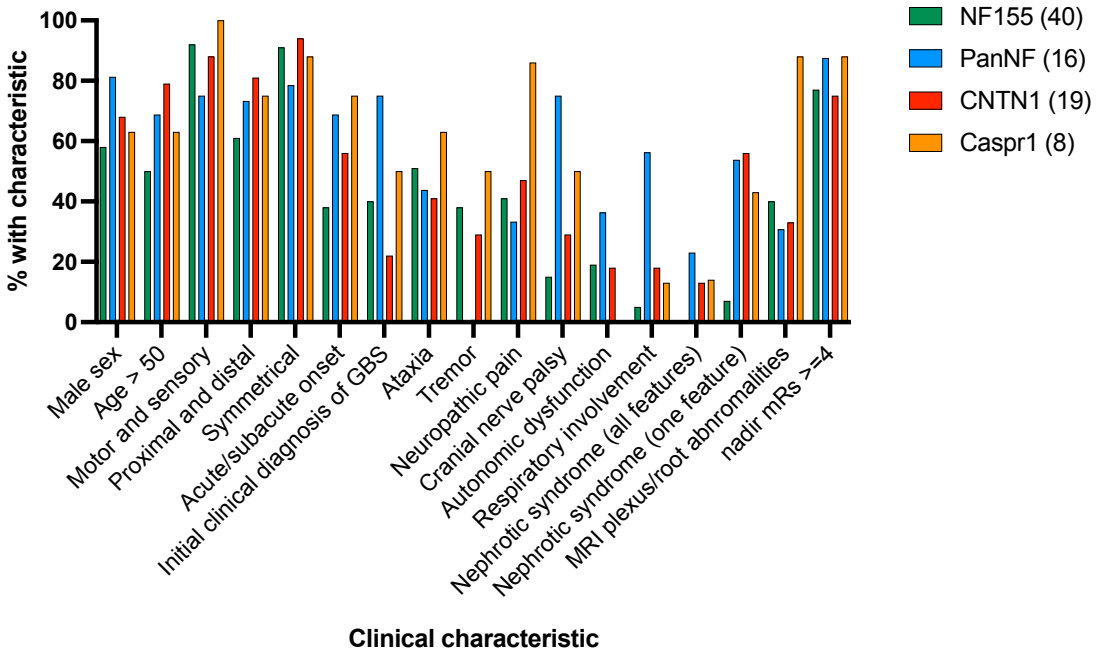
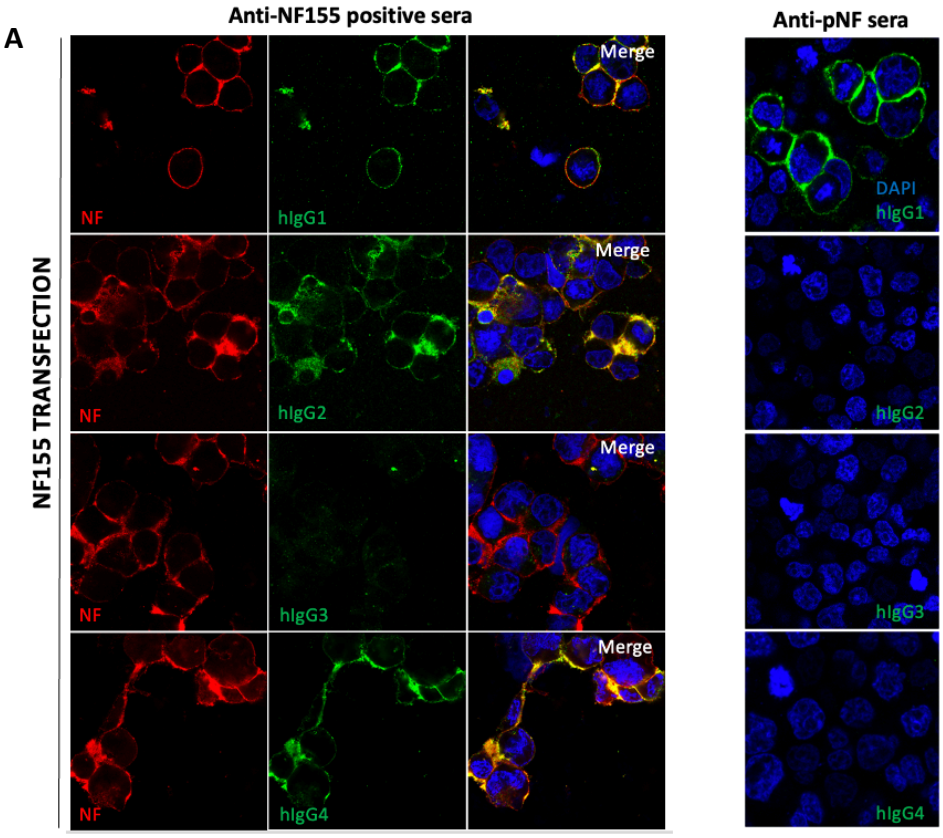


Figure 24: Clinical characteristics in each (para)nodal antibody group (table, heat map and bar chart)

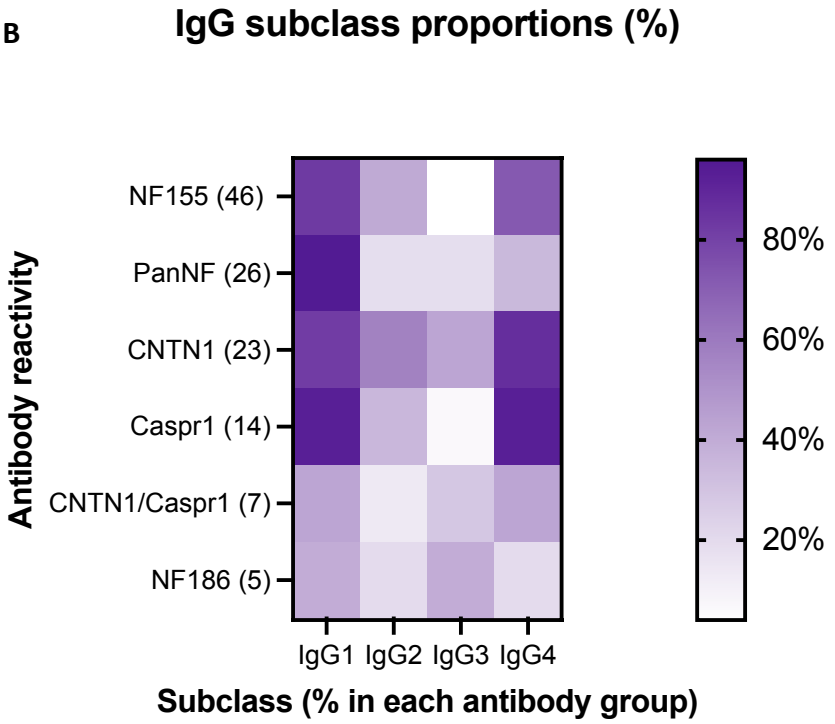
Proportion of patients in each group with clinical features as specified by referring clinician. If no response was provided on the clinical questionnaire this was reflected in the denominator used to calculate percentage. Proximal and distal weakness, as well as symmetry of distribution of weakness was scored as present if these were recorded as present in either or both of the upper and lower limbs. Features of nephrotic syndrome assessed included proteinuria, hypoalbuminaemia and peripheral oedema.

3.2.2.2 Serological profiles

Antibody titres and IgG subclass analysis were available for 109 patients. The predominant IgG subclass detected by CBA was IgG1 and 4 (and in over half of cases reactivity was equally as strong) in all except the panNF and NF186 monospecific group, in which IgG1 was detected in almost every case and almost always the dominant subclass, versus IgG4 which was detected in under half of cases (**Figure 25** and **Figure 26**). IgG2 and 3 were less often detected in all groups. For patients whom we tested serial serum samples, the predominant IgG subclass did not change over time. Antibody titres themselves were not found to be related to the mRS (**Figure 27**).



B



	Antibody subgroup (No.)					
	NF155 (46)	PanNF (26)	CNTN1 (23)	Caspr (14)	CNTN1/Caspr1 (7)	NF186 (5)
	% patients					
IgG1	83	96	82	93	43	40
IgG2	41	19	57	36	14	20
IgG3	4	19	43	7	29	40
IgG4	72	35	87	93	43	20

C

	Antibody subgroup (No.)					
	NF155 (46)	PanNF (26)	CNTN1 (23)	Caspr (14)	CNTN1/Caspr1 (7)	NF186 (5)
	% dominant subclass					
IgG1	37	73	35	36	43	20
IgG2	0	8	0	0	0	0
IgG3	0	0	0	0	0	0
IgG4	30	0	22	21	14	0
IgG1=4	22	8	35	29	0	0
IgG1=2	0	0	0	7	0	20
IgG1=3	0	4	0	0	0	0
IgG1=2=4	2	4	0	0	0	0
IgG2=4	0	0	0	7	0	0
IgG3=4	0	0	0	7	0	20
No subclass	7	12	13	14	0	40

Figure 25: Patient IgG subclass testing: CBA appearances, heat map and tables representing proportion and dominance of IgG subclasses detected within each antibody group

Subclass data was available for 121 patients .Criteria for presence of a subclass was reactivity of subclass antibodies to specific antigen with an observer rating of 1 or above for fluorescence intensity on live CBA testing. Dominance was confirmed by that antibody subclass having the strongest reactivity compared to the others, or co-dominance if reactivity was considered equally as strong.

***(A)** Examples are provided for IgG1, 2 and 4 subclass positivity in NF155 positive sera, as well as for only IgG1 reactivity in pan-neurofascin (pNF) sera. 'NF' is commercial neurofascin labelling, DAPI is nuclear staining. **(B)** IgG1 was most frequently detected in NF155 and panNF antibody cohorts. IgG1 was equally reported to IgG4 in Caspr1 and CNTN1/Caspr1 complex cohorts, and to IgG3 in the NF186 monospecific antibody group. IgG4 was marginally more frequently present in the CNTN1 AIN patients. All IgG subclasses were detected, with variable reactivity, in all antibody groups (though not in each patient). **(C)** IgG1 demonstrated most dominant binding in panNF, NF155, Caspr1 and CNTN1/Caspr1 complex AIN patients. IgG1 was most dominant alone or in combination with IgG4 in CNTN1 antibody patients. IgG4 dominance was seen mostly in NF155 AIN patients compared with the other groups, but was strongly co-dominant with IgG1 in CNTN1 and Caspr1 groups.*

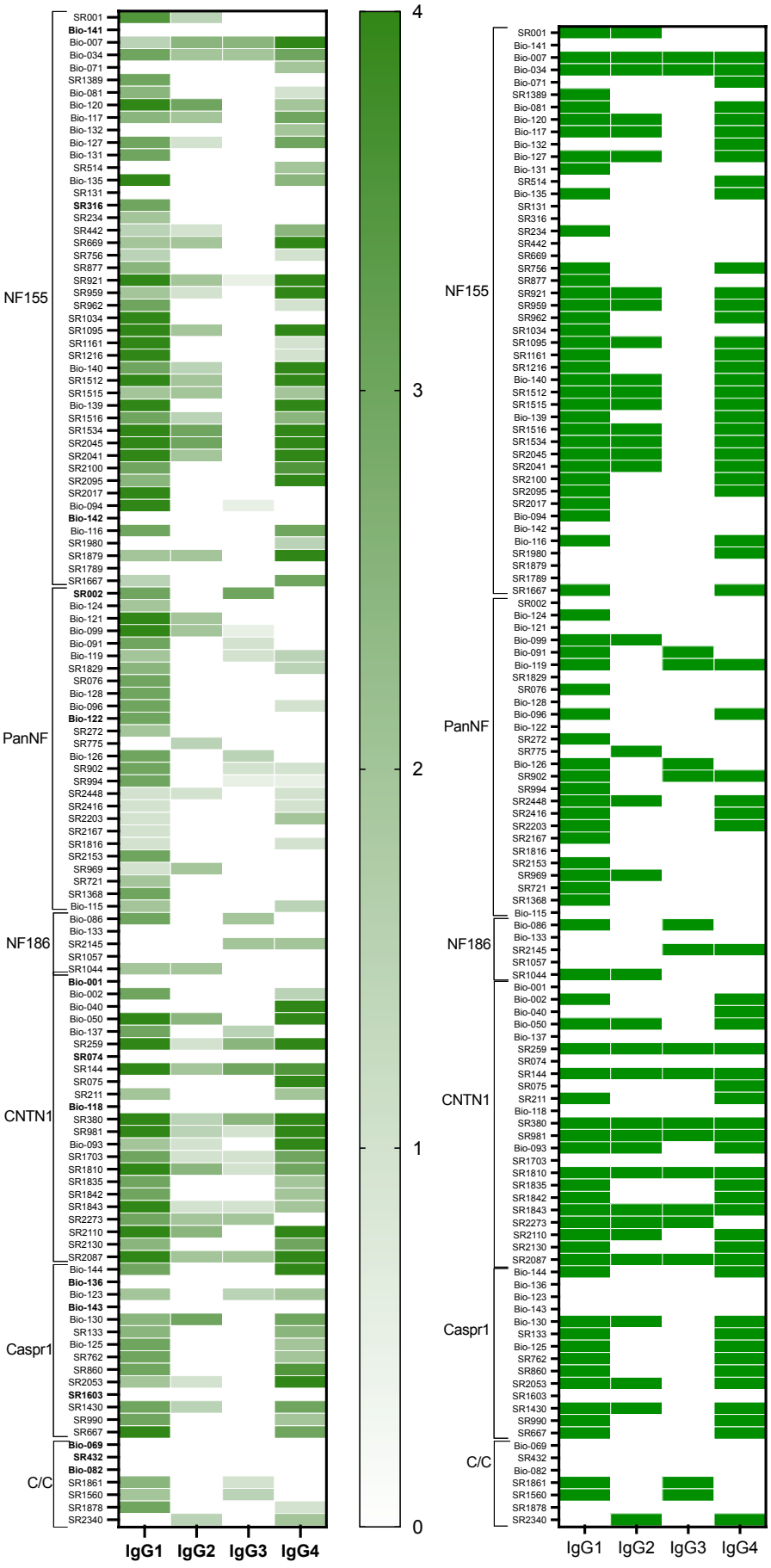

NF155
PanNF
NF186
CNTN1
Caspr1
C/C
IgG1
IgG2
IgG3
IgG4
4
3
2
1
0

Figure 26: Heat map showing IgG subclass positive reactivity scores per patient sample within antibody groups

Left heatmap: Relative proportions of IgG1-4 subclasses per sample (indicated along y-axis). Positivity rating of IgG subclass (0-not present, 1-lower threshold for positive, 4 – strongly positive). IgG1 and 4 are most often found to be strongly positive in NF155, CNTN1 and Caspr1 cohorts, whereas IgG1 is the most reactive subclass in the panNF group.

Right heatmap: Absolute presence of subclass, regardless of positivity score. Green indicates subclass detected, white indicates not present. In some sera no antibody subclasess could be detected.

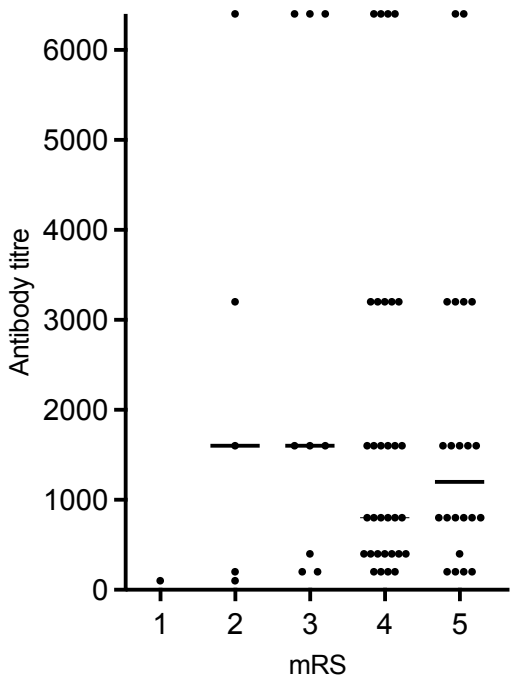


Figure 27: Correlation of (para)nodal antibody titres and mRS

Antibody titres did not correlate to nadir modified rankin scale (mRS) in the autoimmune nodopathy cohort (individual data points for each patient, and median represented by a line). A total of 73 patients had recorded mRS scores at nadir, their antibody titre on the y-axis for each patient is correlated to nadir mRS.

3.2.2.3 Treatment response

In total, treatment data was available for 81 patients testing positive for (para)nodal antibodies (PNAb+) and 127 seronegative patients (PNAb-). The majority of PNAb+ patients (83%) required more than one treatment modality (median = 3), compared with 56% of PNAb- patients (median 2, p< 0001) (**Figure 28**). Within the seropositive group, IVIg, corticosteroids, PLEX then RTX were used in order of frequency, with RTX (56%) most often deemed to have 'good' efficacy by the treating physician (**Figure 29**). Use of IVIg, steroids, and/or PLEX i.e. standard therapies, were deemed to have a good effect only 7%, 19%, and 8% of the time, respectively. Treatment effects were rated overall by the treating physician and categorised as 'none' (clearly no benefit), 'equivocal' (unclear effect), 'partial' (minimal effect or good but unsustained effect), or 'good' (clearly and temporally linked to clinical improvement with sustained effect). Sixteen patients were additionally treated with one or more alternative immunotherapies, most frequently Cyclophosphamide (7), Mycophenolate Mofetil (4) and Methotrexate (3) (**Figure 30**). A similar proportion of the seronegative group had a 'good' response to IVIg, steroids and PLEX, though significantly fewer were felt to respond as well to RTX or other immunosupressants (**Figure 32**).

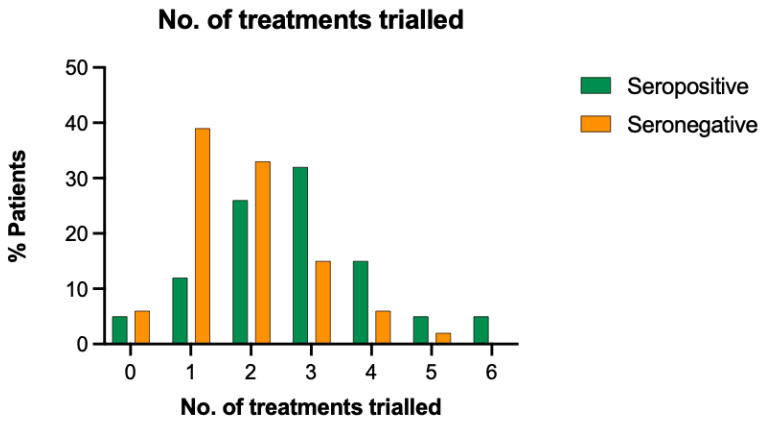


Figure 28: Proportion of seropositive (PNAb+) and seronegative (PNAb-) patients requiring number of treatment modalities.

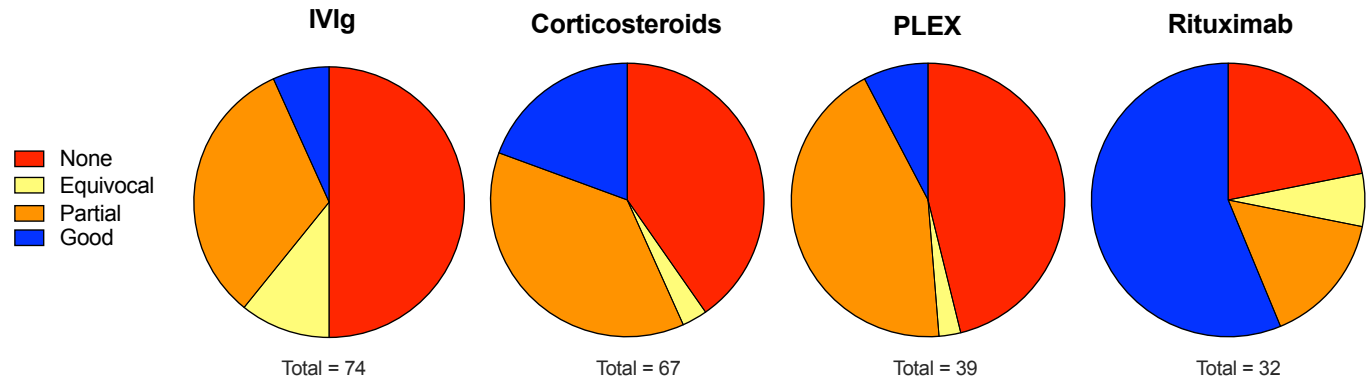


Figure 29: Pie charts showing percentage overall treatment responses in the autoimmune nodopathy cohort

IVIg, corticosteroids and PLEX were most frequently reported to have no, equivocal or partial effect. A good response, deemed by the referring clinician, was significantly more associated with rituximab treatment. Total number of patients who trialled each treatment underneath each chart, data available from 81 individual patient.

IVIg: None (50%), equivocal (11%), partial (32%), good (7%)

Corticosteroids: None (40%), equivocal (3%), partial (37%), good (19%)

PLEX: None (46%), equivocal (3%), partial (43%), good (8%)

Rituximab: None (22%), equivocal (6%), partial (16%), good (56%)

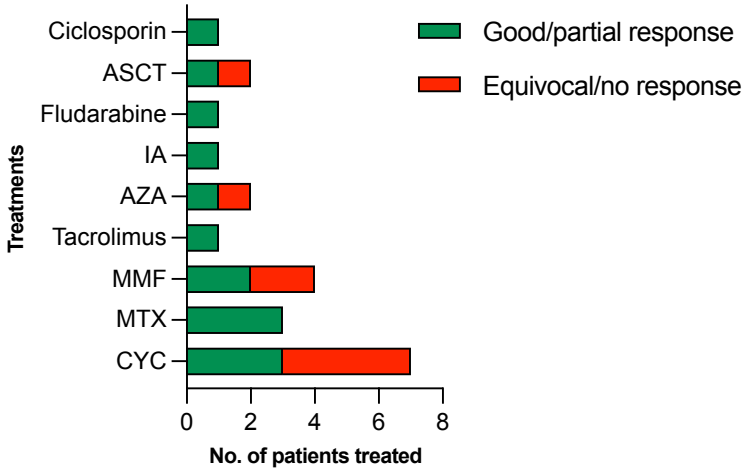


Figure 30: Alternative immunomodulatory therapy use in autoimmune nodopathy patients

Sixteen patients were treated with one or more alternative immunomodulatory treatments in addition to standard therapies/rituximab. The total number of patients treated with each agent is shown on the x-axis and divided into the number of patients who achieved a good or partial response or equivocal to no response. Cyclophosphamide and Methotrexate were most frequently used. Abbreviations: CYC – cyclophosphamide; MTX – methotrexate; MMF – mycophenolate mofetil; AZA – azathioprine; IA – immunoadsorption (protein A); ASCT – autologous stem cell transplant

RTX (in addition to standard therapy) significantly improved disability more than with standard therapy alone (IVIg, steroids, PLEX) (**Figure 31**). In both groups there was a trend of mRS decreasing post-treatment (**Figure 31A**), and although the change in mean mRS was not significantly different between groups, it was within groups (**Figure 31B**). The mRS improved by 2 or more points in 60% of patients in the RTX group, vs 40% of patients who received standard therapy alone, and deteriorated or remained unchanged in 20%, vs 44% if those treated with RTX (**Figure 31C**).

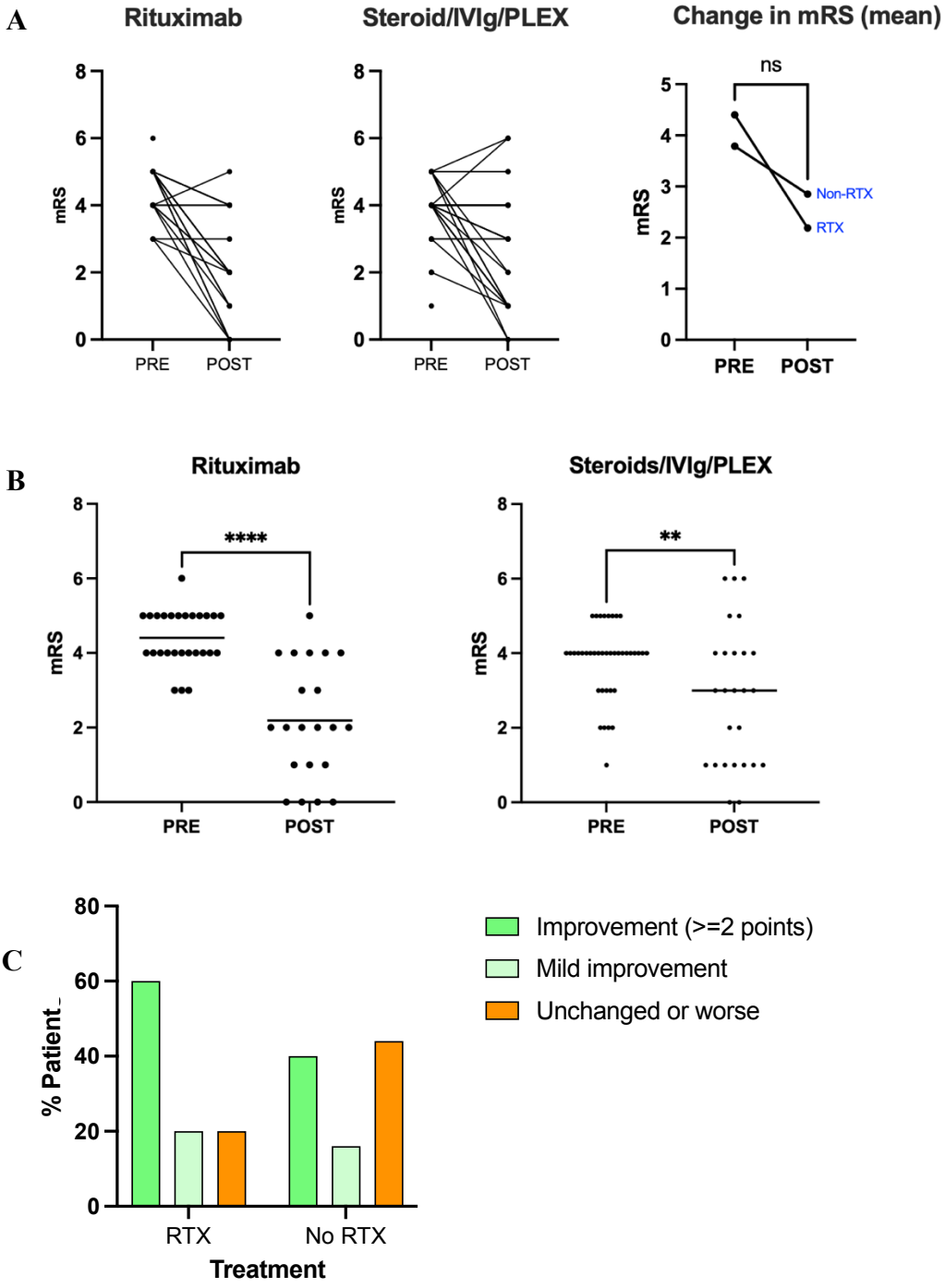


Figure 31: Rituximab treatment led to improved clinical outcome than standard therapy (steroids, IVIg, PLEX) alone.

*(**A**) Pre- and post-treatment modified Rankin scores (mRS) for individual patients (line joins dots for same patient) treated with rituximab in addition to standard therapies or standard therapies alone. Change in mean scores for each group are compared but do not reach statistical significance (p=0.07, unpaired t-test). (**B**) mRS data points pre- and post-treatment (line shows mean values).The change in mean within treatment groups is significant (rituximab treated patients, p<0.0001, paired t-test, steroid/IVIg/PLEX treatment group p=0.001, paired t-test). (**C**) Improvement of 2 or more points on the mRS occurred more frequently in the rituximab-treated group over those only treated with one or a combination of standard therapy (IVig, steroids and PLEX). Those patients treated with alternative immunomodulatory therapy (**Figure 30**) and had a partial or good outcome were not included in this analysis.*

Treatment % treated (% with good response)			Difference in proportion treated/proportion with good response	
	PNAb+	PNAb-		
IVIg	91 (7)	82 (9)	ns/ns	0.0965/0.7953
Corticosteroids	81 (20)	61 (10)	**/ns	0.0029/0.0734
PLEX	48 (8)	24 (10)	***/ns	0.0007/0.8056
RTX	40 (56)	8(10)	****/****	<0.0001/<0.0001
Other (1 and 2)	20 (44)	6 (0)	**/****	0.0054/<0.0001

Figure 32: Physician reported treatment outcomes of autoimmune nodopathy (PNAb+) patients compared with seronegative suspected immune neuropathy patients (PNAb-)

The proportion of patients treated with corticosteroids, PLEX, RTX and other immunosupressants (as stated in **Figure 30***) was statistically significant between the seropositive and seronegative groups, as was the proportion of patients deemed to have a good response to rituximab or other escalation immunotherapies. The responses to IVIg, corticosteroids and PLEX responded comparably between the two groups. Abbreviations –IVIg – intravenous immunoglobulin; ns – not significant; PLEX – plasma exchange; PNAb+ (Para)nodal antibody positive patients; PNAb- (Para)nodal antibody negative patients; RTX - rituximab*

There are 72 patients for whom we have IgG subclass scores recorded and treatment response data available (**Figure 33** and **Table 4**). Since the AINs have predominantly been reported to show IgG4 reactivity, we categorized these into seropositive patient sera that showed IgG4 dominance (or co-dominance, number = 51), contained but were not dominant for IgG4 (number =24), and were negative for IgG4 reactivity (number = 36). For each treatment modality the proportion of patients with or without IgG4 were similar (**Table 4**). If IgG4 was not found in patient sera patients were almost equally as likely to improve (good/partial response) as they were not to (equivocal/no response) (**Figure 33**), Whereas if IgG4 was present a higher proportion of patients who were treated with RTX and/or steroids improved (75% and 59% improved, respectively), and a higher proportion of patients treated with IVIg did not (69% equivocal or no improvement) (**Figure 33**). Those treated with PLEX were almost equally as likely to improve as not (52% vs 48%).

A comparison of proportions between IgG4-dominant vs IgG4 containing but non-dominant groups did not differ greatly (data not shown).

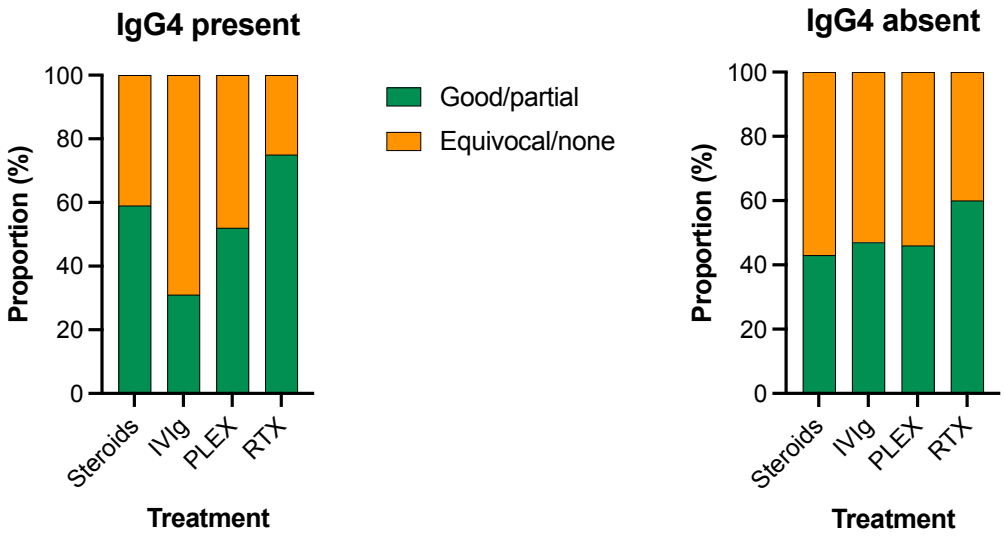


Figure 33: Comparison of treatment responses in 72 autoimmune nodopathy patients with and without IgG4 antibodies

The proportion of patients with a positive response (good or partial) or poor response (equivocal or none) to each treatment modality, categorised by whether IgG4 was present (dominant or not) or absent. Statistical analysis using Fisher's exact test suggests the difference between the proportions of patients in each treatment group responding well or not in the presence or absence of IgG4 is significant for rituximab (p=0.0341), IVIg (p=0.0294 and steroids (p=0.0336), but not PLEX (0.4795).

			No. (%) response to **RTX**			
	Total No.	No. had RTX (%)	Good	Partial	Equivocal	None
IgG4 present	75	20 (27)	11 (55)	4 (20)	1 (5)	4 (20)
IgG4 absent	36	10 (28)	5 (50)	1 (10)	1 (10)	3 (30)

			No. (%) response to **IVIg**			
	Total No.	No. IVIg (%)	Good	Partial	Equivocal	None
IgG4 present	75	45 (60)	1 (2)	13 (29)	7 (16)	24 (53)
IgG4 absent	36	21 (58)	3 (14)	7 (33)	1 (5)	10 (48)

			No. (%) response to **steroids**			
	Total No.	No. Steroids (%)	Good	Partial	Equivocal	None
IgG4 present	75	44 (59)	9 (20)	17 (39)	1 (2)	17 (39)
IgG4 absent	36	14 (39)	2 (14)	4 (29)	0 (0)	8 (57)

			No. (%) response to **PLEX**			
	Total No.	No. PLEX (%)	Good	Partial	Equivocal	None
IgG4 present	75	25 (33)	3 (12)	10 (40)	1 (4)	11 (44)
IgG4 absent	36	13 (36)	0 (0)	6 (46)	0 (0)	7 (54)

Table 4: Treatment responses and IgG subclass dominance in 72 AIN patients.

Tables detailing the numbers and % proportions of patients for whom we have both IgG subclass and treatrment data available. Responses were recorded to each treatment by treating physician.

3.2.3 PanNF-antibody cohort

3.2.3.1 Clinical and serological features

To date (August 2023) we have identified 25 anti-panNF antibody positive AIN patients (25/1940, 1.3% of total cohort screened) and 5 anti-NF186 antibody positive AIN patients (0.26%).

We initially reported the first eight affected panNF AIN adult patients from this group of 25, the results of which are reproduced in the text below (Fehmi, Davies, et al., 2021). At this time, they were compared to seropositive patients with other antibody specificities, consisting of 17 (2.5%) with antibodies against NF155 alone, 1 (0.15%) with monospecific NF186 antibodies, 11 (1.6%) with CNTN1 antibodies alone, and nine (1.3%) with CNTN1/Caspr1 complex antibodies.

Clinical data for panNF patients compared with the other antibody and seronegative group are outlined in **Table 6** and **Table 7** (available for 8/8 panNF, 15/17 NF155, 11/11 CNTN1, 8/9 CNTN1/Caspr1 positive patients, and 194/603 seronegative). The panNF patient cohort developed profound tetraplegia, significantly more likely to be initially diagnosed as GBS ($p=0.03$) compared to NF155 (odds ratio (OR) 6.7, 95% confidence interval (CI) 1.1 - 34.6) or seronegative patients (OR 6.5, 95% CI 1.6 - 24.9), with an acute/subacute deterioration (vs NF155: OR ∞, 95% CI 2 - ∞, vs seronegative: OR ∞, 95% CI 4.8 - ∞). Their peak mRS (median 5.5, range 5-6) was also significantly higher than NF155 (median 4, range 2-5, $p=0.005$), CNTN1 (median 4, range 2-6, $p=0.05$) and seronegative (median 3, range 1-5, $p<0.001$) counterparts, but not patients with CNTN1/Caspr1 complex only reactive antibodies (median 4, range 4-5, $p=0.59$, Kruskal-Wallis test with Dunn's correction for multiple comparisons) (**Table 6** and **Figure 36A**). PanNF patients were also much more likely to develop cranial nerve palsies, respiratory and autonomic dysfunction ($p<0.001$, multiple Chi-square tests), when compared to all of the other antibody and seronegative groups. Ataxia (38%) and neuropathic pain (50%) were present in some, but more noteworthy in CNTN1/Caspr1 patients (71%). Although an association with nephrotic syndrome was evident (38%), this was not as frequent as for CNTN1 patients (82%). The cerebrospinal fluid (CSF) protein concentration was

notably lower in the panNF group ($p<0.001$), though the frequency of MRI plexus/root abnormalities were not significantly different to the other groups (Fehmi, Davies, et al., 2021).

3.2.3.2 Laboratory fundings

Those with anti-panNF antibodies were exclusively found to be of the IgG1 subclass on CBA, whereas using the same assays in all the other antibody groups, IgG4 was most often the dominant subclass detected, with IgG1 only exclusively being present in two NF155 patients. Other (non-dominant) IgG subclasses (IgG2 and 3) were detected in all but the panNF group (Fehmi, Davies, et al., 2021). Six of the seven patient sera tested against neurofascin antigen in ELISA were positive, though had lower end point titres than in CBA (1:400-1:3200) (**Figure 10C**). Additionally, optical density for IgG1 neurofascin reactive antibodies was only above background in two patient samples on ELISA (vs 8 on CBA) (**Figure 10B**) (Fehmi, Davies, et al., 2021). Subclass analysis of (para)nodal antibodies has since been updated in **Figure 25** and **Figure 26**, and although the majority of sera containing panNF reactive antibodies (now 26 patients) remain IgG1 dominant, they have been shown to contain other subclasses (IgG2-4), and a handful of samples show either co-dominance between IgG1, 2 and 4, or are IgG2 dominant.

All panNF patients were negative for standard neuropathy screening blood tests, which included anti-GM1 and GQ1b-ganglioside antibodies. In close temporal relationship to the onset of their neuropathy, an IgG-lambda paraprotein was detected in 2 panNF patients, who were subsequently diagnosed with lymphoproliferative disorders (P3 and 4 - **Table 7**). Both kappa and lambda light-chain containing panNF antibodies were detected using ELISA in these patients' sera however (data not shown). A third patient (P8) was found to have a clonal urinary lambda light chain, though without a serum paraprotein, prior to his death. In two of the three patients who developed nephrotic syndrome in parallel to their neuropathy, urinary protein levels confirmed nephrotic range proteinuria, with peripheral oedema and hypoalbuminaemia only in the third.

In contrast to the majority of patients with AIN, these panNF patients (7 tested, all within 14 days of onset) had normal or only slightly elevated CSF protein (median 0.51 g/L, range 0.34-0.62). This was significantly lower than all other seropositive patients ($p=0.007$ v CNTN1 and $p<0.001$ v NF155 or CNTN1/Caspr1, Kruskal-Wallis with Dunn's correction for multiple comparisons) (**Figure 36, 2D**), but not than the seronegative patients (median 0.87 g/L, range 0.18-6, $p=0.09$). White cell counts (range 1-3/μL), cytology and flow cytometry in the CSF were normal in all cases (range 1-3/μL) (Fehmi, Davies, et al., 2021).

3.2.3.3 Neurophysiological, radiological and histological findings

In the majority of panNF patients who underwent neurophysiological testing (4/6) (**Table 8**), there was evidence of conduction slowing, suggesting demyelination, and in 5/6 conduction block, though without temporal dispersion (usually a surrogate for segmental demyelination), suggestive of nodal pathology (Uncini et al., 2013). Inexcitable nerves were reported in one patient upon testing 2 weeks after onset. Follow-up assessment after 3-4 weeks in 3 patients showed reduced or unrecordable compound muscle action potentials and electromyographic features suggestive of severe axonal degeneration (Fehmi, Davies, et al., 2021).

MRI (performed in 4/8 patients) was normal in 2 patients, revealed enhancement and thickening of nerve roots in the lumbosacral plexi, as well as enhancement of paraspinal and proximal lower limb muscles in one patient, and T2 hyperintensities without thickening/enhancement of the brachial plexus and lumbosacral nerve roots in another (Fehmi, Davies, et al., 2021)

Nerve biopsy was performed in patient 1 and 6, showing axonal loss in both (in keeping with their neurophysiological findings), without evidence of cellular infiltration or inflammation, segmental demyelination, amyloid or vasculitis (**Figure 34E** and **Figure 35**). Further, there was no paranodal detachment visualised upon electron microscopy, performed only in one patient. Muscle biopsy in one patient showed a necrotising myopathy, with a normal creatine kinase (Fehmi, Davies, et al., 2021).

3.2.3.4 Treatment and outcome

All 8 patients received IVIg initially, only 2 of these deemed to be associated with a mild and/or transient neurological improvement. Six went on to have PLEX, only 3 showing slight unsustained improvement. Two patients similarly had a partial response to steroids, though 4 patients ultimately died. Ventilatory support was withdrawn at day 10 for one who had a cardiorespiratory arrest only a week after presentation and showed no recovery of cortical function, and in another at day 108 who failed to respond to IVIg and PLEX in the context of recurrent pulmonary infections. A third patient, with metastatic breast cancer, and refractory to steroids, IVIg, PLEX and cyclophosphamide, declined artificial ventilation and died on day 93. It was felt inappropriate for the fourth patient, who developed breathlessness and tachypnoea on day 12, to receive mechanical ventilation during the COVID-19 pandemic (SARS- CoV-2 PCR negative). He died 2 days later. More detailed assessment of treatment response as reported by the referring clinicians are provided in in **Table 7** and **Table 9**, as well as treatment time lines (
Figure 37).

The remaining 4 patients, who still had detectable anti-panNF antibodies following poor or unsustained treatment responses with IVIg, PLEX and steroids, went on to receive RTX (2 x 1g separated by 2 weeks) 3-4 months into their illness. Combination chemotherapy for haematological disorders was additionally administered in two patients; concurrently in P4, and 5 months later in P3. All 4 improved by at least 3 points on the modified rankin scale within 6 months of RTX treatment, ultimately being discharged home, often following a period of rehabilitation. Two were completely asymptomatic by 9 months (P4,P5) (**Figure 36B and Table 7**). In the only RTX-treated patient with nephrotic syndrome, the serum albumin normalised in line with neurological improvement (nephrotic syndrome was still apparent in those who died just prior to death). Neurofascin antibodies were negative when retested in all patients 4-11 months post RTX. One patient (P6) had a clinical and serological relapse 18 months post a single cycle of RTX treatment, having returned to near baseline (mRS 1). They became immobile over several weeks, re-developed nephrotic syndrome (hypoalbuminaemia), and were found to have low titre (1:100 and 1:200) IgG1 panNF antibodies.

Steroids and a second cycle of RTX proved effective and led to sustained functional independence (Fehmi, Davies, et al., 2021).

	Dominant subclass				Subclasses detected			
	PanNF (n=8)	NF155 (n=17)	CNTN1 (n=11)	CNTN1/Caspr1 (n=9)	PanNF (n=8)	NF155 (n=15)	CNTN1 (n=11)	CNTN1/Caspr1 (n=9)
None	0	1	0	0	-	-	-	-
IgG1	8	4	1	2	8	11	8	7
IgG2	0	0	0	0	0	10	6	4
IgG3	0	0	0	0	0	1	4	1
IgG4	0	9	6	5	0	14	11	8
IgG4=1	0	2	4	1	-	-	-	-
IgG4=2	0	1	0	1	-	-	-	-

Table 5: Subclass distribution of pan-neurofascin versus neurofascin-155, contactin-1 and contactin1/caspr1 complex reactive antibodies.

In all cases, IgG1 was the only subclass detected for pan-neurofascin antibodies. In contrast, with other antibody groups, IgG4 was most often the dominant subclass detected, but IgG1 and to a lesser extent IgG2 were frequently observed. [Supplementary table 1 from (Fehmi, Davies, et al., 2021)*]*

Table 1 Clinical features of patients with pan-neurofascin (panNF) antibodies and comparison with patients with neurofascin-155 (NF155), CNTN1, CNTN1/Caspr1 antibodies, and seronegative cohorts

Clinical feature (n, %)	PanNF (n=8)	NF155 (n=15)	CNTN1 (n=11)	CNTN1/Caspr1 (n=8)	Seronegative (n=194)	OR vs NF155	95% CI	OR vs seronegative	95% CI
Initial clinical diagnosis of GBS	5/8 (63%)	3/15 (20%)	3/11 (27%)	4/7 (57%)	38/185 (21%)	6.7	1.1 to 34.5	6.5	1.6 to 24.9
Acute/subacute progression	8/8 (100%)	7/15 (47%)	4/11 (36%)	5/7 (71%)	56/184 (30%)	∞	2.0 to ∞	∞	4.8 to ∞
Ataxia	3/8 (38%)	7/15 (47%)	7/11 (64%)	5/7 (71%)	62/158 (39%)	0.7	0.1 to 3.4	0.9	0.2 to 3.7
Tremor	0/8 (0%)	5/15 (33%)	3/11 (27%)	3/7 (43%)	39/154 (25%)	0	0 to 1.3	0	0 to 1.4
Neuropathic pain	4/8 (50%)	1/15 (7%)	7/11 (64%)	5/7 (71%)	49/134 (37%)	14	1.3 to 180	1.7	0.5 to 6.2
Cranial nerve palsy	8/8 (100%)	5/15 (33%)	5/11 (45%)	1/7 (14%)	41/156 (26%)	∞	3.3 to ∞	∞	5.7 to ∞
Autonomic dysfunction	6/8 (75%)	0/15 (0%)	2/11 (18%)	0/2	9/71 (13%)	∞	6.1 to ∞	20.7	3.9 to 105.4
Respiratory involvement	7/8 (88%)	0/15 (0%)	3/11 (27%)	0/7	25/185 (14%)	∞	9.9 to ∞	44.8	7.3 to 506.3
Nephrotic syndrome	3/8 (38%)	0/15 (0%)	9/11 (82%)	0/7	5/147 (3%)	∞	1.9 to ∞	17	3.5 to 73.7
MRI plexus/root abnormalities	2/4 (50%)	2/7 (29%)	2/7 (29%)	5/6 (83%)	15/53 (28%)	6.7	1.1 to 34.5	6.5	1.6 to 24.9
Nadir mRS >4	8/8 (100%)	3/15 (20%)	4/11 (36%)	2/7 (29%)	38/185 (21%)				
						Significant vs NF155	P value	Significant vs seronegative	P value
Nadir mRS (median, range)	5.5 (5–6)	4 (2–5)	4 (2–6)	4 (4–5)	3 (1–5)	**	0.006	***	<0.001
CSF protein (g/L) (median, range)	0.48 (0.34–0.62)	1.65 (0.61–7.05)	2 (0.24–5.9)	2.7 (0.91–4.46)	0.87 (0.18–6.0)	***	<0.001	*	0.04

The 95% CI of the OR was calculated by the Baptista-Pike method. Nadir mRS and CSF protein were compared by a two-tailed Kruskal-Wallis test with Dunn's correction for multiple comparisons. The patients with CNTN1 and CNTN1/Caspr1 antibodies were included in previous studies.[11 13]
*p<0.05, **p<0.01, *** p<0.001.
Caspr1, contactin-associated protein; CNTN1, contactin-1; CSF, cerebrospinal fluid; GBS, Guillain-Barré syndrome; mRS, modified Rankin Scale.

Table 6: A comparison of clinical features of panNF AIN patients to other antibody cohorts

[Table 1 from (Fehmi, Davies, et al., 2021)*]*

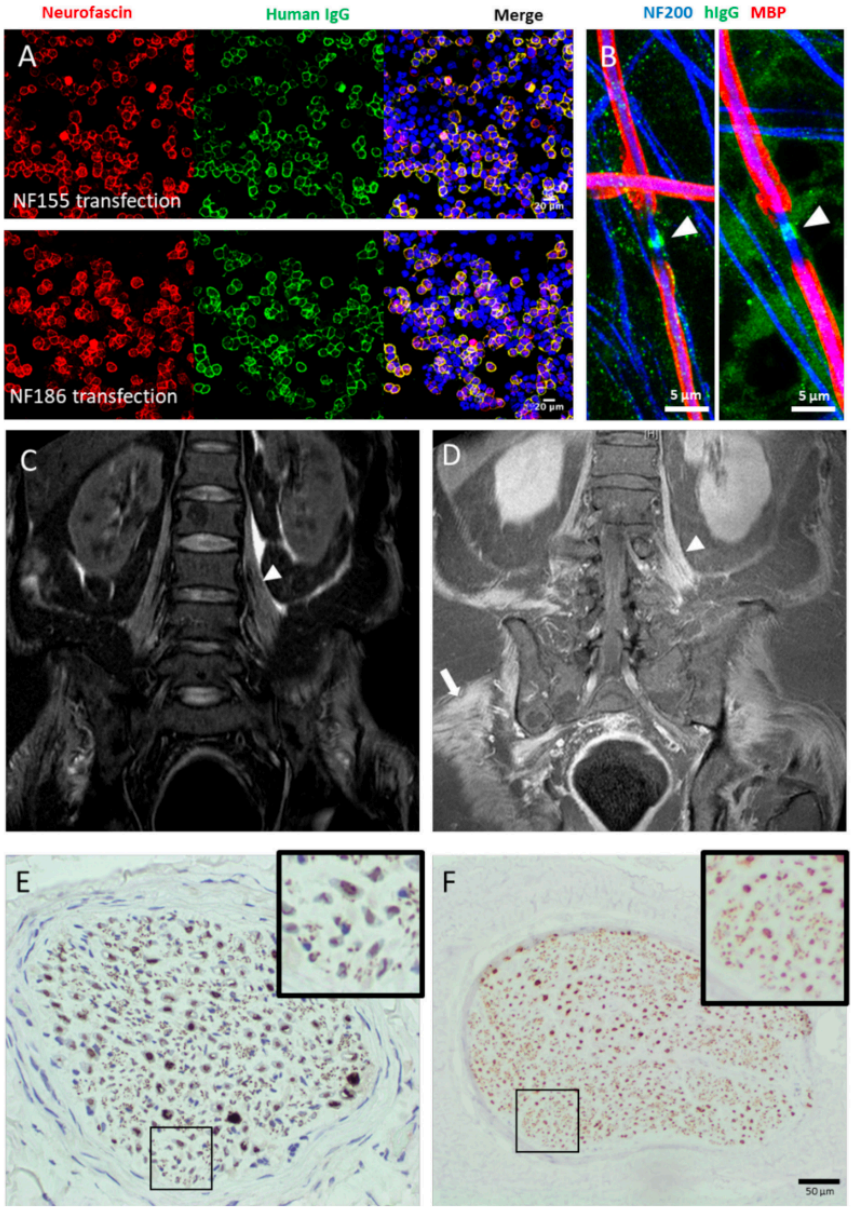


Figure 34: Serological, radiological and histological findings.

(A) *Cell- based assays using HEK293T cells transiently transfected to overexpress neurofascin-155 (NF155) (upper panels) or neurofascin-186 (NF186) (lower panels). Neurofascin (red) expression in the cell membrane is revealed by a commercial polyclonal antibody, and colocalises with human IgG (green) after exposure to acute- phase serum from the patients described in this series.* ***(B)*** *IgG (green) from two pan-neurofascin antibody- positive patient sera (left, P1; right, P6) is deposited at the node of Ranvier (arrowhead) after exposure to myelinating co-cultures. Axons (neurofilament- heavy, NF200, blue) were also observed weakly labelled with punctate IgG deposition in P1. Neither nodal or axonal labelling was observed in sera from healthy controls (data not shown). Myelin basic protein (MBP, red) defines the myelinated internode.* ***(C,D)*** *MRI of the lumbar spine, with coronal short tau inversion recovery (C) and post- contrast T1 (D) sequences, shows diffuse symmetric thickening and enhancement of lumbosacral plexus nerve roots (arrowhead), and enhancement of paraspinal, psoas, pelvic and proximal leg skeletal muscles (arrow).* ***(E)*** *Nerve biopsy from P6 stained for NFP shows reduced numbers of NFP positive axons (more clearly seen in the inset panels), and dense patches of staining, consistent with axonal degeneration. 'Near normal' NFP staining* ***(F)*** *is shown for comparison. [Figure 1 from* (Fehmi, Davies, et al., 2021)*]*

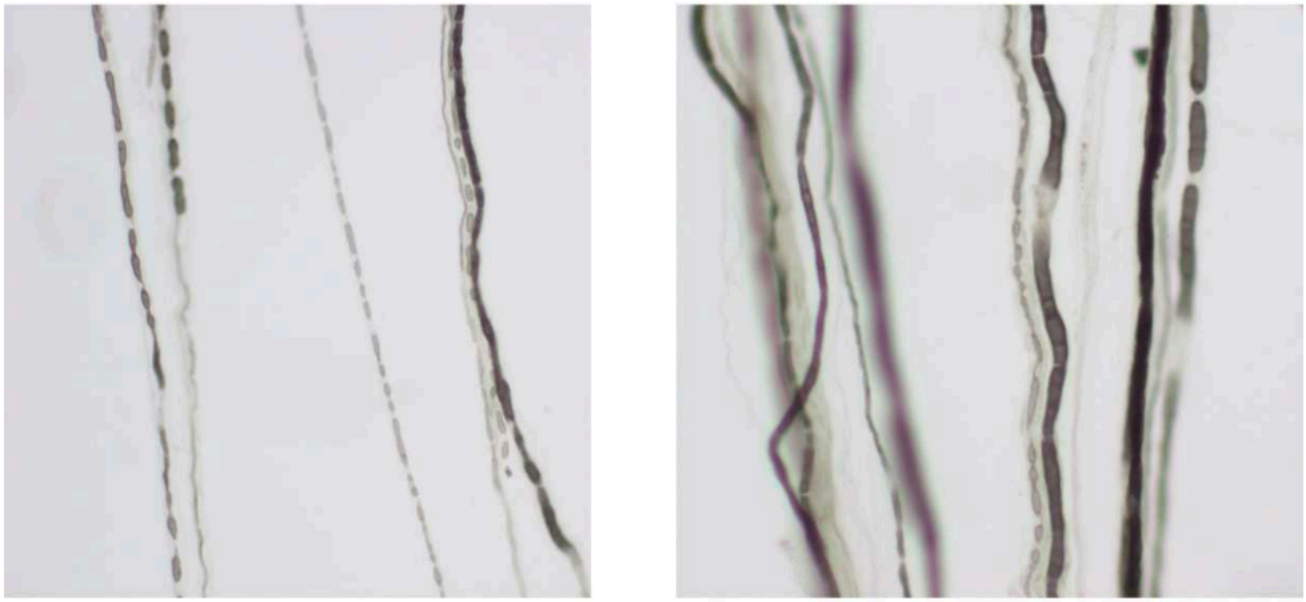


Figure 35: Teased nerve fibre.

The teased nerve fibres from the sural nerve biopsy of patient 6 show myelin ovoids consistent with axonal degeneration (left panel) and occasional short internodes (right panel). [Supplementary figure 5 from (Fehmi, Davies, et al., 2021)*]*

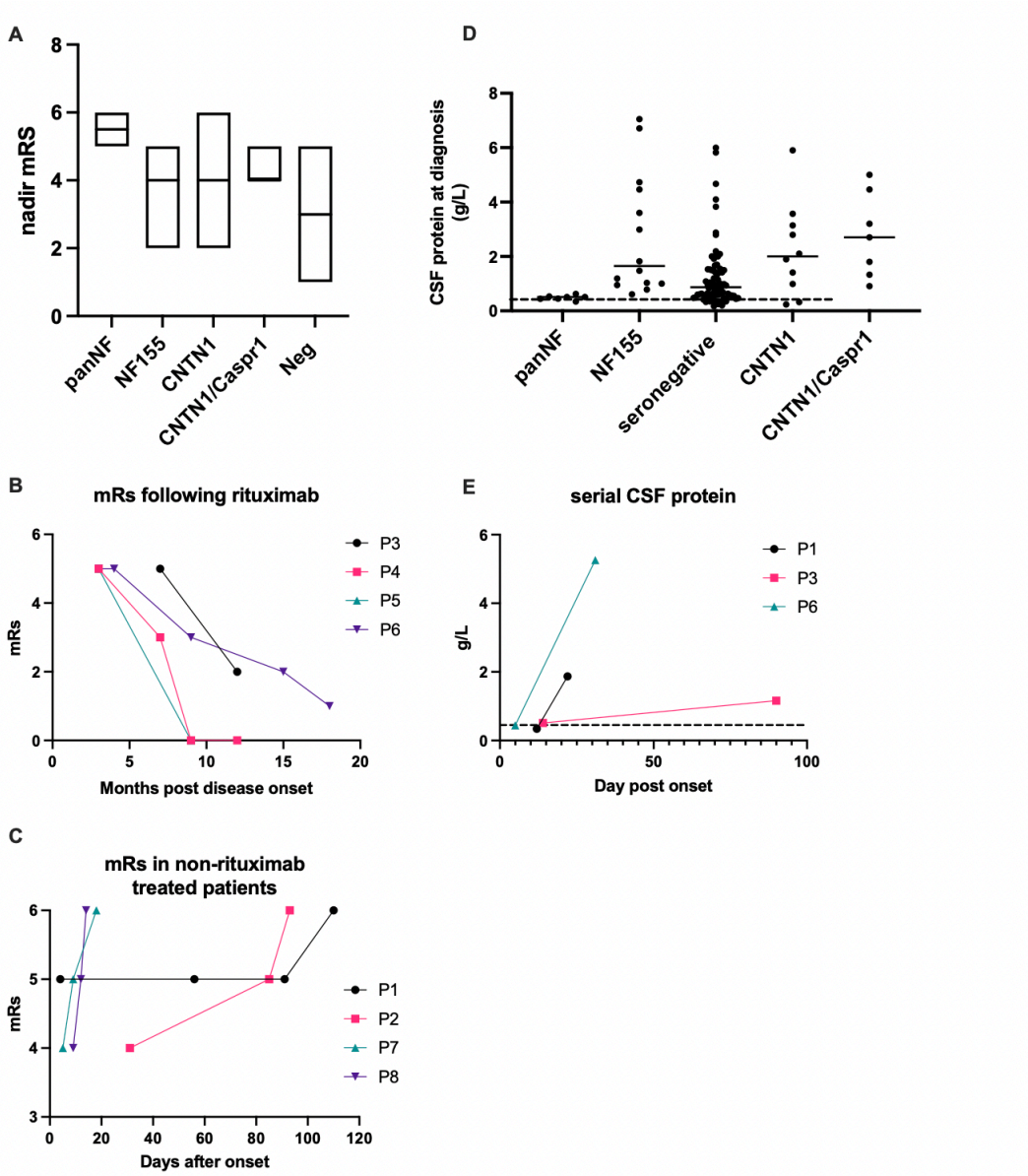


Figure 36: Modified Rankin scores and CSF protein levels.

(A) The median nadir modified Rankin score (mRs) in the pan-neurofascin (panNF) antibody group was significantly higher than that in both the neurofascin-155 (NF155) antibody positive and seronegative groups. (B) Change in mRs in the 4 rituximab treated patients. The first datapoint for each patient represents the time of the first dose of rituximab. (C) Change in disability of non-rituximab treated patients. (D) CSF protein in the panNF group was either normal or only marginally elevated at diagnosis, and significantly lower than in both NF155 antibody positive and seronegative patients. (E) When performed, repeat CSF sampling showed abnormally increased protein levels at later time-points. Dashed lines indicate the upper limit of normal for CSF protein (0.45 g/L). (Fehmi, Davies, et al., 2021)

Age at onset / Gender	Clinical									Investigations				Treatment (response)					Outcome
	Initial Clinical Diagnosis	Motor/ Sensory	CN palsy	Autonomic	Ataxia	Pain	Associated conditions	ITU / MV	Nadir mRS	Para-protein	NCS (Overall impression)	Nerve biopsy	Anti-NF155/ 186 Titre (CBA)	Steroids	IVIg	PLEx	RTX	Other	
P1	GBS	M&S	✓[a]	✓	×	✓	Nephrotic syndrome	✓	6	ND	Inexcitable	×	1:6400/ 1:3200	×	✓	✓	×	×	Death (Day 110)
P2	CIDP	Motor only	✓[b]	✓	×	✓	Breast Cancer	✓ (declined MV)	6	ND	Demyelinating	×	1:3200/ 1:3200	✓	✓	✓	×	CYC	Death (Day 93)
P3	CIDP	M&S	✓[c]	×	×	×	Hodgkin lymphoma	✓	5	IgG-Lambda	Demyelinating	Axonal loss	1:3200/ 1:1600	✓	✓	✓	✓	ChlVPP	mRS 2 (1 year post RTX)
P4	Atypical MMN	Motor only	✓[d]	×	×	×	CLL	×	5	IgG-Lambda	Axonal	×	1:800/ 1:1800	✓	✓	✓	✓	CYC FDB	mRS 0 (9 months post RTX)
P5	GBS	M&S	✓[e]	✓	✓	×	No	✓	5	ND	Demyelinating	×	1:400/ 1:800	✓	✓	✓	✓	×	mRS 0 (9 months post RTX)
P6	GBS	M&S	✓[f]	✓	✓	✓	Nephrotic syndrome	✓	5	ND	Mixed	Axonal loss	1:3200/ 1:6400	✓	✓	✓	✓	×	mRS 1 (18 months post RTX)
P7	GBS	M&S	✓[b]	✓	×	×	No	✓	6	ND	×	×	1:800/ 1:800	×	✓	×	×	×	Death (Day 18)
P8	GBS	Motor only	✓[g]	✓	✓	✓	Nephrotic syndrome	× (deemed unsuitable)	6	ND[h]	×	×	1:400/ 1:400	×	✓	×	×	×	Death (Day 14)

Supplementary Table 2 - Clinical features of pan-neurofascin antibody positive patients

Key:
✓ Given but no response
✓ Given but only partial and/ or transient response
✓ Given with good response
× Not given / not present / not done

[a] II-VII, IX-XII including optic disc swelling
[b] Facial diplegia, subtle gaze palsy
[c] Bilateral III, IV and VI nerve palsies, facial diplegia
[d] Mild bulbar weakness
[e] Facial diplegia, dysphonia
[f] Facial diplegia, complete opthalmoplegia, optic disc swelling with reduced visual acuity, bulbar dysfunction
[g] Facial diplegia
[h] Clonal urinary lambda light chain

ND: Not detected
CN: Cranial Nerve
CLL: Chronic Lymphocytic Leukaemia
MV: Mechanical ventilation
mRS: modified Rankin Score
CYC: Cyclophsphamide
FDB: Fludarabine
IVIg: Intravenous Immunoglobulin
PLEx: Plasma Exchange
ChlVPP: Combination chemotherapy for Hodgkins Lymphoma (Chlorambucil, Vinblastine, Procarbazine, Predinisolone)

Table 7: Clinical features of panNF antibody positive patients

[Supplementary table 2 from (Fehmi, Davies, et al., 2021)*]*

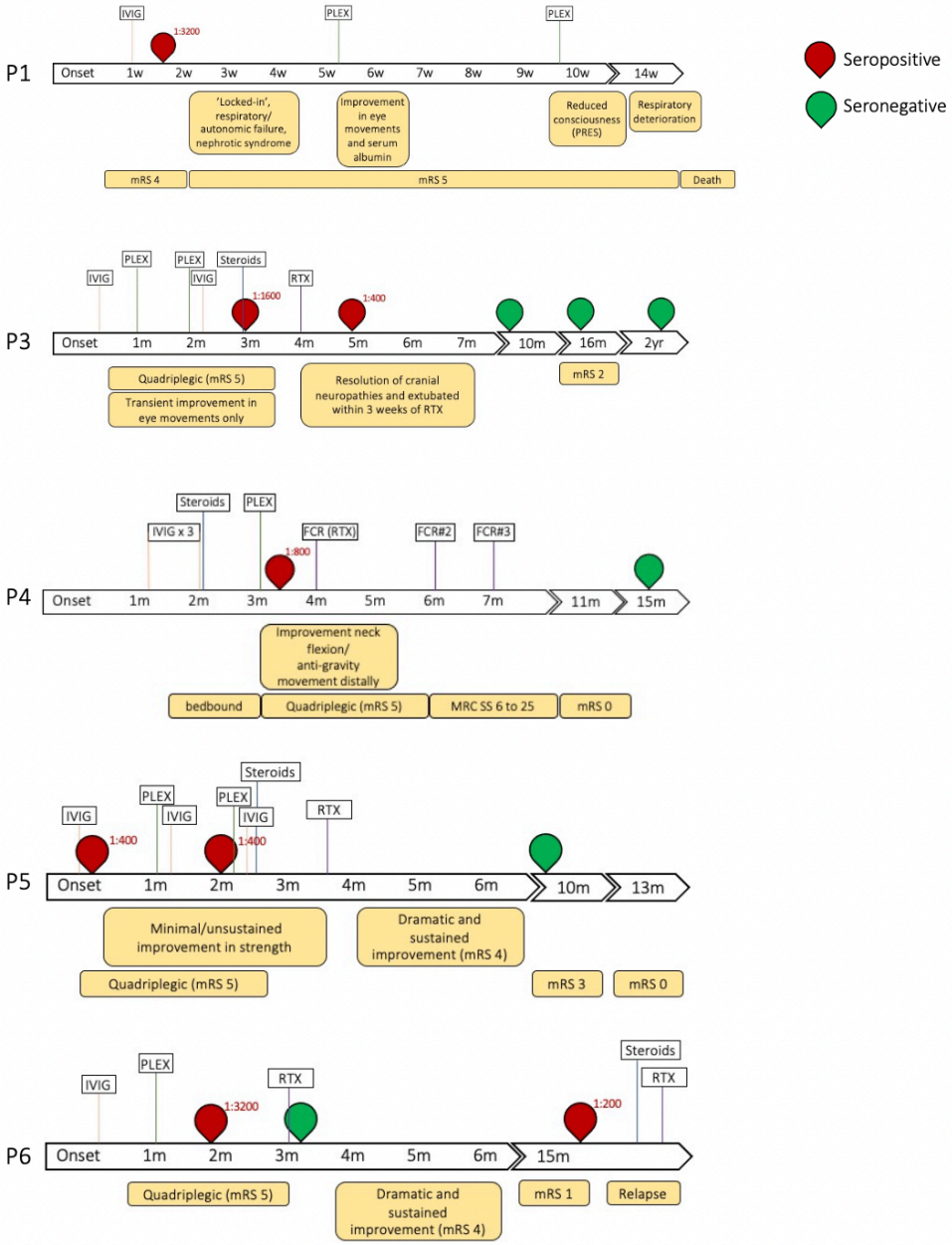


Figure 37: Treatment timelines of anti-panNF AIN patients

Treatments are indicated by flags at timepoints after onset lf symptoms (m – months, w – weeks). Functional status and recorded responses are noted in yellow boxes. Serological status, with antibody titre if positive, are indicated by red and green markers (see key in figure), and included where these were serially performed.

ChlVPP – Chlorambucil, Vinblastine, Procarbazine, Prednisolone (started for Hodgkins Lymphoma) FCR – Fludarabine, Cyclophosphamide and rituximab (started for CLL in absence of haematological indication as felt to be driving panNF antibody production), mRS – modified rankin score, PRES – Posterior Reversible Encephalopathy Syndrome. [Supplementary figure 6 from (Fehmi, Davies, et al., 2021)*]*

Patient	Time from symptom onset	SNAPs	Motor Studies											EMG	Neurophysiologist's report
			Prolonged distal motor latency		Slowed conduction velocity			Abnormal F-waves			Conduction block		TD	CMAP	
			>110 %	>150 %	<90%	<85%	<70%	>120 %	>150 %	absent	>0.7	>0.5			
P1	2 weeks	Absent UL preserved sural												Globally absent	No signs of acute denervation	Inexcitable
	4 weeks	Globally absent												Globally absent	Positive sharp waves and fibrillations	Inexcitable
	8 weeks	Globally absent												Globally absent	Florid denervation with no recordable motor units	Inexcitable
P2	4 weeks	Marginal reductions in amplitude and velocity	1		3	3	1	2			3	2		<50% LLN x 1	ND	Demyelinating
P3	3 weeks [a]	Marginal reductions in amplitude and velocity	2		4	3				8	7	4		<80% LLN x1	Relative paucity of active denervation changes	Demyelinating
	6 weeks [a]	Absent UL SNAPs												Globally absent	Profuse acute denervation	Severe axonal loss
P4	4 weeks	Normal	4		2	2		2		6	4	4		<80% LLN x1		Conduction block
P5	Day 5	Mildly reduced UL amplitudes	3	2	2	1					1			<80% x6 <50% x 3	No spontaneous or voluntary activity	Demyelinating
	2 weeks		2											<80% x1 <50% x 1	Normal	Subtle demyelinating features, some improvement
	6 weeks	Absent / reduced	4	4	1	1	1	1	1	1				<20% x4 <10% x3	Pronounced active denervation	Secondary axonal loss
P6	3 weeks	Absent / reduced	3	2	2	2	1			1	2	1		<50% x5 <10% x4 NR x3	No spontaneous activity	Demyelinating
	5 weeks	Globally absent	1	1										<10% x4 NR x2	Profuse positive sharp waves and fibrillations	Severe axonal loss

Table 8: Detailed neurophysiological findings.

Numbers refer to how many individual nerves met the criteria stated. SNAP – sensory nerve action potential, CMAP – compound muscle action potential, ND – not done. Studies in this patient were performed 3 and 6 weeks after an acute neurological deterioration, which itself occurred after 4 months of insidiously progressive left leg weakness. Note the frequent presence of conduction block, absence of temporal dispersion, and frequent switch from a demyelinating/AIDP to axonal pattern on repeat testing, suggestive of nodal pathology ("nodopathy") (Uncini et al., 2013). *[Supplementary table 3 from* (Fehmi, Davies, et al., 2021)*]*

	Treatment response (% of treated, n)															
	Steroids				IVIg				Plasma exchange				Rituximab			
Antibody (n)	Total	Good	Partial	None/ deteriorated	Total	Good	Partial	None/ deteriorated	Total	Good	Partial	None/ deteriorated	Total	Good	Partial	None/ deteriorated
PanNF (8)	4	0	0	0	8	0	25% (2)	75% (6)	6	0	50% (3)	50% (3)	4	100% (4)	0	0
NF155 (17)	16	19% (3)	37% (6)	44% (7)	15	6% (1)	27% (4)	67% (10)	8	0	25% (2)	75% (6)	6	50% (3)	33% (2)	17% (1)
CNTN1 (11)	11	36% (4)	27% (3)	36% (4)	8	0	50% (4)	50% (4)	4	0	0	100% (4)	4	50% (2)	25% (1)	25% (1)
CNTN1/Caspr1 (9)	8	13% (1)	50% (4)	37% (3)	8	0	13% (1)	87% (7)	4	0	50% (2)	50% (2)	6	67% (4)	33% (2)	0
Seronegative (194)	62	8% (5)	34% (21)	58% (36)	83	8% (7)	43% (36)	48% (40)	27	30% (8)	30% (8)	41% (11)	1	0	0	100% (1)

Table 9: Physician reported treatment response by serological group

[Supplementary table 4 from (Fehmi, Davies, et al., 2021)*]*

A cohort of four paediatric cases (aged 2-5) were also found to possess antibodies reactive against neurofascin isoforms: 2 to all neurofascin isoforms (panNF), 1 to NF186/140 only and 1 to NF155. They were reported by Harris et al (R. E. Harris et al., 2023), and three of which were importantly the first cases of immunotherapy-responsive AIN that were predominantly of the IgG2 subclass. These responded favourably to IVIg, in comparison to the IgG1/4 predominant case which responded to steroids.

3.2.4 CNTN1-antibody AIN cohort with neuropathy and nephropathy

3.2.4.1 Contactin-1 links autoimmune neuropathy and membranous glomerulonephritis

The following results from an observational study have been previously published, showing anti-CNTN1 antibodies can link AIN to nephrotic syndrome caused by membranous glomerulonephritis (MGN) (Fehmi et al., 2023). At this time, 15 patients with an immune-mediated neuropathy, positive for IgG4 CNTN1 antibodies, and concurrent nephrotic syndrome (biopsy proven MGN in 12/12) were identified (summarised in **Table 11**). Their clinical features were compared to seronegative counterparts, and CNTN1 protein or immune complexes identified in both nerve (iPSC derived) and kidney (in those with tissue available) to demonstrate shared target pathogenicity.

For this study we tested sera from patients with suspected immune-mediated neuropathies for (para)nodal targets (CNTN1, Caspr1, NF155, NF186), in our testing centre (Oxford), using a live CBA. At the time of reporting 468 individual patient sera had been prospectively screened, and 36 (7.7%) were found to be seropositive for antibodies targeting one of these. Ten (27.8% of the seropositive group) were anti-CNTN1 antibody positive, and 8 of these also had nephrotic syndrome. In contrast, of the 147 patients who were assessed for nephrotic syndrome from the seronegative group (147/432; 34%), only 5/147 (3.4%) had features suggestive of nephrotic syndrome ($p<0.001$, Fisher's exact test, OR for nephrotic syndrome with CNTN1 antibodies versus seronegative patients = 113.6, 95% CI 11.2 to 169.1). Two patients with (para)nodal antibodies from our cohort (not CNTN1) were additionally found to have nephrotic syndrome.

In light of these findings a subsequent 7 patients with an anti-CNTN1 antibody positive AIN and confirmed nephrotic syndrome (MGN confirmed on biopsy) were retrospectively sought out from international testing centres.

Serologically, of the 9 patient sera that we tested in our laboratory using CBA and ELISA (subclasses undetectable in 2 sera on ELISA), IgG4 was found to be the predominant IgG subclass in 5, and IgG1 was equally reactive in 3 and dominant in 1 (**Figure 11**).

We further tested 295 sera from patients with a nephropathy (idiopathic MGN), but without an apparent neuropathy, and found 4 (1.4%) to be positive for anti-CNTN1 antibodies (**Figure 38**). The antibody targeting glomerular podocyte antigen phospholipase A2 receptor antigen (anti-PLA2R), most often frequent antibody to MGN (anti-PLA2R antibody) (Beck Jr. et al., 2009) was not identified in these 4 as a cause of their nephrotic syndrome, nor was it found in 10 of the 15 patients in our cohort with CNTN1 antibodies, nephropathy and neuropathy (remaining sera unavailable for further testing). Testing for other novel pathogenic antibodies in MGN was not done due to lack of clinical assay availability.

Two hundred and fifty-six control patient sera (90 with other neurological diseases, 46 with lupus nephritis, 12 with class V membranous lupus nephritis, and 120 with other non-neurological/non-renal diseases) were negative for anti-CNTN1 antibodies (Fehmi et al., 2023).

3.2.4.2 Patients with CNTN1 antibodies have a distinct clinical syndrome

The majority of patients with anti-CNTN1 antibodies, neuropathy and nephropathy presented with a rapidly progressive, severe, sensory-motor neuropathy in association with nephrotic syndrome, characterised by oedema, hypoalbuminaemia, and urinary proteinuria (**Table 10**). Additional features, such as pain, tremor,

cranial neuropathies and autonomic dysfunction were common, and over one quarter had an existing diagnosis of diabetes (Fehmi et al., 2023).

3.2.4.3 The nephropathy and neuropathy are immunotherapy responsive and improve in parallel with a reduction in CNTN1 antibody titres

Three quarters of patients improved significantly, achieving complete remission or at least stabilisation of neuropathy and nephropathy in parallel. However, up to four different treatment modalities (including escalation immunotherapy i.e RTX) were typically required to induce a good response, with only 20% (3/15) deemed to respond well to first-line treatment (**Table 10**). There was a 20% mortality rate within this cohort, with two of the oldest patients dying from multi-organ or respiratory failure, and another from complications of coronavirus disease-19 (COVID-19) following prior treatment with IVIg, steroids and RTX. Clinical (neuropathy and nephropathy) and serological remission occurred in parallel, with CNTN1 antibody titres decreasing after immunosuppressive treatment in all 6 patients in whom post-treatment samples were available (**Figure 39A**) ($p = 0.001$). Specifically, clinical improvement could be seen by a reduction on the CIDP Disease Activity Scale (CDAS) (**Figure 39B**), and more detailed serial assessments in one patient show improvements in strength and disability paralleled the fall in CNTN1 antibody titres, and a fall in urinary protein levels followed shortly after (**Figure 39C**).

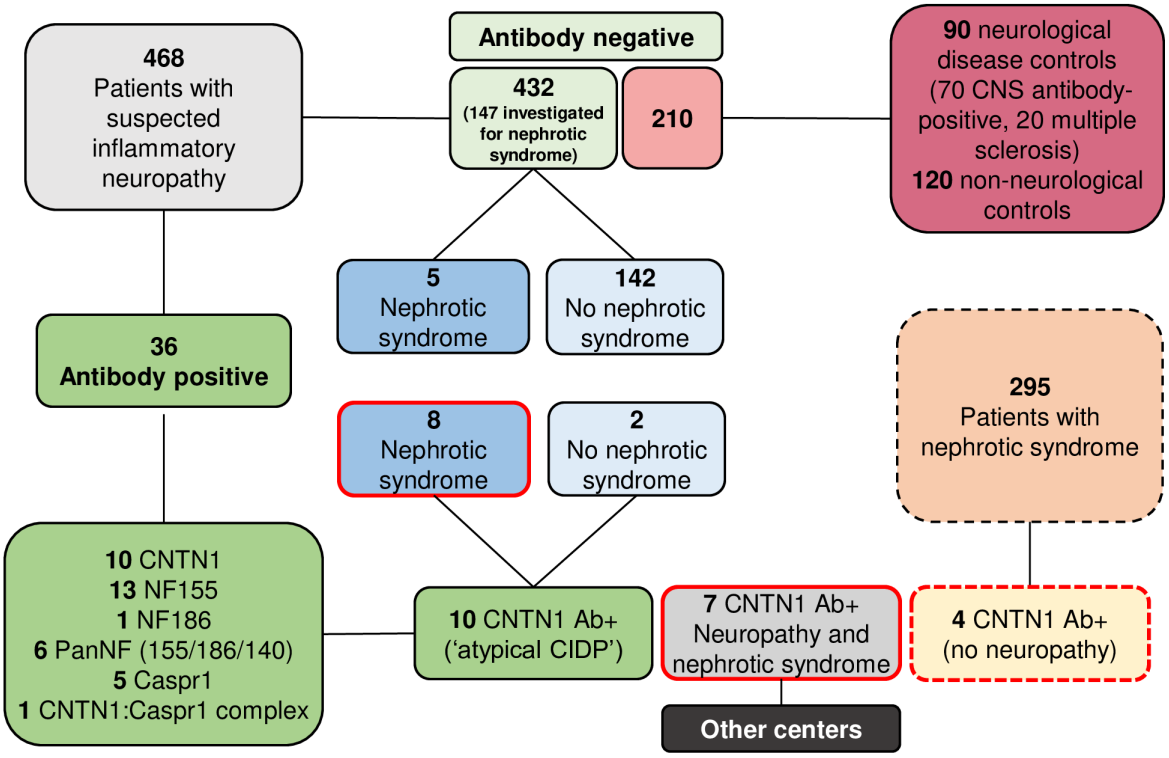


Figure 38: Flowchart summarising detection of patients with CIDP, nephrotic syndrome and CNTN1 antibodies through prospective (para)nodal autoantibody screening

Detection of 8 patients with definite CIDP, nephrotic syndrome and CNTN1 antibodies through prospective testing of sera from patients with suspected inflammatory neuropathies. Subsequently, seven patients were identified from other testing centres, and sera from a further 295 patients with known nephrotic syndrome caused by idiopathic membranous glomerulonephritis were tested only for CNTN1 antibodies using cell-based assay, and 4 were weakly positive (IgG fluorescence labelling to CNTN1-treansfected cells clearly visible, but weakly above background). Patients with central nervous system (CNS) autoimmunity, including 70 antibody-mediated disorders (n=21 anti-aquaporin 4, n=9 anti-NMDA receptor, n=20 anti-glycine receptor, n=20 anti-myelin oligodendrocyte glycoprotein) were used as neurological controls; all were negative for NF186/140, NF155, CNTN1 and Caspr1 antibodies, as were all of the 120 non-neurological controls, which included healthy individuals and those with uncomplicated viral infections, and all 46 patients with secondary membranous lupus nephritis. NMDA, N-Methyl-D-aspartate. Sera from an additional seven patients with neuropathy and nephropathy were provided by other centres. Patients with anti-CNTN1 antibodies, neuropathy and nephropathy are shown in boxes outlined in red; dashed line indicates lack of diagnosed neuropathy [Supplementary figure S1 from (Fehmi et al., 2023)*]*

	SUMMARY OF KEY CHARACTERISTICS		
	Characteristic		**Patients % (No.)**
CLINICAL	Age (median, range)		59 (39–79)
	Male		80 (12/15)
	Diabetes		26.7 (4/15)
	Acute/Subacute onset		86.7 (13/15)
	Additional clinical features (inc ataxia, tremor, cranial nerve palsy, autonomic dysfunction and abdominal weakness)		93.3 (14/15)
	Pain		53.3 (8/15)
	Median nadir disability—mRS (range)		5 (2–6)
INVESTIGATIONS	CSF	Median protein g/l (range)	1.99 (0.24–5.93)
		Normal protein	21.4 (3/14)
		WCC >5	28.6 (4/14)
	Meets electrodiagnostic criteria for CIDP [A]		93.3 (14/15)
	Median serum albumin g/l (range)		22 (11–36)
	Median urinary PCR mg/mmol (range)		1032 (633–4638)
	Median urinary protein g/24hr (range)		3.35 (2.2–10)
	Clinical criteria met for nephrotic syndrome[B]		92.3 (12/13)[C]
	MGN on renal biopsy		100 (12/12)
	Complement (C3 or C1q) deposition noted		58 (7/12)
	PLA_2R negative (IHC or serum antibodies)		100 (10/10)
TREATMENT RESPONSE [D]	First line therapy (Steroids +/-IVIg +/- PE)	Responders	20 (3/15)
		Non-responders	66.7 (10/15)
	Escalation therapy[E] (inc. RTX)	Responders	73 (8/11)
		Non-responders	27 (3/11)
OUTCOME	mRS (median, range)		1 (0–6)
	Complete remission (of both neuropathy/nephropathy)		31 (5/15)
	Significant improvement (≥ 2 points mRS)		38 (6/15)
	Minimal improvement/stabilisation (of both neuropathy/nephropathy)		6 (1/15)
	Death		25 (3/15)

Table 10: Summary of patients with neuropathy, nephrotic syndrome and CNTN1 antibodies.

[Table 1 from (Fehmi et al., 2023)*]*

[A] *As per EFNS/PNS* (Van den Bergh et al., 2021)

[B] *One or more of urinary PCR >300mg/mmol, proteinuria >3g/24 hours, serum albumin <35g/l*

[C] *1 patient did not meet clinical criteria for nephrotic syndrome, and 2 did not have nephrotic investigations available. All 3 of these had biopsy proven MGN.*

[D] *Definition of treatment response*

Responder: Complete remission, Sustained functional improvement > = 2 points mRS

Non-responder: Death, no response, transient response or improvement by only 1 point on the mRS

[E] *Escalation therapy includes (in order of frequency used): Rituximab, Cyclophosphamide, Azathioprine, Tacrolimus, Autologous stem cell transplant, Mycophenolate Mofetil, Immunoadsorption*

Abbreviations: CIDP–chronic inflammatory demyelinating polyneuropathy, CSF–Cerebrospinal fluid, IHC–Immunohistochemistry, IVIg–Intravenous immunoglobulin, mRS–Modified Rankin score, PE–Plasma exchange, PCR–Protein:Creatinine ratio, RTX–Rituximab, WCC–White cell count.

PATIENTS	P1	P2	P3	P4	P5	P6	P7
Demographic	56 M	49 M	39 M	50 M	79 M	74 M	62 M
PMH/FH	-T2DM -Bilateral carpel tunnel -Pulmonary emboli -Two 1st degree relatives: diabetes -Two sisters: HTLV-1 -1st degree relative: Lupus	-HTN -Gout -1st degree relative: GBS	-T2DM Optic neuritis (OPA1 mutation) -15 years relapsing-remitting painful paraesthesia (tongue, hands and feet) and co-existent MGN	None	None	None	-BPH -Hyperlipidaemia -Pulmonary emboli
Neuropathy onset	Subacute	Subacute	Subacute on chronic	Subacute	Subacute	Subacute	>2 months to nadir, rapid progression

Limb symptoms (15/16 'definite CIDP')*	Typical phenotype† (proximal ULs, distal LLs predominant)	Typical phenotype	Typical phenotype (deterioration in sensory symptoms with mild weakness)	Typical phenotype (paraesthesia ULs followed 3 months later by weakness all limbs)	Typical phenotype	Typical phenotype	Typical phenotype
Additional clinical features	Postural tremor Abdominal bloating & weakness**	Back pain Sensory ataxia Abdominal bloating & weakness**	Neuropathic pain Postural tremor (ULs, voice, head)	Dysphonia Unilateral ptosis Gait ataxia	Facial palsy	Neuropathic Pain Sensory ataxia	Neuropathic pain Autonomic disturbance (Hyperhidrosis and constipation)
Nadir Disability	Mild (mRS 2)	Moderate (mRS 3)	Moderate (mRS 3)	Mod-severe (mRS 4)	Death (mRS 6)	Death (mRS 6)	Mod-severe (mRS 4)
Notable blood results	↑ ESR	↑ ESR 109mm/hr IgA Kappa paraprotein	NA	NA	NA	NA	NA

PATIENTS	P1	P2	P3	P4	P5	P6	P7
CSF WCC	<5	<5	<5	↑ 28 (100% monocytes)	<5	<5	↑ 14
CSF Protein g/l	0.32	↑ 2.1	0.24	↑ 2.8	↑ 2.4	↑ 1.5	↑ 2.08
Imaging	MRI neuroaxis/ CT CAP/ PET normal	MRI neuroaxis/ CT CAP normal	ND	MRI neuroaxis/ PET-CT normal	ND	ND	MRI neuroaxis normal
Clinical Evidence of nephrotic syndrome/renal dysfunction §	Within 5 months Oedema ↓ albumin (11g/L) ↑ PCR (1142mg/ mmol)	Within weeks (No oedema) ↓ albumin (24g/L) ↑ PCR (633mg/ mmol)	Within 2 months Oedema ↓ albumin (26g/L) Proteinuria (3.5g/24hr) ↑ PCR	Within a month Oedema ↓albumin (12g/L) ↑ PCR (4638mg/ mmol)	Oedema Creatinine 100µmol/L Proteinuria (3g/24hr) PCR (180mg/mmol)	Albumin (36g/L) Creatinine 87µmol/L Proteinuria (3.35g/24hr) ↑ PCR (718mg/ mmol)	Oedema Creatinine stated to be within ‘normal range’ ↓ albumin (20g/l) Proteinuria (8.3g/24hr)

			(1032mg/ mmol)				↑ PCR
Renal Biopsy	MGN Positive: IgG, C3 Negative:IgA, C1q	MGN Positive: IgG, C3, IgA Negative: IgM, C1q	MGN Positive: Immune complex deposition, IgG, C3	MGN Positive: IgG, C3/4 Negative: IgA, C1q, IgM	MGN	MGN	ND
PLA_2R status ||	Negative IHC	Negative IHC	ND	Antibody negative	Antibody negative	Antibody negative	ND
Treatment (response if clear	Concurrent steroids and CYC (good)	Steroids (good) IVIg (partial)	Steroids (partial) IVIg (good) Tacrolimus (good) Thalatomy (for tremor)	Steroids IVIg PE CYC RTX (unresponsive to all above) ASCT (Good)	Steroids IVIg PE	Steroids IVIg PE RTX	Steroids IVIg AZA PE (unresponsive to all above) RTX (good)

PATIENTS	P1	P2	P3	P4	P5	P6	P7
OUTCOME (neuropathy)	Complete remission (mRS 0) (Steroid dependent)	Good (mRS 1)	Good (mRS 1)	Good (mRS 2)	Death (Multi-organ failure)	Death (Multi-organ failure	Complete remission (mRS 0)
OUTCOME (nephropathy)	Stabilised	Complete remission	Complete remission				

PATIENTS	P8	P09	P10	P11	P12	P13	P14	P15
Demographic	58 M	62 M	66 M	39 F	52F	60 F	72 M	59 M
PMH/FH	Graves' disease	-IDDM -HTN -BPH	None	None	Two 1st degree Relatives - diabetes	-T2DM -HTN -Hashimoto's thyroiditis -ITP -Severe AS -2 year history progressive tremor and gait disturbance (diagnosed CIDP 2015)	-T2DM -HTN -Chronic pancreatitis -Hyperlipidaemia -CKD (baseline ACR 35) – obstructive uropathy and recent bladder neck surgery	None
Neuropathy onset	Subacute	Subacute	Subacute	Subacute	Subacute	Subacute on chronic	Subacute	Chronic progressive
Limb symptoms (15/16 'definite CIDP')*	Typical phenotype	Typical phenotype	Typical phenotype	Typical phenotype	Typical phenotype	Typical phenotype	Typical phenotype	Typical phenotype (prox-dominant weakness)

Additional clinical features	Sensory ataxia	-Back pain -Facial paralysis -Autonomic disturbance (Urinary urgency, orthostatic hypotension)	-Facial palsy -Tremor	-Sensory Ataxia -Tremor	-Sciatic-like pain -Sensory ataxia	-Tremor -Gait ataxia	Back pain	-Neuropathic pain -Sensory ataxia -Autonomic disturbance -Rash -Hyper-somnolence -REM-BD -Cognitive decline -Constitutional symptoms (sweats, weight loss)
Nadir Disability	Severe (mRS 5)	Severe (mRS 5) Tetraparesis, Required artificial ventilation	Severe (mRS 5)	Mild (mRS 2)	Severe (mRS 5)	Moderately severe (mRS 4) prior to death due to COVID19	Severe (mRS 5) Tetraparesis, Required artificial ventilation	Moderately severe (mRS 4)

PATIENTS	P8	P09	P10	P11	P12	P13	P14	P15
Notable blood results	NA	↑ ESR >120mm/hr	NA	NA	↑ Eosinophils	NA	NA	↑ ESR, WCC, eosinophils, serum IgG4
CSF WCC	<5	<5	<5	<5	<5	ND	↑ 40 (100% lymphocytes)	↑ 5-8
CSF Protein g/l	↑ 1.4	↑ 1.9	0.46	↑ 2.25	↑ 3.14 (CSF/Serum albumin ratio 69.64)	ND	↑ >6	↑ 0.99
Imaging	Lumbar spine MRI: mild enlargement cauda equina nerve roots (no gadolinium)	ND	ND	ND	MRI Brain, Spine and plexi enhancement and thickening of roots PET-CT – lymph nodes 'reactive'	ND	CT CAP (enlarged para aortic lymph node)	MRI brain and spine, CT CAP unremarkable
Clinical	Within 2 months Oedema			Not available		Oedema		

Evidence of nephrotic syndrome/renal dysfunction §	Creatinine 55-96mol/L ↓ albumin Proteinuria (10g/24hrs)	Creatinine 60-67mol/L ↓ albumin (12g/l) ↑ PCR (716 mg/mmol)	Creatinine 82µmol/L PCR (220mg/mmol) Proteinuria (2.2g/24hrs)		Proteinuria	↓ albumin (27g/l) ↑ PCR (1300mg/ mmol)	↓albumin (18g/l) Proteinuria (3.05g/24hrs) ↑ PCR (1015mg/mmol)	↓ albumin (24g/l) Proteinuria (8.4g/24hrs)
Renal Biopsy	MGN Positive: IgG, C3	MGN and Diabetic nephropathy Positive: IgG, IgA	MGN Positive: IgG, C3/4	MGN	MGN Positive: IgG Negative: IgM, IgA, C3, C1q	MGN Positive: IgG4, C1q	ND	ND
PLA_2R status ||	ND	Antibody negative	Antibody negative	Antibody negative	Negative IHC and antibodies	Negative IHC and antibodies	ND	ND

PATIENTS	P8	P09	P10	P11	P12	P13	P14	P15
Treatment (response if clear)	IVIg (mild) Steroids (none) CYC and PE (good)	Steroids IVIg PE (unresponsive to all above) RTX Protein A (IA) CYC	Steroids IVIg PE RTX	Steroids IVIg AZA MMF	Steroids (more effective than IVIg) IVIg	Steroids IVIg (transient) RTX	IVIg (transient) Steroids (none) PE (none) RTX (good)	Steroids (good)
OUTCOME (neuropathy)	Complete remission (mRS 0)	Good (mRS 3)	Stabilised (mRS 4)	Complete remission (mRS 0)	Good (mRS 1)	Death (COVID19) Prior treatment not effective	Good (mRS 2)	Significant and spontaneous resolution followed by relapse, successfully treated with steroids
OUTCOME (nephropathy)		Good		Stabilised	Good		Good	

								(mRS 0, lost to follow up)

Table 11: Key characteristics of 15 patients with immune-mediated neuropathy and nephrotic syndrome with positive anti-CNTN1 antibodies (patients 1-7 and 8-15)

** According to EFNS/PNS criteria*

*** Associated with severe denervation of rectus abdominis and iliopsoas on EMG when tested for in one patient*

† Symmetrical non-length dependent weakness and sensory disturbance in all limbs

§ 'nephrotic' range (PCR > 300mg/mmol or proteinuria >3g/24hr), suggestive of glomerular pathology (PCR >100mg/mmol), normal serum albumin (35-55g/l). Proteinuria is in grams over a 24 hour period. Timing relative to neuropathy stated where available.

|| IgG subclass was only available for one patient (P13)

 # PLA_2R was specifically tested for only where status is confirmed

Abbreviations:

ACR – Albumin: Creatinine ratio, AS – Aortic Stenosis, ASCT – Autologous Stem Cell Transplant, AZA – Azathioprine, BPH – Benign prostatic hyperplasia, CKD – Chronic kidney disease, CT CAP – Computed tomography chest abdomen pelvis, CYC – Cyclophosphamide, ESR – Erythrocyte sedimentation rate, FH – Family history, HTN – Hypertension, HTLV-1 – Human T-lymphocytic virus 1, IA – Immunoadsorption, IDDM – Insulin dependent diabetes mellitus, IHC – Immunohistochemistry, ITP -Idiopathic Thrombocytopenic Purpura, IVIg – Intravenous Immunoglobulin, LL – Lower limb, MGN – Membranous Glomerulonephritis, MMF – Mycophenolate Mofetil, MRI – Magnetic resonance Imaging, mRS – Modified rankin score, ND – Not done, OPA1 – Optic atrophy type 1, PCR – Protein:Creatinine Ratio, PE - Plasma Exchange, PET – Positron emission tomography, RTX – Rituximab, T2DM – Type two diabetes mellitus, UL – Upper limb, WCC – White Cell Count (Fehmi et al., 2023)

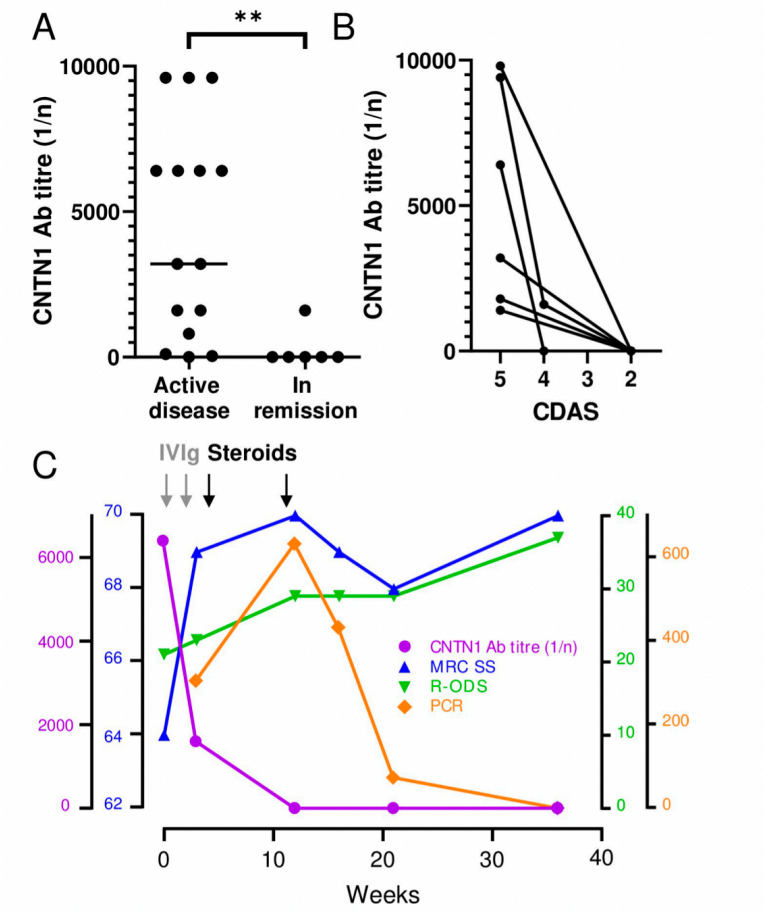


Figure 39: CNTN1 antibody titres correlate with disease activity.

(A) *CNTN1 antibody titres were significantly higher in active disease (on or pre-treatment) (n = 15), compared to remission of ftreatment) (n = 6, p = 0.001, Mann-Whitney).* ***(B)*** *In all 6 patients for whom serial samples were available, CNTN1 antibody titres fell in parallel with a reduction in neuropathy disease activity (measured using the CIDP Disease Activity Scale–CDAS) and became undetectable in 5 patients who achieved treatment-free remission.* ***(C)*** *In one patient, where this level of detail was available, serial assessments showed that improvements in strength (Medical Research Council sum score, MRC-SS), functional abilities (inflammatory neuropathy Rasch-built Overall Disability Scale, iR-ODS) and normalisation of renal function (Protein Creatinine Ratio, PCR) correlated with falling CNTN1 antibody titres. Grey arrows indicate IVIg administration (2g/kg over 5 days), and black arrows pulsed dexamethasone (40mg daily for 4 days, repeated after 4 weeks). [Figure 3 from* (Fehmi et al., 2023)]

3.2.5 Discussion

The prevalence of AINs in our cohort of patients screened for (para)nodal antibodies is slightly lower than reported in the literature (up to 18%). The main reason for this is likely to be that we identified patients from a much larger more varied cohort than others, but additionally, variation in the diagnostic assays used to confirm antibody presence may lead to more false positives in some cohorts. In line with existing literature we found antibodies were most frequently reactive to NF155, but we report a slightly higher frequency of panNF antibodies than CNTN1, which is contrary to prior published reports. This may be due to only recent testing of patient sera to both NF155 and NF186 antigenic targets, resulting in a prior overestimation of patients with NF155 mono-specific antibodies, and underestimation of panNF- reactive antibodies.

Serological profiles of (para)nodal antibodies have almost always reported IgG4 as the predominant subclass in the literature. Indeed our results have been concordant with this in our prior publications. However, the most recent analysis of IgG subclasses suggests IgG1 to be the most dominant subclass in all antibody groups. This is closely followed by either equally reactive IgG1 and 4 subclasses or solely IgG4 dominance in all of the groups except panNF antibody positive patients. In the latter group, contrary to prior reports, the antibody subclass with the strongest reactivity is IgG1, only a few with IgG4 or IgG2 subclasses being equally dominant to IgG1.Our latest data also reveals that all antibody groups had some reactivity to all IgG subclasses, except those with CNTN1/Caspr1 complex monospecific antibodies. Other studies have reported IgG3 reactivity to NF186 or panNF antibodies, with similar clinical phenotypes to our cohort (Burnor et al., 2018; Stengel et al., 2019; J. M. Vallat et al., 2018). Although IgG1 and IgG3 are both notable for being potent activators of complement, this difference in detectable IgG subclass between laboratories could not be explained by the multicentre, inter-laboratory, blinded comparison study of diagnostic assays that we were part of conducting (Rinaldi et al., 2022), and it has similarly been reported with other antigenic targets (Waters et al., 2016). It may have been due to technical aspects of the assays, though the secondary antibodies used in our laboratory recognised the relevant subclass of recombinant human IgG in ELISA (**Figure 10A**), did not cross-react between subclasses, and we used the same tertiary antibody for detection.

NF155 AN patients also more frequently had IgG1 than IgG4 antibodies in our cohort, though both were strongly reactive.

The emergence of IgG1 as a dominant subclass in our AIN dataset, even exclusive of those with panNF antibodies, is not one that has been reported before, and may be a result of technical aspects of the assay and/or subclass antibodies used. Further, studies reporting IgG4 predominance do not seem to state whether other subclasses were present or not, even if only weakly. These findings, though, are relevant, as the absolute presence or absence of IgG subclasses able to bind complement and FcγR could influence the pathogenic mechanism/s at play, independent of apparent strength of reactivity in diagnostic assays. Further, determining the IgG subclass is important, as this may have potential to predict the clinical phenotype and potentially response to treatment.

As a group, those with an AIN in our cohort presented significantly more acutely than seronegative neuropathy patients, and were more likely to acquire an initial diagnosis of GBS. They were also more severely affected, with a median mRS of 4 (5 in the panNF group), signifying the inability to walk or attend to their own bodily needs independently, versus 3 in the seronegative group, who could mobilise independently. The presence of nephrotic syndrome, most often associated with the panNF than CNTN1 group, was significantly more common in the AIN than seronegative group, although the increased proportion of AIN patients with other clinical features considered ‘atypical’ or uncommon in inflammatory neuropathies i.e. ataxia, tremor, cranial nerve palsies, respiratory and autonomic dysfunction, did not reach statistical significance.

All individual antibody groups had a high proportion of male patients above the age of 50, in particular those with anti-CNTN1 antibodies, and presented with a symmetrical, proximal and distal, motor and sensory neuropathy. Consistent with NF155 seropositive patient cohorts reported in the literature, this group were the youngest in our cohort (42% < age 50), and they had the highest proportion of patients presenting

with distal symptoms (39%). The mRS at nadir was equal to or above 4 (moderately severe – inability to mobilise unaided) in at least three quarters of patients in each group, but particularly notable in panNF and Caspr1 patients (88%). The nadir mRS however did not correlate with peak antibody titres across the cohort. Serial clinical-serological data obtained for individual patients however, does suggest antibody titres correlate with clinical course, and highlight the potential for their use in disease monitoring on an individual basis. In some cases, for example where clinical recovery only has a limit i.e. if disease activity started long before treatment initiation, antibodies may dramatically deplete with therapy without a similar improvement in clinical functioning (Querol et al., 2015).

Individual antibody groups were notable for an increased frequency of specific clinical features, namely cranial nerve palsies (75% vs 26% seronegative), autonomic (36% vs 13% seronegative) and respiratory dysfunction (56% vs 14% seronegative) in panNF patients, and ataxia, tremor and neuropathic pain in the Caspr1 group, the latter feature consistent with the very first reported cases of anti-Caspr1 antibody positive patients. The association of nephrotic syndrome with panNF patients is not well recognised, and based on this latest data, has now superseded it's association more widely appreciated in connection with CNTN1 AIN patients.

Surprisingly, ataxia and tremor were only slightly more frequently observed in NF155 AIN patients compared with seronegative patients, two features often reported to be a distinguishing feature in NF155 patients. Similarly, MRI evidence of nerve root thickening/enhancement is a feature usually ascribed to NF155 cohorts, and indeed an earlier analysis of ours did show this (Fehmi, Vale, et al., 2021), but the latest data found this to be associated with 88% of Caspr1 patients, vs 40% of NF155. This highlights the importance of defining patterns of clinical features using larger datasets, and not restricting testing to specific (para)nodal antibodies on the basis of the presence of specific clinical features at this early stage in their recognition.

Autoimmune nodopathy patients were largely refractory to standard treatment with IVIg, steroids and PLEX. Of 81 AIN patients, 83% trialled more than one treatment, and over half trialled three or more, including alternative immunotherapies, most often RTX. Standard therapy was most often ineffective or equivocal (range: 43-66%), but reported to be partially effective in over a third of patients (range: 32 – 43%). RTX was clearly most effective, with reportedly 'good' outcomes, implying effective and sustained response, in over half of patients (56%), compared with IVIg (7%), PLEX (8%) and corticosteroids (19%). Those treated with RTX (and not reported to have a good response to any other alternative immunotherapy) had an improved mRS by at least 2 points in 60% of patients, compared with 40% in those only treated with standard therapies.

It is important to note that the nature of the study in which this data was collected is observational, thus the assessment of treatment responses were obtained at different timepoints per patient, and serial data were only acquired for some. At the time of completing the questionnaire, patient responses to treatment may not have been complete, or conversely may have subsequently deteriorated after the response from the clinician was submitted, thus not accurately reflecting their 'final' response. Additionally, treatments were often given in close succession, and in the case of steroids and RTX, together. Thus without serial assessments, or periods of treatment cessation in between each one, these responses may inaccurately be ascribed to the last administered.

Further, clinical data gathered relied upon the referring clinician completing the data collection form accurately, with potential variability in different clinicians' subjective assessment of treatment response into one of the four categories ('none' to 'good').

A more in depth analysis, and publication, of the initial 8 panNF AIN patients identified within our cohort was the first to report patients with IgG1-subclass panNF antibodies (Fehmi, Davies, et al., 2021). Whereas prior literature had suggested patients with non-IgG4-subclass antibodies may not be part of the AINs

(Cortese et al., 2020), we were able to demonstrate that our series of patients, in comparison with similarly identified seronegative controls, presented with a more rapidly progressive and severe neuropathy, frequently diagnosed as GBS at onset. Five patients did not go on to meet criteria for CIDP (Van den Bergh et al., 2021), something that had been largely described in those with (para)nodal antibodies, though in three, transient fluctuations occurred after treatment but within 8 weeks of onset (Ruts et al., 2010). Currently, it is the ongoing deterioration beyond 8 weeks of onset that most confidently distinguishes GBS from CIDP, though clearly this cannot helpfully inform therapeutic decisions in the early phases of a rapidly progressive neuropathy, which is paramount, given the potential for chronic disease and treatable nature of immune-mediated neuropathies. Thus, we believe testing for (para)nodal antibodies is justified in any patient with a 'GBS-like' presentation, as it would prompt earlier use of potent immunotherapy, and the need for longer term immunosuppression in a case that otherwise resembles GBS, typically considered monophasic and short-lived, only calling for one course of treatment. This could otherwise expose patients to a persistent autoimmune response which can potentially drive ongoing axonal loss leading to long-term disability, and preventing a good response to subsequent treatment. Our observations of inadequate responses to steroids, IVIg and/or PLEX followed by improvements after RTX occurring several months into their illness suggests a more prolonged suppression of antibody titres may be required to achieve sustained neurological improvement in patients with (para)nodal antibodies. A prior study assessing repeated apheresis in AIN patients supports this notion (A. J. Davies et al., 2020). The use of targeted immunotherapy at earlier timepoints in serologically defined cohorts should be assessed to determine the impact on such a severe disease course. Further, the potential for AIN patients to make such a meaningful recovery with appropriate treatment should drive the initiation of a clinical trial, addressing the use of RTX versus standard therapy. Although other alternative immunomodulatory agents are likely to be effective in some cases, the differences in treatment modalities, timelines, variable follow up and documented outcome measures across AIN cohorts means there is insufficient evidence to support their use preferentially over RTX

It is unknown whether RTX would have been as effective in the 4 patients who died should they have survived long enough to receive it, or indeed whether one of the other treatments they did receive would have taken effect. The extent to which chemotherapy for the haematological disorders in several panNF patients contributed to their neurological recovery is also unclear. The fact that 50% (4/8) of this cohort had an IgG/lambda paraprotein-associated lymphoproliferative disorder or solid organ malignancy, in the absence of any onconeural antibodies having been identified in the rare cases where cancer has been associated with GBS/CIDP (Rajabally & Attarian, 2018), suggests panNF antibodies may be pathogenic in such AIN patients.

Two of five patients in this cohort of 8 were found to have an associated nephrotic syndrome, the frequency of which in panNF patients has already superseded that of CNTN1 cohorts, since this paper was published. This may be explained by the expression of NF186 by glomerular podocytes as well as neurons (Sistani et al., 2013).

We conducted a prior analysis of CNTN1 AIN patients with nephrotic syndrome, and along with other studies have contributed to the recognition of this neuro-renal syndrome. By identifying CNTN1 as novel antigenic target in membranous glomerulonephritis (MGN), we highlight the importance of considering (and testing for) nephrotic syndrome in nodopathy patients, but also a neuropathy in patients with nephrotic syndrome. A previous report suggests that these presentations may not be temporally related (Nazarali et al., 2020), emphasising the need for monitoring. Given that half of patients with MGN may develop end-stage renal failure (Glassock, 2003), and CNTN1 AIN patients are often refractory to standard therapies, the need to identify and treat them early is paramount. Indeed, the use of escalation immunotherapies in our cohort of CNTN1 AIN and MGN patients substantially improved disability from the neuropathy, and the associated renal disease invariably improved in parallel, as has been found in another study (Plaisier et al., 2021).

The identification of IgG4 anti-PLA2R antibodies in 70% of patients with suspected idiopathic MGN (Beck Jr. et al., 2009) has been transformative in negating the need for more invasive diagnostic biopsies. In anti-PLA2R negative, anti-CNTN1 positive nephropathy patients, a similar approach could potentially be taken, providing an opportunity for earlier therapeutic intervention. We did however find renal glomerular CNTN1-immune-complex deposition in one patient despite being anti-CNTN1 antibody seronegative at the time (following steroid treatment), highlighting the careful consideration of renal biopsy in seronegative patients otherwise suspected to have antibody-mediated nephrotic syndrome.

Anti-CNTN1 antibodies may also be a helpful biomarker for disease monitoring and prognosis, given their levels mirrored clinical course. Indeed, high titre PLA2R antibodies were shown to predict a worse prognosis (Hoxha et al., 2014), and reduced titres found to precede remission (Beck et al., 2011). As with anti-PLA2R MGN (Burbelo et al., 2020), we found CNTN1 antibodies often preceded the onset of proteinuria, further supporting their utility as biomarkers.

3.3 Mechanistic studies of nodal and paranodal auto-antibody-mediated pathogenicity

3.3.1 Abstract

We have shown IgG from patients with AINs are able to bind to nodal and paranodal targets in live, myelinated, human stem-cell-derived sensory neurons. Further, through pre-adsorption assays with suspected protein targets, we can demonstrate they are specific. Axonal and myelin injury can be visualised using this live culture model, and cytotoxicity, through antibody and/or complement-mediated mechanisms, can be measured using commercial assays, and specifically axonal injury using neurofilament light within the supernatant. Initial investigation reveals that serum CNTN1 protein, previously reported to be significantly reduced in AINs, is unlikely to be a surrogate marker of neuronal injury in AIN patients.

Further objective assessment of (para)nodal antibody-mediated pathogenic effects in culture, and which factors influence this, is required. We have shown complement binding to transfected HEK cells targeted by (para)nodal antibodies, but methods to objectively assess the dependence of cell cytotoxicity on complement require optimisation.

In CNTN1 AIN patients with a concurrent renal injury we have been able to show CNTN1 immune complexes within renal glomeruli, as well as patient antibodies bound to the nodes of animal and human-derived peripheral nerves, thus establishing a shared pathogenic mechanism and treatment target, linking these two disorders.

There is promise in using the live myelinated neuron culture system to further define human (para)nodal IgG topographical binding patterns and determinants of neuronal injury, as well as extracting supernatant from injured cultures to further analyse potential fluid biomarkers of active disease.

3.3.2 Topographical patterns of antibody binding in myelinated co-cultures and investigation of in-vitro evidence of pathogenicity

Topographical binding of serum IgG from a proportion of patients with a confirmed AIN (by CBA) can be seen when applied to live myelinated sensory neuron cultures (**Figure 15**). Five of 7 panNF sera tested in our earlier cohort (Fehmi, Davies, et al., 2021) showed nodal binding, and two additional axonal binding, in live myelinating co-cultures (**Figure 34B** and **Figure 41A**), a distinct pattern to that observed with anti-NF155 monospecific IgG.

The antigen specificity of (para)nodal antibodies was further confirmed by pre-adsorption assays (with relevant soluble target protein) in both CBA (**Figure 9C** and **D**) and myelinating co-cultures (**Figure 40** and **Figure 41**), or exposure of sera pre- and post-successful immunotherapy (**Figure 42H** and **I**), which abrogated IgG binding.

3.3.2.1 Contactin-1 in patients with a peripheral neuropathy and nephrotic syndrome

In those patients with an anti-CNTN1 antibody AIN who also have evidence of nephrotic syndrome, both neuronal (**Figure 40** and **Figure 42E-H**) and glomerular binding (**Figure 42** and **Figure 43**) of IgG can be demonstrated. Further, CNTN1-containing immune complexes could be found in the renal glomeruli of patients with CNTN1 antibodies, but not in control kidneys. The following are extracts taken from the results of recently published material detailing this anti-CNTN1 AIN cohort with associated nephrotic syndrome:

3.3.2.1.1 CNTN1-containing immune complexes are found in the glomeruli of patients with CNTN1 antibodies

For 12 of the 15 anti-CNTN1 antibody positive patients with nephrotic syndrome renal biopsies were performed by referring centres, all characteristic of MGN (glomerular capillary wall thickening, basement membrane spikes and lucencies on silver stain). IgG (**Figure 42A**) and complement (C3 – not shown)

immunolabelling, with subepithelial electron dense deposits on electron microscopy (**Figure 42B**), representative of immune complexes, was further demonstrated in the glomerular capillary wall. Immunohistochemistry revealed CNTN1 protein deposition along the glomerular basement membranes (**Figure 42C** and **Figure 43**), and laser dissection of glomeruli followed by LC-MS/MS proteomic analysis revealed a peptide in CNTN1-immunopositive renal tissue, which matched with recombinant CNTN1 protein (**Figure 44**). By contrast, there was no positive CNTN1 protein staining found in control healthy human glomeruli or PLA2R antibody-induced MGN renal tissue (**Figure 42D**), though low level CNTN1 protein was detected by western blot (

Figure 45), as was CNTN1 mRNA by PCR in healthy human kidney (Fehmi et al., 2023).

3.3.2.1.2 Low serum CNTN1 protein levels correlated with immune complex formation

Levels of serum CNTN1 protein (sCNTN1) were shown by to be significantly lower in AIN patients with (para)nodal antibodies in comparison to seronegative and healthy control subjects (Wieske et al., 2021). In line with this recent data, and in collaboration with Wieske *et al*, I could show that sCNTN1 levels were significantly lower in anti-CNTN1 AIN patients with nephrotic syndrome (median 1.02 ng/ml, range 0.02 to 36.37) compared with 25 seronegative CIDP patients (four with concurrent nephrotic syndrome, median 10.67 ng/ml, range 3.96 to 30.06) and 25 non-neuropathy patients with only nephrotic syndrome (median 13.91 ng/ml, range 4.37 to 26.72) ($p = 0.003$ and $p<0.001$, Kruskal-Wallis) (**Figure 46A**). The trend for sCNTN1 and CNTN1 antibody levels to be inversely correlated was not significant ($p = 0.099$, $R2 = 0.1088$, simple linear regression) (**Figure 46B**), though interestingly in 5/8 patients in whom CNTN1 antibody levels became undetectable, sCNTN1 levels remained low. Finally, I detected CNTN1 protein using western blot from the PEG precipitates (immune complexes) obtained from a patient during active neurological and renal disease (patient 14 in **Table 11**), but not from the same patient during remission, nor in a healthy human donor (**Figure 46C** and **Figure 47**). In keeping with the existing data showing low levels of sCNTN1 in other anti-CNTN1 antibody patient sera samples (**Figure 46A**), CNTN1 protein was undetectable by

western blot in the soluble fraction (supernatant) of PEG-treated serum of P14 during active disease (**Figure 47**) (Fehmi et al., 2023).

3.3.2.1.3 CNTN1 antibodies from seropositive patients target peripheral nerves and paranodes

Incubation of anti-CNTN1 antibody positive patient sera with teased mouse nerve fibres showed IgG reactivity to paranodes, colocalising with Caspr1 (work performed by Dr Alex Davies) (**Figure 42E–G**). Further, I showed IgG labelling of unmyelinated axons (**Figure 42H**) and paranodal regions of myelinated axons (**Figure 42H**, inset) in live hiPSC-derived co-cultures. Subsequent incubation of patient sera depleted of CNTN1 antibodies from immunosuppressive treatment (as determined by CBA) (**Figure 42J** and **1K**) abrogated all IgG labelling from neuronal axons (**Figure 42I**). Further, the re-application to live CBA or neuronal co-cultures of CNTN1 antibody-containing sera pre-adsorbed with recombinant CNTN1 protein led to markedly reduced immunolabelling (**Figure 40**), confirming CNTN1 as the antigen for serum IgG binding in these live cell culture systems (Fehmi et al., 2023).

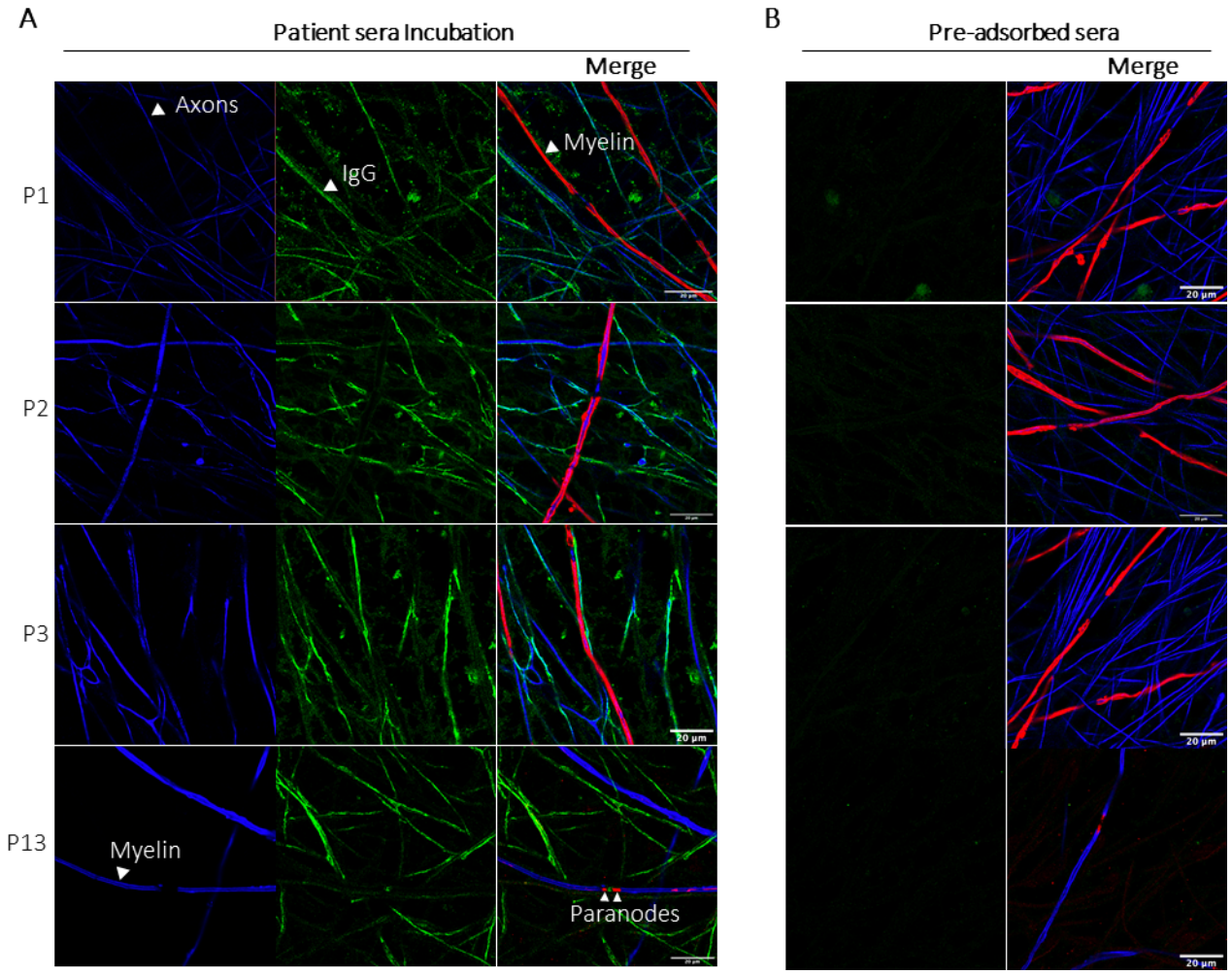


Figure 40: Axonal pattern of IgG binding from CNTN1-positive patients in myelinated neuronal co-cultures is specific to the CNTN1 antigen.

Patient sera tested on myelinated co-cultures were available for nine patients (four shown above). Sera for P4 was available but tested negative for IgG reactivity against neurons, and is not shown. Sera for P09 was only available at the time of initial testing, and not pre-adsorption experiments. ***(A)*** *Human IgG binding (green immunofluorescence, middle column) to human iPSC-derived axons (blue, immunolabelled with Neurofilament antibody NF200, first column) is demonstrated for P1-P3, and P13. These can be seen to co-localise (merged image, third column), but not with myelin (red, immunolabelled with myelin basic protein – MBP). For P13 there was some additional IgG labelling at the node. This can be better appreciated, as shown, with paranodes labelled with anti-caspr antibodies (red), and myelin in blue. Images showing independently marked are not shown.* ***(B)*** *Sera were pre-adsorbed with CNTN1 protein and re-applied to co-cultures. Patient IgG binding was abrogated in all cases tested. [Supplementary figure S4 from* (Fehmi et al., 2023)]

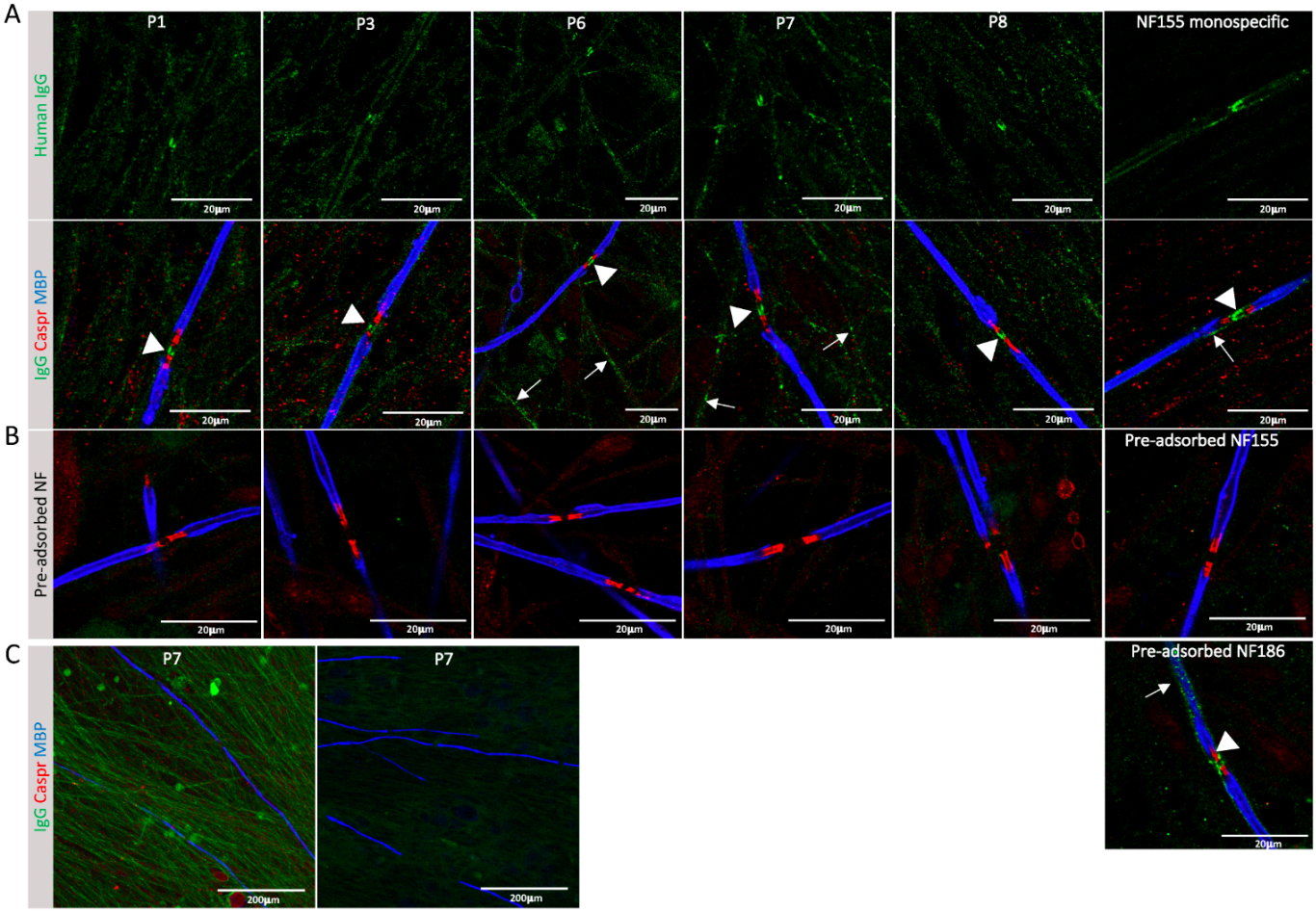


Figure 41: Pan-neurofascin serum is specific to NF155 and NF186 in live myelinating co- cultures.

In myelinating co-cultures, high magnification confocal microscopy (x63 objective) reveals ***(A)*** *IgG (green) is deposited at the node of Ranvier (arrowhead), flanked by paranodes labelled with Caspr (red), in patients 1, 3 and 8, with additional IgG labelling along axons (marked by arrow, axons not co-labelled in these images) in patients 6 and 7. There was no IgG binding observed for P2 and P5, and no sera was available for P4 for testing on cultures. Incubation of cultures with NF155 monospecific sera reveals IgG deposition over the outer surface of the myelin sheath (MBP, blue - arrow) and at the node. Nodal IgG staining was abrogated following pre-adsorption of panNF sera with either neurofascin 155 or 186 protein (pre-adsorption with NF186 shown in figure)* ***(B)****. Axonal IgG labelling was also reduced following pre-adsorption in P6 and P7, best appreciated using lower magnification (x20 objective)* ***(C)****. In contrast IgG labelling from NF155 monospecific sera is only abrogated when sera is pre-adsorbed with NF155, and is retained following pre-incubation with recombinant NF186 protein (far right column). [Supplementary figure 4 from* (Fehmi, Davies, et al., 2021)*]*

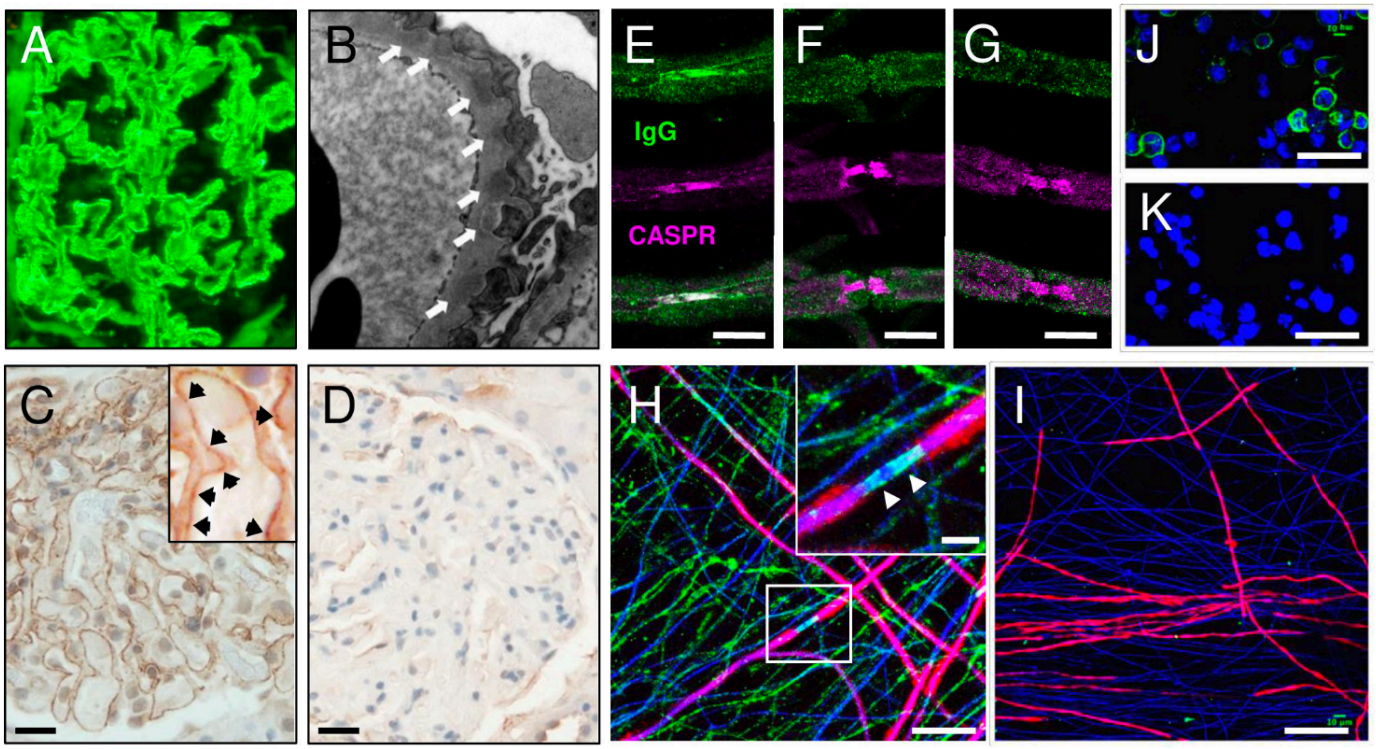


Figure 42: Contactin-1 immunoreactivity in kidney immune deposits and peripheral nerve tissue

(A) *Immunofluorescence of IgG deposition along glomerular capillary wall in anti-CNTN1 positive MGN patient kidney (P12 from* ***Error! Reference source not found.****). **(B)** Electron microscopy reveals immune complex deposits on the extracapillary side of the glomerular basement membrane, visible as electron dense material (white arrows). **(C)** Diaminobenzidine immunohistochemistry for CNTN1 is observed along the basement membrane of glomeruli from the same anti-CNTN1 positive MGN patient. Higher magnification image of a glomerulus demonstrating enrichment of CNTN1 in deposits lining the thickened basement membrane, characteristic of primary MGN (inset, black arrows). Equivalent results were obtained from biopsies of three further patients (S5 Fig). **(D)** No CNTN1 labelling was observed in biopsy sections from an anti-PLA2R-positive patient with MGN. Scale bars in C-D, 20 µm. **(E-G)** Labelling of the paranode in teased fibres from mouse sciatic nerve with IgG (green) from pre-treatment anti-CNTN1-positive human sera (E) is abrogated post-treatment (F) and absent in healthy control sera (G). Bound human IgG co-localises with CASPR at the paranode (magenta). Scale bars, 10µm. **(H)** Human IgG binding (green) to myelinated co-cultures treated with patient sera sampled before steroid treatment. Cultures were permeabilised with methanol prior to sera incubation. Note diffuse axonal pattern and paranodal localisation of human IgG (green) (arrowheads in inset). Myelin basic protein (MBP, red) indicates myelin, and neurofilament (NF200, blue) indicates axons. Scale bar, 25µm (5µm in inset) **(I)** Loss of human IgG binding (green) to myelinated co-cultures treated with patient sera sampled after steroid treatment. Scale bar 50 µm. **(J, K)** CNTN1-transfected HEK293 cells (CBA) treated with patient sera sampled before (J) and after (K) steroid treatment. Serum titration in CNTN1 CBA shows a fall ofanti-CNTN1 titre from 1:6400 to negative subsequent to steroid treatment. [Figure 1 from* (Fehmi et al., 2023)]

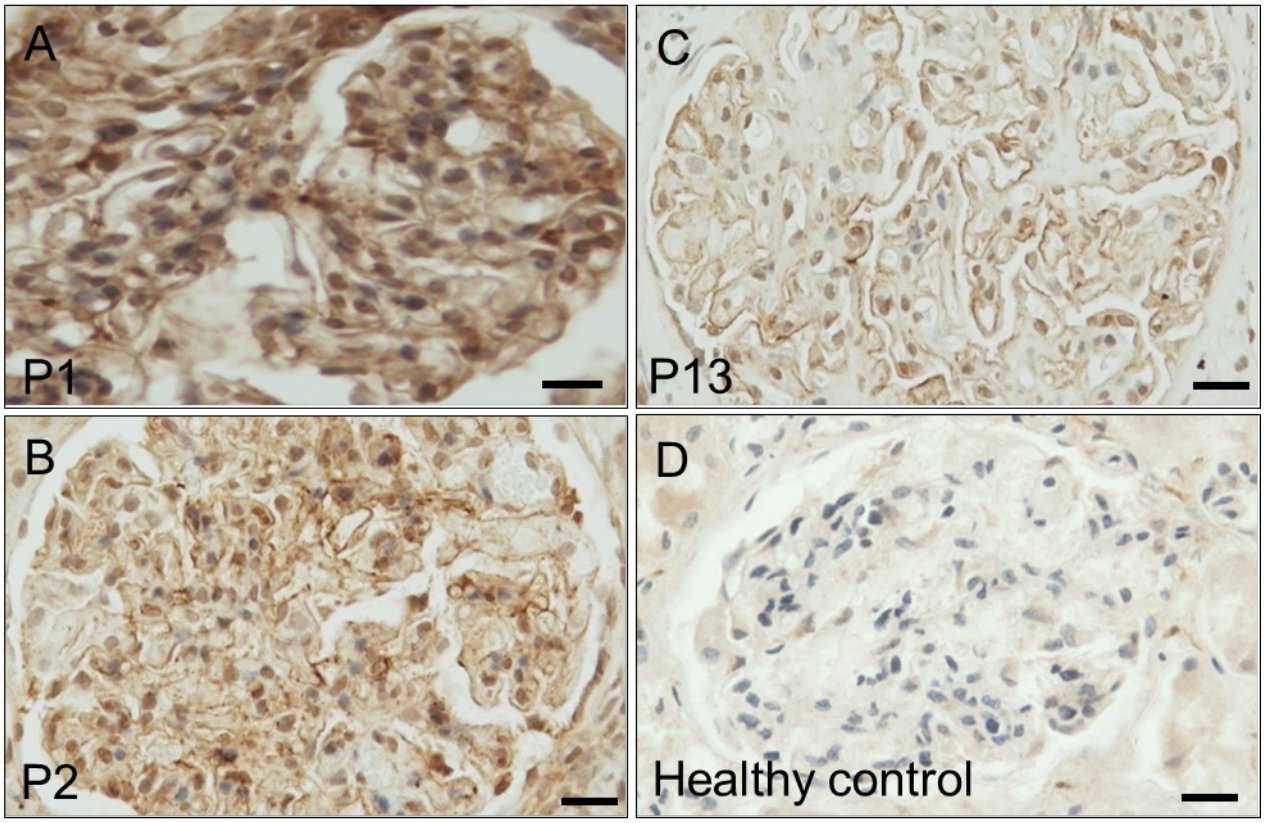


Figure 43: Contactin-1 immunoreactivity in kidney immune deposits for patents 1, 2 and 13

Diaminobenzidine immunohistochemistry for CNTN1 is observed along the basement membrane of glomeruli from patients 1, 2 and 13 in ***(A)****,* ***(B)*** *and* ***(C)****, respectively.* ***(D)*** *No positive CNTN1 staining can be seen in a healthy control kidney specimen. Scale bars 20µm. [Supplementary figure S5 from* (Fehmi et al., 2023)*]*

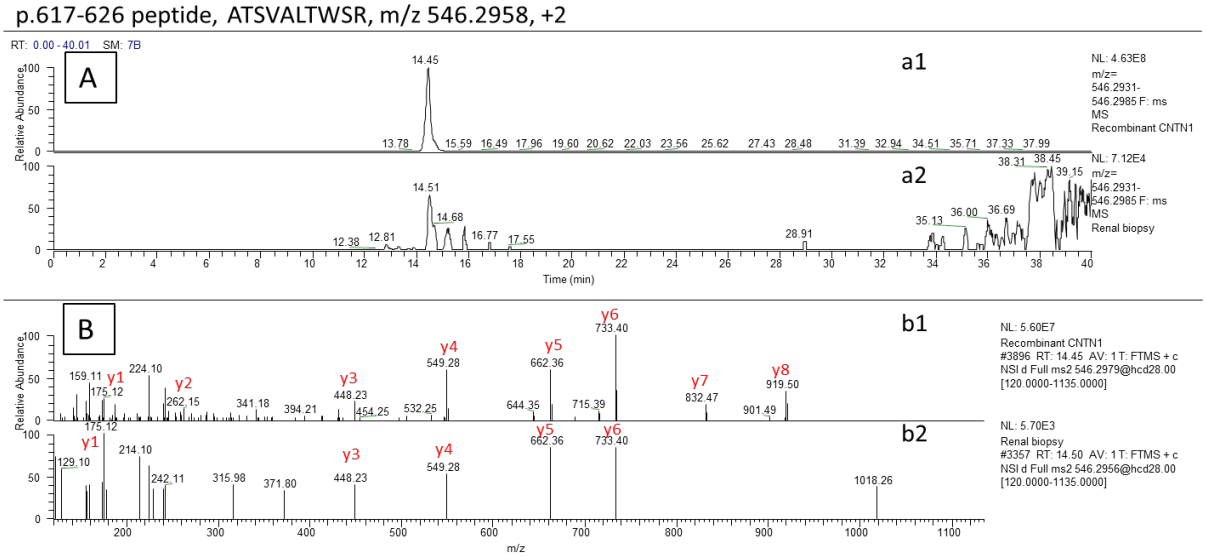


Figure 44: LC-MS/MS of CNTN1 peptides.

(A) *Extracted-ion chromatograms for p.617-626 peptide (MH_2^{2+} m/z 546.2958) from recombinant CNTN1 (above, a1) and laser-dissected CNTN1-immunopositive kidney biopsy (below, a2). The p.617-626 peptide elutes ~ 14.5 min in both samples.* ***(B)*** *HCD mass spectra for p.617-626 peptide from recombinant CNTN1 (above, b1) and CNTN1-immunopositive kidney biopsy (below, b2). HCD spectra with a prevalence of y series fragment ions confirming the identity of the peptide. [Supplementary figure S6 from* (Fehmi et al., 2023)*]*

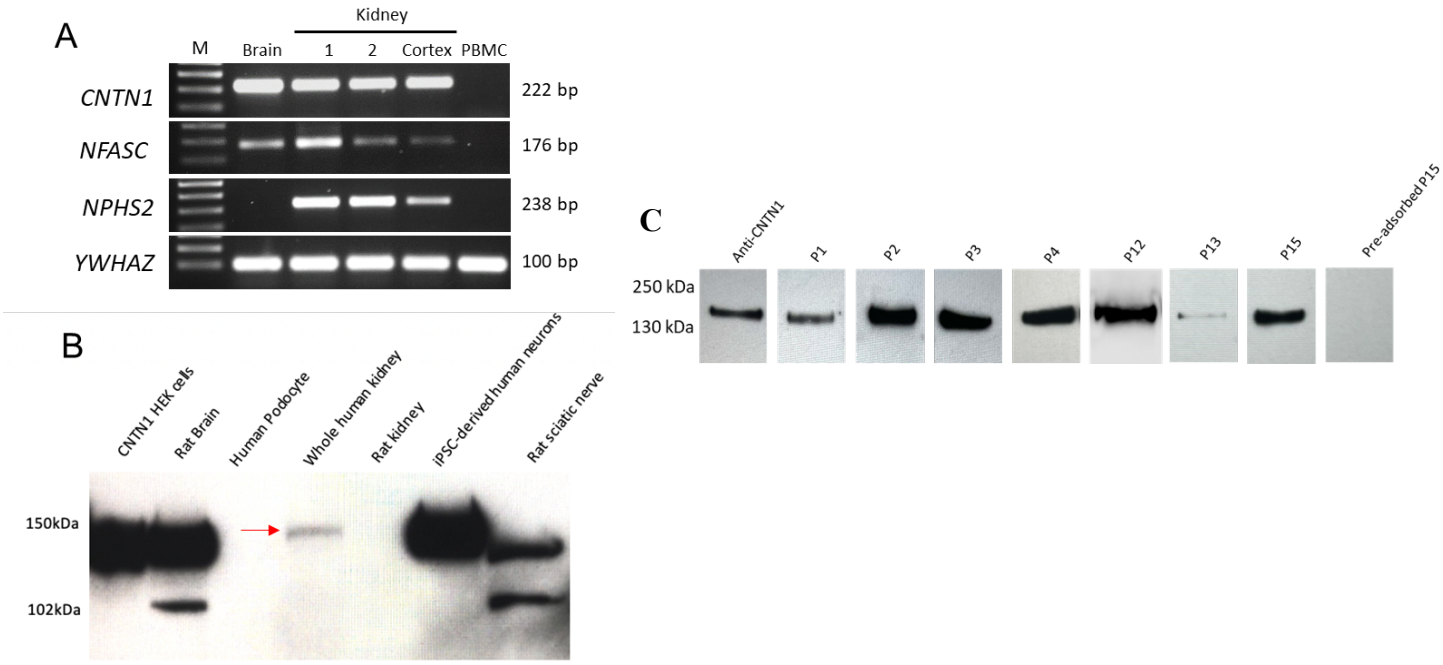


Figure 45: CNTN1 is expressed in healthy human kidney

(A) *Gel electrophoresis of contactin 1 (CNTN1), pan-neurofascin (pan) (NFASC), podocin (NPHS2) and house-keeping gene 14-3-3 protein zeta/delta (YWHAZ) PCR products in human brain, kidney (whole tissue lysate from two patients, as well as isolated cortex) and peripheral blood mononuclear cells (PBMC) from a healthy donor.* ***(B)*** *Western blot of human and rat tissue lysates with anti-CNTN1 antibody showing weak detection of CNTN1 protein in healthy human kidney. Faint band around 150 kDa in whole human kidney lysate (arrow, lane 4) corresponds to prominent bands in positive control samples for CNTN1 detection: lysate of HEK cells transfected with untagged CNTN1 (lane 1), rat brain (lane 2), human iPSC-derived sensory neurons (lane 6) and rat sciatic nerve (lane 7). An additional band is detected around 100 kDa in rat brain and sciatic nerve tissue, which may represent an alternative isoform of CNTN1. No bands are seen in lysate of a differentiated human podocyte cell line or rat kidney. Protein loading: CNTN1 transfected HEK cells (30µg); rat brain (5µg); podocyte lysate (40µg); healthy human kidney (30µg); iPSC-derived sensory neurons (40µg); rat sciatic nerve (60µg).* ***(C)*** *Western blot shows bands at approximately 150kDa when patient sera (P1, 2, 3, 4, 12, 13 and 15) is used as a primary antibody against recombinant CNTN1 protein loaded onto the gel. As all sera contain predominantly IgG4 subclass antibodies, anti-IgG4 HRP was used as a secondary antibody against sera. These bands align with the band produced when a commercial anti-CNTN1 antibody (lane 1) is used as a primary antibody, and can be abrogated by pre-adsorbing the sera with CNTN1 protein (lane 9), confirming the antibodies are specific for CNTN1. [Supplementary figure S7 from* (Fehmi et al., 2023)]

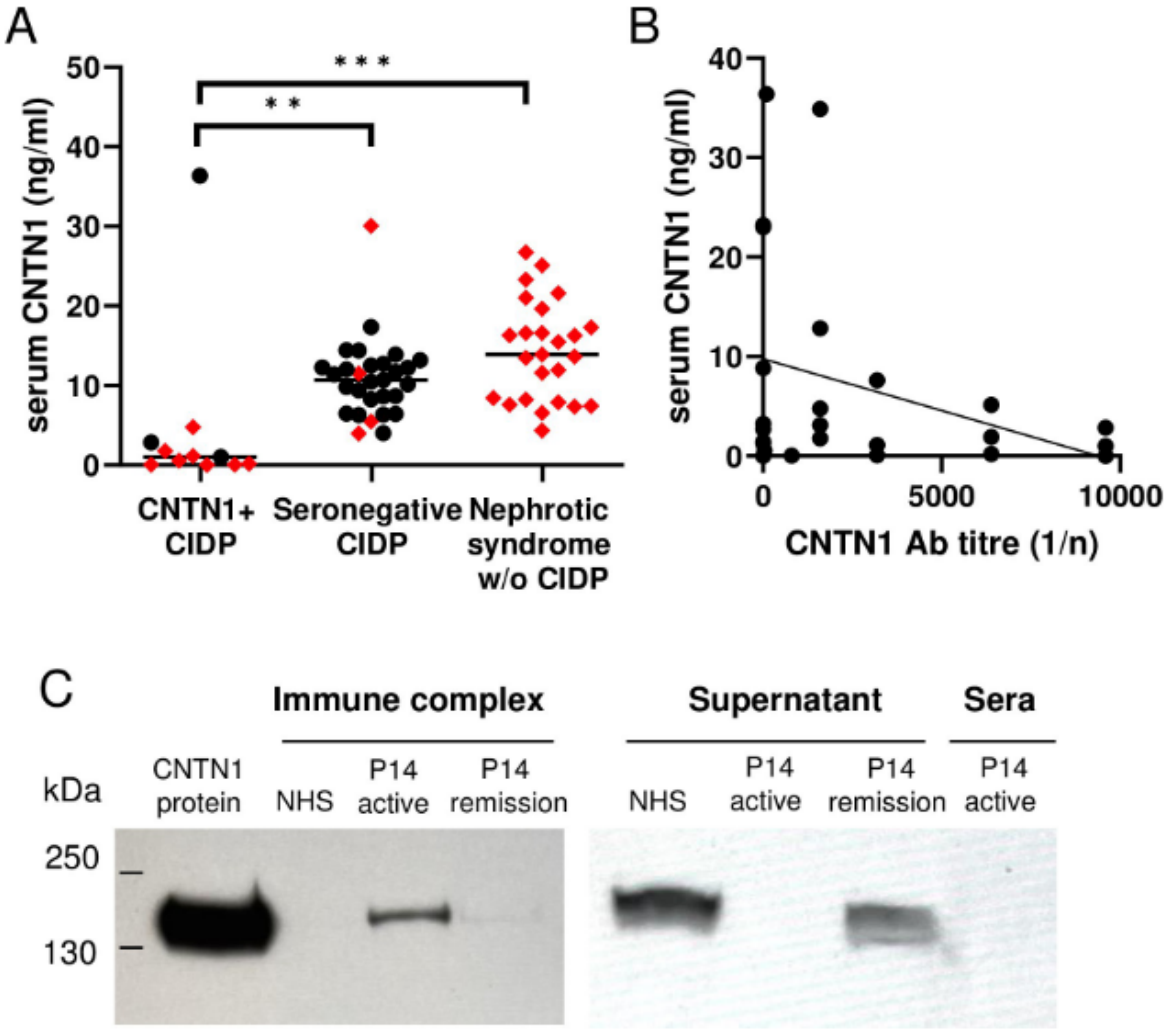


Figure 46: Fall in serum CNTN1 protein is associated with immune complex formation in active disease.

(A) *Serum CNTN1 (sCNTN1) protein levels are significantly lower in CNTN1 antibody seropositive CIDP (n = 11; sera available for testing from 10 patients in prospective group and 1 in retrospective group) vs seronegative CIDP patients (n = 29), and those with nephrotic syndrome but without CIDP (n = 25). Red diamonds and black dots indicate patients with and without nephrotic syndrome, respectively. Although 9/11 patients from the CNTN1 Ab+ CIDP group developed MGN, at the time of testing for sCNTN1 only 8/ 11 had nephrotic syndrome. Kruskal-Wallis p<0.001 overall, with post-test pairwise comparisons (CNTN1 Ab+ vs. seronegative CIDP, p = 0.003, vs. nephrotic syndrome alone p<0.001, seronegative CIDP vs. nephrotic syndrome ns, p = 0.19).* ***(B)*** *Overall, there was a non-significant trend for sCNTN1 and CNTN1 antibody levels to be negatively correlated (p = 0.099, R2 = 0.1088, simple linear regression). However in 5/8 patients where CNTN1 antibodies later became undetectable, sCNTN1 remained low.* ***(C)*** *Western blot for CNTN1 in the insoluble fraction of polyethylene glycol (PEG) treated healthy control normal human serum (NHS) and serum of patient 14 at nadir of active disease compared to remission. Recombinant CNTN1 protein (0.003 µg) loading; 5µl immune complexes purified from 300µl of patient serum. A repeat blot reveals reciprocal CNTN1 bands detectable only from the soluble fraction of the NHS and P14 serum in remission, but not during nadir of active disease (5µl loaded). [Figure 2 from* (Fehmi et al., 2023)*]*

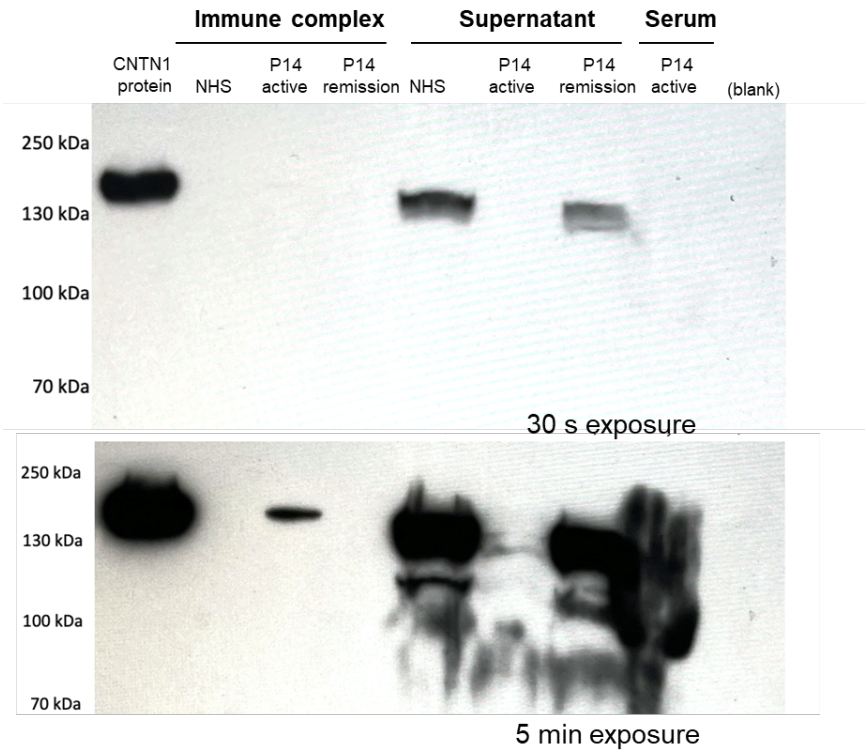


Figure 47: CNTN1-containing immune complexes are present in serum at disease nadir.

Repeat of full western blots from ***Figure 46*** *at two different exposure times: 30s (above) and 5 min (below). Gel was loaded with 5µl of precipitate (immune complexes) or 1µl of the remaining supernatant purified from 300µl serum; 5µl of whole sera was also loaded. Recombinant CNTN1 protein loading, 0.01 µg. [Supplementary figure 8 from* (Fehmi et al., 2023)*]*

3.3.3 Evidence of complement activation

3.3.3.1 CBA

A live HEK cell CBA was used to assess for the dependence of complement on (para)nodal antibody-complement fixation and cell cytotoxicity. Heat inactivated patient sera containing (para)nodal IgG antibodies was used, and I have shown that heat inactivation of patient sera can successfully abolish endogenous complement but not antibody activity (**Figure 48**), such that a defined concentration of exogenous complement can be added ('NHS' – normal human serum). As a control, anti-Aquaporin 4 (AQP4) antibody-containing sera (provided by Professor Sarosh Irani, University of Oxford) was used to confirm antibody-complement binding to the cell membrane of AQP4-transfected HEK cells (**Figure 49A**) in the presence of NHS (20-50%). Similarly, using NF155 or NF186- transfected HEK cells exposed to anti-NF155 and anti-panNF antibody-containing sera, respectively, human IgG fixes complement and C3c binding can be visualised faintly when incubated with 20-50% exogenous source of complement (NHS) (**Figure 49B** and **C**).

Repeated experiments to assess complement binding gave variable binding appearances, and was vulnerable to high background staining of IgG and C3c when transfected HEK cells were exposed to increasing concentrations of NHS (**Figure 50A**). Qualitative assessment of complement-dependent cell cytotoxicity suggested that exposure of transfected cells to (para)nodal antibody-containing sera and exogenous NHS may lead to acceleration of cell death (**Figure 50B-D**). Specifically, membrane human IgG staining and complement was consistently weaker, more fragmented, and more intense in an intracellular (vs membrane) distribution when exposed to 50% NHS (vs lower concentrations). No quantitative measurements of complement-dependent HEK cell cytotoxicity could reliably be obtained.

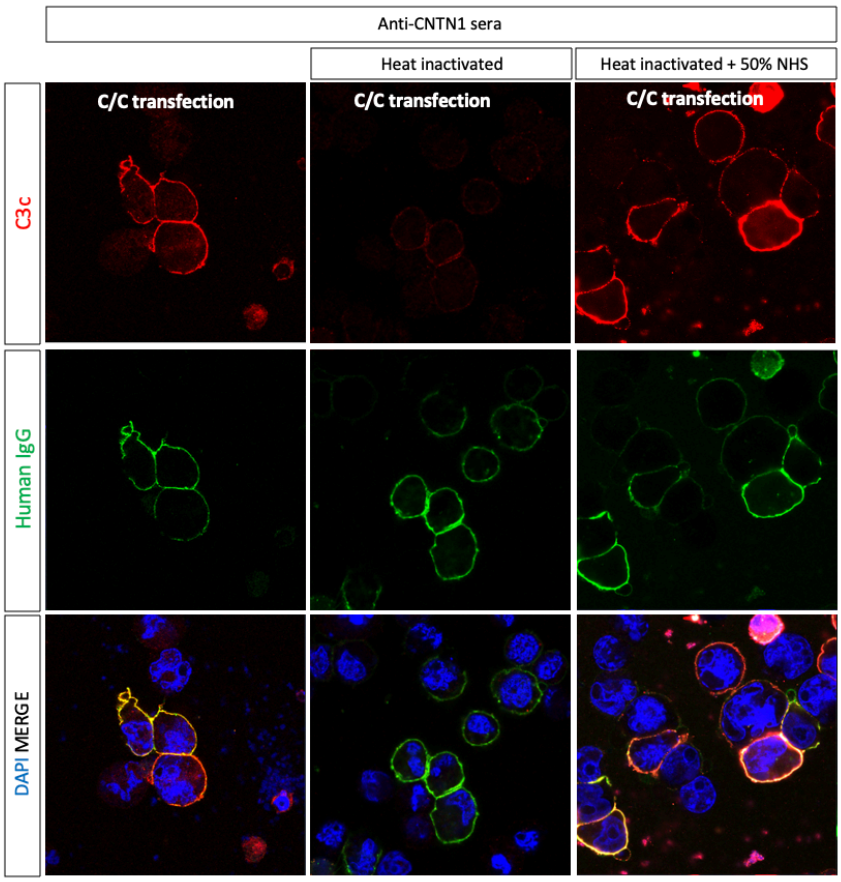
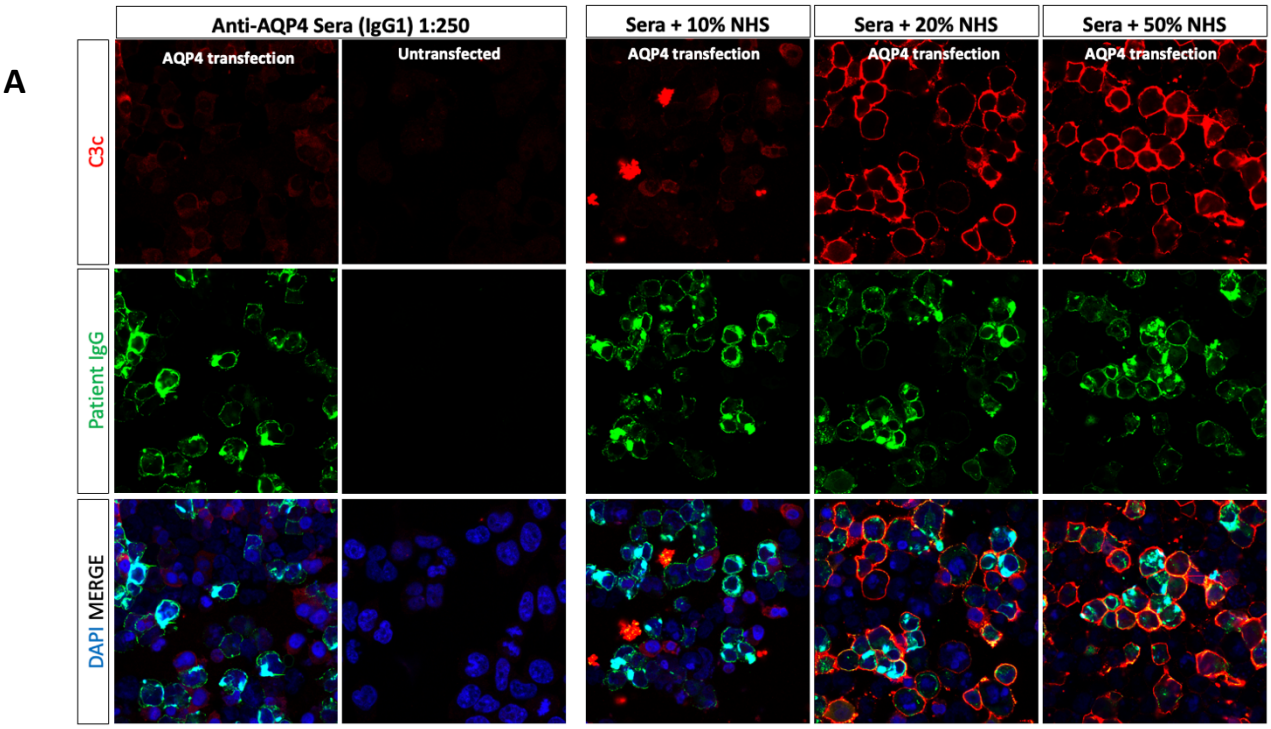
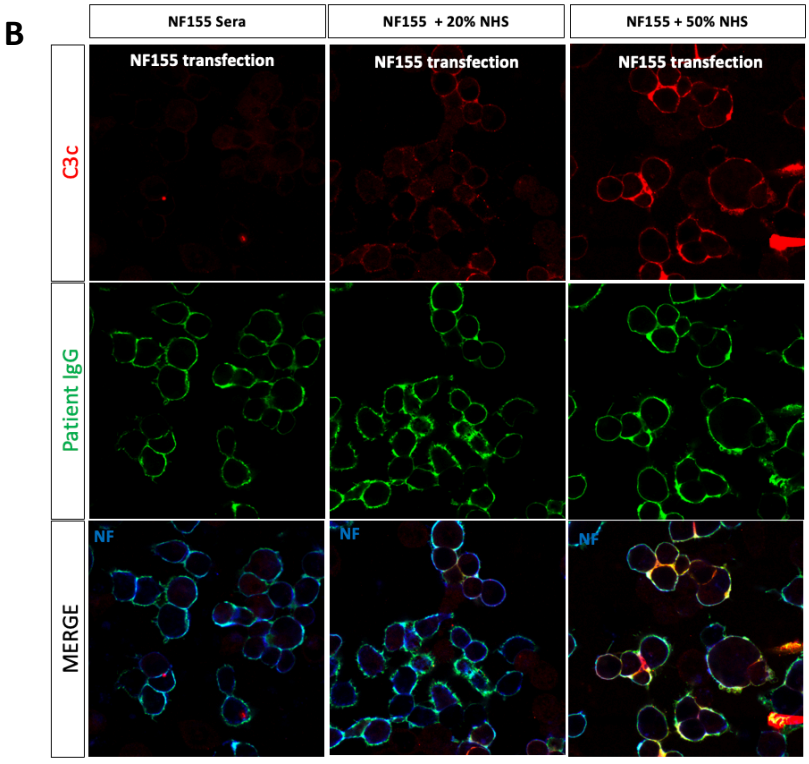


Figure 48: Heat inactivation eliminates endogenous complement but not antibody binding

HEK cells co-transfected with CNTN1 and Caspr1 (C/C) bind human IgG from anti-CNTN1 antibody containing sera (green) and complement (C3c – red) on their cell membrane. If sera is heat inactivated (2nd column), complement activity is lost and no/minimal antibody-complement binding can be seen. If an exogenous source of complement (50% NHS) is added to the heat inactivated sera, complement activity and binding is restored (3rd column). Images taken at x 60 magnification.

Abbreviations: C/C – CNTN1/Caspr1; C3c – complement component; DAPI - 4',6-diamidino-2-phenylindole); NHS – Normal human serum; IgG - Immunoglobulin


A
Anti-AQP4 Sera (IgG1) 1:250
Sera + 10% NHS
Sera + 20% NHS
Sera + 50% NHS
AQP4 transfection
Untransfected
AQP4 transfection
AQP4 transfection
AQP4 transfection
C3c
Patient IgG
DAPI MERGE


B
NF155 Sera
NF155 + 20% NHS
NF155 + 50% NHS
NF155 transfection
NF155 transfection
NF155 transfection
C3c
Patient IgG
MERGE
NF
NF
NF

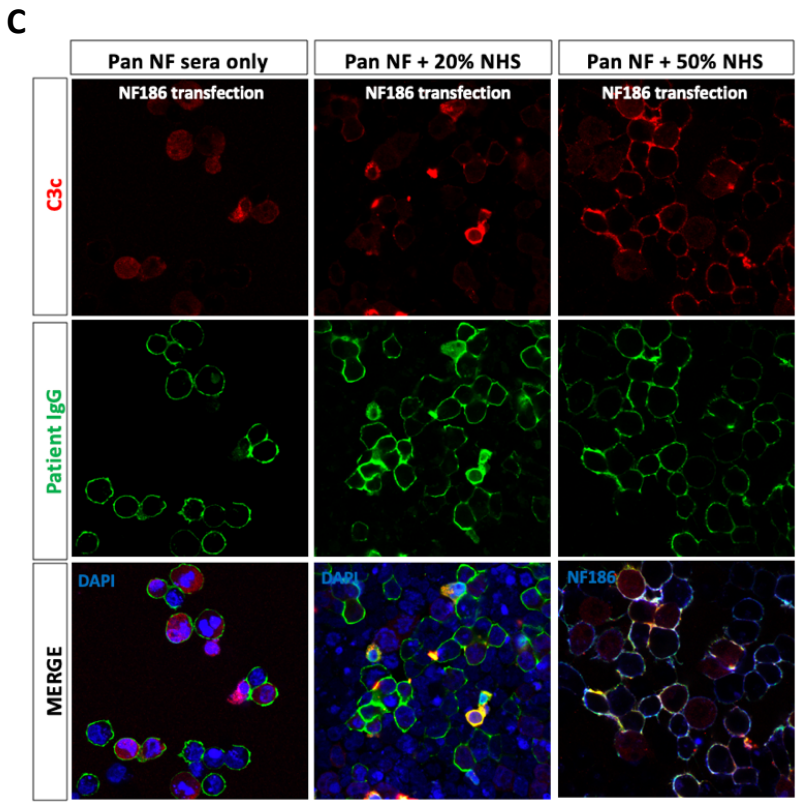


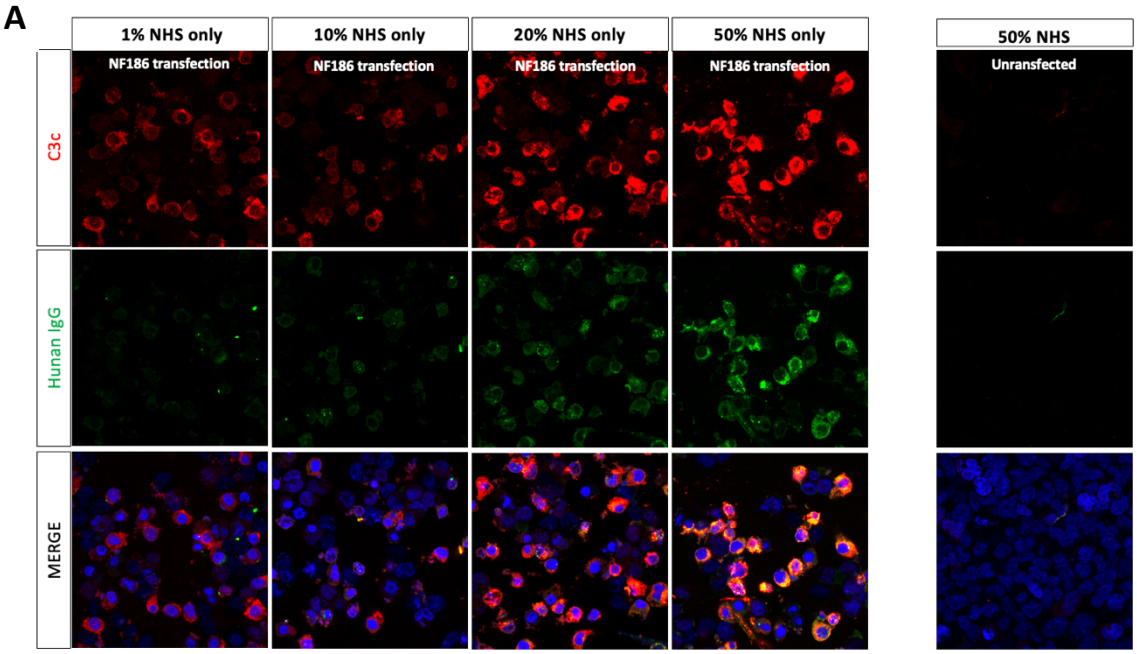
Figure 49: Assessment of (para)nodal antibody and complement fixation in HEK cells

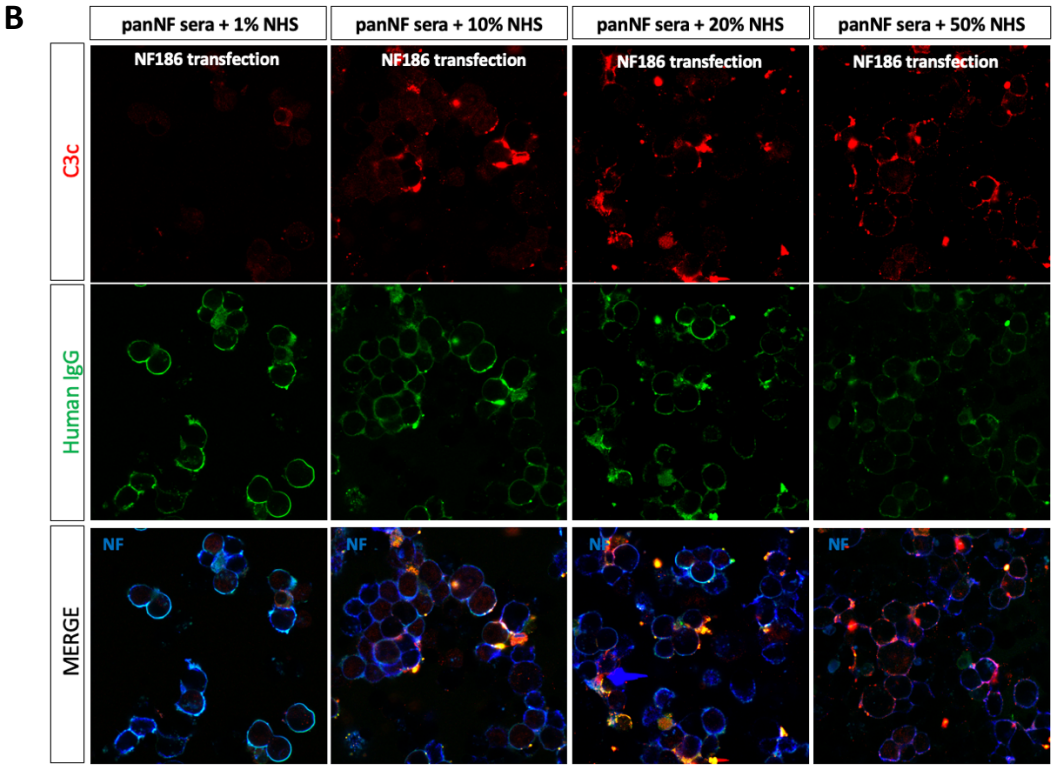
Column headings – indicates incubation with sera positive for specified IgG +/- normal human serum 'NHS' as a source of complement.

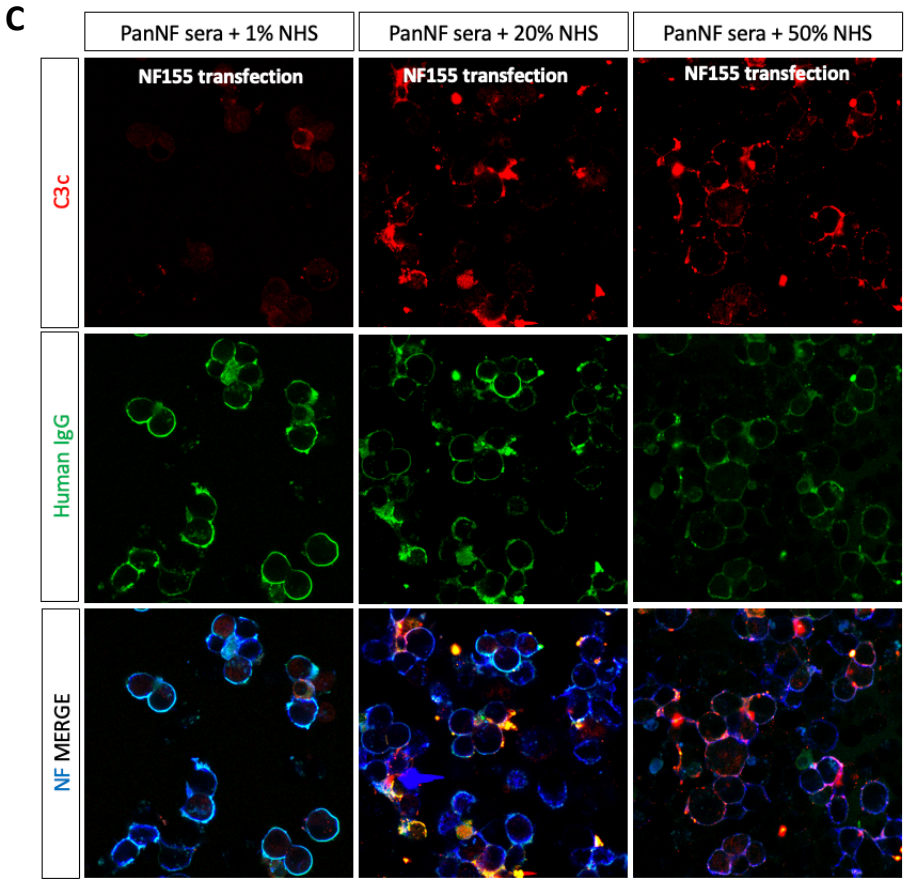
Row headings – fluorescent immunolabelling

***(A)** IgG1 anti-Aquaporin-4 antibody (AQP4 - provided by Professor Sarosh Irani, University of Oxford) is used as a positive control of complement-dependent antibody-mediated complement fixation. Green fluorescent protein (GFP)-tagged AQP4 protein confirms successful cell transfection, and only in the presence of at least 20% exogenous source of complement (NHS) can C3c fixation (red) be observed. **(B)** In NF155 transfected cells, C3c fixation can only be convincingly observed upon exposure to sera with anti-NF155 antibodies with a final concentration of 50% NHS. Patient antibodies (green) can be seen to co-localise with C3c and commercial neurofascin antibody (NF – blue). **(C)** Similar appearances can be seen with NF186-transfected cells exposed to panNF positive sera and 50% NHS. Images taken at x40 magnification.*

Abbreviations: GFP – green fluorescent protein; C3c – complement component; DAPI - 4',6-diamidino-2-phenylindole)


A
1% NHS only
10% NHS only
20% NHS only
50% NHS only
50% NHS
NF186 transfection
NF186 transfection
NF186 transfection
NF186 transfection
Unransfected
C3c
Human IgG
MERGE


B
panNF sera + 1% NHS
panNF sera + 10% NHS
panNF sera + 20% NHS
panNF sera + 50% NHS
NF186 transfection
NF186 transfection
NF186 transfection
NF186 transfection
C3c
Human IgG
MERGE
NF
NF
NF
NF


C
PanNF sera + 1% NHS
PanNF sera + 20% NHS
PanNF sera + 50% NHS
NF155 transfection
NF155 transfection
NF155 transfection
C3c
Human IgG
NF MERGE

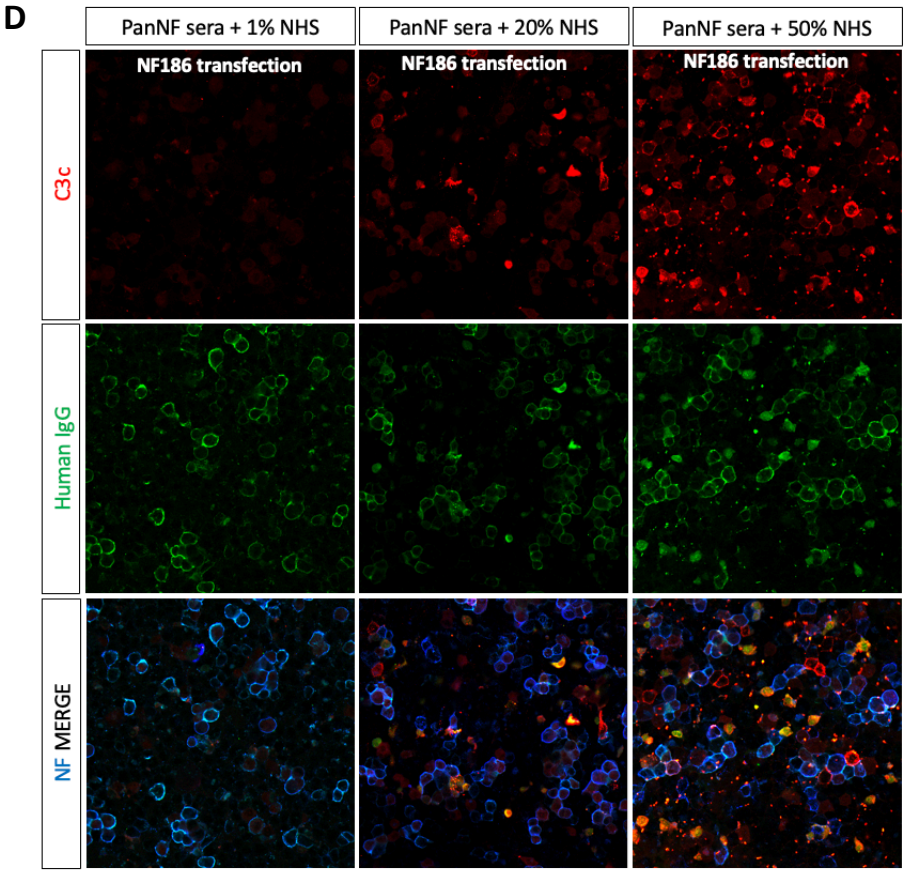

D
PanNF sera + 1% NHS
PanNF sera + 20% NHS
PanNF sera + 50% NHS
NF186 transfection
NF186 transfection
NF186 transfection
C3c
Human IgG
NF MERGE

Figure 50: High background staining and complement dose dependent HEK cell cytotoxicity

(A) *In NF186-transfected cells only exposed to increasing NHS (1-50%), but no (para)nodal IgG containing serum, high background staining of anti-C3c and anti-human IgG antibody reactivity can be seen.* ***(B)*** *As NHS concentration increases (esp at 50%) in the presence of anti-panNF antibody-containing sera and NF186-transfected HEK cells human IgG cell membrane staining becomes weaker, and although complement fixation can be seen to co-localise with IgG staining, it is fragmented and more intracellular. These findings suggest possible cell cytotoxicity at this concentration of NHS. Similar appearances can be seen in* ***(C)*** *and* ***(D)****. Similar results were observed with either NF155 or NF186 transfection.* ***Images from A-C taken at x40 magnification, images D at x 20 magnification.***

3.3.3.2 Myelinated co-cultures

Preliminary studies using myelinated co-cultures were similarly conducted to assess complement binding, using the same primary antibody as in CBA. In untreated cultures (media only) there was no visible complement binding (data not shown). Using dilutions of normal human sera (NHS) from 1:100 (1%) to 1:5 (20%) in media (no disease patient sera) complement binding could be seen to myelinating and non-myelinating SCs, with varying intensities. Binding was absent at 1%, barely visible at 5%, and particularly apparent with concentrations of 10% or more (**Figure 51**). NHS added to patient sera containing IgG known to bind to (and induce injury in the presence of a source of complement) myelin seemed to show more intense (qualitative assessment) complement binding to myelinating SCs than the background seen with NHS alone (**Figure 52**). This implies complement may specifically rely on and be bound to IgG targeting the myelinating SCs. Further, the intensities of fluorescence reactivity did not correlate with the concentrations of NHS added but rather the duration i.e 20% NHS incubation showed most vivid staining at

2 hrs and 5% NHS showed more vivid staining at 5 hrs than 20% NHS (

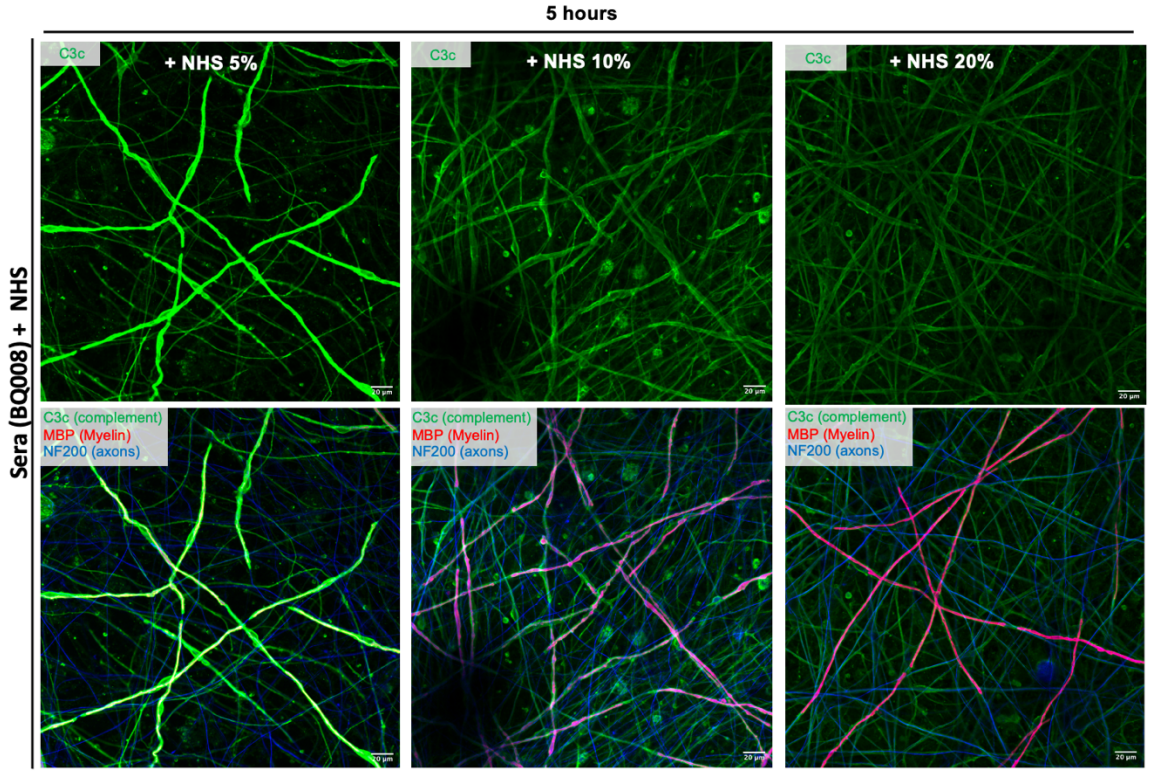


Figure 53). This perhaps reflects a dynamic process of complement binding and activation that may not be captured if cultures are fixed and analysed at one timepoint. There was also variation observed between individual sera, potentially suggesting complement binding was dependent on the specific antibody bound to the specific neuronal component. Incubation of patient sera alone (not heat inactivated), despite showing IgG binding at the same timepoint, demonstrated complement binding in some but not all samples (**Figure 54**). Using sera containing antibodies known to induce axonal injury in the presence of a source of complement, complement can be seen to bind to axons, co-localising with IgG, after 1 hour incubation (

Figure 55). When a source of complement is added (NHS 20%) axonal damage can now be seen, though both IgG and complement show non-specific binding (

Figure 55). This perhaps implies that complement binding precedes any injury. Upon heat inactivation (inactivation of complement) of NHS and application in the same culture conditions axonal injury is not

seen, nor complement binding, implying that the complement within the NHS is likely to be the component involved in inducing injury to the neuronal culture (

Figure 55).

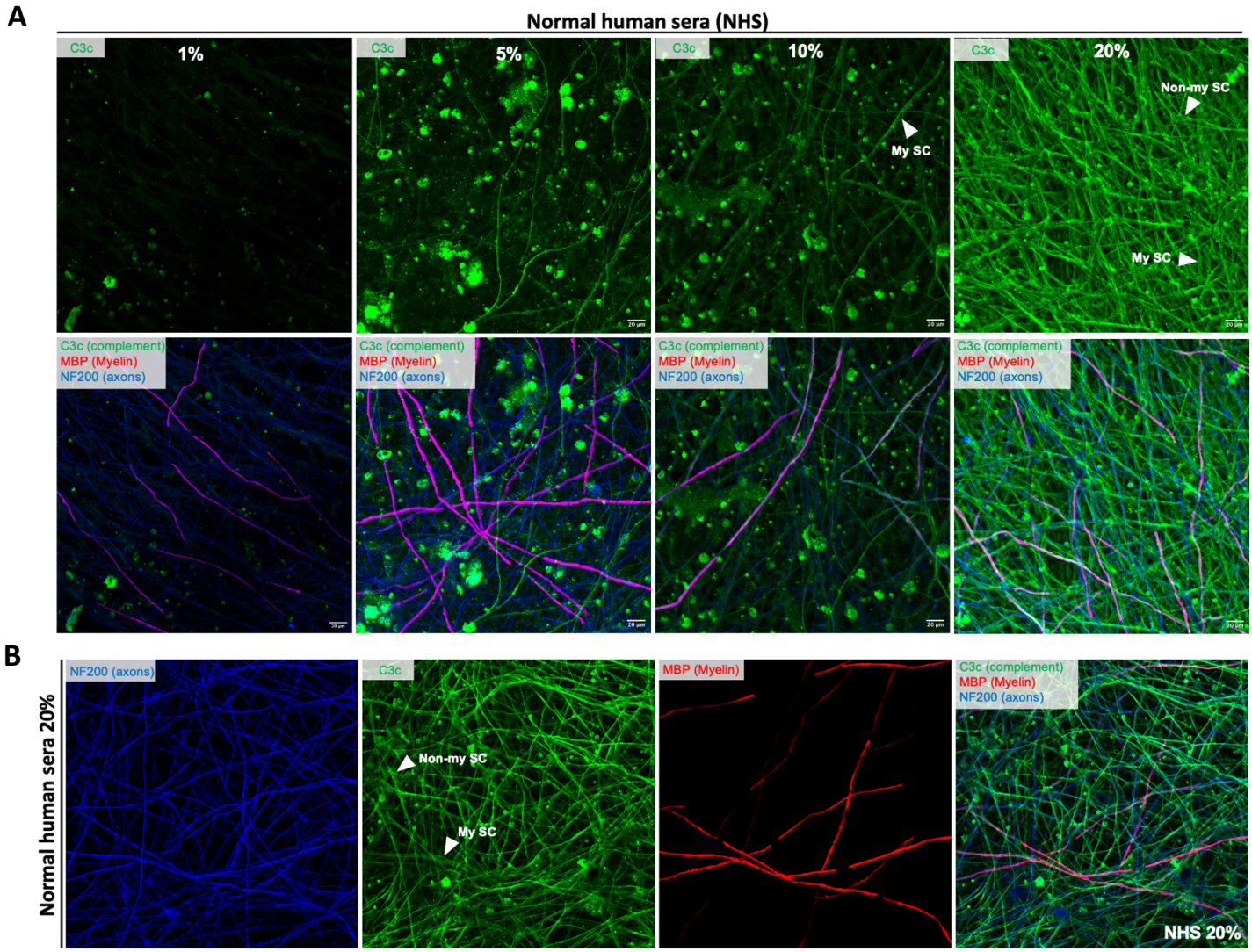


Figure 51: Normal human sera (NHS) binding in myelinated co-cultures.

(A) *Complement (anti-C3c antibody) binding in green, and merged with red (MBP - myelin) and blue (NF200 – axons) channels when cultures treated with NHS 1-20% for 1 hour. Specific binding of myelinating Schwann cells (My SC) can be seen with 10% and 20% NHS, and non-myelinating SCs (non-my SC) at 20%.* ***(B)*** *Separation of each channel with 20% NHS*

Abbreviations: MBP – Myelin basic protein; NF200 – Neurofilament 200; NHS – Normal human sera; SCs – Schwann cells

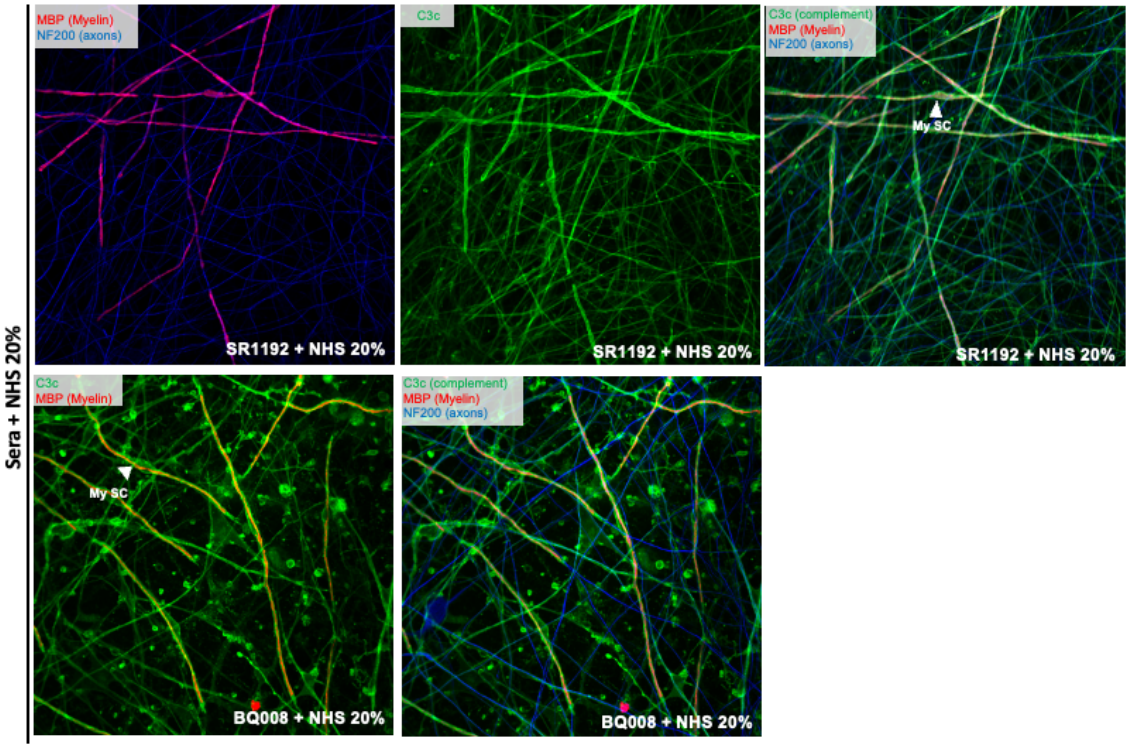


Figure 52: Antibody-containing sera and NHS (top row sera SR1192, bottom row sera BQ008)

*Two sera containing IgG antibodies known to bind myelin and induce injury in the presence of a source of complement (SR1192, BQ008), incubated with cultures and supplemented with 20% NHS (1 hour) showed more intense (qualitatively assessed) green fluorescence staining to myelinating SCs than the 'background' staining that can be seen with NHS alone (**Figure 51**).*

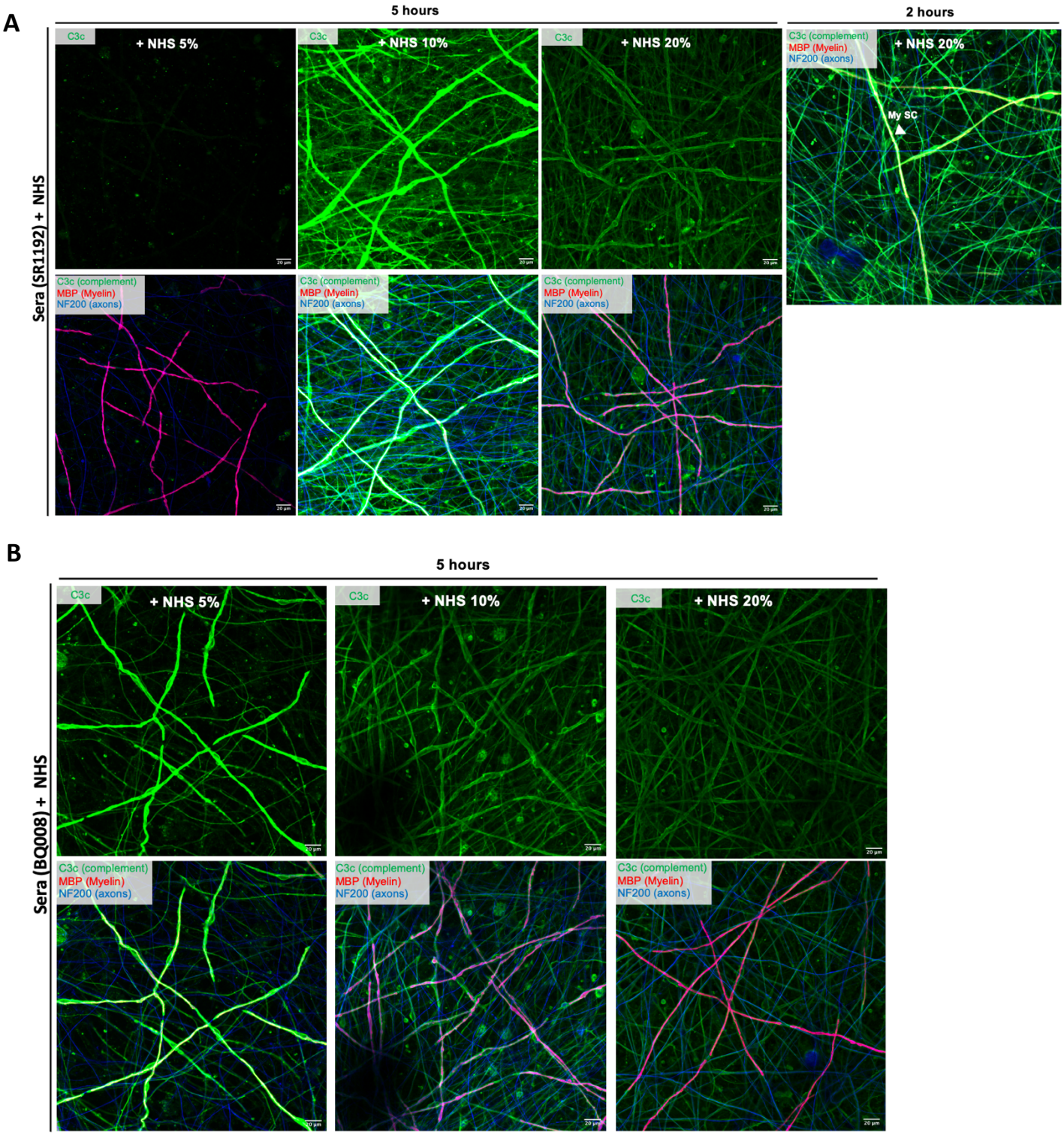


Figure 53: Factors affecting strength of antibody binding.

Intensity of complement staining can depend on properties of individual patient sera, time, and concentration of NHS (same confocal microscopy settings used for comparisons). **(A)** *SR1192 sera incubated for 5 hours with varying concentrations of NHS shows strongest IgG staining with 10%. The addition of 20% NHS incubation at 2 hours shows mor vivid staining than at 5 hours.* ***(B)*** *Under the same conditions but using BQ008 sera a lower concentration of NHS (5%) shows most vivid staining at 5 hours.*

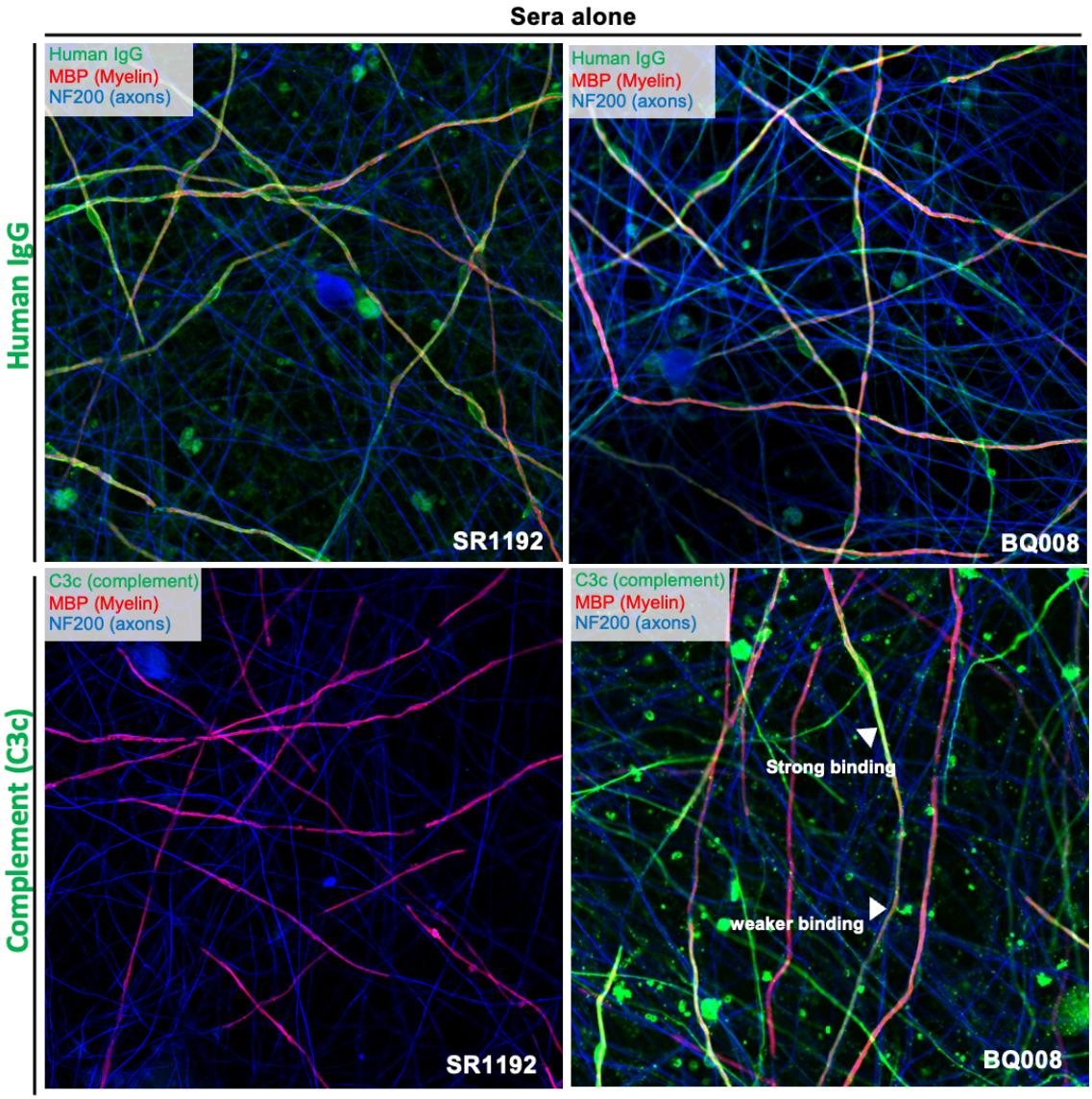


Figure 54: Complement binding in the presence of antibody-containing sera alone.

Despite IgG binding to myelin in co-culture when sera (SR1192 or BQ008 top row) is incubated alone for 1 hour, variable complement binding can be seen. No complement is seen to bind with SR1192 sera incubation, but BQ008 shows some strong fluorescence signal from complement bound to myelinating SCs.

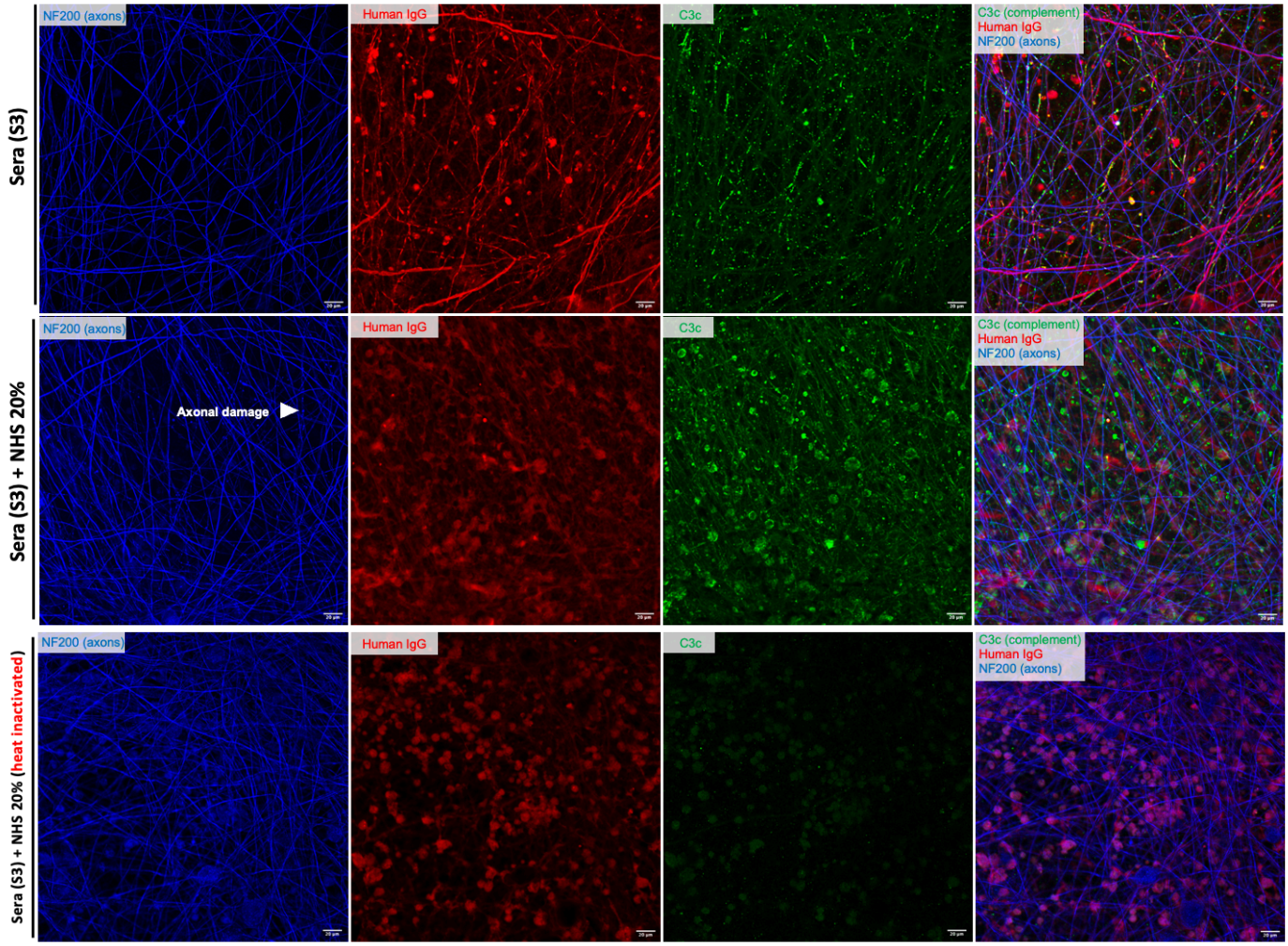


Figure 55: Complement binding precedes axonal injury in the presence of a source of complement.

Top row: Incubation of S3 sera alone in co-culture (from a patient with GBS and anti-GQ1b antibodies) causes human IgG to bind to axons, and co-localises with bound complement.

Middle row: Sera with the addition of 20% NHS results in axonal injury (blebbing indicated by arrow), though IgG and complement can no longer be visualised to specifically bind.

Bottom row: Heat inactivating the NHS prior to adding to sera prevents axonal injury, and there is no IgG or complement bound.

Abbreviations: GBS – Guillain-Barre Syndrome; GQ1b - Ganglioside Q1b

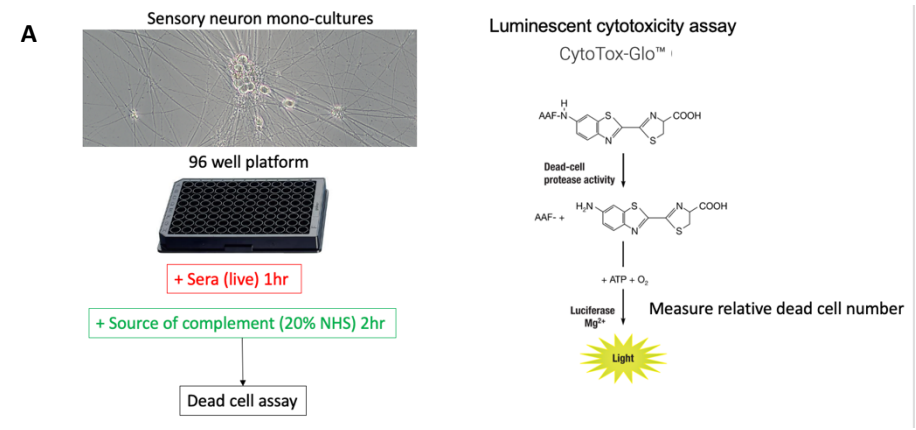
3.3.4 Assessment of complement dependent neuronal injury

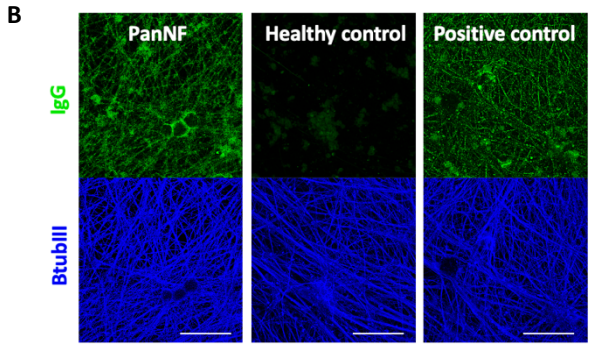
3.3.4.1 Luminescent cytotoxicity assay

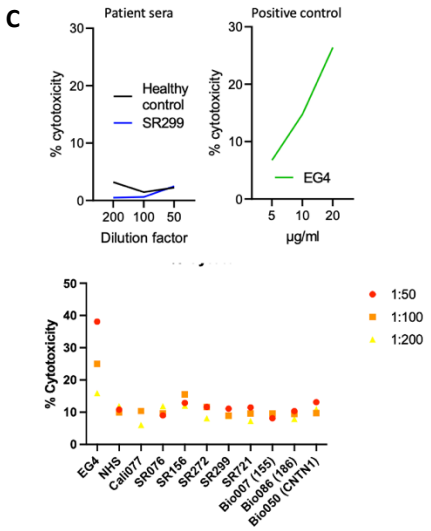
Assessment of complement-dependent cell cytotoxicity induced by (para)nodal antibodies was performed by incubating sera and a source of complement with hiPSC-derived sensory neuron mono-cultures and measuring cell cytotoxicity using the same CytoTox-Glo™ luminescence assay (**Figure 56A**). This has already been shown by Dr Alexander Davies, within Dr Simon Rinaldi's laboratory, to be a sensitive method in the detection of complement-mediated cytotoxicity induced by mouse and human monoclonal antibodies targeting GD2 ganglioside (data not shown).

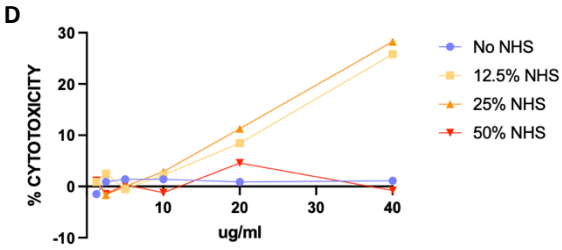
As a positive control of complement-induced cell cytotoxicity, a complement-fixing mouse IgG2A antibody against disialosyl glycolipids (EG4) was used. IgG labelling of human sensory neurons in culture after incubation with (para)nodal antibody-containing sera and EG4, compared with no labelling of NHS (negative control), was demonstrated prior to cytotoxicity experiments (**Figure 56B**). Cytotoxicity of sensory neurons reached 27% following 2 hour incubation with the positive control antibody EG4 (7% at 5µg/ml – 27% at 20µg/ml) and a source of complement (20% NHS). Treatment of neurons with serial dilutions up to 1:50 of patient sera containing anti-panNF antibodies and 20% NHS did not induce cytotoxicity beyond that of normal human sera (**Figure 56C**). Similar results were yielded through treatment of neurons with sera from 9 different patients under the same conditions (6 panNF, 1 NF186, 1 NF155, 1 CNTN1) (**Figure 56C**). Different concentrations of NHS (0, 12.5%, 25%, 50%) were applied to serial dilutions of EG4 (control antibody, 0-40µg/ml) and whole sera from a panNF antibody positive patient (1:5000 – 1:5) (**Figure 56D** and **E**). This reproduced % cytotoxicity of almost 30% in EG4 in a dose dependent manner, though only with 12.5-25% NHS. Beyond this, at 50% NHS, luminescence readings fell and indicated less cytotoxicity. Using the panNF sera, at each dilution, alone or with the addition of up to 50% NHS did not induce cytotoxicity. However, at 1:5 dilution, up to 12% cytotoxicity can be observed with sera alone. The percentage of total cell lysis measured, relative to maximum cell lysis within a well, was inversely proportional to the amount of NHS added as a source of complement. Three healthy control

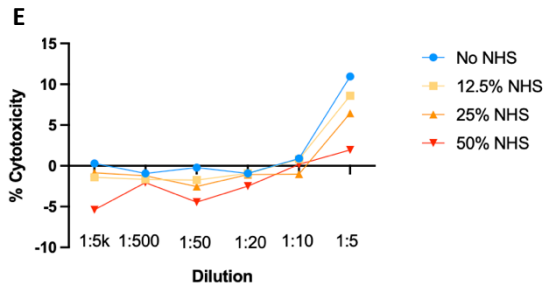
patient sera were used at the same serial dilutions, alone or with the addition of the same NHS, and did not show any convincing dose-dependent cytotoxicity (**Figure 56F**).











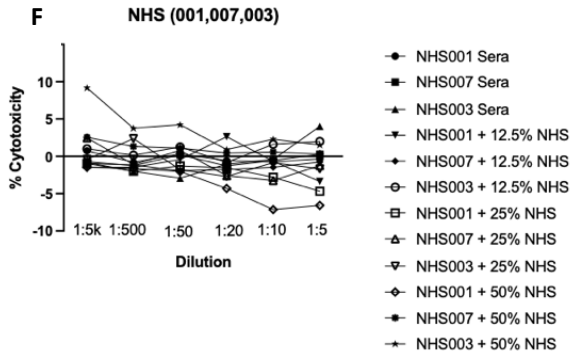


Figure 56: IgG labelling and complement-dependent cytotoxicity in human sensory neurons.

(A) *Abbreviation of methodology for functional complement-dependent cytotoxicity assay using Cytotox-Glo™ commercial assay. Patient sera or 'positive control' mouse IgG2A anti-disialosyl glycolipid antibody (EG4) were applied to human sensory neurons derived from induced pluripotent stem cells for 1h. Normal human serum (NHS) was added to a final concentration of 20% as a source of complement and cells were incubated a further 2h. Complement-dependent cytotoxicity was measured using a dead cell protease luminescence detection assay in a 96 well plate format. Luminescence reads were background subtracted from wells to which only NHS was added, and percentage cytotoxicity was calculated relative to maximum lysis by digitonin (50 µg/ml) (see methods for more detail).* ***(B)*** *IgG labelling (green) of human sensory neurons (BtubIII in blue – neurons) in culture after incubation with serum (1:100) from a panNF patient, healthy control, and a positive control complement-fixing mouse IgG2A antibody against disialosyl glycolipids (EG4) (10 µg/ml).* ***(C)*** *Percentage cytotoxicity of sensory neurons after treatment with different concentrations (1:50-1:200 dilution) of panNF sera (SR299) or monoclonal antibody (EG4), and a cohort of panNF sera (Cali077, SR076, SR156, SR272, SR299, SR721), NF155 antibody-positive sera (Bio007), NF186 only antibody-positive sera (Bio086), and CNTN1 antibody-positive sera (Bio050).* ***(D and E)*** *Using a positive control (EG4) and one panNF positive sera from one patient (1:5 to 1:5000 dilution) either without a source of complement, or with up to 50% NHS as a source of complement, percentage cytotoxicity is recorded.* ***(F)*** *Sera from three different healthy controls (NHS001, 003 and 007) are tested in the same way (1:5 to 1:5000 dilution), alone or with the addition of the same NHS added to panNF sera or the positive control. Abbreviations: BtubIII – class III β-tubulin*

3.3.4.2 Measurement of fluid biomarkers Neurofilament light (NfL) and Contactin-1 protein

Neurofilament light (NfL) and CNTN1 protein were measured in the supernatant generated from myelinated co-cultures, either untreated, or treated over 1 and 24 hours, with a source of complement from healthy human donors (normal human serum - NHS) as control sera, or antibody-containing sera known to induce either axonal or myelin injury in the presence of a source of complement. These experiments were performed on two different occasions, initially using a 24 well plate platform ('experiment 1'), and subsequently 96 well plates ('experiment 2').

NfL levels were undetectable in media alone (not exposed to culture), and low level and static in untreated culture supernatant over 24 hours (mean 145pg/ml in 96 well plate and 660pg/ml in 24 well plate) (**Table 12** and **Figure 57**). In cultures treated with NHS (from 3 different donors – 'A, B and C'), NfL levels increased

over 24 hours to between 1.9 and 10 fold without visible injury to neurons using confocal microscopy (**Figure 58**).

The concentration of NfL increased following the incubation of cultures with sera containing anti-GQ1b antibodies ('axonal injury' sera), again without visible injury to the cultures, though significantly increased levels were seen in parallel to diffuse axonal fragmentation following the addition of NHS to the sera (96,393pg/ml at 24 hours in a 24 well platform, 5777pg/ml in a 96 well platform). These findings were consistent using two different NHS donors. Absolute NfL levels were significantly higher in experiment 1, and although a greater relative increase was seen at 1 hour in the presence of additional complement (x28 fold vs x2.4 fold), the same relative increase (8 x fold) was seen at 24 hours in the presence of additional complement.

Incubation with sera containing antibodies known to cause myelin degradation in the presence of complement, did not cause NfL levels to rise above controls at both timepoints, and with or without the addition of NHS. Correlation with microscopy appearances revealed only visible myelin injury (**Figure 58**).

Overall, absolute NfL values were increased by between 4 and 18 x fold in experiment 1 (24 well) compared to experiment 2 (96 well).

From experiment 2 it was clear that contactin-1 protein levels were below the lower limit of detection (LLOD) in the supernatants of cultures treated with healthy or antibody-containing sera, but consistently raised in the presence of 20% NHS, either alone or in addition to antibody-containing sera. This did not change over time up to 24 hours (**Figure 59**).

Sample		Neurofilament level (pg/ml), mean (range)						Overall imaging appearances (qualitative)	
		Not exposed to culture		Exposure to culture					
				Experiment 1		Experiment 2			
		Exp 1	Exp 2	1 hr	24 hr	1 hr	24 hr	Axon injury	Myelin injury
Media (untreated)		<LLOQ	<LLOQ	-	660 (611-743)	213 (198-228)	145 (84-207)	No	
NHS A 20%		<LLOQ		926	9109 (x10)	-	-	No	
NHS B 20%		-	<LLOQ	-	-	247 (196-299)	2069 (1066-3916) (x8)	No	
NHS C 20%			<LLOQ			625 (470-918)	1179 (1059–1260) (x1.9)	No	
'Axonal injury' sera	Alone	-	<LLOQ	884	12,200	253 (168-336)	707 (573-837)	No	No
	+ complement (NHS B 20%)		<LLOQ	25,000 (x28)	96,393 (x8)	612 (573-670) (x2.4)	5777 (3888–8857) (x8)	Yes	No
	+ complement (NHS C 20%)		7.1 (0.6-17)			800 (661-947)	5702 (5253–6438)		
'Demyelination' sera	Alone		5.3	682	12,562	241 (126-368)	635 (450-827)	No	
	+ complement (NHS B 20%)		<LLOQ	785	10,842	284 (201-379)	1157 (995-1394)	No	Yes (24hrs)

Table 12: NfL measurements compared from supernatant extracted from experiment 1 and 2. Assessment of imaging for experiment 2 is ongoing

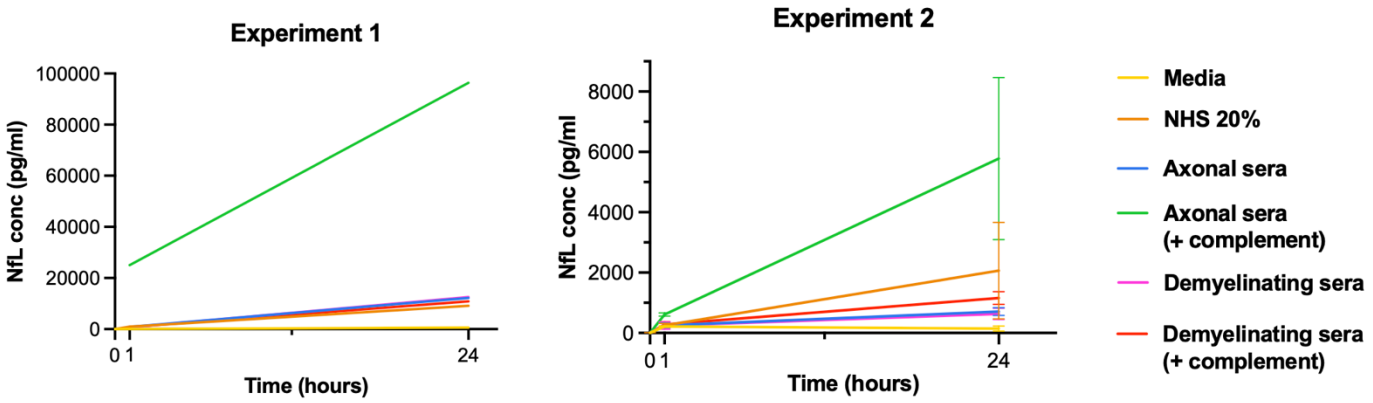


Figure 57: Graphs illustrating figures from table 12

NHS A 20% used as a source of complement in experiment 1, NHS B 20% used in experiment 2.

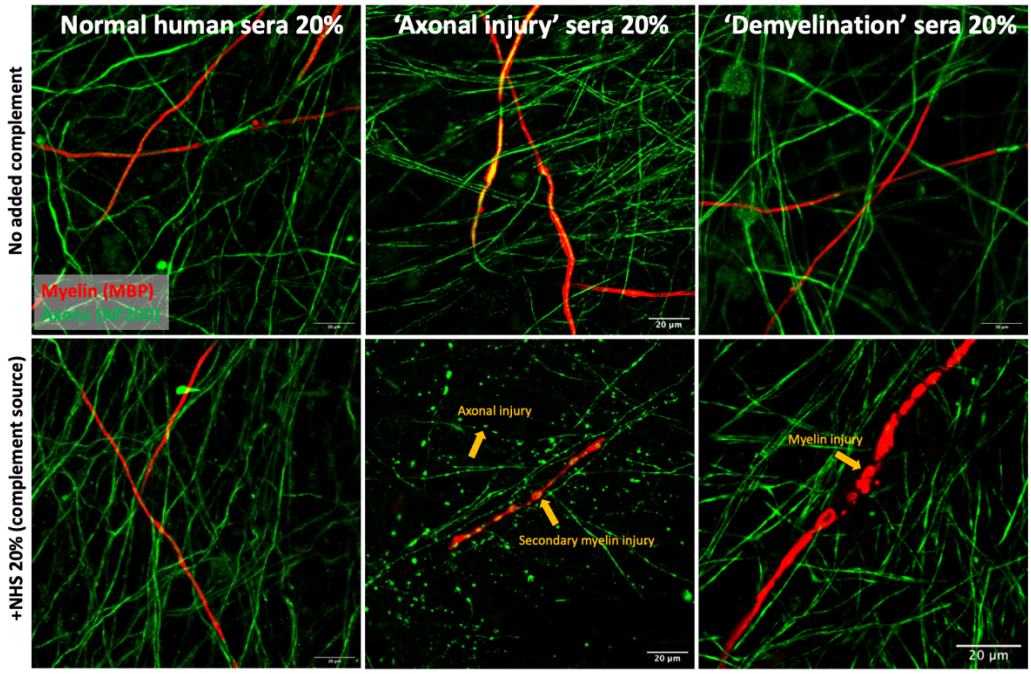


Figure 58: Examples of culture appearances seen using confocal microscopy with and without the addition of NHS 20%.

(A) No significant damage can be seen after 24 hour incubation with NHS B 20% MBP – Myelin basic protein; NF200 – Neurofilament 200

(B) Axonal injury (and likely secondary myelin injury) can be seen as early as 1 hour incubation with 'Axonal injury' sera 1:50 and NHS 20%

(C) 'Demyelinating' sera 1:50 and NHS 20% induces myelin injury at 24 hours

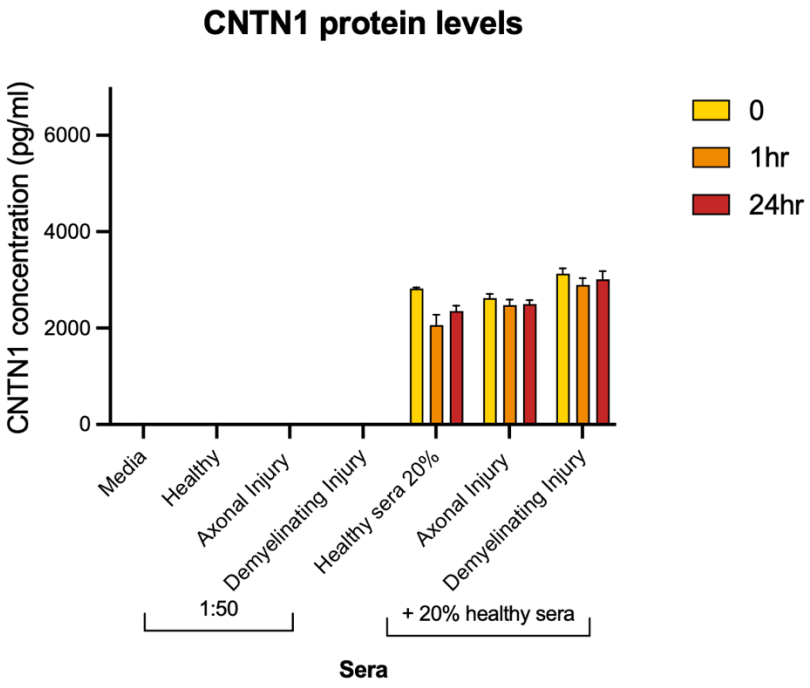


Figure 59: CNTN1 protein levels in healthy and nerve injury conditions, from experiment 2.

CNTN1 protein is consistently raised in 20% healthy sera, or disease sera only where NHS 20% added. Levels are static over 24 hours

3.3.5 Discussion

3.3.5.1 Topographical IgG binding

Existing peripheral nerve models used to test patient sera for potentially pathogenic autoantibodies are limited to those of a different species, or unmyelinated axons, the results of which may not easily be clinically meaningful. The recently developed model of partially human, myelinated peripheral nerve cells in live co-culture by Clark *et al* (Clark et al., 2017) more closely mimic the native environment of the human peripheral nerve and offers a deeper insight into how nerve reactive antibodies from patient sera may be causing injury. By introducing a cryopreservation step into this model, and plating cells into a 96 well microplate, we can now permit higher throughput testing of patient sera suspected to possess nerve reactive auto-antibodies, in a more clinically relevant context.

Overall, preliminary testing shows known nodal or paranodal antibodies from over half of seropositive patient sera bind to live myelinated neurons in vitro. A higher proportion of CNTN1 and Caspr1 antibody positive sera were scored as positive for axonal binding, which one can expect due to diffuse expression of these antigens along the axonal membrane, and thus more striking appearances of immunofluorescence if positive. This suggests that at least some of the lack of observed binding in NF155 and PanNF positive sera is due to more subtle staining patterns i.e. node and/or myelin. In this case, the quality of myelination within a given culture and/or well may more heavily influence the observers' ability to detect positive IgG immunofluorescence. In NF155 seropositive sera, binding was predominantly observed at the node and/or along the myelin, and for panNF sera binding at the node and sometimes axon. Neurofascin is known to be enriched at the node (186) and paranode (155), but IgG staining at the paranode was presumably lacking due to the tight paranodal junctions. Indeed permeabilization of cultures did sometimes permit access of the antibodies to the paranodes. Binding to myelin was not expected, though these are of rat origin, and the specificity of these antibodies as anti-neurofascin could be confirmed as staining was abrogated through pre-adsorption with neurofascin protein.

The lack of observed binding in almost half of overall samples known to possess pathogenic antibodies may be accounted for by a number of variables, including stem cell line and quality of cell culture/degree of myelination, quality of sera sample neurons exposed to (stored and thawed at different timepoints), and experimenter/observer technique. However, our validation testing suggests that any discrepancies in scoring for IgG positivity were not heavily influenced by one individual variable. Where disagreement did occur it was more often between equivocal/positive than negative/positive binding, and when IgG was observed to bind to one vs multiple neuronal components.

Positive IgG immunolabelling was detected in 10% of samples known to be seronegative for (para)nodal antibodies on CBA testing, with binding to either axonal or glial structures, indicating that there may be novel pathogenic antibodies targeting neuronal antigens, warranting further investigation in this subset of patients.

Our results suggest that sensory neuron myelinated co-cultures can be used to demonstrate topographical IgG binding of (para)nodal antibodies from seropositive patient sera, although is not as reliable as a CBA to detect the four known pathogenic antibodies (CNTN1, Caspr1, NF155, NF168/140), and thus would not currently be useful for stand-alone diagnostic testing for these antibodies. However, in those patients who are classified as seronegative by CBA but who have clinical symptoms suggestive of an immune-mediated peripheral nerve disorder, identifying specific IgG reactivity to human derived components of this live culture system can provide supporting evidence that an antibody-mediated process may be driving the disease, and assist clinicians in therapeutic decision making. Further, this subset of patients provide an opportunity for novel antibody discovery.

With regard to specific antibody groups we have shown that panNF antibodies target three neurofascin isoforms (140/186 and 155), and other studies have previously also shown that they specifically target the

immunoglobulin domain common to each isoform (Delmont et al., 2018; Stengel et al., 2019), in contrast to NF155 antibodies which require the third fibronectin domain specific to this isoform in order to bind (Devaux et al., 2016; Ng et al., 2012).

3.3.5.2 Evidence of pathogenicity

It is yet to be confirmed whether panNF antibodies are actually pathogenic or in fact an epiphenomenon i.e as a byproduct of nodal and paranodal damage. The consistent dominance of the IgG1 subclass in our panNF antibody cohort, and IgG3 in other reported cohorts, implies complement activation is likely to play a role in antibody pathogenicity, though this needs to be more robustly addressed in future studies.

I have provided a mechanistic explanation for numerous clinical observations of nephrotic syndrome, caused by MGN, co-occuring with immune-mediated neuropathies
(Cortese et al., 2020; Delmont et al., 2017; Doppler et al., 2015; Hashimoto et al., 2018; Taieb et al., 2018), implicating CNTN1 antibodies as the pathological link. Firstly, I have confirmed the presence of CNTN1 in animal and human-derived peripheral nerve as well as human renal tissue, and that they are targeted by anti-CNTN1 antibodies. The finding of low-level CNTN1 protein expression in healthy human kidney is further supported by recent studies, through the identification of CNTN1 in podocytes by single cell transcriptomic profiling of human kidney (Stewart et al., 2019), as well as CNTN1 expression in normal kidney glomeruli and co-localisation of CNTN1 and IgG4 in the glomerular basement membrane of a patient with MGN (Le Quintrec et al., 2021). This implies there may be a similar initial mechanism to anti-PLA2R antibody-mediated MGN, whereby circulating autoantibodies bind directly to the target antigen in situ, which shed and accumulate in the glomerular space (W. Liu et al., 2019). (Fehmi et al., 2023)

However, in contrast to PLA2R, which is currently undetectable in anti-PLA2R MGN patient or control sera (Beck Jr. et al., 2009), CNTN1 protein has been demonstrated in healthy human sera and seronegative CIDP patients, and different levels can reflect (para)nodal antibody status and neurological disease activity in

CIDP (Wieske et al., 2021). The fact that CNTN1 protein was specifically detected in the PEG precipitates (the fraction containing the immune complexes) and not in the supernatant from patient sera containing high anti-CNTN1 antibody titre indicates CNTN1 likely exists as circulating immune complexes in CNTN1 antibody-positive patients. The subepithelial pattern of CNTN1 deposition may indicate small (and undetectable through our methods) immune complexes causing injury in renal glomeruli, but the absence of immune complexes found in mesangial and/or capillary cells in CNTN1 antibody-positive patient renal biopsies argue against these directly causing nephrotic syndrome (Nangaku & Couser, 2005). The reasons for concurrent renal and nerve disease in CNTN1 antibody-positive, versus the preferential injury to either, is not clear. It is possible that one or other disease may not reach clinical detection, or pre-existing renal disease may predispose patients to subsequent immune-mediated glomerular attack. Indeed over a quarter of the patients in our cohort had a pre-existing diagnosis of diabetes, and as evidenced in mice, upregulated expression of CNTN1 in kidney occurs in the context of prior glomerular injury (Murakoshi et al., 2011). An alternative mechanism may be driven by malignancy. Six patients in our cohort of CNTN1 antibody-associated neuropathy and nephropathy were radiologically screened for malignancy, and despite none being positive, CNTN1 is known to be associated with solid organ cancers (Liang et al., 2020), and it remains possible that these patients may have developed cancer subsequent to their diagnosis (Lefaucheur et al., 2006). Indeed, there is an increased risk of cancer-associated MGN in patients with antibodies against glomerular antigen THSD7A (Pozdzik et al., 2018).

3.3.5.3 Complement binding and complement-mediated cell cytotoxicity

In both a live CBA and myelinated co-culture model I have shown complement binding.

The interpretation of whether antibody-containing sera alone or only with the addition of a source of complement (NHS) could fix/activate complement was confounded by the fact that there is a degree of background complement binding to transfected cells when NHS is added alone, and also that fragmented cells seemed to occur more when higher concentrations of NHS were added, affecting the clarity of membrane bound complement. Further, repeated experiments did not always yield consistent staining

patterns, likely due to the variation in cell quality and density. Assessment at different timepoints may also affect the presence or intensity of complement staining, given this is a dynamic process, and would need to be further investigated.

In myelinated co-cultures it was clear that the level of background staining with NHS alone was high, and although the addition of antibody-containing sera seemed to intensify any complement staining, this was not assessed quantitatively, and varied between individual samples and duration of incubation.

These data suggest that complement fixation studies must use robust control healthy sera. Heat inactivation should be used to eliminate endogenous complement, but not antibody, activity in patient sera to control the total proportion of NHS from an exogenous source. Heat inactivation of the exogenous NHS can also be used to confirm any observations that complement fixation and subsequent injury of neuronal components are indeed from the complement in the NHS and not other sera components.

Sera from patients with IgG1 panNF reactive antibodies incubated with human stem cell-derived sensory neurons did not induce levels of cytotoxicity beyond healthy sera, and were not comparable to that induced by a positive control monoclonal antibody known to induce complement mediated cytotoxicity. Interestingly, the percentage of total cell lysis measured, relative to maximum cell lysis within a well, was inversely proportional to the amount of NHS added as a source of complement. This is likely due to the increasing concentration of serum inhibiting the effect of the detergent used to induce lysis, and remains a confounding factor with the use of this assay. Together, these preliminary findings suggest (para)nodal antibodies may induce cytotoxicity, particularly at higher concentrations, although we did not see any convincing evidence of cytotoxicity above what could be seen for healthy sera in the presence of a source of complement. There may be a number of reasons for not seeing significant complement activity, such as lack of sensitivity of the assay, insufficient amount or duration of IgG exposure, or complement source.

Measurement of neurofilament light (NfL) in the supernatant of these cultures under conditions deprived of or supplemented with (para)nodal antibodies and complement could be another method of assessing neuronal injury in vitro. We found that NfL levels did indeed increase in accordance with visible axonal injury, and these preliminary data strengthen the concept that NfL could be a useful biomarker of axonal injury in this in vitro model and in patient sera. Measurement of serum CNTN1 protein under the same conditions did not fluctuate with observable injury, but consistently increased with the addition of NHS as a source of complement, thus the reason for the low levels seen in autoimmune nodopathy patients (Wieske et al., 2021) remains elusive, and CNTN1 protein is not a biomarker that can be used as a surrogate for neuronal or nodal injury. This quantitative assessment of supernatant constituents in this model of peripheral nerve injury holds promise as it most closely mimics the human peripheral nerve in vitro, and may provide more accurate and reproducible assessment of neuronal injury than visual assessment with confocal microscopy. We observed differences in protein concentration between wells and experiments, which may be due to multiple variables, including differences in well size, culture density, changes in serum activity, and storage of supernatant. Fluid biomarkers of active peripheral nerve injury are lacking in clinical practice, and are needed to guide prompt treatment initiation/changes. Thus, developing a more robust in vitro model in which to further understand these biomarkers is necessary.

4 CONCLUSION AND FUTURE WORK

This data clearly supports the growing body of evidence that autoimmune nodopathy patients have core, phenotypically distinct characteristics that set them apart from the most common demyelinating forms of GBS and CIDP. Most relevant in clinical practice is that they respond poorly to standard therapy used for these disorders, hence are now classified separately within international guidelines and NHS England commissioning policy (NHSE, 2021), encouraging specific identification by way of diagnostic antibody testing and initiation of an alternative therapeutic agent. It is clear from our patient cohort that they require more aggressive therapy, in the form of repeated or multiple standard treatment modalities, to induce meaningful clinical responses, and that these are much more often transient. To achieve a sustained good response B-cell depleting therapy is required, and should be used at the offset, particularly in severe cases where the risk of axonal injury and irreversible neuronal damage may occur more rapidly. Steroids should be considered as an early treatment, if not used alongside RTX. Currently, IVIg has a limited role in the treatment of AINs, and until we understand more about whether the predominance of specific subclasses may offer a more favourable response to IVIg, it should not be standard care for these patients. PLEX may be a useful interim treatment until RTX can be commenced, but has yet to be shown to change the outcome of patients just receiving RTX. The fact that IVIg has been suggested to inhibit the very functions that IgG4 antibodies classically do not exhibit, e.g Fc receptor recruitment of immune cells, cross-linking of antigens and immune complex formation, and antibody-dependent cellular cytotoxicity, may help explain why these patients do not respond to this treatment. However, we have shown a larger proportion of patients (not only the panNF patients) have a predominance of IgG1subclass antibodies, and they also do not respond to IVIg. Data concerning longer term outcomes and relapse rates of patients who have received different treatments are emerging now, but a prospective trial comparing a large group of patients using the same outcome measures at standardised timepoints is required to draw more robust conclusions about the longer-term efficacy of RTX.

Diagnostic testing for (para)nodal antibodies is currently performed for patients with atypical clinical features of an immune mediated neuropathy and/or poor response to standard therapies. This has led to a skewed cohort being tested, and has limited our understanding of the clinical relevance of these antibodies in healthy individuals and other patients with a less phenotypically distinct presentation. Future studies will hopefully address this issue and may also help our understanding of the relevance of antibody isotype on potential pathogenicity. Although a comparison of diagnostic assays, in particular CBA, across laboratories in Europe have shown good accuracy, there should be ongoing interval inter-lab validation studies to ensure consistency in reporting and standardisation of international testing.

Using analysis of a unique human stem cell-derived in vitro model of the myelinated peripheral neuron (hiPSC co-cultures) we can identify topographical patient IgG binding to it's suspected antigenic target. Interpreting any potential pathogenic effects of this, and the dependence on factors such as complement activation could allow subsequent manipulation of antibody and other environmental factors to determine their specific effects on pathogenicity. Indeed, glycosylation of neurofascin antibodies has been shown to influence it's ability to bind to an antigenic target (Devaux et al., 2016). Similarly, altering accessibility of the paranodal loops may provide insights into why antibodies targeting paranodal and juxtaparanodal targets may only be pathogenic if exposed environmental factors predisposing the nerves to injury i.e. concurrent autoimmune, malignant or genetic disease. This has been speculated in Caspr2 related diseases, where there is differential targeting of antigens in the CNS and PNS (Binks et al., 2018; Ferrara et al., 2023). Why, despite shared (para)nodal proteins in both the PNS and CNS, we have not observed more frequent clinical overlap in our patient cohort, is not clear, though there may also be subtle regional or fibre-type differences in the conformation, clustering, or accessibility of paranodal adhesion molecules, all influencing their interaction with antibodies and potential to induce injury. Using the co-culture model however, does not account for potential inaccessibility of antibodies (and other inflammatory or mediating cells) through the blood nerve barrier (BNB). Pathogenicity of antibodies in vitro may not reflect their effects in vivo, or may

be dependent on external factors influencing BNB permeability. Indeed this may determine clinical phenotypes (Shimizu & Kanda, 2015), though fully humanised peripheral nerve models with a BNB are lacking.

Through the acquisition of more quantitative measures (automated imaging and analysis software) to assess axonal and myelin injury in this live peripheral nerve model, the effects of time of antibody exposure, an additional complement source, and antibody deglycosylation can be more reliably determined. The measurement of fluid constituents generated from these models, such as NfL, can complement these studies by providing a more dynamic measure of neuronal injury.

Finally, we have shown that apparently (para)nodal antibody seronegative patients may still have nerve-reactive antibodies, that if further characterised, could provide impetus to consider offering more patients targeted and effective therapy that they may not have otherwise been considered for. This finding eludes to the fact that there are probably as yet unidentified pathogenic antibodies which may be pathologically relevant. The observed difference in their binding patterns in iPSC cultures suggest numerous antigenic targets may be responsible, a proportion of which seem to be at the node/paranode. As yet human Schwann cells have not successfully been differentiated, though ideally, a fully humanised model may provide more representative topographical binding data in order to more accurately identify candidate antigenic targets through immunoprecipitation assays and mass spectrometry.

5 BIBLIOGRAPHY

Allen, J. A. (2020). The Misdiagnosis of CIDP: A Review. *Neurology and Therapy*, *9*(1), 43–54. https://doi.org/10.1007/s40120-020-00184-6

Allen, J. A., Gorson, K. C., & Gelinas, D. (2018). Challenges in the diagnosis of chronic inflammatory demyelinating polyneuropathy. *Brain and Behavior*, *8*(3), 1–5. https://doi.org/10.1002/brb3.932

Amor, V., Zhang, C., Vainshtein, A., Zhang, A., Zollinger, D. R., Eshed-Eisenbach, Y., Brophy, P. J., Rasband, M. N., & Peles, E. (2017). The paranodal cytoskeleton clusters Na(+) channels at nodes of Ranvier. *ELife*, *6*. https://doi.org/10.7554/eLife.21392

Appeltshauser, L., Brunder, A. M., Heinius, A., Körtvélyessy, P., Wandinger, K. P., Junker, R., Villmann, C., Sommer, C., Leypoldt, F., & Doppler, K. (2020). Antiparanodal antibodies and IgG subclasses in acute autoimmune neuropathy. *Neurology - Neuroimmunology Neuroinflammation*, *7*(5), 817. https://doi.org/10.1212/NXI.0000000000000817

Appeltshauser, L., Junghof, H., Messinger, J., Linke, J., Haarmann, A., Ayzenberg, I., Baka, P., Dorst, J., Fisse, A. L., Grüter, T., Hauschildt, V., Jörk, A., Leypoldt, F., Mäurer, M., Meinl, E., Michels, S., Motte, J., Pitarokoili, K., Stettner, M., … Doppler, K. (2022). Anti-pan-neurofascin antibodies induce subclass-related complement activation and nodo-paranodal damage. *Brain*, *146*(5), 1932–1949. https://doi.org/10.1093/brain/awac418

Appeltshauser, L., Linke, J., Heil, H. S., Karus, C., Schenk, J., Hemmen, K., Sommer, C., Doppler, K., & Heinze, K. G. (2023). Super-resolution imaging pinpoints the periodic ultrastructure at the human node of Ranvier and its disruption in patients with polyneuropathy. *Neurobiology of Disease*, *182*(February), 106139. https://doi.org/10.1016/j.nbd.2023.106139

Armbruster, D. A., & Pry, T. (2008). Limit of blank, limit of detection and limit of quantitation. *The Clinical Biochemist. Reviews*, *29 Suppl 1*(August), S49-52.

http://www.ncbi.nlm.nih.gov/pubmed/18852857%0Ahttp://www.pubmedcentral.nih.gov/articlerender.fcgi?artid=PMC2556583

Asbury, A. K., Arnason, B. G., & Adams, R. D. (1969). The inflammatory lesion in idiopathic polyneuritis. Its role in pathogenesis. *Medicine*, *48*(3), 173–215. https://doi.org/10.1097/00005792-196905000-00001

Bangdiwala, S. I., & Shankar, V. (2013). The agreement chart. *BMC Medical Research Methodology*, *13*(1), 1–7. https://doi.org/10.1186/1471-2288-13-97/FIGURES/3

Beck Jr., L. H., Bonegio, R. G., Lambeau, G., Beck, D. M., Powell, D. W., Cummins, T. D., Klein, J. B., & Salant, D. J. (2009). M-type phospholipase A2 receptor as target antigen in idiopathic membranous nephropathy. *N Engl J Med*, *361*(1), 11–21. https://doi.org/10.1056/NEJMoa0810457

Beck, L. H., Fervenza, F. C., Beck, D. M., Bonegio, R. G. B., Malik, F. A., Erickson, S. B., Cosio, F. G., Cattran, D. C., & Salant, D. J. (2011). Rituximab-induced depletion of anti-PLA2R autoantibodies predicts response in membranous nephropathy. *Journal of the American Society of Nephrology*, *22*(8), 1543–1550. https://doi.org/10.1681/ASN.2010111125

Bellanti, R., Keddie, S., Lunn, M. P., & Rinaldi, S. (2024). Ultrasensitive assay technology and fluid biomarkers for the evaluation of peripheral nerve disease. *Journal of Neurology, Neurosurgery, and Psychiatry*, *95*(2), 114–124. https://doi.org/10.1136/jnnp-2023-332031

Berg, B. van den, Bunschoten, C., Doorn, P. A. van, & Jacobs, B. C. (2013). Mortality in Guillain-Barré syndrome. *Neurology*, *80*(18), 1650 LP – 1654. https://doi.org/10.1212/WNL.0b013e3182904fcc

Bermingham, J. R. J., Shearin, H., Pennington, J., O'Moore, J., Jaegle, M., Driegen, S., van Zon, A., Darbas, A., Ozkaynak, E., Ryu, E. J., Milbrandt, J., & Meijer, D. (2006). The claw paw mutation reveals a role for Lgi4 in peripheral nerve development. *Nature Neuroscience*, *9*(1), 76–84. https://doi.org/10.1038/nn1598

Bhat, M. A. (2003). Molecular organization of axo-glial junctions. *Current Opinion in Neurobiology*, *13*(5), 552–559. https://doi.org/10.1016/j.conb.2003.09.004

Bhat, M. A., Rios, J. C., Lu, Y., Garcia-Fresco, G. P., Ching, W., St Martin, M., Li, J., Einheber, S., Chesler, M., Rosenbluth, J., Salzer, J. L., & Bellen, H. J. (2001). Axon-glia interactions and the domain organization of myelinated axons requires neurexin IV/Caspr/Paranodin. *Neuron*, *30*(2), 369–383. https://doi.org/10.1016/S0896-6273(01)00294-X

Binks, S. N. M., Klein, C. J., Waters, P., Pittock, S. J., & Irani, S. R. (2018). LGI1, CASPR2 and related antibodies: a molecular evolution of the phenotypes. *Journal of Neurology, Neurosurgery, and Psychiatry*, *89*(5), 526–534. https://doi.org/10.1136/jnnp-2017-315720

Boyle, M. E., Berglund, E. O., Murai, K. K., Weber, L., Peles, E., & Ranscht, B. (2001). Contactin orchestrates assembly of the septate-like junctions at the paranode in myelinated peripheral nerve. *Neuron*, *30*(2), 385–397. https://doi.org/10.1016/S0896-6273(01)00296-3

Bunschoten, C., Jacobs, B. C., Van den Bergh, P. Y. K., Cornblath, D. R., & van Doorn, P. A. (2019). Progress in diagnosis and treatment of chronic inflammatory demyelinating polyradiculoneuropathy. *The Lancet Neurology*, *18*(8), 784–794. https://doi.org/10.1016/S1474-4422(19)30144-9

Burbelo, P. D., Joshi, M., Chaturvedi, A., Little, D. J., Thurlow, J. S., Waldman, M., & Olson, S. W. (2020). Detection of PLA2R autoantibodies before the diagnosis of membranous nephropathy. *Journal of the American Society of Nephrology*, *31*(1), 208–217. https://doi.org/10.1681/ASN.2019050538

Burnor, E., Yang, L., Zhou, H., Patterson, K. R., Quinn, C., Reilly, M. M., Rossor, A. M., Scherer, S. S., & Lancaster, E. (2018). Neurofascin antibodies in autoimmune, genetic, and idiopathic neuropathies. *Neurology*, *90*(1), E31–E38. https://doi.org/10.1212/WNL.0000000000004773

Burt, R. K., Balabanov, R., Tavee, J., Han, X., Sufit, R., Ajroud-Driss, S., Jovanovic, B., Quigley, K., Arnautovic, I., Helenowski, I., & Sharrack, B. (2020). Hematopoietic stem cell transplantation for chronic inflammatory demyelinating polyradiculoneuropathy. *Journal of Neurology*, *267*(11), 3378–3391. https://doi.org/10.1007/S00415-020-10010-6/TABLES/3

Chambers, S. M., Qi, Y., Mica, Y., Lee, G., Zhang, X.-J., Niu, L., Bilsland, J., Cao, L., Stevens, E., Whiting, P., Shi, S.-H., & Studer, L. (2012). Combined small-molecule inhibition accelerates developmental timing and converts human pluripotent stem cells into nociceptors. *Nature Biotechnology*, *30*(7), 715–720. https://doi.org/10.1038/nbt.2249

Chiu, S. Y., & Ritchie, J. M. (1984). On the physiological role of internodal potassium channels and the security of conduction in myelinated nerve fibres. *Proceedings of the Royal Society of London. Series B, Biological Sciences*, *220*(1221), 415–422. https://doi.org/10.1098/rspb.1984.0010

Cifuentes-Diaz, C., Dubourg, O., Irinopoulou, T., Vigny, M., Lachkar, S., Decker, L., Charnay, P., Denisenko, N., Maisonobe, T., Léger, J.-M., Viala, K., Hauw, J.-J., & Girault, J.-A. (2011). Nodes of ranvier and paranodes in chronic acquired neuropathies. *PloS One*, *6*(1), e14533. https://doi.org/10.1371/journal.pone.0014533

Clark, A. J., Kaller, M. S., Galino, J., Willison, H. J., Rinaldi, S., & Bennett, D. L. H. (2017). Co-cultures with stem cell-derived human sensory neurons reveal regulators of peripheral myelination. *Brain*, *45*(2), 846–860. https://doi.org/10.1093/brain/awx012

Cocito, D., Paolasso, I., Antonini, G., Benedetti, L., Briani, C., Comi, C., Fazio, R., Jann, S., Matà, S., Mazzeo, A., Sabatelli, M., & Nobile-Orazio, E. (2010). A nationwide retrospective analysis on the effect of immune therapies in patients with chronic inflammatory demyelinating polyradiculoneuropathy. *European Journal of Neurology*, *17*(2), 289–294. https://doi.org/10.1111/j.1468-1331.2009.02802.x

Cortese, A., Lombardi, R., Briani, C., Callegari, I., Benedetti, L., Manganelli, F., Luigetti, M., Ferrari, S., Clerici, A. M., Marfia, G. A., Rigamonti, A., Carpo, M., Fazio, R., Corbo, M., Mazzeo, A., Giannini, F., Cosentino, G., Zardini, E., Curro, R., … Franciotta, D. (2020). Antibodies to neurofascin, contactin-1, and contactin-associated protein 1 in CIDP: Clinical relevance of IgG isotype. *Neurol Neuroimmunol Neuroinflamm*, *7*(1). https://doi.org/10.1212/NXI.0000000000000639

Csurhes, P. A., Sullivan, A.-A., Green, K., Pender, M. P., & McCombe, P. A. (2005). T cell reactivity to P0, P2, PMP-22, and myelin basic protein in patients with Guillain-Barre syndrome and chronic inflammatory demyelinating polyradiculoneuropathy. *Journal of Neurology, Neurosurgery, and Psychiatry*, *76*(10), 1431–1439. https://doi.org/10.1136/jnnp.2004.052282

Cunningham, M. E., McGonigal, R., Meehan, G. R., Barrie, J. A., Yao, D., Halstead, S. K., & Willison, H. J. (2016). Anti-ganglioside antibodies are removed from circulation in mice by neuronal endocytosis. *Brain*, *139*(6), 1657–1665. https://doi.org/10.1093/brain/aww056

Dalakas, M. C. (2002). Mechanisms of action of IVIg and therapeutic considerations in the treatment of acute and chronic demyelinating neuropathies. *Neurology*, *59*(12 Suppl 6), S13-21. https://doi.org/10.1212/wnl.59.12_suppl_6.s13

Davidson, A. I., Halstead, S. K., Goodfellow, J. A., Chavada, G., Mallik, A., Overell, J., Lunn, M. P., McConnachie, A., van Doorn, P., & Willison, H. J. (2017). Inhibition of complement in Guillain-Barré syndrome: the ICA-GBS study. *Journal of the Peripheral Nervous System*, *22*(1), 4–12. https://doi.org/10.1111/jns.12194

Davies, A., Fehmi, J., Senel, M., Tumani, H., Dorst, J., & Rinaldi, S. (2020). Immunoadsorption and Plasma Exchange in Seropositive and Seronegative Immune-Mediated Neuropathies. *Journal of Clinical Medicine*, *9*(7), 2025. https://doi.org/10.3390/jcm9072025

Davies, A. J., Fehmi, J., Senel, M., Tumani, H., & Dorst, J. (2020). *Immunoadsorption and Plasma Exchange in Seropositive and Seronegative Immune-Mediated Neuropathies*. 1–24. https://doi.org/10.3390/jcm9072025

De Simoni, D., Ricken, G., Winklehner, M., Koneczny, I., Karenfort, M., Hustedt, U., Seidel, U., Abdel-Mannan, O., Munot, P., Rinaldi, S., Steen, C., Freilinger, M., Breu, M., Seidl, R., Reindl, M., Wanschitz, J., Lleixà, C., Bernert, G., Wandinger, K. P., … Höftberger, R. (2020). Antibodies to nodal/paranodal proteins in paediatric immune-mediated neuropathy. *Neurology(R) Neuroimmunology & Neuroinflammation*, *7*(4), 1–5. https://doi.org/10.1212/NXI.0000000000000763

Delmont, E., Brodovitch, A., Kouton, L., Allou, T., & Beltran, S. (2020). Antibodies against the node of Ranvier : a real - life evaluation of incidence , clinical features and response to treatment based on a prospective analysis of 1500 sera. *Journal of Neurology*, *0123456789*. https://doi.org/10.1007/s00415-020-10041-z

Delmont, E., Manso, C., Querol, L., Cortese, A., Berardinelli, A., Lozza, A., Belghazi, M., Malissart, P., Labauge, P., Taieb, G., Yuki, N., Illa, I., & Attarian, S. (2018). *Autoantibodies to nodal isoforms of neurofascin in chronic inflammatory demyelinating polyneuropathy*. *May*, 1851–1858. https://doi.org/10.1093/brain/awx124

Delmont, E., Manso, C., Querol, L., Cortese, A., Berardinelli, A., Lozza, A., Belghazi, M., Malissart, P., Labauge, P., Taieb, G., Yuki, N., Illa, I., Attarian, S., & Devaux, J. J. (2017). Autoantibodies to nodal isoforms of neurofascin in chronic inflammatory demyelinating polyneuropathy. *Brain*, *140*(7), 1851–1858. https://doi.org/10.1093/brain/awx124

Demichelis, C., Franciotta, D., Cortese, A., Callegari, I., Serrati, C., Mancardi, G. L., Schenone, A., Leonardi, A., & Benedetti, L. (2018). Remarkable Rituximab Response on Tremor Related to Acute-Onset Chronic Inflammatory Demyelinating Polyradiculoneuropathy in an Antineurofascin155 Immunoglobulin G4–Seropositive Patient. In *Movement Disorders Clinical Practice* (Vol. 5, Issue 5, pp. 559–560). Wiley-Blackwell. https://doi.org/10.1002/mdc3.12662

D'Este, E., Kamin, D., Balzarotti, F., & Hell, S. W. (2017). Ultrastructural anatomy of nodes of Ranvier in the peripheral nervous system as revealed by STED microscopy. *Proceedings of the National Academy of Sciences of the United States of America*, *114*(2), E191–E199. https://doi.org/10.1073/pnas.1619553114

Devaux, J. J., Miura, Y., Fukami, Y., Inoue, T., Manso, C., Belghazi, M., Sekiguchi, K., Kokubun, N., Ichikawa, H., Wong, A. H. Y., & Yuki, N. (2016). Neurofascin-155 IgG4 in chronic inflammatory demyelinating polyneuropathy. *Neurology*, *86*(9), 800–807. https://doi.org/10.1212/WNL.0000000000002418

Devaux, J. J., Odaka, M., & Yuki, N. (2012). Nodal proteins are target antigens in Guillain-Barré syndrome. *Journal of the Peripheral Nervous System*, *17*(1), 62–71. https://doi.org/10.1111/j.1529-8027.2012.00372.x

Doneddu, P. E., Cocito, D., Manganelli, F., Fazio, R., Briani, C., Filosto, M., Benedetti, L., Mazzeo, A., Marfia, G. A., Cortese, A., Fierro, B., Jann, S., Beghi, E., Clerici, A. M., Carpo, M., Schenone, A., Luigetti, M., Lauria, G., Antonini, G., … Nobile-Orazio, E. (2018). Atypical CIDP: diagnostic criteria, progression and treatment response. Data from the Italian CIDP Database. *Journal of Neurology, Neurosurgery & Psychiatry*, *1*, jnnp-2018-318714. https://doi.org/10.1136/jnnp-2018-318714

Doneddu, P. E., Dentoni, M., & Nobile-Orazio, E. (2021). Atypical chronic inflammatory demyelinating polyradiculoneuropathy: recent advances on classification, diagnosis, and pathogenesis. *Current Opinion in Neurology*, *34*(5), 613–624. https://doi.org/10.1097/WCO.0000000000000979

Doppler, K., Appeltshauser, L., Villmann, C., Martin, C., Peles, E., Kr??mer, H. H., Haarmann, A., Buttmann, M., & Sommer, C. (2016). Auto-antibodies to contactin-associated protein 1 (Caspr) in two patients with painful inflammatory neuropathy. *Brain*, *139*(10), 2617–2630. https://doi.org/10.1093/brain/aww189

Doppler, K., Appeltshauser, L., Wilhelmi, K., Villmann, C., Dib-Hajj, S. D., Waxman, S. G., Maurer, M., Weishaupt, A., & Sommer, C. (2015). Destruction of paranodal architecture in inflammatory neuropathy with anti-contactin-1 autoantibodies. *J Neurol Neurosurg Psychiatry*, *86*(7), 720–728. https://doi.org/10.1136/jnnp-2014-309916

Doppler, K., Schuster, Y., Appeltshauser, L., Biko, L., Villmann, C., Weishaupt, A., Werner, C., & Sommer, C. (2019). Anti-CNTN1 IgG3 induces acute conduction block and motor deficits in a passive transfer rat model. *Journal of Neuroinflammation*, *16*(1), 73. https://doi.org/10.1186/s12974-019-1462-z

Doppler, K., Schuster, Y., Appeltshauser, L., Biko, L., Villmann, C., Weishaupt, A., Werner, C., Sommer, C., & Doppler, K. (2017). Complement deposition induced by binding of anti-contactin-1 auto-antibodies is modified by immunoglobulins. *Experimental Neurology*, *287*, 84–90. https://doi.org/10.1016/j.expneurol.2016.10.006

Doppler, K., Stengel, H., Appeltshauser, L., Grosskreutz, J., Man Ng, J. K., Meinl, E., & Sommer, C. (2018). Neurofascin-155 IgM autoantibodies in patients with inflammatory neuropathies. *Journal of Neurology, Neurosurgery and Psychiatry*, 1145–1151. https://doi.org/10.1136/jnnp-2018-318170

Doppler, K., Werner, C., & Sommer, C. (2013). Disruption of nodal architecture in skin biopsies of patients with demyelinating neuropathies. In *Journal of the Peripheral Nervous System* (Vol. 18). https://onlinelibrary.wiley.com/doi/pdf/10.1111/jns5.12023

Dubey, D., Honorat, J. A., Shelly, S., Klein, C. J., Komorowski, L., Mills, J. R., Brakopp, S., Probst, C., Lennon, V. A., Pittock, S. J., & McKeon, A. (2020). Contactin-1 autoimmunity: Serologic, neurologic, and pathologic correlates. *Neurology(R) Neuroimmunology & Neuroinflammation*, *7*(4). https://doi.org/10.1212/NXI.0000000000000771

Dustin, E., Suarez-Pozos, E., Stotesberry, C., Qiu, S., Palavicini, J. P., Han, X., & Dupree, J. L. (2023). Compromised Myelin and Axonal Molecular Organization Following Adult-Onset Sulfatide Depletion. *Biomedicines*, *11*(5). https://doi.org/10.3390/biomedicines11051431

Dzhashiashvili, Y., Zhang, Y., Galinska, J., Lam, I., Grumet, M., & Salzer, J. L. (2007). Nodes of Ranvier and axon initial segments are ankyrin G-dependent domains that assemble by distinct mechanisms. *Journal of Cell Biology*, *177*(5), 857–870. https://doi.org/10.1083/jcb.200612012

Einheber, S., Zanazzi, G., Ching, W., Scherer, S., Milner, T. A., Peles, E., & Salzer, J. L. (1997). The axonal membrane protein Caspr, a homologue of neurexin IV, is a component of the septate-like paranodal junctions that assemble during myelination. *Journal of Cell Biology*, *139*(6), 1495–1506. https://doi.org/10.1083/jcb.139.6.1495

Emilien, D., & Hugh, W. (2015). Diagnostic Utility of Auto Antibodies in Inflammatory Nerve Disorders. In *Journal of Neuromuscular Diseases* (Vol. 2, Issue 2, pp. 107–112). IOS Press. https://doi.org/10.3233/JND-150078

Eshed, Y., Feinberg, K., Poliak, S., Sabanay, H., Sarig-Nadir, O., Spiegel, I., Bermingham, J. R., & Peles, E. (2005). Gliomedin mediates Schwann cell-axon interaction and the molecular assembly of the nodes of Ranvier. *Neuron*, *47*(2), 215–229. https://doi.org/10.1016/j.neuron.2005.06.026

Fehmi, J., Davies, A. J., Antonelou, M., Keddie, S., Pikkupeura, S., Querol, L., Delmont, E., Cortese, A., Franciotta, D., Persson, S., Barratt, J., Pepper, R., Farinha, F., Rahman, A., Canetti, D., Gilbertson, J. A., Rendell, N. B., Radunovic, A., Minton, T., … Rinaldi, S. (2023). Contactin-1 links autoimmune neuropathy and membranous glomerulonephritis. *PLoS ONE*, *18*(3 March), 1–15. https://doi.org/10.1371/journal.pone.0281156

Fehmi, J., Davies, A. J., Walters, J., Lavin, T., Keh, R., Rossor, A. M., Munteanu, T., Delanty, N., Roberts, R., Bäumer, D., Lennox, G., & Rinaldi, S. (2021). IgG1 pan-neurofascin antibodies identify a severe yet treatable neuropathy with a high mortality. *Journal of Neurology, Neurosurgery, and Psychiatry*, *92*(10), 1089–1095. https://doi.org/10.1136/jnnp-2021-326343

Fehmi, J., Scherer, S. S., Willison, H. J., & Rinaldi, S. (2018). Nodes, paranodes and neuropathies. *Journal of Neurology, Neurosurgery and Psychiatry*, *89*(1). https://doi.org/10.1136/jnnp-2016-315480

Fehmi, J., Vale, T., Keddie, S., & Rinaldi, S. (2021). Nodal and paranodal antibody-associated neuropathies. *Practical Neurology*, *21*(4), 284–291. https://doi.org/10.1136/practneurol-2021-002960

Feinberg, K., Eshed-Eisenbach, Y., Frechter, S., Amor, V., Salomon, D., Sabanay, H., Dupree, J. L., Grumet, M., Brophy, P. J., Shrager, P., & Peles, E. (2010). A glial signal consisting of gliomedin and NrCAM clusters axonal Na+ channels during the formation of nodes of Ranvier. *Neuron*, *65*(4), 490–502. https://doi.org/10.1016/j.neuron.2010.02.004

Ferrara, J. M., Wiid, M., & Burke, S. (2023). Contactin-Associated Protein-Like 2-Related Peripheral Nerve Hyperexcitability Associated With Charcot-Marie-Tooth Type 4F. *The Neurohospitalist*, *13*(2), 164–168. https://doi.org/10.1177/19418744221140182

Forsberg, A., Press, R., & Holmqvist, L. W. (2012). Residual disability 10 years after falling ill in Guillain-Barré syndrome: A prospective follow-up study. *Journal of the Neurological Sciences*, *317*(1–2), 74–79. https://doi.org/10.1016/j.jns.2012.02.026

Gabriel, C. M., Gregson, N. A., & Hughes, R. A. (2000). Anti-PMP22 antibodies in patients with inflammatory neuropathy. *Journal of Neuroimmunology*, *104*(2), 139–146. https://doi.org/10.1016/s0165-5728(99)00269-6

Garcia-Fresco, G. P., Sousa, A. D., Pillai, A. M., Moy, S. S., Crawley, J. N., Tessarollo, L., Dupree, J. L., & Bhat, M. A. (2006). Disruption of axo-glial junctions causes cytoskeletal disorganization and degeneration of Purkinje neuron axons. *Proceedings of the National Academy of Sciences of the United States of America*, *103*(13), 5137–5142. https://doi.org/10.1073/pnas.0601082103

Garssen, M. P. J., Van Koningsveld, R., & Van Doorn, P. A. (2006). Residual fatigue is independent of antecedent events and disease severity in Guillain-Barré syndrome. *Journal of Neurology*, *253*(9), 1143–1146. https://doi.org/10.1007/s00415-006-0163-6

Glassock, R. J. (2003). Diagnosis and natural course of membranous nephropathy. *Seminars in Nephrology*, *23*(4), 324–332. https://doi.org/10.1016/S0270-9295(03)00049-4

Godil, J., Barrett, M. J., Ensrud, E., Chahin, N., & Karam, C. (2020). Refractory CIDP: Clinical characteristics, antibodies and response to alternative treatment. *Journal of the Neurological Sciences*, *418*. https://doi.org/10.1016/J.JNS.2020.117098

Grüner, J., Stengel, H., Werner, C., Appeltshauser, L., Sommer, C., Villmann, C., & Doppler, K. (2021). Anti-contactin-1 Antibodies Affect Surface Expression and Sodium Currents in Dorsal Root Ganglia. *Neurology(R) Neuroimmunology & Neuroinflammation*, *8*(5), 1–14. https://doi.org/10.1212/NXI.0000000000001056

Guillain, G., Barré, J. A., & Strohl, A. (1999). [Radiculoneuritis syndrome with hyperalbuminosis of cerebrospinal fluid without cellular reaction. Notes on clinical features and graphs of tendon reflexes. 1916]. *Annales de medecine interne*, *150*(1), 24–32.

Gupta, P., Mirman, I., Shahar, S., & Dubey, D. (2023). Growing Spectrum of Autoimmune Nodopathies. *Current Neurology and Neuroscience Reports*, *23*(5), 201–212. https://doi.org/10.1007/s11910-023-01264-4

Hadden, R. D. M., Cornblath, D. R., Hughes, R. A. C., Zielasek, J., Hartung, H. P., Toyka, K. V, & Swan, A. V. (1998). Electrophysiological classification of guillain-barré syndrome: Clinical associations and outcome. *Annals of Neurology*, *44*, 780–788. https://doi.org/DOI 10.1002/ana.410440512

Hafer-Macko, C. E., Sheikh, K. A., Li, C. Y., Ho, T. W., Cornblath, D. R., McKhann, G. M., Asbury, A. K., & Griffin, J. W. (1996). Immune attack on the Schwann cell surface in acute inflammatory demyelinating polyneuropathy. *Annals of Neurology*, *39*(5), 625–635. https://doi.org/10.1002/ana.410390512

Hafer-Macko, C., Hsieh, S. T., Yan Li, C., Ho, T. W., Sheikh, K., Cornblath, D. R., McKhann, G. M., Asbury, A. K., & Griffin, J. W. (1996). Acute motor axonal neuropathy: An antibody-mediated attack on axolemma. *Annals of Neurology*, *40*(4), 635–644. https://doi.org/10.1002/ana.410400414

Harkiss, G. D., & Brown, D. L. (1979). Detection of immune complexes by a new assay, the polyethylene glycol precipitation-complement consumption test (PEG-CC). *Clinical and Experimental Immunology*, *36*(1), 117–129.

Harris, P. A., Taylor, R., Minor, B. L., Elliott, V., Fernandez, M., O'Neal, L., McLeod, L., Delacqua, G., Delacqua, F., Kirby, J., & Duda, S. N. (2019). The REDCap consortium: Building an international community of software platform partners. *Journal of Biomedical Informatics*, *95*(December 2018), 103208. https://doi.org/10.1016/j.jbi.2019.103208

Harris, P. A., Taylor, R., Thielke, R., Payne, J., Gonzalez, N., & Conde, J. G. (2009). Research electronic data capture (REDCap)-A metadata-driven methodology and workflow process for

providing translational research informatics support. *Journal of Biomedical Informatics*, *42*(2), 377–381. https://doi.org/10.1016/j.jbi.2008.08.010

Harris, R. E., Atherton, M., Naude, J. T. W., Bird-Lieberman, G. A., Ramdas, S., Fehmi, J., Rinaldi, S., & Ong, M. T. (2023). Antineurofascin IgG2-associated paediatric autoimmune nodopathy. *Developmental Medicine and Child Neurology*, *November 2021*, 1118–1122. https://doi.org/10.1111/dmcn.15493

Hashimoto, Y., Ogata, H., Yamasaki, R., Sasaguri, T., Ko, S., Yamashita, K., Xu, Z., Matsushita, T., Tateishi, T., Akiyama, S., Maruyama, S., Yamamoto, A., & Kira, J. I. (2018). Chronic Inflammatory Demyelinating Polyneuropathy With Concurrent Membranous Nephropathy: An Anti-paranode and Podocyte Protein Antibody Study and Literature Survey. *Front Neurol*, *9*(November), 997. https://doi.org/10.3389/fneur.2018.00997

Haymaker, W. E., & Kernohan, J. W. (1949). The Landry-Guillain-Barré syndrome; a clinicopathologic report of 50 fatal cases and a critique of the literature. *Medicine*, *28*(1), 59–141.

Hecker, K., Grüner, J., Hartmannsberger, B., Appeltshauser, L., Villmann, C., & Sommer, C. (2023). *Different binding and pathogenic effect of neurofascin and contactin – 1 autoantibodies in autoimmune nodopathies*. *June*, 1–10. https://doi.org/10.3389/fimmu.2023.1189734

Henderson, R. D., Lawn, N. D., Fletcher, D. D., McClelland, R. L., & Wijdicks, E. F. M. (2003). The morbidity of Guillain-Barré syndrome admitted to the intensive care unit. *Neurology*, *60*(1), 17–21. https://doi.org/10.1212/01.wnl.0000035640.84053.5b

Hoxha, E., Harendza, S., Pinnschmidt, H., Panzer, U., & Stahl, R. A. (2014). PLA2R antibody levels and clinical outcome in patients with membranous nephropathy and non-nephrotic range proteinuria under treatment with inhibitors of the renin-angiotensin system. *PLoS ONE*, *9*(10), e110681. https://doi.org/10.1371/journal.pone.0110681

Hughes, R. A. C., Swan, A. V, & van Doorn, P. A. (2014). Intravenous immunoglobulin for Guillain-Barré syndrome. *The Cochrane Database of Systematic Reviews*, *2014*(9), CD002063. https://doi.org/10.1002/14651858.CD002063.pub6

Huijbers, M. G., Vergoossen, D. L., Fillié-Grijpma, Y. E., van Es, I. E., Koning, M. T., Slot, L. M., Veelken, H., Plomp, J. J., van der Maarel, S. M., & Verschuuren, J. J. (2019). MuSK myasthenia gravis monoclonal antibodies: Valency dictates pathogenicity. *Neurology(R) Neuroimmunology & Neuroinflammation*, *6*(3), e547. https://doi.org/10.1212/NXI.0000000000000547

Iijima, M., Tomita, M., Morozumi, S., Kawagashira, Y., Nakamura, T., Koike, H., Katsuno, M., Hattori, N., Tanaka, F., Yamamoto, M., & Sobue, G. (2009). Single nucleotide polymorphism of TAG-1 influences IVIg responsiveness of Japanese patients with CIDP. *Neurology*, *73*(17), 1348–1352. https://doi.org/10.1212/WNL.0b013e3181bd1139

Ikeda, S., Koike, H., Nishi, R., Kawagashira, Y., Iijima, M., Katsuno, M., & Sobue, G. (2019). Clinicopathological characteristics of subtypes of chronic inflammatory demyelinating polyradiculoneuropathy. *Journal of Neurology, Neurosurgery and Psychiatry*, *90*(9), 988–996. https://doi.org/10.1136/jnnp-2019-320741

Illa, I., Ortiz, N., Gallard, E., Juarez, C., Grau, J. M., & Dalakas, M. C. (1995). Acute axonal Guillain-Barré syndrome with IgG antibodies against motor axons following parenteral gangliosides. *Annals of Neurology*, *38*(2), 218–224. https://doi.org/10.1002/ana.410380214

Irani, S. R., Alexander, S., Waters, P., Kleopa, K. A., Pettingill, P., Zuliani, L., Peles, E., Buckley, C., Lang, B., & Vincent, A. (2010). Antibodies to Kv1 potassium channel-complex proteins leucine-rich, glioma inactivated 1 protein and contactin-associated protein-2 in limbic encephalitis, Morvan's syndrome and acquired neuromyotonia. *Brain : A Journal of Neurology*, *133*(9), 2734–2748. https://doi.org/10.1093/brain/awq213

Ishibashi, T., Dupree, J. L., Ikenaka, K., Hirahara, Y., Honke, K., Peles, E., Popko, B., Suzuki, K., Nishino, H., & Baba, H. (2002). A myelin galactolipid, sulfatide, is essential for maintenance of ion channels on myelinated axon but not essential for initial cluster formation. *Journal of Neuroscience*, *22*(15), 6507–6514. https://doi.org/10.1523/jneurosci.22-15-06507.2002

Jenkins, S. M., & Bennett, V. (2002). Developing nodes of Ranvier are defined by ankyrin-G clustering and are independent of paranodal axoglial adhesion. *Proceedings of the National Academy of*

Sciences of the United States of America, *99*(4), 2303–2308. https://doi.org/10.1073/pnas.042601799

Jentzer, A., Attal, A., Roué, C., Raymond, J., Lleixà, C., Illa, I., Querol, L., Taieb, G., & Devaux, J. (2022). IgG4 Valency Modulates the Pathogenicity of Anti-Neurofascin-155 IgG4 in Autoimmune Nodopathy. *Neurology(R) Neuroimmunology & Neuroinflammation*, *9*(5), 1–12. https://doi.org/10.1212/NXI.0000000000200014

Jiao, L., Xiang, Y., Li, S., Zhang, F., Ruan, X., & Guo, S. (2020). Efficacy of low dose rituximab in treatment-resistant CIDP with antibodies against NF-155. *Journal of Neuroimmunology*, *May*, 577280. https://doi.org/10.1016/j.jneuroim.2020.577280

Kadoya, M., Kaida, K., Koike, H., Takazaki, H., Ogata, H., Moriguchi, K., Shimizu, J., Nagata, E., Takizawa, S., Chiba, A., Yamasaki, R., Kira, J. ichi, Sobue, G., & Ikewaki, K. (2016). IgG4 anti-neurofascin155 antibodies in chronic inflammatory demyelinating polyradiculoneuropathy: Clinical significance and diagnostic utility of a conventional assay. *Journal of Neuroimmunology*, *301*, 16–22. https://doi.org/10.1016/j.jneuroim.2016.10.013

Kanda, T. (2013). Biology of the blood-nerve barrier and its alteration in immune mediated neuropathies. *Journal of Neurology, Neurosurgery, and Psychiatry*, *84*(2), 208–212. https://doi.org/10.1136/jnnp-2012-302312

Kawamura, N. (2015). Anti-neurofascin antibody in combined central and peripheral demyelination. *Nihon Rinsho. Japanese Journal of Clinical Medicine*, *73*, 347–351. https://doi.org/10.1111/cen3.12061

Kegel, L., Aunin, E., Meijer, D., & Bermingham, J. R. (2013). LGI proteins in the nervous system. *ASN Neuro*, *5*(3), 167–181. https://doi.org/10.1042/AN20120095

Khalil, M., Teunissen, C. E., Otto, M., Piehl, F., Sormani, M. P., Gattringer, T., Barro, C., Kappos, L., Comabella, M., Fazekas, F., Petzold, A., Blennow, K., Zetterberg, H., & Kuhle, J. (2018). Neurofilaments as biomarkers in neurological disorders. *Nature Reviews Neurology*, *14*(10), 577–589. https://doi.org/10.1038/s41582-018-0058-z

Kieseier, B. C., Hartung, H. P., & Wiendl, H. (2006). Immune circuitry in the peripheral nervous system. *Current Opinion in Neurology*, *19*(5), 437–445. https://doi.org/10.1097/01.wco.0000245365.51823.72

Kim, Y. H., Kim, Y. H., Shin, Y. K., Jo, Y. R., Park, D. K., Song, M.-Y., Yoon, B.-A., Nam, S. H., Kim, J. H., Choi, B.-O., Shin, H. Y., Kim, S. W., Kim, S. H., Hong, Y. Bin, Kim, J. K., & Park, H. T. (2019). p75 and neural cell adhesion molecule 1 can identify pathologic Schwann cells in peripheral neuropathies. *Annals of Clinical and Translational Neurology*, *6*(7), 1292–1301. https://doi.org/10.1002/acn3.50828

Klein, C. J., Lennon, V. A., Aston, P. A., McKeon, A., O'Toole, O., Quek, A., & Pittock, S. J. (2013). Insights From LGI1 and CASPR2 Potassium Channel Complex Autoantibody Subtyping. *JAMA Neurology*, *70*(2), 229–234. https://doi.org/10.1001/jamaneurol.2013.592

Klein, C. J., Lennon, V. A., Aston, P. A., McKeon, A., & Pittock, S. J. (2012). Chronic pain as a manifestation of potassium channel-complex autoimmunity. *Neurology*, *79*(11), 1136–1144. https://doi.org/10.1212/WNL.0b013e3182698cab

Koike, H., Fukami, Y., Nishi, R., Kawagashira, Y., Iijima, M., Katsuno, M., & Sobue, G. (2020). Ultrastructural mechanisms of macrophage-induced demyelination in Guillain-Barré syndrome. *Journal of Neurology, Neurosurgery &Amp; Psychiatry*, *91*(6), 650 LP – 659. https://doi.org/10.1136/jnnp-2019-322479

Koike, H., Kadoya, M., Kaida, K. I., Ikeda, S., Kawagashira, Y., Iijima, M., Kato, D., Ogata, H., Yamasaki, R., Matsukawa, N., Kira, J. I., Katsuno, M., & Sobue, G. (2017). Paranodal dissection in chronic inflammatory demyelinating polyneuropathy with anti-neurofascin-155 and anti-contactin-1 antibodies. *Journal of Neurology, Neurosurgery and Psychiatry*, *88*(6), 465–473. https://doi.org/10.1136/jnnp-2016-314895

Koike, H., Nishi, R., Ikeda, S., Kawagashira, Y., Iijima, M., Katsuno, M., & Sobue, G. (2018). Ultrastructural mechanisms of macrophage-induced demyelination in CIDP. In *Neurology* (Vol.

91, Issue 23, pp. 1051–1060). Lippincott Williams and Wilkins. https://doi.org/10.1212/WNL.0000000000006625

Komada, M., & Soriano, P. (2002). βIV-spectrin regulates sodium channel clustering through ankyrin-G at axon initial segments and nodes of Ranvier. *Journal of Cell Biology*, *156*(2), 337–348. https://doi.org/10.1083/jcb.200110003

Kouton, L., Boucraut, J., Devaux, J., Rajabally, Y. A., Adams, D., Antoine, J. C., Bourdain, F., Brodovitch, A., Camdessanché, J. P., Cauquil, C., Ciron, J., Dubard, T., Echaniz-Laguna, A., Grapperon, A. M., Juntas-Morales, R., Kremer, L., Kuntzer, T., Labeyrie, C., Lanfranco, L., … Delmont, E. (2020). Electrophysiological features of chronic inflammatory demyelinating polyradiculoneuropathy associated with IgG4 antibodies targeting neurofascin 155 or contactin 1 glycoproteins. *Clinical Neurophysiology*, *131*(4), 921–927. https://doi.org/10.1016/j.clinph.2020.01.013

Kozar-Gillan, N., Velichkova, A., Kanatouris, G., Eshed-Eisenbach, Y., Steel, G., Jaegle, M., Aunin, E., Peles, E., Torsney, C., & Meijer, D. N. (2023). LGI3/2-ADAM23 interactions cluster Kv1 channels in myelinated axons to regulate refractory period. *The Journal of Cell Biology*, *222*(4). https://doi.org/10.1083/jcb.202211031

Kusunoki, S., Shimizu, J., Chiba, A., Ugawa, Y., Hitoshi, S., & Kanazawa, I. (1996). Experimental sensory neuropathy induced by sensitization with ganglioside GD1b. *Annals of Neurology*, *39*(4), 424–431. https://doi.org/10.1002/ana.410390404

Kuwabara, S., Yuki, N., Koga, M., Hattori, T., Matsuura, D., Miyake, M., & Noda, M. (1998). IgG anti-GM1 antibody is associated with reversible conduction failure and axonal degeneration in Guillain-Barre syndrome. *Annals of Neurology*, *44*(2), 202–208. https://doi.org/10.1002/ana.410440210

Kuwahara, M., Suzuki, H., Samukawa, M., Hamada, Y., Takada, K., & Kusunoki, S. (2013). Clinical features of CIDP with LM1-associated antibodies. *Journal of Neurology, Neurosurgery, and Psychiatry*, *84*(5), 573–575. https://doi.org/10.1136/jnnp-2012-303440

Labasque, M., Hivert, B., Nogales-Gadea, G., Querol, L., Illa, I., & Faivre-Sarrailh, C. (2014). Specific contactin N-glycans are implicated in neurofascin binding and autoimmune targeting in peripheral neuropathies. *The Journal of Biological Chemistry*, *289*(11), 7907–7918. https://doi.org/10.1074/jbc.M113.528489

Lambert, S., Davis, J. Q., & Bennett, V. (1997). Morphogenesis of the node of ranvier: Co-clusters of ankyrin and ankyrin-binding integral proteins define early developmental intermediates. *Journal of Neuroscience*, *17*(18), 7025–7036. https://doi.org/10.1523/jneurosci.17-18-07025.1997

Lancaster, E., Huijbers, M. G. M., Bar, V., Boronat, A., Wong, A., Martinez-Hernandez, E., Wilson, C., Jacobs, D., Lai, M., Walker, R. W., Graus, F., Bataller, L., Illa, I., Markx, S., Strauss, K. A., Peles, E., Scherer, S. S., & Dalmau, J. (2011). Investigations of caspr2, an autoantigen of encephalitis and neuromyotonia. *Annals of Neurology*, *69*(2), 303–311. https://doi.org/10.1002/ana.22297

Le Quintrec, M., Teisseyre, M., Bec, N., Delmont, E., Szwarc, I., Perrochia, H., Machet, M. C., Chauvin, A., Mavroudakis, N., Taieb, G., Lanfranco, L., Rigothier, C., José, B., Concetta, C., Geneste, C., Pernin, V., Larroque, C., Devaux, J., & Beyze, A. (2021). Contactin-1 is a novel target antigen in membranous nephropathy associated with chronic inflammatory demyelinating polyneuropathy. *Kidney International*, *100*(6), 1240–1249. https://doi.org/10.1016/J.KINT.2021.08.014

Lefaucheur, C., Stengel, B., Nochy, D., Martel, P., Hill, G. S., Jacquot, C., & Rossert, J. (2006). Membranous nephropathy and cancer: Epidemiologic evidence and determinants of high-risk cancer association. *Kidney International*, *70*(8), 1510–1517. https://doi.org/10.1038/SJ.KI.5001790

Leonhard, S. E., Mandarakas, M. R., Gondim, F. A. A., Bateman, K., Ferreira, M. L. B., Cornblath, D. R., van Doorn, P. A., Dourado, M. E., Hughes, R. A. C., Islam, B., Kusunoki, S., Pardo, C. A., Reisin, R., Sejvar, J. J., Shahrizaila, N., Soares, C., Umapathi, T., Wang, Y., Yiu, E. M., … Jacobs, B. C. (2019). Diagnosis and management of Guillain–Barré syndrome in ten steps. *Nature Reviews Neurology*, *15*(11), 671–683. https://doi.org/10.1038/s41582-019-0250-9

Liang, Y., Ma, C., Li, F., Nie, G., & Zhang, H. (2020). The Role of Contactin 1 in Cancers: What We Know So Far. *Frontiers in Oncology*, *10*(October), 1–7. https://doi.org/10.3389/fonc.2020.574208

Lieverloo, G. G. A., Wieske, L., Verhamme, C., Vrancken, A. F. J., Doorn, P. A., Michalak, Z., Barro, C., Schaik, I. N., Kuhle, J., & Eftimov, F. (2019). Serum neurofilament light chain in chronic inflammatory demyelinating polyneuropathy. *Journal of the Peripheral Nervous System*, *24*(2), 187–194. https://doi.org/10.1111/jns.12319

Lindner, M., Ng, J. K. M., Hochmeister, S., Meinl, E., & Linington, C. (2013). Neurofascin 186 specific autoantibodies induce axonal injury and exacerbate disease severity in experimental autoimmune encephalomyelitis. *Experimental Neurology*, *247*, 259–266. https://doi.org/10.1016/j.expneurol.2013.05.005

Liu, B., Hu, J., Sun, C., Qiao, K., Xi, J., Zheng, Y., Sun, J., Luo, S., Zhao, Y., Lu, J., Lin, J., & Zhao, C. (2023). Effectiveness and safety of rituximab in autoimmune nodopathy: a single-center cohort study. *Journal of Neurology*, *20*(0123456789). https://doi.org/10.1007/s00415-023-11759-2

Liu, B., Zhou, L., Sun, C., Wang, L., Zheng, Y., Hu, B., Qiao, K., Zhao, C., Lu, J., & Lin, J. (2023). *Clinical profile of autoimmune nodopathy with anti-neurofascin 186 antibody*. 944–952. https://doi.org/10.1002/acn3.51775

Liu, W., Gao, C., Dai, H., Zheng, Y., Dong, Z., Gao, Y., Liu, F., Zhang, Z., Liu, Z., Liu, W., Liu, B., Liu, Q., & Shi, J. (2019). Immunological Pathogenesis of Membranous Nephropathy: Focus on PLA2R1 and Its Role. In *Frontiers in immunology* (Vol. 10, p. 1809). NLM (Medline). https://doi.org/10.3389/fimmu.2019.01809

Lonigro, A., & Devaux, J. J. (2009). Disruption of neurofascin and gliomedin at nodes of Ranvier precedes demyelination in experimental allergic neuritis. *Brain*, *132*(1), 260–273. https://doi.org/10.1093/brain/awn281

Lustig, M., Zanazzi, G., Sakurai, T., Blanco, C., Levinson, S. R., Lambert, S., Grumet, M., & Salzer, J. L. (2001). Nr-CAM and neurofascin interactions regulate ankyrin G and sodium channel clustering at the node of Ranvier Voltage-dependent sodium (Na) channels are myelinated axons

and play a key role in promoting rapid and efficient conduction of action potentials b. *Current Biology*, *11*, 1864–1869.

Lux, A., Yu, X., Scanlan, C. N., & Nimmerjahn, F. (2013). Impact of Immune Complex Size and Glycosylation on IgG Binding to Human FcγRs. *The Journal of Immunology*, *190*(8), 4315–4323. https://doi.org/10.4049/jimmunol.1200501

Manso, C., Querol, L., Lleixà, C., Poncelet, M., Mekaouche, M., Vallat, J. M., Illa, I., & Devaux, J. J. (2019). Anti-Neurofascin-155 IgG4 antibodies prevent paranodal complex formation in vivo. *The Journal of Clinical Investigation*, *130*. https://doi.org/10.1172/JCI124694

Manso, C., Querol, L., Mekaouche, M., Illa, I., & Devaux, J. J. (2016). Contactin-1 IgG4 antibodies cause paranode dismantling and conduction defects. *Brain*, *139*(6), 1700–1712. https://doi.org/10.1093/brain/aww062

Martín-Aguilar, L., Camps-Renom, P., Lleixà, C., Pascual-Goñi, E., Díaz-Manera, J., Rojas-García, R., De Luna, N., Gallardo, E., Cortés-Vicente, E., Muñoz, L., Alcolea, D., Lleó, A., Casasnovas, C., Homedes, C., Gutiérrez-Gutiérrez, G., Jimeno-Montero, M. C., Berciano, J., Sedano-Tous, M. J., García-Sobrino, T., … Querol, L. (2021). Serum neurofilament light chain predicts long-term prognosis in Guillain-Barré syndrome patients. *Journal of Neurology, Neurosurgery and Psychiatry*, *92*(1), 70–77. https://doi.org/10.1136/jnnp-2020-323899

Martín-Aguilar, L., Lleixà, C., & Pascual-Goñi, E. (2022). Autoimmune nodopathies, an emerging diagnostic category. *Current Opinion in Neurology*, *35*(5), 579–585. https://doi.org/10.1097/WCO.0000000000001107

Martín-Aguilar, L., Lleixà, C., Pascual-Goñi, E., Caballero-Ávila, M., Martínez-Martínez, L., Díaz-Manera, J., Rojas-García, R., Cortés-Vicente, E., Turon-Sans, J., de Luna, N., Suárez-Calvet, X., Gallardo, E., Rajabally, Y., Scotton, S., Jacobs, B. C., Baars, A., Cortese, A., Vegezzi, E., Höftberger, R., … Querol, L. (2022). Clinical and Laboratory Features in Anti-NF155 Autoimmune Nodopathy. *Neurology(R) Neuroimmunology & Neuroinflammation*, *9*(1). https://doi.org/10.1212/NXI.0000000000001098

Mathey, E. K., Derfuss, T., Storch, M. K., Williams, K. R., Hales, K., Woolley, D. R., Al-Hayani, A., Davies, S. N., Rasband, M. N., Olsson, T., Moldenhauer, A., Velhin, S., Hohlfeld, R., Meinl, E., & Linington, C. (2007). Neurofascin as a novel target for autoantibody-mediated axonal injury. *The Journal of Experimental Medicine*, *204*(10), 2363–2372. https://doi.org/10.1084/jem.20071053

McGonigal, R., Barrie, J. A., Yao, D., McLaughlin, M., Cunningham, M. E., Rowan, E. G., & Willison, H. J. (2019). Glial sulfatides and neuronal complex gangliosides are functionally interdependent in maintaining myelinating axon integrity. *Journal of Neuroscience*, *39*(1), 63–77. https://doi.org/10.1523/JNEUROSCI.2095-18.2018

McGonigal, R., Cunningham, M. E., Yao, D., Barrie, J. A., Sankaranarayanan, S., Fewou, S. N., Furukawa, K., Yednock, T. A., & Willison, H. J. (2016). C1q-targeted inhibition of the classical complement pathway prevents injury in a novel mouse model of acute motor axonal neuropathy. *Acta Neuropathologica Communications*, *4*(1), 23. https://doi.org/10.1186/s40478-016-0291-x

McGonigal, R., Rowan, E. G., Greenshields, K. N., Halstead, S. K., Humphreys, P. D., Rother, R. P., Furukawa, K., & Willison, H. J. (2010). Anti-GD1a antibodies activate complement and calpain to injure distal motor nodes of Ranvier in mice. *Brain*, *133*(7), 1944–1960. https://doi.org/10.1093/brain/awq119

McKie, S. J., Nicholson, A. S., Smith, E., Fawke, S., Caroe, E., Williamson, J. C., Butt, B. G., Kolářová, D., Peterka, O., Holčapek, M., Lehner, P. J., Graham, S. C., & Deane, J. E. (2022). Altered plasma membrane abundance of the sulfatide-binding protein NF155 links glycosphingolipid imbalances to demyelination. *BioRxiv*, 2022.09.15.508082. https://doi.org/10.1101/2022.09.15.508082

Menon, D., Katzberg, H. D., & Bril, V. (2021). Treatment Approaches for Atypical CIDP. *Frontiers in Neurology*, *12*, 319. https://doi.org/10.3389/FNEUR.2021.653734/BIBTEX

Miller, J. A. L., Spyropoulos, A., Jaros, E., Galban-Horcajo, F., Whittaker, R. G., & Willison, H. J. (2014). Anti-GQ1b ganglioside positive Miller Fisher syndrome - evidence of paranodal pathology on nerve biopsy. *Journal of Neuromuscular Diseases*, *1*(2), 191–195.

Misawa, S., Kuwabara, S., Sato, Y., Yamaguchi, N., Nagashima, K., Katayama, K., Sekiguchi, Y., & Iwai, Y. (2018). *Safety and efficacy of eculizumab in Guillain-Barré syndrome : a multicentre , double-blind , randomised phase 2 trial*. *17*(June), 519–529. https://doi.org/10.1016/S1474-4422(18)30114-5

Miura, Y., Devaux, J. J., Fukami, Y., Manso, C., Belghazi, M., Wong, A. H. Y., Yuki, N., Fujimura, H., Fukutake, T., Iwanami, H., Kusaka, H., Kuwabara, S., Okuma, Y., Ueda, M., & Yamamoto, T. (2015). Contactin 1 IgG4 associates to chronic inflammatory demyelinating polyneuropathy with sensory ataxia. *Brain*, *138*(6), 1484–1491. https://doi.org/10.1093/brain/awv054

Murakoshi, M., Tanimoto, M., Gohda, T., Hagiwara, S., Takagi, M., Horikoshi, S., & Tomino, Y. (2011). Mindin: A novel marker for podocyte injury in diabetic nephropathy. *Nephrology Dialysis Transplantation*, *26*(7), 2153–2160. https://doi.org/10.1093/ndt/gfq708

Nangaku, M., & Couser, W. G. (2005). Mechanisms of immune-deposit formation and the mediation of immune renal injury. In *Clinical and Experimental Nephrology* (Vol. 9, Issue 3, pp. 183–191). Clin Exp Nephrol. https://doi.org/10.1007/s10157-005-0357-8

Nazarali, S., Mathey, E. K., Tang, D., Margetts, P. J., & Baker, S. K. (2020). Chronic Inflammatory Demyelinating Polyneuropathy and Concurrent Membranous Nephropathy. *Canadian Journal of Neurological Sciences*, *47*(4), 585–587. https://doi.org/10.1017/CJN.2020.46

Ng, J. K. M., Malotka, J., Kawakami, N., Derfuss, T., Khademi, M., Olsson, T., Linington, C., Odaka, M., Tackenberg, B., Prüss, H., Schwab, J. M., Harms, L., Harms, H., Sommer, C., Rasband, M. N., Eshed-Eisenbach, Y., Peles, E., Hohlfeld, R., Yuki, N., … Meinl, E. (2012). Neurofascin as a target for autoantibodies in peripheral neuropathies. *Neurology*, *79*(23), 2241–2248. https://doi.org/10.1212/WNL.0b013e31827689ad

NHSE. (2021). *Clinical Commissioning Policy Rituximab therapy for the treatment of nodal / paranodal antibody positive inflammatory / autoimmune neuropathy in adults and post- pubescent children [210602P] (URN : 2001)*. https://www.england.nhs.uk/publication/rituximab-therapy-

for-the-treatment-of-nodal-paranodal-antibody-positive-inflammatory-autoimmune-neuropathy-in-adults-and-postpubescent-children/

Oaklander, A. L., Lunn, M. P., Hughes, R. A., van Schaik, I. N., Frost, C., & Chalk, C. H. (2017). Treatments for chronic inflammatory demyelinating polyradiculoneuropathy (CIDP): an overview of systematic reviews. *The Cochrane Database of Systematic Reviews*, *1*(1), CD010369. https://doi.org/10.1002/14651858.CD010369.pub2

Ogata, H., Matsuse, D., Yamasaki, R., Kawamura, N., Matsushita, T., Yonekawa, T., Hirotani, M., Murai, H., & Kira, J. (2016). A nationwide survey of combined central and peripheral demyelination in Japan. *Journal of Neurology, Neurosurgery, and Psychiatry*, *87*(1), 29–36. https://doi.org/10.1136/jnnp-2014-309831

Ogata, H., Yamasaki, R., Hiwatashi, A., Oka, N., Kawamura, N., Matsuse, D., Kuwahara, M., Suzuki, H., Kusunoki, S., Fujimoto, Y., Ikezoe, K., Kishida, H., Tanaka, F., Matsushita, T., Murai, H., & Kira, J.-I. (2015). Characterization of IgG4 anti-neurofascin 155 antibody-positive polyneuropathy. *Annals of Clinical and Translational Neurology*, *2*(10), 960–971. https://doi.org/10.1002/acn3.248

Ogawa, Y., Schafer, D. P., Horresh, I., Bar, V., Hales, K., Yang, Y., Susuki, K., Peles, E., Stankewich, M. C., & Rasband, M. N. (2006). Spectrins and ankyrinB constitute a specialized paranodal cytoskeleton. *Journal of Neuroscience*, *26*(19), 5230–5239. https://doi.org/10.1523/JNEUROSCI.0425-06.2006

Park, H. T., Kim, J. K., & Tricaud, N. (2019). The conceptual introduction of the “demyelinating Schwann cell” in peripheral demyelinating neuropathies. *Glia*, *67*(4), 571–581. https://doi.org/10.1002/glia.23509

Park, H. T., Kim, Y. H., Lee, K. E., & Kim, J. K. (2020). Behind the pathology of macrophage-associated demyelination in inflammatory neuropathies: demyelinating Schwann cells. *Cellular and Molecular Life Sciences : CMLS*, *77*(13), 2497–2506. https://doi.org/10.1007/s00018-019-03431-8

Pascual-Goñi, E., Fehmi, J., Lleixà, C., Martin-Aguilar, L., Devaux, J., Höftberger, R., Delmont, E., Doppler, K., Sommer, C., Radunovic, A., Carvajal, A., Smyth, S., Williams, L., Mazanec, R., Potočková, V., Hinds, N., Cassereau, J., Viala, K., Lefilliatre, M., … Querol, L. (2020). Antibodies to the Caspr1/contactin-1 complex in chronic inflammatory demyelinating polyneuropathy. *Brain (in Press)*.

Pascual-Goñi, E., Fehmi, J., Lleixà, C., Martín-Aguilar, L., Devaux, J., Höftberger, R., Delmont, E., Doppler, K., Sommer, C., Radunovic, A., Carvajal, A., Smyth, S., Williams, L., Mazanec, R., Potočková, V., Hinds, N., Cassereau, J., Viala, K., Lefilliatre, M., … Querol, L. (2021). Antibodies to the Caspr1/contactin-1 complex in chronic inflammatory demyelinating polyradiculoneuropathy. *Brain*, *144*(4), 1183–1196. https://doi.org/10.1093/brain/awab014

Peles, E., Nativ, M., Lustig, M., Grumet, M., Schilling, J., Martinez, R., Plowman, G. D., & Schlessinger, J. (1997). Identification of a novel contactin-associated transmembrane receptor with multiple domains implicated in protein-protein interactions. *EMBO Journal*, *16*(5), 978–988. https://doi.org/10.1093/emboj/16.5.978

Pillai, A. M., Thaxton, C., Pribisko, A. L., Cheng, J.-G., Dupree, J. L., & Bhat, M. A. (2009). Spatiotemporal ablation of myelinating glia-specific neurofascin (Nfasc NF155) in mice reveals gradual loss of paranodal axoglial junctions and concomitant disorganization of axonal domains. *Journal of Neuroscience Research*, *87*(8), 1773–1793. https://doi.org/10.1002/jnr.22015

Plaisier, E., Not, A., Buob, D., Ronco, P., & Debiec, H. (2021). Contactin-1–associated membranous nephropathy: complete immunologic and clinical remission with rituximab. *Kidney International*, *100*(6), 1342–1344. https://doi.org/10.1016/J.KINT.2021.08.029

Poliak, S., Salomon, D., Elhanany, H., Sabanay, H., Kiernan, B., Pevny, L., Stewart, C. L., Xu, X., Chiu, S.-Y., Shrager, P., Furley, A. J. W., & Peles, E. (2003). Juxtaparanodal clustering of Shaker-like K+ channels in myelinated axons depends on Caspr2 and TAG-1. *The Journal of Cell Biology*, *162*(6), 1149–1160. https://doi.org/10.1083/jcb.200305018

Pozdzik, A., Brochériou, I., David, C., Touzani, F., Goujon, J. M., & Wissing, K. M. (2018). Membranous Nephropathy and Anti-Podocytes Antibodies: Implications for the Diagnostic Workup and Disease Management. *BioMed Research International*, *2018*. https://doi.org/10.1155/2018/6281054

Querol, L., Crabtree, M., Herepath, M., Priedane, E., Viejo Viejo, I., Agush, S., & Sommerer, P. (2021). Systematic literature review of burden of illness in chronic inflammatory demyelinating polyneuropathy (CIDP). *Journal of Neurology*, *268*(10), 3706–3716. https://doi.org/10.1007/s00415-020-09998-8

Querol, L., Nogales-Gadea, G., Rojas-Garcia, R., Diaz-Manera, J., Pardo, J., Ortega-Moreno, A., Sedano, M. J., Gallardo, E., Berciano, J., Blesa, R., Dalmau, J., & Illa, I. (2014). Neurofascin IgG4 antibodies in CIDP associate with disabling tremor and poor response to IVIg. *Neurology*, *82*(10), 879–886. https://doi.org/10.1212/WNL.0000000000000205

Querol, L., Nogales-Gadea, G., Rojas-Garcia, R., Martinez-Hernandez, E., Diaz-Manera, J., Suarez-Calvet, X., Navas, M., Araque, J., Gallardo, E., & Illa, I. (2013). Antibodies to contactin-1 in chronic inflammatory demyelinating polyneuropathy. *Ann Neurol*, *73*(3), 370–380. https://doi.org/10.1002/ana.23794

Querol, L., Rojas-Garcia, R., Diaz-Manera, J., Barcena, J., Pardo, J., Ortega-Moreno, A., Sedano, M. J., Sero-Ballesteros, L., Carvajal, A., Ortiz, N., Gallardo, E., & Illa, I. (2015). Rituximab in treatment-resistant CIDP with antibodies against paranodal proteins. *Neurol Neuroimmunol Neuroinflamm*, *2*(5), e149. https://doi.org/10.1212/NXI.0000000000000149

Rajabally, Y. A., & Attarian, S. (2018). Chronic inflammatory demyelinating polyneuropathy and malignancy: A systematic review. *Muscle & Nerve*, *57*(6), 875–883. https://doi.org/10.1002/mus.26028

Rajabally, Y. A., Durand, M.-C., Mitchell, J., Orlikowski, D., & Nicolas, G. (2015). Electrophysiological diagnosis of Guillain-Barré syndrome subtype: could a single study suffice?

Journal of Neurology, Neurosurgery, and Psychiatry, *86*(1), 115–119. https://doi.org/10.1136/jnnp-2014-307815

Raphaël, J. C., Chevret, S., Hughes, R. A. C., & Annane, D. (2012). Plasma exchange for Guillain-Barré syndrome. *The Cochrane Database of Systematic Reviews*, *7*, CD001798. https://doi.org/10.1002/14651858.CD001798.pub2

Rinaldi, S., Brennan, K. M., Kalna, G., Walgaard, C., van Doorn, P., Jacobs, B. C., Yu, R. K., Mansson, J.-E., Goodyear, C. S., & Willison, H. J. (2013). Antibodies to Heteromeric Glycolipid Complexes in Guillain-Barré Syndrome. *PLoS ONE*, *8*(12), e82337. https://doi.org/10.1371/journal.pone.0082337

Rinaldi, S., Halstead, S., Rodrigues, M. C. L., Titulaer, M., Mgbachi, V., Fehmi, J., Elba-Pascual-Goni, Franken, S., Paunovic, M., Zhu, L., Rohrbacher, S., Sommer, C., Willison, H., Querol, L., Huizinga, R., & Doppler, K. (2022). Inter-laboratory validation of nodal/paranodal antibody testing. *Journal of the Peripheral Nervous System*, *27*(S3), 154–155. https://doi.org/10.1111/jns.12506

Rosch, R. E., Bamford, A., Hacohen, Y., Wraige, E., Vincent, A., Mewasingh, L., & Lim, M. (2014). Guillain-Barr?? syndrome associated with CASPR2 antibodies: Two paediatric cases. *Journal of the Peripheral Nervous System*, *19*(3), 246–249. https://doi.org/10.1111/jns.12089

Roux, T., Debs, R., Maisonobe, T., Lenglet, T., Delorme, C., Louapre, C., Leblond, V., & Viala, K. (2018). Rituximab in chronic inflammatory demyelinating polyradiculoneuropathy with associated diseases. *Journal of the Peripheral Nervous System*, *July*, 1–6. https://doi.org/10.1111/jns.12287

Ruts, L., Drenthen, J., Jacobs, B. C., & Van Doorn, P. A. (2010). Distinguishing acute-onset CIDP from fluctuating guillain-barré syndrome: A prospective study. *Neurology*, *74*(21), 1680–1686. https://doi.org/10.1212/WNL.0b013e3181e07d14

Shelly, S., Klein, C. J., Dyck, P. J. B., Paul, P., Mauermann, M. L., Berini, S. E., Howe, B., Fryer, J. P., Basal, E., Bakri, H. M., Laughlin, R. S., McKeon, A., Pittock, S. J., Mills, J., & Dubey, D. (2021).

Neurofascin-155 Immunoglobulin Subtypes. *Neurology*, *97*(24), e2392 LP-e2403. https://doi.org/10.1212/WNL.0000000000012932

Shimizu, F., & Kanda, T. (2015). Breakdown of blood-nerve barrier in immune-mediated neuropathy. *Neuroimmunology*, *6*, 139–148.

Sistani, L., Rodriguez, P. Q., Hultenby, K., Uhlen, M., Betsholtz, C., Jalanko, H., Tryggvason, K., Wernerson, A., & Patrakka, J. (2013). Neuronal proteins are novel components of podocyte major processes and their expression in glomerular crescents supports their role in crescent formation. *Kidney Int*, *83*(1), 63–71. https://doi.org/10.1038/ki.2012.321

Stengel, H., Vural, A., Brunder, A.-M., Heinius, A., Appeltshauser, L., Fiebig, B., Giese, F., Dresel, C., Papagianni, A., Birklein, F., Weis, J., Huchtemann, T., Schmidt, C., Körtvelyessy, P., Villmann, C., Meinl, E., Sommer, C., Leypoldt, F., & Doppler, K. (2019). Anti–pan-neurofascin IgG3 as a marker of fulminant autoimmune neuropathy. *Neurology - Neuroimmunology Neuroinflammation*, *6*(5), e603. https://doi.org/10.1212/NXI.0000000000000603

Stewart, B. J., Ferdinand, J. R., Young, M. D., Mitchell, T. J., Loudon, K. W., Riding, A. M., Richoz, N., Frazer, G. L., Staniforth, J. U. L., Braga, F. A. V., Botting, R. A., Popescu, D. M., Vento-Tormo, R., Stephenson, E., Cagan, A., Farndon, S. J., Polanski, K., Efremova, M., Green, K., … Clatworthy, M. R. (2019). Spatiotemporal immune zonation of the human kidney. *Science*, *365*(6460), 1461–1466. https://doi.org/10.1126/science.aat5031

Susuki, K., Baba, H., Tohyama, K., Kanai, K., Kuwabara, S., Hirata, K., Furukawa, K., Furukawa, K., Rasband, M. N., & Yuki, N. (2007). Gangliosides contribute to stability of paranodal junctions and ion channel clusters in myelinated nerve fibers. *Glia*, *55*(7), 746–757. https://doi.org/10.1002/glia.20503

Susuki, K., Rasband, M. N., Tohyama, K., Koibuchi, K., Okamoto, S., Funakoshi, K., Hirata, K., Baba, H., & Yuki, N. (2007). Anti-GM1 Antibodies Cause Complement-Mediated Disruption of Sodium Channel Clusters in Peripheral Motor Nerve Fibers. *Journal of Neuroscience*, *27*(15), 3956–3967. https://doi.org/10.1523/JNEUROSCI.4401-06.2007

Taieb, G., Jentzer, A., Vegezzi, E., Lleixà, C., Illa, I., Querol, L., & Devaux, J. J. (2023). Effect of monovalency on anti-contactin-1 IgG4. *Frontiers in Immunology*, *14*(March), 1–9. https://doi.org/10.3389/fimmu.2023.1021513

Taieb, G., Le Quintrec, M., Pialot, A., Szwarc, I., Perrochia, H., Labauge, P., & Devaux, J. J. (2018). "Neuro-renal syndrome" related to anti-contactin-1 antibodies. *Muscle & Nerve*. https://doi.org/10.1002/mus.26392

Taieb, G., Le Quintrec, M., Pialot, A., Szwarc, I., Perrochia, H., Labauge, P., & Devaux, J. J. (2019). "Neuro-renal syndrome" related to anti-contactin-1 antibodies. *Muscle Nerve*, *59*(3), E19–E21. https://doi.org/10.1002/mus.26392

Taylor, A. M., Saifetiarova, J., & Bhat, M. A. (2017). Postnatal Loss of Neuronal and Glial Neurofascins Differentially Affects Node of Ranvier Maintenance and Myelinated Axon Function . In *Frontiers in Cellular Neuroscience* (Vol. 11). https://www.frontiersin.org/articles/10.3389/fncel.2017.00011

Thaxton, C., Pillai, A. M., Pribisko, A. L., Dupree, J. L., & Bhat, M. A. (2011). Nodes of Ranvier act as barriers to restrict invasion of flanking paranodal domains in myelinated axons. *Neuron*, *69*(2), 244–257. https://doi.org/10.1016/j.neuron.2010.12.016

Thomma, R. C. M., Fokke, C., Walgaard, C., Vermeulen-de Jongh, D. M. C., Tio-Gillen, A., van Rijs, W., van Doorn, P. A., Huizinga, R., & Jacobs, B. C. (2023). High and Persistent Anti-GM1 Antibody Titers Are Associated With Poor Clinical Recovery in Guillain-Barré Syndrome. *Neurology - Neuroimmunology Neuroinflammation*, *10*(4). https://doi.org/10.1212/NXI.0000000000200107

Tüzün, E., Kinay, D., Hacohen, Y., Aysal, F., & Vincent, A. (2013). Guillain-Barré-like syndrome associated with lung adenocarcinoma and CASPR2 antibodies. *Muscle & Nerve*, *48*(5), 836–837. https://doi.org/10.1002/mus.23851

Uncini, A., & Kuwabara, S. (2012). Electrodiagnostic criteria for Guillain–Barrè syndrome: A critical revision and the need for an update. *Clinical Neurophysiology*, *123*(8), 1487–1495. https://doi.org/10.1016/j.clinph.2012.01.025

Uncini, A., Santoro, M., Corbo, M., Lugaresi, A., & Latov, N. (1993). Conduction abnormalities induced by sera of patients with multifocal motor neuropathy and anti-GM1 antibodies. *Muscle & Nerve*, *16*(6), 610–615. https://doi.org/10.1002/mus.880160606

Uncini, A., Susuki, K., & Yuki, N. (2013). Nodo-paranodopathy: Beyond the demyelinating and axonal classification in anti-ganglioside antibody-mediated neuropathies. *Clinical Neurophysiology*, *124*(10), 1928–1934. https://doi.org/10.1016/j.clinph.2013.03.025

Uncini, A., & Vallat, J. M. (2018). Autoimmune nodo-paranodopathies of peripheral nerve: The concept is gaining ground. *Journal of Neurology, Neurosurgery and Psychiatry*, *89*(6), 627–635. https://doi.org/10.1136/jnnp-2017-317192

Vabnick, I., Novaković, S. D., Levinson, S. R., Schachner, M., & Shrager, P. (1996). The clustering of axonal sodium channels during development of the peripheral nervous system. *Journal of Neuroscience*, *16*(16), 4914–4922. https://doi.org/10.1523/jneurosci.16-16-04914.1996

Vallat, J. M., Mathis, S., Magy, L., Bounolleau, P., Skarzynski, M., Heitzmann, A., Manso, C., Devaux, J., & Uncini, A. (2018). Subacute nodopathy with conduction blocks and anti-neurofascin 140/186 antibodies: An ultrastructural study. *Brain*, *141*(7), e56. https://doi.org/10.1093/brain/awy134

Vallat, J. M., Mathis, S., Vegezzi, E., Richard, L., Duchesne, M., Gallouedec, G., Corcia, P., Magy, L., Uncini, A., & Devaux, J. (2019). Antibody- and macrophage-mediated segmental demyelination in chronic inflammatory demyelinating polyneuropathy: clinical, electrophysiological, immunological and pathological correlates. *European Journal of Neurology*. https://doi.org/10.1111/ene.14133

Vallat, J.-M., Magy, L., Corcia, P., Boulesteix, J.-M., Uncini, A., & Mathis, S. (2019). Ultrastructural Lesions of Nodo-Paranodopathies in Peripheral Neuropathies. *Journal of Neuropathology & Experimental Neurology*, *79*(3), 247–255ff. https://doi.org/10.1093/jnen/nlz134

Vallat, J.-M., Yuki, N., Sekiguchi, K., Kokubun, N., Oka, N., Mathis, S., Magy, L., Sherman, D. L., Brophy, P. J., & Devaux, J. J. (2017). Paranodal lesions in chronic inflammatory demyelinating polyneuropathy associated with anti-Neurofascin 155 antibodies. In *Neuromuscular Disorders* (Vol. 27, Issue 3). https://doi.org/10.1016/j.nmd.2016.10.008

Van Den Berg, B., Walgaard, C., Drenthen, J., Fokke, C., Jacobs, B. C., & Van Doorn, P. A. (2014). Guillain-Barré syndrome: Pathogenesis, diagnosis, treatment and prognosis. *Nature Reviews Neurology*, *10*(8), 469–482. https://doi.org/10.1038/nrneurol.2014.121

Van den Bergh, P. Y. K., van Doorn, P. A., Hadden, R. D. M., Avau, B., Vankrunkelsven, P., Allen, J. A., Attarian, S., Blomkwist-Markens, P. H., Cornblath, D. R., Eftimov, F., Goedee, H. S., Harbo, T., Kuwabara, S., Lewis, R. A., Lunn, M. P., Nobile-Orazio, E., Querol, L., Rajabally, Y. A., Sommer, C., & Topaloglu, H. A. (2021). European Academy of Neurology/Peripheral Nerve Society guideline on diagnosis and treatment of chronic inflammatory demyelinating polyradiculoneuropathy: Report of a joint Task Force—Second revision. *Journal of the Peripheral Nervous System*, *26*(3), 242–268. https://doi.org/10.1111/JNS.12455/SUPINFO

van Sonderen, A., Ariño, H., Petit-Pedrol, M., Leypoldt, F., Körtvélyessy, P., Wandinger, K.-P., Lancaster, E., Wirtz, P. W., Schreurs, M. W. J., Sillevis Smitt, P. A. E., Graus, F., Dalmau, J., & Titulaer, M. J. (2016). The clinical spectrum of Caspr2 antibody-associated disease. *Neurology*, *87*(5), 521–528. https://doi.org/10.1212/WNL.0000000000002917

Visser, N. A., Notermans, N. C., Linssen, R. S. N., van den Berg, L. H., & Vrancken, A. F. J. E. (2015). Incidence of polyneuropathy in Utrecht, the Netherlands. *Neurology*, *84*(3), 259–264. https://doi.org/10.1212/WNL.0000000000001160

Vural, A., Doppler, K., & Meinl, E. (2018). Autoantibodies Against the Node of Ranvier in Seropositive Chronic Inflammatory Demyelinating Polyneuropathy: Diagnostic, Pathogenic, and Therapeutic Relevance. *Front Immunol*, *9*, 1029. https://doi.org/10.3389/fimmu.2018.01029

WAKSMAN, B. H., & ADAMS, R. D. (1955). Allergic neuritis: an experimental disease of rabbits induced by the injection of peripheral nervous tissue and adjuvants. *The Journal of Experimental Medicine*, *102*(2), 213–236. https://doi.org/10.1084/jem.102.2.213

Wang, Y., Shi, Q., Lv, H., Hu, M., Wang, W., Wang, Q., Qiao, B., Zhang, G., Lv, Z., Kjellman, C., Järnum, S., Winstedt, L., Zhang, Y., Wen, J., Hao, Y., & Yuki, N. (2017). IgG-degrading enzyme of Streptococcus pyogenes (IdeS) prevents disease progression and facilitates improvement in a rabbit model of Guillain-Barré syndrome. *Experimental Neurology*, *291*, 134–140. https://doi.org/https://doi.org/10.1016/j.expneurol.2017.02.010

Waters, P., Reindl, M., Saiz, A., Schanda, K., Tuller, F., Kral, V., Nytrova, P., Sobek, O., Nielsen, H. H., Barington, T., Lillevang, S. T., Illes, Z., Rentzsch, K., Berthele, A., Berki, T., Granieri, L., Bertolotto, A., Giometto, B., Zuliani, L., … Marignier, R. (2016). Multicentre comparison of a diagnostic assay: Aquaporin-4 antibodies in neuromyelitis optica. *Journal of Neurology, Neurosurgery and Psychiatry*, *87*(9). https://doi.org/10.1136/jnnp-2015-312601

Wieske, L., Martín-Aguilar, L., Fehmi, J., Lleixà, C., Koel-Simmelink, M. J. A., Chatterjee, M., Van Lierop, Z., Killestein, J., Verhamme, C., Querol, L., Rinaldi, S., Teunissen, C. E., Eftimov, F., & Org/Coe, N. (2021). Serum Contactin-1 in CIDP A Cross-Sectional Study Class of Evidence Criteria for rating therapeutic and diagnostic studies. *Neurol Neuroimmunol Neuroinflamm*, *8*. https://doi.org/10.1212/NXI.0000000000001040

Willison, H. J. (2018). Anti-ganglioside Antibodies in Peripheral Nerve Pathology. *Methods in Molecular Biology (Clifton, N.J.)*, *1804*, 173–188. https://doi.org/10.1007/978-1-4939-8552-4_7

Willison, H. J., Veitch, J., Paterson, G., & Kennedy, P. G. (1993). Miller Fisher syndrome is associated with serum antibodies to GQ1b ganglioside. *Journal of Neurology, Neurosurgery & Psychiatry*, *56*(2), 204 LP – 206. https://doi.org/10.1136/jnnp.56.2.204

Winer, J. B., Hughes, R. A., & Osmond, C. (1988). A prospective study of acute idiopathic neuropathy. I. Clinical features and their prognostic value. *Journal of Neurology, Neurosurgery, and Psychiatry*, *51*(5), 605–612. https://doi.org/10.1136/jnnp.51.5.605

Witsch, J., Galldiks, N., Bender, A., Kollmar, R., Bösel, J., Hobohm, C., Günther, A., Schirotzek, I., Fuchs, K., & Jüttler, E. (2013). Long-term outcome in patients with Guillain-Barré syndrome requiring mechanical ventilation. *Journal of Neurology*, *260*(5), 1367–1374. https://doi.org/10.1007/s00415-012-6806-x

Yan, W., Nguyen, T., Yuki, N., Ji, Q., Yiannikas, C., Pollard, J. D., & Mathey, E. K. (2014). Antibodies to neurofascin exacerbate adoptive transfer experimental autoimmune neuritis. *Journal of Neuroimmunology*, *277*(1), 13–17. https://doi.org/10.1016/j.jneuroim.2014.09.012

Yan, W. X., Taylor, J., Andrias-Kauba, S., & Pollard, J. D. (2000). Passive transfer of demyelination by serum or IgG from chronic inflammatory demyelinating polyneuropathy patients. *Annals of Neurology*, *47*(6), 765–775. https://doi.org/10.1002/1531-8249(200006)47:6<765::AID-ANA9>3.0.CO;2-8

Yang, Y., Lacas-Gervais, S., Morest, D. K., Solimena, M., & Rasband, M. N. (2004). βIV spectrins are essential for membrane stability and the molecular organization of nodes of Ranvier. *Journal of Neuroscience*, *24*(33), 7230–7240. https://doi.org/10.1523/JNEUROSCI.2125-04.2004

Yuki, N. (2007). Campylobacter sialyltransferase gene polymorphism directs clinical features of Guillain-Barré syndrome. *Journal of Neurochemistry*, *103 Suppl*, 150–158. https://doi.org/10.1111/j.1471-4159.2007.04707.x

Yuki, N., & Uncini, A. (2014). Acute and chronic ataxic neuropathies with disialosyl antibodies: A continuous clinical spectrum and a common pathophysiological mechanism. *Muscle and Nerve*, *49*(5), 629–635. https://doi.org/10.1002/mus.24192

Yuki, N., Yamada, M., Koga, M., Odaka, M., Susuki, K., Tagawa, Y., Ueda, S., Kasama, T., Ohnishi, A., Hayashi, S., Takahashi, H., Kamijo, M., & Hirata, K. (2001). Animal model of axonal Guillain-Barré syndrome induced by sensitization with GM1 ganglioside. *Annals of Neurology*, *49*(6), 712–720. http://www.ncbi.nlm.nih.gov/pubmed/11409422

Yuki, N., Yoshino, H., Sato, S., & Miyatake, T. (1990). Acute axonal polyneuropathy associated with anti-GM1 antibodies following Campylobacter enteritis. *Neurology*, *40*(12), 1900–1902. https://doi.org/10.1212/wnl.40.12.1900

Zhang, C., Susuki, K., Zollinger, D. R., Dupree, J. L., & Rasband, M. N. (2013). Membrane domain organization of myelinated axons requires βII spectrin. *Journal of Cell Biology*, *203*(3), 437–443. https://doi.org/10.1083/jcb.201308116

Zhang, G., Lin, J., Ghauri, S., & Sheikh, K. A. (2017). Modulation of IgG–FcRn interactions to overcome antibody-mediated inhibition of nerve regeneration. *Acta Neuropathologica*, *134*(2), 321–324. https://doi.org/10.1007/s00401-017-1730-x

Zhang, X., Kira, J. I., Ogata, H., Imamura, T., Mitsuishi, M., Fujii, T., Kobayashi, M., Kitagawa, K., Namihira, Y., Ohya, Y., Maimaitijiang, G., Yamasaki, R., Fukata, Y., Fukata, M., Isobe, N., & Nakamura, Y. (2023). Anti-LGI4 Antibody Is a Novel Juxtaparanodal Autoantibody for Chronic Inflammatory Demyelinating Polyneuropathy. *Neurology(R) Neuroimmunology & Neuroinflammation*, *10*(2), 1–14. https://doi.org/10.1212/NXI.0000000000200081

Zhang, X., Zheng, P., Devaux, J. J., Wang, Y., Liu, C., Li, J., Guo, S., Song, Y., Wang, Q., Feng, X., & Wang, Y. (2019). Chronic inflammatory demyelinating polyneuropathy with anti-NF155 IgG4 in China. *Journal of Neuroimmunology*, *337*(August). https://doi.org/10.1016/j.jneuroim.2019.577074

Zhang, Y., Yoko bekku, Yulia Dzhashiashvil, Steven Arementi, Xiasong Meng, Yo Sasaki, Jeffrey Millbrandt, & Salzer, J. L. (2012). Assembly and maintenance of nodes of Ranvier rely on distinct sources of proteins and targeting mechanisms. *Neuron*, *73*(1), 92–107. https://doi.org/10.1016/j.neuron.2011.10.016.Assembly

6 APPPENDIX

Request Form for Paranodal / Nodal Antibody Testing

Clinical Data

Date of neuropathy onset: Age at diagnosis:

☐ Prodromal illness/trigger (please specify):
Start date for prodrome/trigger:

Initial diagnosis
☐ GBS ☐ Typical CIDP ☐ MMN
☐ Atypical CIDP / Other (specify):

Current diagnosis
☐ GBS ☐ CIDP ☐ MMN
☐ Atypical CIDP / Other (specify):

If the current diagnosis is GBS, CIDP, or MMN please answer the following (tick all that apply):

Clinical course
☐ Relapsing-remitting ☐ Progressive ☐ Monophasic

Onset / progression
☐ Acute (<4 weeks) ☐ Subacute (4-8 weeks) ☐ Chronic (>8 weeks)

Weakness (Yes/No) (Tick all that apply)
☐ Arms
☐ Proximal ☐ Distal
☐ Asymmetric ☐ Symmetric
☐ Legs
☐ Proximal ☐ Distal
☐ Asymmetric ☐ Symmetric

Sensory deficit (Tick all that apply)
☐ Arms
☐ Vibration ☐ Pinprick ☐ JPS
☐ Legs
☐ Vibration ☐ Pinprick ☐ JPS

☐ Ataxia ☐ Tremor ☐ Neuropathic pain 0 /10 Severity (1-10)

Reflexes
☐ Absent ☐ Decreased ☐ Normal ☐ Brisk

☐ Cranial nerve involvement (specify)

☐ Autonomic involvement (please specify)

Respiratory involvement ☐ Current ☐ Previous ☐ None

Evidence of nephrotic syndrome
☐ Proteinuria (level:)
☐ Hypoalbuminaemia (nadir level: g/L)
☐ Oedema ☐ Not assessed
☐ None

Severity
Modified Rankin score (at nadir): 1 ☐ 2 ☐ 3 ☐ 4 ☐ 5 ☐ 6 ☐

Investigations

☐ CSF (at diagnosis) Date:
Protein: g/L WCC: RCC:
OCBs: (select from drop down menu) Other:

Neurophysiology
Overall impression: ☐ Demyelinating ☐ Axonal ☐ Mixed Other (specify)

☐ Motor involvement (describe core features):
☐ Sensory involvement (describe core features):

Other Antibodies
Gangliosides ☐ Positive ☐ Negative ☐ Not done
Anti-MAG ☐ Positive ☐ Negative ☐ Not done

Paraprotein ☐ Positive ☐ Negative ☐ Not done
☐ IgG ☐ IgM ☐ IgA ☐ Kappa ☐ Lambda
Level: g/L

Imaging
MRI lumbar roots ☐ Abnormal ☐ Normal ☐ Not done
Specify:

Treatment and Outcome

	Trialled		**Response**			
			Good	Partial	None	Worse
IVIg	Yes ☐	No ☐	☐	☐	☐	☐
Steroids	Yes ☐	No ☐	☐	☐	☐	☐
Plasma Ex.	Yes ☐	No ☐	☐	☐	☐	☐
Other (specify)			☐	☐	☐	☐
Other (specify)			☐	☐	☐	☐

Current Disease Activity

1.Cure: ≥5 years off treatment
- ☐ A. Normal examination
- ☐ B. Abnormal examination, stable/improving

2. Remission: <5 years off treatment
- ☐ A. Normal examination
- ☐ B. Abnormal examination, stable/improving

3. Stable active disease: ≥1 year, on treatment
- ☐ A. Normal examination
- ☐ B. Abnormal examination, stable/improving

4. Improvement: ≥3 months <1 year, on Treatment
- ☐ A. Normal examination
- ☐ B. Abnormal examination, stable/improving

5. Unstable active disease: abnormal examination with progressive or relapsing course*
- ☐ A. Treatment naïve or <3 months
- ☐ B. Off treatment
- ☐ C. On treatment

Modified Rankin score (at best post treatment):
0 ☐ 1 ☐ 2 ☐ 3 ☐ 4 ☐ 5 ☐ 6 ☐